2018

Formulation and in Vitro Characterisation of Fungal Chitosan Nanoparticles Coated With Zein for Improved Oral Delivery of Selenoamino Acids

Giuliana Vozza
Technological University Dublin, giuliana.vozza@tudublin.ie

Formulation and *in vitro* characterisation of fungal chitosan nanoparticles coated with zein for improved oral delivery of selenoamino acids

Giuliana Vozza BSc (Hons)

A thesis submitted to the Dublin Institute of Technology for the Award of Doctor of Philosophy (PhD)

Supervisors:

Prof. Jésus Frías, Dr Sinéad Ryan and Prof. Hugh J Byrne

FOCAS Research Institute

School of Food Science and Environmental Health

Dublin Institute of Technology

Submission Date: May 2018

Declaration

I certify that this thesis which I now submit for examination for the award Doctor of Philosophy (PhD), is entirely my own work and has not been taken from the work of others, save and to the extent that such work has been cited and acknowledged within the text of my work.

This thesis was prepared according to the regulations for postgraduate study by research of the Dublin Institute of Technology and has not been submitted in whole or in part for another award in any other third level institution. The work reported on in this thesis conforms to the principles and requirements of the DIT's guidelines for ethics in research.

DIT has permission to keep, lend or copy this thesis in whole or in part, on condition that any such use of the material of the thesis be duly acknowledged.

Candidate Signature _____Date _____

Abstract

Selenium (Se) is an essential micronutrient in both human and animal nutrition that exists in a wide array of different forms, both organic and inorganic. Selenoamino acids (SeAAs), such as selenocystine ($SeCys_2$), selenomethionine (SeMet), and methylselenocysteine (MSC) are organic species with reported health benefits of cancer prevention, increased fertility and improved immunological status. However, supplementation of SeAAs can be challenging, due to their reported narrow therapeutic range of indices, low bioavailability and increased susceptibility to oxidation. To address this, SeAAs were encapsulated into nanoparticles (NPs) to lower their toxicity profiles in comparison to their native form, in addition to offering them protection from the harsh conditions present in the gastrointestinal tract. The ionotropic gelation method was employed to produce NPs, using the cationic polyelectrolyte chitosan (Cs) crosslinked with the polyanion tripolyphosphate (TPP). The NP physicochemical properties were optimised using a Design of Experiments (DoE) and mathematical modelling approach.

First, a central composite design (CCD) was used to identify a feasible region in which unloaded NPs with target properties for oral delivery (size~300 nm, PDI < 0.5 and ZP > 30 mV) could be achieved, indicating that optimum conditions to be 6:1 mass ratios of Cs:TPP. Following that, SeMet was used as a prototype encapsulant and a second DoE approach was employed, namely a Box Behnken design (BBD). In that study, Cs:TPP ratio, Cs solvent pH, and drug load concentration were independently varied and the dependent variables assessed were encapsulation efficiency (EE%), particle size, PDI and ZP. The BBD highlighted the optimum conditions for NP production, although EE% remained relatively low (≈40 %). By varying the pH of the ionotropic solution components and coating the NPs with zein (a prolamine rich protein), EE% was doubled

(≈80 %), diameters increased from 187±58nm to 377±47nm and PDI and ZP values were maintained. The formulation performed well indicating good suitability for oral delivery, in terms of stability, cytotoxicity (intestinal and liver cell lines) and release profiles, as determined by *in vitro* techniques. The models generated from the BBD were then applied to the SeAAs, $SeCys_2$ and MSC and further refinement of the zein coating was investigated. NPs with similar physicochemical properties to those of SeMet loaded Cs were produced, indicating the strength of the DoE models and their usefulness in formulation design. These NPs also performed well in *in vitro* assessments for stability and release profiles. However, $SeCys_2$ showed cytotoxicity to liver cell lines which was reduced after encapsulation within the NP matrix, inferring its protective effects and thus use as a delivery system.

Chitin was extracted from the cultivated mushroom *Agaricus bisporus* in order to derive fungal Cs (fCs) with equivalent physicochemical properties to the commercial Cs (CL113) that had been employed for NP production. fCs with comparable properties to CL113 were produced, although fCs possessed a higher molecular weight (MW) (180±19 vs 110±4 kDa). Trimethyl chitosan was then synthesised from the fCs and assessed for permeation enhancing capabilities on intestinal cell monolayer models, which implicated its potential application as a permeation enhancer.

fCs was used for the production of synthetic $SeCys_2$ loaded NPs using the knowledge gained from the previously developed DoE models and *in vitro* methodologies. Lastly, a preliminary study to assess the feasibility of Irish mushrooms providing Se species for supplementation purposes was conducted, implicating them as a viable source for $SeCys_2$.

Acknowledgments

The work presented in this thesis would not have been possible without the encouragement and recommendations of many others and I would like to take this opportunity to show my appreciation.

Firstly, I would like to express my sincerest gratitude to my three supervisors, Prof. Jesús Frías, Dr. Sinéad Ryan and Prof. Hugh Byrne, for all your guidance, help and understanding during my research. To Jesús, thank you for always helping me find a remedy, to problems, that had garnered, my interest, for example: funding for microwave digestion vessels or multi-plate stirrers (which you rightly predicted would turn into margarita mixers). Thank you for being so sound and approachable for the last 4 years! To Sinéad, thank you for putting up with the many times I popped into your office, essentially talking in tongues about lab work not going well and managing to instill a sense of calm over me to talk the issues through properly, I hope you know just how much I appreciated it. To Hugh, thank you for always having an open door, for always offering your guidance and support, for encouraging me to address things I wanted to avoid and for the wonderful environment that you have created in FOCAS, so much so that I truly consider it my second home.

I would like to thank our project collaborators in UCD, Prof David Brayden and Shane Forde, for all the assistance and feedback during our collaboration and express my gratitude to all the research team at Monaghan Mushrooms. A special mention to Catriona O' Reilly and Dr. Juan Valverde for the multiple lifts to Monaghan, for sending samples externally when I hit instrumentation walls and whose encouragement and support aided my development over the course of this PhD. I would also like to thank Alltech, Biotechnology in Dunboyne, especially Dr Cathal Connolly who was always on hand to offer advice and feedback on the project.

To all the staff who assisted me in my researches, particularly: Marcus Maher and Alan Casey (Nanolab); Joythi Nair and Noel Grace (CBS); Martin Kitson in (Kevin St); Martin Feeny and Tom Conroy (TCD) and last but most certainly not least, my squirrel friends Fiona Mc Carthy and John Gleeson (UCD), thank you; your resolute assistance during this research was majorly appreciated and you are all an absolute testament to your institutes.

To the FOCAS ~~crew~~ ~~friends~~ family, of which there are too many to list, you are all superstars!! I can't imagine having done this project without you all there to lend an ear during the lows, to blow off steam on nights out (or table quizzes in) and to celebrate the highs with. Special mention to Minna Danish who will be glad to hear I'm no longer "dying inside" and to Craig Mullen whom I've walked the work-cosmos with for the last 12 years and all going well for another 40 years to come.

I would also like to thank all my friends for their unyielding support and encouragement throughout the years, especially my dear, formatting prowess, friend Caoimhe. You are the most amazing friend a girl could ever dream of and I am honored to have had your friendship these last 25 years.

My highest appreciation to my family: Alessia; Stefano; Pauline; Antonello; Lucia and especially my parents, Eileen and Antonio for all their love and support over the years. To my kind, loving, supportive partner Darren for making me believe in myself and my abilities when I'd lost my own faith, and for providing me with copious amounts of tea to keep me functioning when I felt I couldn't go on! Lastly, I would like to thank my ~~guurrll~~ ~~twin~~ rock Emilio, who I have walked this life with longer than I have walked without, who has encouraged, supported and even contributed physical data to this project, thank you from the bottom of my heart. I honestly don't know what I'd do without you.

Table of Contents

List of Figures

List of Tables

1 INTRODUCTION

1.1 Background

Drug discovery and development involves highly challenging, laborious, and expensive processes. On average, it can take 15 years, with an estimated cost of US $802 million, for the development of a new drug, from bench to bedside, which is markedly increasing at an annual rate of 7.4 % above general price inflation (Cousin *et al.*, 2016). Technological advances such as quantitative structure activity relationships (QSAR) and high throughput screening (HTS) have assisted in the identification, synthesis and activity assessment of new bioactive (BA) compounds, more rapidly than that of conventional discovery (Park, 2014). However, in spite of QSAR and HTS techniques, most drugs fail to achieve favourable clinical outcomes in the clinical phase, due to their inability to reach the target site of action (Park *et al.*, 2010, Estanqueiro *et al.*, 2015). Although BAs may show high potency for target sites *in vitro*, the oral delivery of such compounds *in vivo* can often raise a challenge, for example:

- Stability in the gastrointestinal tract (GIT) -reducing bio-accessibility
- Low permeability through intestinal epithelial and/or transporter restrictions
- Instability under processing conditions (temperature, oxygen, light)
- Degradation in the GIT by pH, enzymes or presence of other nutrients

all of which may limit the activity and potential health benefits of nutraceutical molecules (Agrawal *et al.*, 2014, Gleeson, Ryan and Brayden, 2016).

Targeted drug delivery systems, that release drugs or BA agents at the desired site of action, are an effective approach to overcome these critical issues, as they can improve therapeutic efficacy through the modulation of pharmacokinetic and biodistribution

fate (Hagens *et al.*, 2007). In this context, nanoparticle (NP) delivery systems have been investigated, as they have been shown to be more biologically active, due to their enhanced surface area per mass compared with larger-sized particles of the same chemistry (Oberdörster *et al.*, 2005). By using NPs as a drug delivery vehicle, it might be possible to enhance a range of characteristics for a given BA, such as increased protection ensuring stability and better oral uptake (Nair *et al.*, 2010).

The gold standard for BA delivery is considered the oral route, due to ease of dosing, patient acceptance and compliance. Because of this, encapsulation systems now are of the upmost importance (Benshitrit *et al.*, 2012). Recently, consumers, industry and researchers alike are recognising the potential of BA compounds naturally present in common food stuffs (Vattem and Maitin, 2016). There is a consumer perception on the need to reduce animal testing for everyday products and dietary supplements, favouring "naturally derived" BAs (Vanhonacker and Verbeke, 2014). Chitosan (Cs), a biocompatible, mucopolysaccharide, typically derived from crustaceans, has been investigated as a system for cargo delivery to the colon, due to its capacity to protect therapeutic agents from the hostile conditions of the upper gastrointestinal tract (Benshitrit *et al.*, 2012) and to facilitate release of entrapped agents (Chen *et al.*, 2013), whilst its glycosidic linkages undergo degradation by colonic microflora (Amidon, Brown and Dave, 2015). Improving the bioavailability of drugs through NP drug delivery systems is possible using Cs prepared either as a hydrogel or as NPs, whereby its polycationic amino groups interact with the drug's anionic groups, in the presence of an anionic crosslinker (Janes, Calvo and Alonso, 2001). However, because of its high solubility in acid gastric fluids (such as the stomach environment (pH 1.2)), Cs has limited suitability in colonic targeting of drugs, sometimes resulting in a burst release of the drug in this environment (Garapati *et al.*, 2015). To alleviate

this problem, the coating of Cs NPs has been proposed, whereby an improved controlled release of encapsulated BA can be achieved, as the coating serves as a rate limiting barrier (Katouzian and Jafari, 2016). It is worth noting however, that the release from these NPs is strongly dependent on the chemical nature and physical structure of the coating material and its interaction with Cs. Zein, a prolamine rich protein derived from maize, has been employed for the formulation and coating of Cs:NP oral delivery systems, due to its ability to increase the encapsulation efficiency (EE%) of BAs and to improve their controlled release in the GIT (Luo *et al.*, 2010; Luo and Wang, 2014; Paliwal and Palakurthi, 2014). This coating strategy harnesses both the protein (zein) and polysaccharide (Cs) properties in a NP delivery system in which a broader range of physical, chemical and colloidal stability can be achieved (Benshitrit *et al.*, 2012).

Selenium (Se) is an essential micronutrient that exists in different forms, both inorganic and organic and exerts its biological functions through >25 selenoproteins (Xia *et al.*, 2005). Nutritional deficiency of the element decreases the expression of selenoproteins and thereby impairs selenium's biological functions. Selenoamino acids (SeAAs) have attracted attention as Se supplements due to their potential immune enhancing, fertility improving and anti-cancer properties (El-Bayoumy, Sinha and Richie Jr, 2015; Kamwesiga *et al.*, 2015; Shanmugam *et al.*, 2015). However, Se from *A. bisporus* has been reported to have poor bioavailability (Thiry *et al.*, 2012), which is further reduced upon cooking (Khanam and Platel, 2016). As such, there is substantial interest in developing an oral formulation of Se, although, due to its susceptibility to oxidation, this has not proved possible to date.

As a consequence of depleting finite resources, food shortages, and climate change, the concept of a circular economy and the importance of obtaining maximum value from organic resources have been highlighted (Walsh *et al.*, 2017). *A. bisporus* offers a renewable source for Cs which is more sustainable than that of crustacean sources and can potentially contribute to the creation of a circular economy for the mushroom industry (Kaur *et al.*, 2014). More specifically, estimations of by-products produced globally from industrial mushroom cultivation per annum have been reported to be in excess of 50,000 tonnes (Wu *et al.*, 2004) and as such may offer an opportunity to acquire high purity products such as fungal-derived Cs (fCs) and SeAAs. Within this sustainability view-point, fCs, due to the controlled environments in which the mushrooms are cultivated may produce Cs with greater reproducible properties than those derived from crustaceans (Muzzarelli *et al.*, 2012). Whereas Se-fortified *A. bisporus* have demonstrated the ability to assimilate inorganic Se (such as sodium selenite) from the growth substrate and convert it to organic Se, such as SeAAs (Maseko *et al.*, 2013).

This project aims to develop a robust formulation for SeAA loaded fCs NPs intended for oral delivery, using a systematic approach to design and extensive *in vitro* analysis. Additionally, the extraction and characterisation of SeAAs from Se supplemented *A. bisporus* will be conducted with the objective of demonstrating the feasibility of obtaining these compounds for supplement production.

1.2 Delivery of bioactive peptides

Bioactive peptides and proteins have garnered much interest in the nutraceutical and pharmaceutical industry over the last decade. This interest has been attributed to

several factors such as: selectivity (Arkin, 2005; Soudy *et al.*, 2016), effective and potent actions (Frokjaer and Otzen, 2005; Elzoghby, Samy and Elgindy, 2012) and reduced side effects (Morishita and Peppas, 2006). Ophthalmic, dermatological and oral are delivery routes that have been investigated for peptides and proteins over the last few years (Van Der Walle, 2011), the latter typically identified as the most convenient and desired mode of delivery, due to its ease of administration and reported patient compliance, particularly when repeat administration is required (Mahato *et al.*, 2003).

The oral delivery of peptides and proteins has proven challenging to date, due to their susceptibility to enzymatic degradation (Woodley, 1993) and poor intestinal absorption across epithelial cells found in the GIT (Hamman, Enslin and Kotzé, 2005). Several approaches to overcoming these limitations have been investigated, for example: enteric coatings (Toorisaka *et al.*, 2005), permeation enhancers (Karavasili *et al.*, 2015), protease inhibitors (Chuang *et al.*, 2015) and the employment of carrier systems (Jain *et al.*, 2013). Amongst these, the latter has shown particular promise in the form of NP delivery systems, particularly with regards to polymers that possess mucoadhesive properties and have the ability to protect molecules from the harsh conditions that are found in the GIT (Ensign, Cone and Hanes, 2012). Furthermore, NPs have been shown to possess the ability to be absorbed into mucosal tissue, although this has also been shown to be related to the size and surface charge, manifest as zeta potential (ZP), of the NP. In terms of oral delivery, optimum sizes for NPs have been reported as 100 – 500 nm, with ZP of approximately +30 mV being reported as a good indication of NP dispersibility (He *et al.*, 2010). Additionally, the polydispersity index (PDI) of a NP suspension should be as close to zero as possible, a value of 0.5 generally accepted as the upper limit for PDI (Gaumet *et al.*, 2008).

1.3 Selenium

Selenium is a chemical element with the symbol Se and atomic number 34. Many health benefits of Se, such as cancer prevention (Abdulah *et al.*, 2005; Nie *et al.*, 2016) increased immunological status (Narayan *et al.*, 2015) and increased fertility (Aréchiga *et al.*, 1998; Shanmugam *et al.*, 2015) have been identified in recent years. However, as a result of diverse geological conditions, the Se status of humans, plants and animals can differ significantly. Most rock types contain very low concentrations of Se, although high concentrations are associated with some phosphatic rocks, organic rich black shales, coals and sulphide mineralisation, which has led to more Se deficient soils than there are seleniferous ones, worldwide (Khanal and Knight, 2010). Soils containing > 0.5 mg Se kg^{-1} are considered to be seleniferous and the forages produced on such soils absorb Se to levels in excess of what is permissible for animal consumption (Fordyce, 2013). In seleniferous parts of the world, such as parts of Ireland, Canada, western USA and some zones in China, adverse effects on Se toxicity in livestock have been reported (Navarro-Alarcon and López-Martınez, 2000).

The physical and chemical form of an element is referred to as speciation, meaning its oxidation state, stoichiometry or possible presence of various ligands (Reeder, Schoonen and Lanzirotti, 2006). Selenium is typically present as Se^{2-}, Se^{2+}, Se^{4+}, or Se^{6+}, associated with organic and inorganic species. The oxyanions selenite (SeO_3^{2-} or Se(IV)) and selenate (SeO_4^{2-} or Se(VI)) are some of the best-known inorganic species of Se, while selenomethionine (SeMet), selenocystine ($SeCys_2$) and methylselenocysteine (MSC) are some of the best-known organic Se species (Uden *et al.*, 2004). In amino acids, when an atom of Se replaces the atom of sulphur (S), such as methionine and cysteine, Se analogues are produced and referred to as selenoamino

acids (SeAAs). As the bioactivity of Se is highly dependent on its chemical form (Rayman, 2000), it is an important consideration when proposing a health supplement. Organic forms of Se, such as SeMet, $SeCys_2$ and MSC, have been found to be more bioavailable than inorganic forms (Zeng *et al.*, 2011) and several human health studies have shown their antioxidant and anticancer activity (Abdulah *et al.*, 2005; Thiry *et al.*, 2012). Health benefits of MSC and $SeCys_2$ have been linked to the body's endogenous antioxidant defence system, protecting cellular components such as cell membranes, lipids, lipoproteins and DNA from oxidative damage by free radicals, reactive oxygen and reactive nitrogen species (Ponnampalam *et al.*, 2009). As oxidative damage is linked to the development of cardiovascular and neurodegenerative diseases as well as cancers, several experimental *in vivo* studies, on the effects of administration of Se compounds, have been undertaken (Valko *et al.*, 2007; Lobo *et al.*, 2010; de Souza *et al.*, 2014). For example, SeMet may have some potential in degenerative disease by decreasing oxidative stress of small molecule antioxidants used as a buffer for free radicals in brain tissue (Song *et al.*, 2014; Reddy *et al.*, 2017), $SeCys_2$ has been shown to reduce tobacco-derived nitrosamine-induced lung tumour growth and enhance hepatic chemoprotective enzyme activities in mice (Fan *et al.*, 2013), whereas MSC has been shown to offer selective protection against organ specific toxicity induced by clinically active antitumor agents, cisplatin, oxaliplatin, and irinotecan in rat models (Cao *et al.*, 2014). A number of benefits regarding oncology treatments due the modulation of the therapeutic efficacy and selectivity of anticancer drugs has been reported for these SeAAs also (Evans, Khairuddin and Jameson, 2017).

Although essential, Se possesses a low therapeutic index, meaning that there is a fine line between beneficial and toxic doses. Generally, organic Se shows a greater degree

of bioavailability than the inorganic forms, as well as a higher threshold for toxicity (Amoako, Uden and Tyson, 2009). For humans and animals, increased aging, increased risk of cardiovascular disease and an increased risk of other degenerative diseases are among the consequences of Se intake below the daily recommended amount of 42 µg per day (Levander, 1991). On the other hand, hair loss, nail brittleness, gastrointestinal disturbances, garlic breath, skin rash, irritability, fatigue and nervous system abnormalities are all side effects of a Se intake above the tolerable upper intake level of 400 µg per day (www.nap.edu). Despite the associated health benefits, Se intake in Ireland is remarkably low, whereby, nearly 50% of females and 20% of males aged between 18 – 64 years fail to meet the average recommended requirement (ARR) of 40 µg per day (Murphy and Cashman, 2002). This low Se intake in the Irish population has been attributed to the drop in imports of high-protein wheat for bread-making flour from North America and Canada (Barclay and Macpherson, 1992), which are Se-rich in comparison to Irish flour varieties (Murphy and Cashman, 2001). Suffice to say, the narrow safety margin and form of Se must be carefully considered when designing an optimal Se supplement to ensure high bioactivity and low toxicity impact (Whanger, 2002)

SeAAs possess lower bond energies for C-Se and Se-Se than those of C-S and S-S (C-S 272 kJ mol^{-1} , S-S 240 kJ mol^{-1} , C-Se 244 kJ mol^{-1} , Se-Se 172 kJ mol^{-1}) respectively (Kildahl, 1995). As such, delivery of these compounds can be challenging, due to their distinctive electronegativity and atomic radius (i.e. larger radius and less E^- than S), which makes oxidation easier vs their S analogue counterparts (Xu, Cao and Zhang, 2013). By using NPs as a drug delivery vehicle, it is possible to provide or enhance a wide range of optimal characteristics for a given BA compound, including: increased stability (Nair *et al.*, 2010), reduction in

dose/toxicity of free drug to non-target organs in the body whilst maintaining therapeutic effects (De Jong and Borm, 2008), incorporation of both hydrophobic and hydrophilic substances (Ron *et al.*, 2010) and suitability for the various routes of administration such as oral, pulmonary and topical applications (Helson, 2013).

With this in mind, an opportunity arises to improve human and animal health by the provision of SeAAs through use of nanoparticulate delivery systems, as this strategy can potentially improve the bioavailability, decrease toxicity and confer protection from oxidative environments such found in the GIT.

1.4 Chitosan

Cs is a well-known, positively charged polyelectrolyte that has been extensively investigated for NP delivery systems (Kwon, 2008; Kleine-Brueggeney *et al.*, 2015). This interest has been attributed to its high bio-compatibility, bio-degradability and muco-adhesive properties (Pillai, Paul and Sharma, 2009). Furthermore, it has been reported that Cs has the ability to transiently open the tight junctions found between epithelial cells (Dodane, Khan and Merwin, 1999; Smith, Wood and Dornish, 2004) which can in turn increase absorption of a given bioactive.

Invertebrates (Crustacean shells and insect cuticles) and fungi are considered the predominant sources of Cs, the latter origin garnering much interest over the last decade (Muzzarelli *et al.*, 2012). This is due to the fact that mushroom bodies are produced within a highly controlled production environment, which typically results in Cs with highly reproducible physicochemical properties being manufactured on a batch to batch basis (Plapied *et al.*, 2010). Additionally, 50,000 tonnes of mushroom waste are produced annually (Wu *et al.*, 2004) by the commercial industry and it is

considered a potential way of utilising by-products produced from the cultivation process. In contrast, animal derived Cs suffers from seasonal shortages, heavy metal contamination and inconsistent physicochemical characteristics (also attributed to seasonal circumstances) on a batch to batch basis (Brine and Austin, 1981; Plapied *et al.*, 2010). In Ireland, the mushroom industry is the largest horticultural sector, employing over 3,500 people, with a farm gate value of €136 million, of which approximately 80% is exported to the UK (www.teagasc.ie). *A. bisporus* is the most commonly consumed cultivated mushroom in Ireland, consisting of the three main stages of maturity (Figure 1.1) (www.bordbia.ie). The Irish Food Board, Bord Bia, have indicated that the UK market for mushrooms is growing steadily in recent years at about 2% per year, with Button/Closed cup mushrooms holding the largest share of the market, followed by Flat/Breakfast mushrooms. However, during white mushroom (*A. bisporus)* cultivation, high quantities of by-products are generated, as between 5 and 20% of fruiting bodies are discarded due to misshaped cups and stalks that do not meet the specifications set by retailers (Wu *et al.*, 2004). For example, in the USA alone, mushroom production results in nearly 50,000 metric tons of mushroom waste material per year, with no suitable commercial application (Philibert, Lee and Fabien, 2017).

Figure 1.1 The different types of *A. bisporus* (pictures acquired from www.monaghan-mushrooms.com).

Production of Cs, predominately by acid and alkaline hydrolysis, is relatively straight-forward, and is typically sourced from shellfish or mushroom waste. Depending on the source and treatment method employed for Cs manufacture, the physicochemical properties, such as the degree of deacetylation (DDA%) (which is defined in terms of the percentage of primary amino groups present in the polymer backbone) and molecular weight (MW) can range from 60-100% and 10-1000 kDa, respectively, and are important characteristics to consider when deciding on the application (Ravi Kumar, 2000). For example, DDA% and MW of the Cs have been shown to directly influence the size, zeta potential and colloidal stability of NPs in biological media (Kleine-Brueggeney *et al.*, 2015). Generally, if the Cs is intended for use as a drug delivery vehicle, a medium molecular weight (110-225kDa) with high DDA% (≥80%) is considered ideal (Bowman and Leong, 2006).

PROTASAN™ CL113, a commercial Cs, derived from crustacean shells and provided as a hydrochloride salt, has been previously promoted for its ability to encapsulate and deliver food derived BAs such as Retinyl Palmitate (a vitamin A isomer) and possesses the following physicochemical properties: MW of 110-150 kDa, DDA% ≥80 % and minimal metal contamination (Fernández-Gutiérrez *et al.*, 2015). It has also been used to slow and control the drug release profile of Triclosan (an efficient anti-malarial drug) (Maestrelli, Mura and Alonso, 2004) and salmon calcitonin (a potential osteoarthritic drug) (Ryan *et al.*, 2013) owing to both its known mucoadhesive and enhancer properties and its demonstrated effectiveness in optimally controlling drug release rate. To date, much of the research involving the employment of Cs as a nanocarrier, has been of animal origin (crustaceans) (Hamed, Özogul and Regenstein, 2016). However, high batch to batch variability of Cs from these sources have been reported, resulting in formulations with variable

physicochemical properties and with potential for inducing allergic responses (Smets and Rüdelsheim, 2018). Hence, an alternative source of Cs, for example edible *A. bisporus* mushrooms, could be well placed for pharmaceutical applications, particularly if available with batch to batch reproducibility and high control over its molecular characteristics, such as molecular weight and DDA%.

1.5 Ionotropic Gelation

A promising tool in the development of bio-compatible NP drug delivery systems is ionotropic gelation (IG). IG is a process whereby polyelectrolytes (of opposite charges) form inter- and intra- molecular cross-linkages mediated by the anionic molecules, in the presence of BAs, to form a hydrogel mesh structure with the bioactive encapsulated within (Calvo *et al.*, 1997; Janes, Calvo and Alonso, 2001). It has also gained popularity due to the eco-friendly nature of the process, whereby only mildly acidic and basic solutions are required, in contrast to the expensive and toxic organic solvents which have been previously employed in delivery systems (Sailaja, Amareshwar and Chakravarty, 2011). The primary amino groups ($-NH_2$) of Cs are predominantly protonated at acidic pH ($-NH_3^+$), and it is this characteristic of Cs that provides it with the ability to form stable complexes when crosslinked with anionic polyelectrolytes, such as tripolyphosphate (TPP) (Janes, Calvo and Alonso, 2001). IG is considered a suitable technique for the development of NP vehicles for the delivery of sensitive drugs, as, once encapsulated within the hydrogel mesh work, their structural integrity has been shown to persist during release (Hennink and Van Nostrum, 2012). With regards to the optimum size of NPs, 100-300 nm in diameter has been found to be enough for a high payload, while smaller than 100 nm may pass through the GIT (Mohanraj and Chen, 2007).

1.6 Trimethyl chitosan as a permeation enhancer

Trimethyl chitosan (TMC), a derivative of Cs in which the primary amine has been quarternised with methyl groups, has shown promising results as a permeation enhancer (PE), due to its intrinsic properties, including mucoadhesion and the ability to transiently open the tight junctions of the intestinal barrier, which can help facilitate both transcellular and paracellular transport of macromolecules (Chen *et al.*, 2013). The transcellular route is both active and passive and is based on the activity of transmembrane pumps, channels, and carriers expressed in a polarised fashion. On the other hand, paracellular transport is only passive and driven by the gradients secondary to transcellular transport mechanisms (Figure 1.2) (Gleeson, Ryan and Brayden, 2016). The major barrier in the paracellular route is the tight junction, which is regulated and varies among epithelia in tightness and ion selectivity (Ghishan and Kiela, 2014).

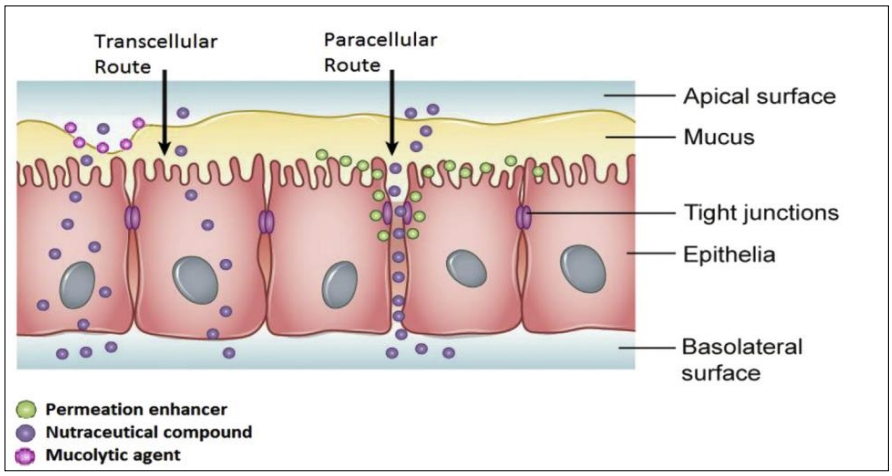

Figure 1.2 A schematic representation of Paracellular and Transcellular transport adapted from (Gleeson, Ryan and Brayden, 2016).

This mucoadhesive feature of TMC may aid in its utility as a potential permeation enhancer for assisting the delivery of drugs to mucosal tissues, such as the GIT, by prolonging residence time through its ability to hold a positive charge at neutral pH.

1.7 Design of Experiments

In the food industry, Design of Experiments (DoE) has become standard practice for research and development (R&D) of improved manufacturing processes (Carneiro and Azevedo, 2017). Employing such methodologies, it is possible to assess and select the most appropriate materials and equipment from available alternatives and subsequently identify variables for further study that can ensure a desired response outcome. Additionally, if more than two variables are under study, their interaction effects (if applicable) can also be evaluated.

Typically, in the early stages of industrial R&D, the main focus is on screening designs, whereby extreme upper and lower bound level setting combinations of process variables are employed, to identify their potential effect on a given response (Politis *et al.*, 2017). In the later stages of this work, the goal shifts from screening of variables, to product and process optimisation, through use of statistical experiment designs commonly termed "response surface methodologies (RSM)."

In addition to trialling experiments with one or more variables at extreme levels, the benefits of RSM, are that midpoints of the study range are also included, allowing for information to be harnessed on direct, interactive and curvilinear variable effects. There are many variations of RSM. In this work, the main focus will be on two commonly employed designs the central composite design (CCD) and Box Behnken design (BBD) (discussed at length in Chapter 3, Section 3.1)) that were used to optimise unloaded and Se loaded Cs:TPP NPs.

1.8 Project Aims and Objectives

The aim of this research is to produce oral formulations of nutraceutical SeAAs using ingredients from the food industry.

To achieve this aim, the following objectives have been set:

1. To assess the method of ionic gelation between the Cs and TPP, for production of NPs with physicochemical properties suitable for oral delivery using CCD optimisation.
2. To employ the SeAA, SeMet as a prototype encapsulant and identify the main variables which affect EE%, particle size, PDI and ZP by use of BBD optimisation and coating with the prolamine rich protein zein
3. To test the strength of the developed DoE models by encapsulating SeAAs with comparable ionisable groups ($SeCys_2$ and MSC) with evaluation of oral compatibility in terms of stability, cytotoxicity and release profiles *in vitro*
4. To extract chitin from the edible basidiomycete mushroom *A. bisporus* and derive to fCs with equivalent properties (DDA%, MW and purity) to that of an ultrapure Cs (CL113) product, for potential use in future NP formulations
5. To chemically derive fCs to TMC and assess if it may offer potential use as a permeation enhancer
6. To validate the strength of the developed DoE models by encapsulating synthetic $SeCys_2$ with the fCs produced in this work
7. To extract and characterise SeAAs in Irish mushrooms with the objective to demonstrate the possible availability of the species for supplement production in the Irish context.

1.9 Thesis outline

Chapter 1 has introduced Se and its associated health benefits, alongside limitations that can occur when designing a Se supplement. The prospects of employing Cs based NPs for use in oral delivery of Se was introduced and the importance of NP physicochemical properties (size, PDI and ZP) for oral delivery purposes was highlighted. The fundamentals of ionotropic gelation were elucidated and its employment for the development of a SeAA loaded Cs NP delivery systems was recommended. TMC, a derivative of Cs that has shown promising results as a permeation enhancer, was also discussed. Finally RSM, a mathematical and statistical technique for empirical model building, was discussed.

Chapter 2 is a review chapter that was published in *Nutrition - Nutrient delivery. In: Nanotechnology in the Food Industry* (Vozza *et al.*, 2016) and gives the reader a broader outlook on nutrient delivery through nanoparticulate systems. Briefly, it discusses functional food and BAs in relation to nanotechnology in the food industry, basic concepts of NPs for nutrient and food grade delivery systems, in addition to common obstacles encountered. Attention is paid to nano systems based on encapsulation technology using polymeric NPs, and studies detailing the delivery of food derived nutraceuticals are presented. Key issues such as enhanced level of nutrient absorption consequences and nanotoxicology are also considered. Lastly, the need for labelling, regulation and recommendations for consumer acceptance of these products is highlighted.

Chapter 3 introduces the key research methodologies employed in Chapters 4-8 and comprises five segments. Section 3.1 details NP experimental design using RSM techniques, specifically CCD and BBD. Section 3.2 describes the physicochemical

techniques employed to assess the produced NP properties (size, PDI and ZP), morphologies and EE%, *via* DLS, SEM and high performance liquid chromatography coupled with a diode array detector (HPLC-DAD). Section 3.3 details the *in vitro* techniques used to evaluate the produced NPs likelihood of oral compatibility in terms of stability, cytotoxicity and release profile. Section 3.4 describes the analytical techniques used to assess the physicochemical properties of chitin and Cs, such as DDA% and MW, with FTIR, NMR (^{1}H and ^{13}C) and Gel permeation chromatography (GPC), in addition to transepithelial electrical resistance (TEER, Ω cm^2) for assessment of TMC as an intestinal permeation enhancer. Lastly, Section 3.5 describes the extraction methods for qualitative and quantitative Se speciation analysis through use of HPLC-DAD.

Chapter 4 details the production of unloaded Cs:TPP NPs *via* ionotropic gelation. A CCD statistical design was employed to generate a mathematical model that identified the optimum mass ratio of Cs:TPP for NPs, with properties reported to be beneficial for oral drug delivery. The results of the CCD identified a feasible region in which NP target properties could be achieved as determined by DLS. Evidence for the formation of NPs was acquired *via* FTIR analysis, through identification of key functional groups on Cs and TPP and identifying their shifts in the crosslinked matrices. The morphology of the NPs was then assessed by SEM analysis.

Chapter 5 presents a manuscript submitted to the *International Journal of Pharmaceutics* (April 2018), detailing the study of SeMet, as a prototype encapsulant for Cs:TPP NPs (Vozza *et al*., 2018a). A BBD statistical design was employed to optimise the main variables that affected NP EE%, particle size, PDI and ZP. Two further studies were then conducted to increase the EE% of SeMet within the NP

matrix, 1) ionisation/protonation of NP formulation components and 2) The use of zein, as a co-formulation component for coating the NPs. Physicochemical properties of the NPs produced from the study were characterised *via* DLS, FTIR and SEM analysis. MTS (3-(4,5-dimethylthiazol-2-yl)-5-(3-carboxymethoxyphenyl)-2-(4-sulfophenyl)-2H-tetrazolium) studies were employed to test for potential cytotoxicity in the human intestinal epithelium (Caco-2), and human liver hepatocellular (HepG2), cell lines. Accelerated thermal stability of the loaded NPs was conducted to assess NP stability under normal storage conditions. Lastly, a compartmental, simulated gastric fluid and membrane analysis model enabled assessment the NP release profile *in vitro*.

Chapter 6 presents a manuscript submitted to the *Journal of Food Hydrocolloids* (May 2018), detailing the encapsulation of the SeAAs, $SeCys_2$ and MSC using the responses estimated from the derived quadratic polynomials identified previously with BBD (Vozza *et al*., 2018b). Further optimisation of the mass ratios of zein:Cs for NP coating was investigated. *In vitro* evaluation of the produced NPs was then conducted, using the previously developed methodologies, to assess the likelihood of oral compatibility in terms of stability, cytotoxicity and release profiles. Differences between the encapsulated SeAAs were then identified in terms of cytotoxicity profiles and release rates by the *in vitro* techniques.

Chapter 7 details a manuscript submitted to the *Journal of Carbohydrate Polymers* (May 2018), for the extraction of chitin and derivatisation to Cs from the edible basidiomycete mushroom *A. bisporus*, using alkaline treatments coupled with microwave irradiation (Vozza *et al*., 2018c). The Cs produced was compared to that of CL113, an ultrapure Cs product that has been assessed extensively for drug delivery applications and assessed for equivalent properties (DDA%, MW and purity), using

FTIR, $^{13}C/^{1}H$ NMR and GPC. A commercially available, fungal sourced Cs, from Sigma Aldrich was also compared to the Cs produced in this work, as an additional reference check point. Following production of Cs with a satisfactory match to CL113, a further chemical modification of the product to TMC was performed to assess whether fungal derived TMC may offer potential use as a permeation enhancer and as an alternative to crustacean derived.

Chapter 8 presents a manuscript to be submitted to the journal of *Innovative Food Science and Emerging Technologies* and considers the employment of fCs to formulate NPs loaded with synthetic $SeCys_2$, by employing the optimised formulation conditions previously identified by the DoE approach. *In vitro* evaluation of the produced NPs was then conducted, using the previously developed methodologies, to assess the likelihood of oral compatibility in terms of stability, cytotoxicity and release profiles. Differences between the CL113 and fCs NPs were then identified in terms of physicochemical properties and release rates by the *in vitro* techniques. Finally, a preliminary study to assess the feasibility of Irish mushrooms providing Se species for supplementation purposes was conducted. In that study, a Reverse phase, high performance liquid chromatography, Photodiode Array Detector (RP-HPLC-PDA) method was validated to analyse Se supplemented *A. bisporus*

Chapter 9 summarises the conclusions of the research findings and includes a detailed discussion on potential considerations and future perspectives.

1.10 References

Abdulah, R. *et al.* (2005) 'Chemical forms of selenium for cancer prevention', *Journal of Trace Elements in Medicine and Biology*, 19(2), pp. 141–150.

Amidon, S., Brown, J. E. and Dave, V. S. (2015) 'Colon-targeted oral drug delivery systems: design trends and approaches', *AAPS Pharmscitech*, 16(4), pp. 731–741.

Amoako, P. O., Uden, P. C. and Tyson, J. F. (2009) 'Speciation of selenium dietary supplements; formation of S-(methylseleno)cysteine and other selenium compounds', *Analytica Chimica Acta*, 652(1–2), pp. 315–323.

Aréchiga, C. F. *et al.* (1998) 'Effect of injection of β-carotene or vitamin E and selenium on fertility of lactating dairy cows', *Theriogenology*, 50(1), pp. 65–76.

Arkin, M. (2005) 'Protein–protein interactions and cancer: small molecules going in for the kill', *Current Opinion in Chemical Biology*, 9(3), pp. 317–324.

Benshitrit, R. C. *et al.* (2012) 'Development of oral food-grade delivery systems: Current knowledge and future challenges', *Food & Function*, 3(1), p. 10.

Bord Bia – Market for horticultural products bordbia.ie. Retrieved 25 March 2018, from:www.bordbia.ie/industry/buyers/industryinfo/hort/pages/marketforhorticulturalproducts.aspx (Accessed Jan 2018).

Bowman, K. and Leong, K. W. (2006) 'Chitosan nanoparticles for oral drug and gene delivery', *International Journal of Nanomedicine*, 1(2), p. 117.

Brine, C. J. and Austin, P. R. (1981) 'Chitin variability with species and method of preparation', *Comparative Biochemistry and Physiology Part B: Comparative Biochemistry*, 69(2), pp. 283–286.

Calvo, P. *et al.* (1997) 'Novel hydrophilic chitosan-polyethylene oxide nanoparticles as protein carriers', *Journal of Applied Polymer Science*, 63(1), pp. 125–132.

Cao, S. *et al.* (2014) 'Se-methylselenocysteine offers selective protection against toxicity and potentiates the antitumour activity of anticancer drugs in preclinical animal models', *British Journal of Cancer*, 110(7), p. 1733.

Carneiro, F. and Azevedo, A. (2017) 'A six sigma approach applied to the analysis of variability of an industrial process in the field of the food industry', in *Industrial Engineering and Engineering Management*, pp. 1672–1679.

Chen, M. C. *et al.* (2013) 'Recent advances in chitosan-based nanoparticles for oral delivery of macromolecules', *Advanced Drug Delivery Reviews*, pp. 865–879.

Chuang, E.-Y. *et al.* (2015) 'Self-assembling bubble carriers for oral protein delivery', *Biomaterials*, 64, pp. 115–124.

Cousin, M. A. *et al.* (2016) 'The Value of Systematic Reviews in Estimating the Cost and Barriers to Translation in Tissue Engineering', *Tissue Engineering. Part B, Reviews*, 22(6), pp. 430–437.

Dodane, V., Khan, M. A. and Merwin, J. R. (1999) 'Effect of chitosan on epithelial permeability and structure', *International Journal of Pharmaceutics*, 182(1), pp. 21–32.

El-Bayoumy, K., Sinha, R. and Richie Jr, J. P. (2015) '7 Forms of Selenium in Cancer Prevention', *Diversity of Selenium Functions in Health and Disease*, 38, p. 137.

Elzoghby, A. O., Samy, W. M. and Elgindy, N. a. (2012) 'Protein-based nanocarriers as promising drug and gene delivery systems', *Journal of Controlled Release*, 161(1), pp. 38–49.

Ensign, L. M., Cone, R. and Hanes, J. (2012) 'Oral drug delivery with polymeric nanoparticles: the gastrointestinal mucus barriers', *Advanced Drug Delivery Reviews*, 64(6), pp. 557–570.

Estanqueiro, M. *et al.* (2015) 'Nanotechnological carriers for cancer chemotherapy: the state of the art', *Colloids and Surfaces B: Biointerfaces*, 126, pp. 631–648.

Evans, S. O., Khairuddin, P. F. and Jameson, M. B. (2017) 'Optimising Selenium for Modulation of Cancer Treatments', *Anticancer Research*, 37(12), pp. 6497–6509.

Fan, C. *et al.* (2013) 'Selenocystine potentiates cancer cell apoptosis induced by 5-fluorouracil by triggering reactive oxygen species-mediated DNA damage and inactivation of the ERK pathway', *Free Radical Biology and Medicine*, 65, pp. 305–316.

Fernández-Gutiérrez, M. *et al.* (2015) 'Bioactive Chitosan Nanoparticles Loaded with Retinyl Palmitate: A Simple Route Using Ionotropic Gelation', *Macromolecular Chemistry and Physics*, 216(12), pp. 1321–1332.

Fordyce, F. M. (2013) 'Selenium deficiency and toxicity in the environment', *Essentials of Medical Geology: Revised Edition*, pp. 375–416.

Frokjaer, S. and Otzen, D. E. (2005) 'Protein drug stability: a formulation challenge', *Nature Reviews Drug Discovery*, 4(4), pp. 298–306.

Garapati, C. *et al.* (2015) 'Tailoring the Release of Drugs Using Excipients', in *Excipient Applications in Formulation Design and Drug Delivery*, pp. 201–236.

Gaumet, M. *et al.* (2008) 'Nanoparticles for drug delivery: the need for precision in reporting particle size parameters', *European Journal of Pharmaceutics and Biopharmaceutics*, 69(1), pp. 1–9.

Ghishan, F. K. and Kiela, P. R. (2014) 'Epithelial transport in inflammatory bowel diseases.', *Inflammatory Bowel Diseases*, 20(6), pp. 1099–109.

Gleeson, J. P., Ryan, S. M. and Brayden, D. J. (2016) 'Oral delivery strategies for nutraceuticals: Delivery vehicles and absorption enhancers', *Trends in Food Science & Technology*, 53, pp. 90–101.

Hagens, W. I. *et al.* (2007) 'What do we (need to) know about the kinetic properties of nanoparticles in the body?', *Regulatory Toxicology and Pharmacology : RTP*, 49(3), pp. 217–29.

Hamed, I., Özogul, F. and Regenstein, J. M. (2016) 'Industrial applications of crustacean by-products (chitin, chitosan, and chitooligosaccharides): A review', *Trends in Food Science & Technology*, 48, pp. 40–50.

Hamman, J. H., Enslin, G. M. and Kotzé, A. F. (2005) 'Oral delivery of peptide drugs', *BioDrugs*, 19(3), pp. 165–177.

He, C. *et al.* (2010) 'Effects of particle size and surface charge on cellular uptake and biodistribution of polymeric nanoparticles', *Biomaterials*, 31(13), pp. 3657–3666.

Helson, L. (2013) 'Curcumin (diferuloylmethane) delivery methods: A review.', *Biofactors*, 39(1), pp. 21–26.

Hennink, W. E. and Van Nostrum, C. (2012) 'Novel crosslinking methods to design hydrogels', *Advanced Drug Delivery Reviews*, 64, pp. 223–236.

Jain, A. *et al.* (2013) 'Peptide and protein delivery using new drug delivery systems', *Critical Reviews™ in Therapeutic Drug Carrier Systems*, 30(4).

Janes, K. A., Calvo, P. and Alonso, M. J. (2001) 'Polysaccharide colloidal particles as delivery systems for macromolecules', *Advanced Drug Delivery Reviews*, 47(1), pp. 83–97.

De Jong, W. H. and Borm, P. J. A. (2008) 'Drug delivery and nanoparticles: Applications and hazards', *International Journal of Nanomedicine*, 3(2), pp. 133–149.

Kamwesiga, J. *et al.* (2015) 'Effect of selenium supplementation on CD4+ T-cell recovery, viral suppression and morbidity of HIV-infected patients in Rwanda: a randomized controlled trial', *AIDS*, 29(9), p. 1045.

Karavasili, C. *et al.* (2015) 'Bioactive Self-Assembling Lipid-Like Peptides as Permeation Enhancers for Oral Drug Delivery', *Journal of Pharmaceutical Sciences*, 104(7), pp. 2304–2311.

Katouzian, I. and Jafari, S. M. (2016) 'Nano-encapsulation as a promising approach for targeted delivery and controlled release of vitamins', *Trends in Food Science & Technology*, 53, pp. 34–48.

Khanal, D. R. and Knight, A. P. (2010) 'Selenium: its role in livestock health and productivity', *Journal of Agriculture and Environment*, 11, pp. 101–106.

Khanam, A. and Platel, K. (2016) 'Bioaccessibility of selenium, selenomethionine and selenocysteine from foods and influence of heat processing on the same', *Food Chemistry*, 194, pp. 1293–1299.

Kildahl, N. K. (1995) 'Bond energy data summarized', *Journal of Chemical Education*, 72(5), p. 423.

Kleine-Brueggeney, H. *et al.* (2015) 'A rational approach towards the design of chitosan-based nanoparticles obtained by ionotropic gelation', *Colloids and Surfaces B: Biointerfaces*, 135, pp. 99–108.

Kaur, S. *et al.* (2014) 'Waste biomass: a prospective renewable resource for development of bio-based economy/processes', in *Biotransformation of Waste Biomass into High Value Biochemicals*, pp. 3–28.

Kwon, I. C. (2008) 'Chitosan-based nanoparticles for cancer therapy; tumor specificity and enhanced therapeutic efficacy in tumor-bearing mice', *Journal of Controlled Release*, 132(3), pp. e69–e70.

Levander, O. A. (1991) 'Scientific rationale for the 1989 recommended dietary allowance for selenium.', *Journal of the American Dietetic Association*, 91(12), pp. 1572–1576.

Lobo, V. *et al.* (2010) 'Free radicals, antioxidants and functional foods: Impact on human health', *Pharmacognosy Review*, 4(8), p. 118.

Luo, Y. *et al.* (2010) 'Preparation, characterization and evaluation of selenite-loaded chitosan/TPP nanoparticles with or without zein coating', *Carbohydrate Polymers*, 82(3), pp. 942–951.

Luo, Y. and Wang, Q. (2014) 'Zein-based micro- and nano-particles for drug and nutrient delivery: A review', *Journal of Applied Polymer Science*, 131(16), pp. 1–12.

Maestrelli, F., Mura, P. and Alonso, M. J. (2004) 'Formulation and characterization of triclosan sub-micron emulsions and nanocapsules', *Journal of Microencapsulation*, 21(8), pp. 857–864.

Mahato, R. I. *et al.* (2003) 'Emerging trends in oral delivery of peptide and protein drugs', *Critical Reviews™ in Therapeutic Drug Carrier Systems*, 20(2&3).

Maseko, T. *et al.* (2013) 'Chemical characterisation and speciation of organic selenium in cultivated selenium-enriched Agaricus bisporus.', *Food Chemistry*, 141(4), pp. 3681–3687.

Mohanraj, V. J. and Chen, Y. (2007) 'Nanoparticles - A review', *Tropical Journal of Pharmaceutical Research*, 5(1), pp. 561–573.

Morishita, M. and Peppas, N. A. (2006) 'Is the oral route possible for peptide and protein drug delivery?', *Drug Discovery Today*, 11(19), pp. 905–910.

Teagasc | Agriculture and Food Development Authority. (2018), from www.teagasc.ie/crops/horticulture/mushrooms/ (Accessed Jan 2018).

Muzzarelli, R. *et al.* (2012) 'Current views on fungal chitin/chitosan, human chitinases, food preservation, glucans, pectins and inulin: A tribute to Henri Braconnot, precursor of the carbohydrate polymers science, on the chitin bicentennial', *Carbohydrate Polymers*, 87(2), pp. 995–1012.

Nair, H. B. *et al.* (2010) 'Delivery of antiinflammatory nutraceuticals by nanoparticles for the prevention and treatment of cancer.', *Biochemical Pharmacology*, 80(12), pp. 1833–43.

Narayan, V. *et al.* (2015) 'Epigenetic regulation of inflammatory gene expression in macrophages by selenium', *The Journal of Nutritional Biochemistry*, 26(2), pp. 138–145.

Navarro-Alarcon, M. and López-Martınez, M. C. (2000) 'Essentiality of selenium in the human body: relationship with different diseases', *Science of the Total Environment*, 249(1), pp. 347–371.

Nie, T. *et al.* (2016) 'Facile synthesis of highly uniform selenium nanoparticles using glucose as the reductant and surface decorator to induce cancer cell apoptosis', *Journal of Materials Chemistry B*, 4(13), pp. 2351–2358.

Oberdörster, G. *et al.* (2005) 'Principles for characterizing the potential human health effects from exposure to nanomaterials: elements of a screening strategy.', *Particle and Fibre Toxicology*, 2, p. 8.

Paliwal, R. and Palakurthi, S. (2014) 'Zein in controlled drug delivery and tissue engineering.', *Journal of Controlled Release*, 189, pp. 108–22.

Park, J. H. *et al.* (2010) 'Targeted delivery of low molecular drugs using chitosan and its derivatives', *Advanced Drug Delivery Reviews*, 62(1), pp. 28–41.

Park, K. (2014) 'Controlled drug delivery systems: past forward and future back', *Journal of Controlled Release*, 190, pp. 3–8.

Philibert, T., Lee, B. H. and Fabien, N. (2017) 'Current status and new perspectives on chitin and chitosan as functional biopolymers', *Applied Biochemistry and Biotechnology*, 181(4), pp. 1314–1337.

Pillai, C. K. S., Paul, W. and Sharma, C. P. (2009) 'Chitin and chitosan polymers: Chemistry, solubility and fiber formation', *Progress in Polymer Science*, 34(7), pp. 641–678.

Plapied, L. *et al.* (2010) 'Bioadhesive nanoparticles of fungal chitosan for oral DNA delivery', *International Journal of Pharmaceutics*, 398(1), pp. 210–218.

Politis, S. N. *et al.* (2017) 'Design of experiments (DoE) in pharmaceutical development', *Drug Development and Industrial Pharmacy*, 43(6), pp. 889–901.

Ponnampalam, E. *et al.* (2009) 'Nutritional strategies to increase the selenium and iron content in pork and promote human health', *Co-operative Research Centre for an Internationally Competitive Pork Industry, Pork CRC, Australian Government*.

Ravi Kumar, M. N. . (2000) 'A review of chitin and chitosan applications', *Reactive and Functional Polymers*, 46(1), pp. 1–27.

Rayman, M. P. (2000) 'The importance of selenium to human health.', *Lancet*, 356(9225), pp. 233–241.

Reddy, V. S. *et al.* (2017) 'A systematic review and meta-analysis of the circulatory, erythrocellular and CSF selenium levels in Alzheimer's disease: A metal meta-analysis (AMMA study-I)', *Journal of Trace Elements in Medicine and Biology*, 42, pp. 68–75.

Reeder, R. J., Schoonen, M. A. A. and Lanzirotti, A. (2006) 'Metal speciation and its role in bioaccessibility and bioavailability', *Reviews in Mineralogy and Geochemistry*, 64(1), pp. 59–113.

Ron, N. *et al.* (2010) 'Beta-lactoglobulin–polysaccharide complexes as nanovehicles for hydrophobic nutraceuticals in non-fat foods and clear beverages', *International Dairy Journal*, 20(10), pp. 686–693.

Ryan, S. M. *et al.* (2013) 'An intra-articular salmon calcitonin-based nanocomplex reduces experimental inflammatory arthritis', *Journal of Controlled Release*, 167(2), pp. 120–129.

Sailaja, A., Amareshwar, P. and Chakravarty, P. (2011) 'Different techniques used for the preparation of nanoparticles using natural polymers and their application', *Int J Pharm Pharm Sci*, 3(suppl 2), pp. 45–50.

Shanmugam, M. *et al.* (2015) 'Dietary organic zinc and selenium supplementation improves semen quality and fertility in layer breeders', *The Indian Journal of Animal Sciences*, 85(2).

Smets, G. and Rüdelsheim, P. (2018) 'Biotechnologically produced chitosan for nanoscale products. A legal analysis', *New Biotechnology*, 42, pp. 42–47.

Smith, J., Wood, E. and Dornish, M. (2004) 'Effect of chitosan on epithelial cell tight junctions', *Pharmaceutical Research*, 21(1), pp. 43–49.

Song, G. *et al.* (2014) "Selenomethionine ameliorates cognitive decline, reduces tau hyperphosphorylation, and reverses synaptic deficit in the triple transgenic mouse model of alzheimer"s disease', *Journal of Alzheimer's Disease*, 41(1), pp. 85–99.

Soudy, R. *et al.* (2016) 'Engineered Peptides for Applications in Cancer Targeted Drug Delivery and Tumor Detection.', *Mini Reviews in Medicinal Chemistry*.

De Souza, V. R. *et al.* (2014) 'Determination of the bioactive compounds, antioxidant activity and chemical composition of Brazilian blackberry, red raspberry, strawberry, blueberry and sweet cherry fruits.', *Food Chemistry*, 156, pp. 362–8.

Thiry, C. *et al.* (2012) 'Current knowledge in species-related bioavailability of selenium in food', *Food Chemistry*, 130(4), pp. 767–784.

Toorisaka, E. *et al.* (2005) 'An enteric-coated dry emulsion formulation for oral insulin delivery', *Journal of Controlled Release*, 107(1), pp. 91–96.

Uden, P. C. *et al.* (2004) 'Selective detection and identification of Se containing compounds—review and recent developments', *Journal of Chromatography A*, 1050(1), pp. 85–93.

Valko, M. *et al.* (2007) 'Free radicals and antioxidants in normal physiological functions and human disease', *The International Journal of Biochemistry & Cell Biology*, 39(1), pp. 44–84.

Van Der Walle, C. (2011) '*Peptide and protein delivery*'. Academic Press.

Vanhonacker, F. and Verbeke, W. (2014) 'Public and consumer policies for higher welfare food products: Challenges and opportunities', *Journal of Agricultural and Environmental Ethics*, 27(1), pp. 153–171.

Vattem, D. A. and Maitin, V. (2016) '*Functional Foods, Nutraceuticals and Natural Products*'. DEStech Publications Lancaster.

Vozza, G. *et al.* (2016) *Nutrition - Nutrient delivery. In: Nanotechnology in the Food Industry, Volume 5*. U. K. E. Oxford.

Vozza, G. *et al.* (2018a) 'Application of box-behnken experimental design for the formulation and optimisation of selenomethionine-loaded chitosan nanoparticles coated with zein for oral delivery', *International Journal of Pharmaceutics*, (submitted for publication, April 2018).

Vozza, G. *et al.* (2018b) 'Formulation, characterisation, and in vitro evaluation of methylselenocysteine and selenocystine loaded chitosan nanoparticles-coated with zein', *Food Hydrocolloids*, (submitted for publication, May 2018).

Vozza, G. *et al.* (2018c) 'Potential of mushroom by-products for nutrient delivery applications: production and characterisation of chitin from agaricus bisporus and its derivatisation to chitosan and trimethyl chitosan', *Carbohydrate Polymers*, (submitted for publication, May 2018).

Walsh, E. *et al.* (2017) 'The Irish Bioeconomy -Definition, Structure, and Situational Analysis Mr Pádraic Ó hUiginn 3a 3b'. Available at: https://www.teagasc.ie/media/website/publications/2017/WP1-Deliverable (Accessed 10 Jan 2018)

Whanger, P. D. (2002) 'Selenocompounds in plants and animals and their biological significance', *Journal of the American College of Nutrition*, 21(3), pp. 223–232.

Woodley, J. F. (1993) 'Enzymatic barriers for GI peptide and protein delivery.', *Critical*

Reviews in Therapeutic Drug Carrier Systems, 11(2–3), pp. 61–95.

Wu, T. *et al.* (2004) 'Chitin and chitosan--value-added products from mushroom waste.', *Journal of Agricultural and Food Chemistry*, 52(26), pp. 7905–7910.

Xia, Y. *et al.* (2005) 'Effectiveness of selenium supplements in a low-selenium area of China', *The American Journal of Clinical Nutrition*, 81(4), pp. 829–834.

Xu, H., Cao, W. and Zhang, X. (2013) 'Selenium-containing polymers: promising biomaterials for controlled release and enzyme mimics', *Accounts of Chemical Research*, 46(7), pp. 1647–1658.

Zeng, H. *et al.* (2011) 'Chemical form of selenium affects its uptake, transport, and glutathione peroxidase activity in the human intestinal Caco-2 cell model', *Biological Trace Element Research*, 143(2), pp. 1209–1218.

2 NUTRITION – NUTRIENT DELIVERY

This chapter is a reproduction of:

Vozza, G., Khalid, M., Byrne, H. J., Ryan, S. and Frías, J. (2016). Nutrition - Nutrient delivery. In: *Nanotechnology in the Food Industry, Volume 5. Nutrient Delivery*, 1st ed. Oxford, United Kingdom: Elsevier, ISBN: 978-0-12-804304.

Vozza, G., was primary author, Khalid, M., contributed to Sections 2.1.1-2.1.5 and 2.1.10. Byrne, H. J., Ryan, S. and Frías, J contributed to layout, design and proofing.

2.1 Introduction

A new area in research and development has been instigated in the functional food industry by the emergence of nanotechnology. In particular, the enhanced delivery of nutrients to both humans and animals has garnered much attention from both academic and industrial bodies over the past decade (Neves *et al.*, 1999; Scrinis and Lyons, 2007; Srinivas *et al.*, 2010; Yao, McClements and Xiao, 2015) . With consumers now acknowledging the ability of certain foods to reduce disease risk or improve health (Hasler, 2000), in addition to the food industry's recognition that they may stand to gain a competitive edge over their competitors by satiating user specific dietary requirements and consumers' diverse demands for foods, it is not surprising that the nutraceutical industry has expanded within the past two decades (DeFelice 1995; Verbeke 2005; Lagos *et al.* 2015). It is estimated that the industry is currently worth $151 billion in annual worldwide sales, and is anticipated to grow to $207 billion by 2016 (BCC research, 2015).

The chief purpose of the diet is to deliver appropriate nutrients to an individual in order to meet their nutritional requirements. Foods and food constituents that provide health benefits beyond rudimentary nutrition are classified as nutraceuticals (Kalra 2003). Nutraceuticals have elements of both foods and medicinal products. If the substance contributes only to the maintenance of healthy tissues and organs, then it may be considered to be a food ingredient. On the other hand, if it can be shown to have a modifying effect on the body's natural physiological functions and is supported by favorable scientific opinion, it is considered a nutraceutical (Ec.europa.eu, 2015).

In the EU, a substance is characterised based on its exhibited effects on the body (JRC Science Hub, 2015). The European Commission (EC) defines nutraceuticals as "substances which are not traditionally recognised nutrients but which have positive physiological effects on the human body" (Coppens, Da Silva and Pettman, 2006). A plethora of scientific evidence has been accumulating, particularly over the last decade, proposing the ability of nutraceuticals to reduce the risk of numerous chronic diseases which has led to a boom in the food supplementation market (Brown and Arthur, 2001; Dickinson and MacKay, 2014; Luo, 2014). In response to this, the EC have published regulation (EC) No 1170/2009, which includes a list of vitamin and mineral ingredients approved in foods and food supplements (European Commission, 2009), in order to "harmonise the legislation and to ensure that these products are safe and appropriately labeled so that consumers can make informed choices" (European Parliament, 2006)

2.2 Functional foods and bioactives

Functional foods have been defined as foods that provide a health benefit beyond the basic nutritional requirements, by virtue of their physiologically active components (Hasler, 2000). For example, soy protein, associated with a reduction in cardiovascular disease, is referred to as a functional food because soy protein is not considered to be an essential nutrient (Song *et al.*, 2007; Kuan *et al.*, 2012).

Most commonly, there are two ways in which a functional food may be presented. One is where the nutraceutical is trapped within the food matrix, for example polyphenol antioxidants found in blackberry fruiting bodies (de Souza *et al.*, 2014), the other being processed foods in which the nutraceutical has been isolated prior to

manufacture and has subsequently been incorporated into the product during processing, for instance, nano-selenium-enriched Nanotea from Shenzhen Become Industry & Trade Co., Ltd (Blasco and Picó, 2011).

Nutraceuticals with prospective health benefits have been identified in several traditional foods such as fruits, vegetables, dairy, soya and whole grains (Brouns, 2002; Liu, 2007; Jelen, 2010; Thilakarathna and Rupasinghe, 2012; Mann, 2015). In addition to traditional foods, new foods have been developed in which isolated bioactives have been amalgamated with a specific food matrix in order to harness their potential health or physiological effects (Wang *et al.*, 2014; McClements, 2015).

The emergence of dietary compounds with health benefits offers an excellent opportunity to improve public health. Presently, a number of functional food components are being explored for their potential roles in disease prevention and/or beneficial health effects (Li-Chan, 2015). These include, but are not limited to vitamins, probiotics, bioactive peptides, anti-oxidants etc. (Ha and Zemel, 2003; Molina *et al.*, 2012; Roberts *et al.*, 2013; Blondeau, 2015).

Nutraceuticals have also emerged in areas such as food supplementation, with more than 50,000 dietary supplements available to date, as well as in the area of oncology research (Nair *et al.* 2010; Braithwaite *et al.* 2014). Table 2.1 details examples of current research regarding common nutraceuticals.

Table 2.1 Examples of some common nutraceuticals.

Nutraceutical	Origin	Physiological Function/Claim	Reference
Chitosan	Fungal mycelium	Reduction of low-density lipoprotein (LDL) cholesterol, triglycerides and increase high-density lipoprotein cholesterol	(Rizzo *et al.*, 2013)
Guggulsterone	Medicinal herbs	Hypoglycemic and hypolipidemic effect for treatment of type 2 diabetes	(Sharma *et al.*, 2009)
Pomegranate juice	Pomegranate	Dyslipidemia treatment	(Jadeja *et al.*, 2010)
Oleocantha	Olive oil	Anti-inflammatory effects	(Guasch-Ferré *et al.*, 2014)
Luteolin	Rosemary, celery, and parsley	Protective role of DNA against hydrogen peroxide-induced toxicity and anti-inflammatory actions	(Seelinger *et al.*, 2008; Moncada-Pazos *et al.*, 2011; Nordeen *et al.*, 2013)
Fucoxanthin	Marine algae	Antioxidant, anticancer and anti-obesity activities	(Fung, Hamid and Lu, 2013)
Omega-3 fatty acids	Nuts seeds, plant and marine oils	Decreased thrombus formation, lower LDL cholesterol; mood-stabilising properties, cardiovascular disease	(Simopoulos, 2002; Blondeau, 2015)
Methyl selenocysteine	Garlic	Prostate cancer, Cholesterol-lowering effects	(Arnault and Auger, 2006)

2.3 Nutraceutical formulation challenges

The effectiveness of nutraceutical products in preventing diseases depends on the preservation and effective provision of the targeted BA of the active ingredients (Ting *et al.*, 2014). Innovative therapies are currently the focus of scientific research and there is a growing interest in optimizing dosage forms and formulation methods to increase the BA of promising natural candidates (Ubbink and Krüger, 2006; Acosta, 2009; Harde, Das and Jain, 2011; Wang *et al.*, 2014).

There are, however, a number of challenges that can be encountered when supplementing a food with a nutraceutical (Augustin and Sanguansri, 2015). For instance, the solubility of the active component in the food product it is being introduced to must be considered. The physicochemical and physiological characteristics of the bioactive are also important:

- Does it have low water solubility that would hinder its uptake in target cells?
- Does it have a high melting point that would be able to withstand high temperature processing methods?
- What is its' chemical stability, does it need to be shielded from harsh pH environments?
- Does it exhibit high or low BA in the body? If not, how can the component/s efficacy as a disease preventing agent be increased?

These considerations must be borne in mind when designing a new product, as harsh conditions may lead to deleterious effects on the overall food properties, hindering food sensory properties and limiting the bio-accessibility and BA of the bioactive compounds (Handford *et al.*, 2014).

Supplements (Bonifácio *et al.*, 2014), food processing (Abbas *et al.*, 2009), agriculture (Chen and Yada, 2011) and food packaging (Duncan, 2011) have been identified as the four major applications of nanotechnology by food technology experts (Institute of Medicine (US) Food Forum, 2009). However, this type of segregation is quite arbitrary, due to the fact that the most interesting applications can be seen when one or more of these areas intersect. For example, interdisciplinary efforts are gaining increasing popularity as food engineers and drug delivery scientists collaborate in order to develop new nutrient delivery systems (Chen, Remondetto and Subirade, 2006; McClements and Li, 2010; Fathi, Mozafari and Mohebbi, 2012; Fathi, Martín and McClements, 2014). By adapting a pharmacological approach, various methods have previously been considered in the development of food-grade delivery systems, which offer the possibility to fabricate products that would protect, control and target the release of the bioactive ingredient to its desired location (Benshitrit *et al.*, 2012). Most approaches share one key methodology: entrapment, encapsulation and coating (Augustin and Hemar, 2009). This not only helps shield the nutraceuticals from their exposure environment but can also enable the release of the active component in a more controlled way (Shoji and Nakashima, 2004; Velikov and Pelan, 2008; McClements and Li, 2010).

Resultant nutraceutical particles occur in an extensive range of shapes and sizes (Figure 2.1). They can also be delivered in a wide array of formations, such as tablets, granules and micro/nanoparticles, the latter arising from the most recent development in drug delivery research areas (Lee, Yun and Park, 2015).

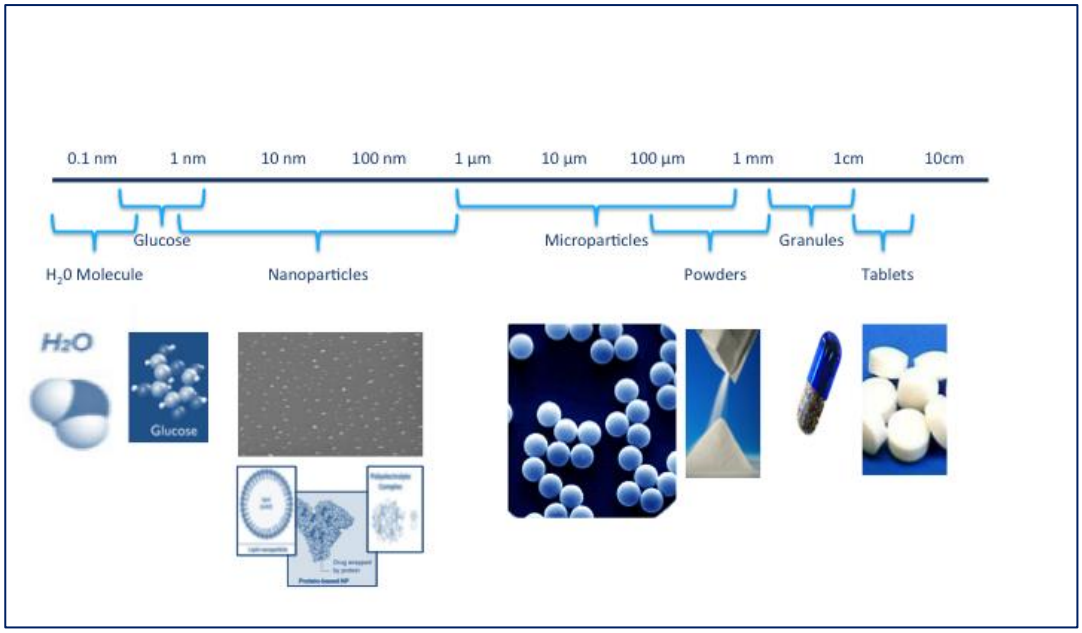

Figure 2.1 Scalar representation of various nutraceutical particles, ranging from nanoparticles to tablets.

Microparticles (MP) have been applied to deliver bioactives and/or drugs over long periods of time (months/weeks) in a variety of formulations, such as, depot administration via subcutaneous or intramuscular injection, pulmonary routes and oral delivery (Chen *et al.*, 2010; Nair *et al.*, 2010; Zhou *et al.*, 2015). MPs delivered intravenously have been shown to accumulate in the minute blood vessels of the lungs and have recently become an attractive approach in treating chronic obstructive pulmonary disease (Nair *et al.*, 2010). Complications can, however, arise when using MPs for drug delivery, as they have been shown to induce higher immune responses than submicron particles (Gutierro *et al.*, 2002).

Table 2.2 details a number of approaches that have been used to formulate nutraceuticals in order optimize their health benefits and/or to avoid harsh conditions during consumption and processing.

Table 2.2 Formulation aspects of current marketed nutraceutical products.

Brand Name	Formulation	Bioactive Compound	Indication	Company
Zacol NMX®	Tablets (controlled release matrix technology)	Calcium Salt of Butyric Acid and Inulin	Intestinal Disorders	Da Cosmo Pharmaceuticals
Berocin CZ	Softgel Capsule	Folic acid	Treatment and prevention of folate deficiencies and megaloblastic anemia.	Eros Pharma Ltd
Meconerv®	Injection	Mecobalamin	Peripheral neuropathies	Micro Labs Ltd
Pediasure®	Liquid supplement	Protein, vitamin and other natural supplementation	Pediatric growth	Abbott nutrition
Betafactor®	Capsules	Beta–glucan	Immune supplement	Ameriden® International Inc.,USA
Chaser®	Tablet	Activated calcium carbonate and vegetable carbon	Hangover supplement	Living Essentials, Walled Lake, MI, USA

2.4 Oral delivery

The fundamental applications of nutraceuticals entail the delivery of nutrients, bioseparation of proteins, rapid sampling of biological/chemical contaminants, and entrapment of nutraceuticals (Sozer and Kokini, 2009). Oral delivery is regarded as the gold standard for nutraceutical delivery due to high levels of patient acceptance, long term compliance and ease of administration (Sastry, Nyshadham and Fix, 2000). Moreover, it is preferable to maintain the natural process of food and nutrient consumption. However, in order for the nutraceutical (such as bioactive peptides, minerals and vitamins) to elicit the desired physiological effects via the oral route, a number of challenges for oral administration must be overcome (Chen, Remondetto and Subirade, 2006). These include insufficient gastric residence time, low permeability and/or solubility within the gut, instability under food processing conditions (temperature, oxygen, light) or in the gastrointestinal tract (GIT) (pH, enzymes, presence of other nutrients), all of which may limit the activity and potential health benefits of nutraceutical molecules (Agrawal *et al.*, 2014).

In order to overcome these challenges, it is necessary to construct an appropriate formulation that will protect and maintain the active ingredient in the relevant location for it to deliver its physiological/therapeutic effect within the required timeframe (McClements 2012). Table 2.3 lists common oral delivery systems for nutraceuticals.

Table 2.3 Common oral delivery systems for nutraceuticals.

Phospholipid based delivery systems	**References**
Amphipathic lipids that can orientate themselves into lipid bilayers, examples include Liposomes and Phytosomes. They have been shown to enhance potency and dose efficiency of both hydrophilic and lipophilic compounds.	(Coimbra *et al*. 2011; Chen *et al.* 2010; Mishra *et al.* 2012)
Emulsion based delivery systems	**References**
Mixture of two or more immiscible liquids stabilised by amphipathic compounds, examples include micro/nano-emulsions and solid lipid NPs. They have been shown to enhance potency and dose efficiency of lipophilic compounds	(Davidov-Pardo & McClements 2014; Wang *et al.* 2014; Josef *et al.* 2010;)
Chemical modification	**References**
Involves the association of non-bioactive pro-moieties (such as functional groups and polymers) with bioactive compounds that can subsequently be dissociated within the body by the action of enzymes or other chemicals. They have been shown to enhance potency and dose efficiency of the parent compound from the molecular level.	(Mulholland *et al.*, 2001; Liang *et al.*, 2013; Zhou *et al.*, 2014)
Chitosan-based delivery systems	**References**
Chitosan is a positively charged polyelectrolyte that is biocompatible, pH responsive and biodegradable. It has been formulated in both micro and nano-sized particles to deliver bioactives. They have been shown to possess muco-adhesive properties that facilitates tight junction widening thus increasing BA of target nutraceutical	(Jang and Lee, 2008; Kwon, 2008; Akhtar, Rizvi and Kar, 2012; Mukhopadhyay *et al.*, 2013)
Nanodispersions	**References**
Bioactives > 100 nm homogeneously distributed within a carrier free solution. Allow for higher dosing of bioactive with minimal processing. They have been shown to enhance potency and dose efficiency of bioactive compounds.	(Chu *et al.*, 2007; Anarjan *et al.*, 2010; Adjonu *et al.*, 2014)
Mesoporous silica particles	**References**
Bioactives > 10 nm distributed within the nanopores of a micro scale silica particle. Allow for the further use of pH or Redox potential sensitive gates to maximise dosing of bioactive in a specific area of the GIT.	(Pérez-Esteve *et al.*, 2015)

NPs have shown promise for oral drug delivery systems, as they posses the potential to provide a remedy to these obstacles whilst maintaining the aforementioned health benefits (Ensign, Cone and Hanes, 2012). For example, a protein or peptide drug can be encapsulated in a nanoparticle environment which can protect against enzymatic degradation, consequently improving the pharmacokinetics and stability of the molecule (Almeida and Souto, 2007; Patel, Cholkar and Mitra, 2014). By using NPs as a drug delivery vehicle, it is possible to provide or enhance a wide range of optimal characteristics for a given nutraceutical drug, including increased stability (Nair *et al.*, 2010), incorporation of both hydrophobic and hydrophilic substances (Ron *et al.*, 2010), high carrier capacity (Yao, McClements and Xiao, 2015) and suitability for the various routes of administration such as oral, pulmonary and topical applications (Helson, 2013).

NPs can also help deliver drugs with low solubility, also providing controlled release in order to sustain the drug. These characteristics enable optimum drug BA and reduction of frequency of drug administration (Huang, Yu and Ru, 2010). NPs made from biocompatible and biodegradable materials found in food, which are generally regarded as safe (GRAS), have the potential to be approved by regulatory bodies faster than alternative compounds (Hans and Lowman, 2002). From here on in, the discussion will focus on an area that has garnered much interest in nutrient delivery the past decade -the use of nanoparticles (NPs) for nutraceutical delivery.

2.5 Bioavailability enhancement with nanoparticles

The drivers for utilizing nanotechnology in foods include taste or flavour enhancement, improved delivery and solubility, protection against oxidation and

enzymatic degradation, prolonged residence time and efficient permeation through the GIT and improved BA at the target site (Chen, Remondetto and Subirade, 2006). Recently, a number of nutraceuticals, such as omega 3 and omega 6 fatty acids, probiotics, prebiotics, vitamins and minerals, have been investigated as bioactive compounds in nanoparticle formulations (Anal and Singh, 2007; Gökmen *et al.*, 2011; Rashidi and Khosravi-Darani, 2011; Luo, Teng and Wang, 2012).

Nanoparticles can be generated both intentionally (for therapeutics or other applications) or unintentionally (e.g. by combustion). In the field of food and medicine, several nanoparticle applications have already been approved for clinical use, and many others are at different stages of development (Wacker, 2014). Table 2.4 shows some examples of marketed nanoformulations of drugs, beverages, foods and health supplements developed from the Pharmaceutical and Food industry targeting the oral delivery route of administration. There are also a number of nanoformulations that are currently in pre-clinical development in order to assist targeting of oncology drugs, such as Folic acid-PAMAM dendrimers for Epithelial cancer (Thomas *et al.*, 2013), Albumin-bound nanoparticles and Glycol chitosan nanoparticles for cancer treatment (Miele *et al.*, 2009; Yoon *et al.*, 2014), Starch-coated iron oxide nanoparticles of magnetically guided Mitoxantrone for tumour angiogenesis (Wahajuddin and Arora, 2012) and Silica-based nanoparticles for photodynamic therapy (Couleaud *et al.*, 2010).

Table 2.4 Current nanomaterial's in the Food and Pharmaceutical industry (websites accessed 16/6/2015).

Current Marketed Drugs (Pharmaceutical)	**Function**	**Trade name**	**Company**	**References**
Liposomal amphotericin B	Fungal infections	Abelcet®	Sigm-Tau	www.sigmatau.com
PEG–L-asparaginase	Acute lymphoblastic leukemia	Oncaspar®	Enzon	www.oncaspar.com
Current Marketed Nanomaterials in Foods/Beverages	**Function**	**Trade name**	**Company**	**References**
Nano-sized self-assembled structured liquids (micelles)	Food	Canola Active Oil	Shemen	www.shemen.co.il (website only in Hebrew).
Nano Zinc Oxide (food grade)	Food additive	AdNano®	Evonik (Degussa)	www.advancednanomaterials.com
Current Marketed Nanomaterials in health supplements	**Function**	**Trade name**	**Company**	**References**
Nano silver	Health supplement	Colloidal Silver Liquid	Skybright Natural Health	hwww.skybright.co.nz
Nano humic and fulvic acid	Health supplement	Nano Humic and Fulvic Acid	Nano Health Solutions	www.fulvic.org

Studies have shown that the enhanced surface area per mass compared with larger-sized particles of the same chemistry renders nanosized particles more biologically active (Oberdörster *et al.*, 2005; Heitbrink, Lo and Dunn, 2015). The biological interactions of a nanoparticle system are highly dependent on the nanoparticles size and size distribution (Hagens *et al.*, 2007). Etheridge *et al.* (2013), state that the enhancement of a drugs BA at the systemic level results from the increased surface area provided by the submicron size of the nanoparticle formulation. For example, a given drug formulated within a smaller sized nanoparticle (approx. 100 nm) has an increased likelihood to be associated on or close to the surface of the particle allowing the drug to be released at a higher rate (Hans and Lowman, 2002). On the other hand, larger particles (>100nm) have a smaller initial burst release and longer sustained release than smaller particles as the load tends to be encapsulated in the core centre of the particle (Hans and Lowman, 2002). Generally, passive diffusion allows for the slow release of the drug into the systemic system, as a result of the drug releasing from the larger NP core (Mohanraj and Chen, 2007).

The higher mobility and cellular uptake of NPs compared to microparticles is another advantage provided by nano-scale formulations. For example, when comparing the uptake of 1 and 10 µm particles against 100 nm particles in *in vitro* models, an increase of 2.5-6 fold higher uptakes were observed respectively (Mohanraj and Chen, 2007). Etheridge *et al*. (2013) also commented that the effect of particle size on cellular intake can be influenced by the constituent material and the particle geometry. With this in mind, it is important to consider the particle size and morphology on a case by case basis that will allow for specific evaluation for formulation processes that use different encapsulating materials for delivery of nutraceuticals (De Jong and Borm, 2008) Encapsulating nutraceuticals within engineered nanoparticle based delivery systems

presents the potential to improve BA and the ability to tailor a given particle in order to withstand detrimental pH, processing and enzymatic environments (Yao, McClements and Xiao, 2015). Further advantages of using nanoparticles as drug carriers can be seen in Table 2.5.

Table 2.5 Advantages associated with Nano-carriers for drug delivery (Abbas, K. A. *et al.* (2009).

Advantages of nanoparticles as drug carriers
Controlled and sustained release profile of the drug to a given target site
Several routes of administration can be applied
High drug loading under mild conditions and in the absence of harsh chemicals
Ability to manipulate particle physicochemical properties such as size and morphology to achieve optimum passive/active drug targeting
Increased retention time of NPs at mucosal surfaces by exploiting mucoadhesive formulation components
Increase the chemical stability of a drug by shielding it from harsh pH environments such that are found in the GIT
Prevent aggregation of proteins/peptides when the pH of the surrounding environment approaches their isoelectric point

It is also important to keep in mind that the main advantage for formulation of NPs is targeted drug delivery, which can be achieved using two different routes, passive targeting and active targeting (Singh and Lillard, 2009). Passive targeting occurs when NPs exhibit localization to specific organs or to sites of disease via biological mechanisms, such as the reticuloendothelial system (RES) or the enhanced permeability and retention (EPR) effect (Maeda *et al.*, 2000). One example is PEGylatyed liposome-doxorubicin, Doxil®, which encapsulates an anti-tumor drug, doxorubicin (Kroon *et al.*, 2014). On the other hand, active targeting is the conjugation of antibodies, peptides, or other ligands onto the nanocarrier surface which will recognise and bind to target cells through ligand–receptor interactions by the expression of receptors or epitopes on the cell

surface (Nobs *et al.*, 2004). For example, monoclonal antibody-conjugated PLGA NPs formulated to actively target cancer cells, resulting in better cancer cell recognition of surface-modified NPs than non-coated NPs (Kocbek *et al.*, 2007).

The European commission recommends that a nanomaterial be defined as (Ec.europa.eu, 2011):

> *A natural, incidental or manufactured material containing particles, in an unbound state or as an aggregate or as an agglomerate and where, for 50 % or more of the particles in the number size distribution, one or more external dimensions is in the size range 1 nm - 100 nm.*
>
> *In specific cases and where warranted by concerns for the environment, health, safety or competitiveness the number size distribution threshold of 50 % may be replaced by a threshold between 1 and 50 %.*
>
> *By derogation from the above, fullerenes, graphene flakes and single wall carbon nanotubes with one or more external dimensions below 1 nm should be considered as nanomaterial's.*

With this in mind, it is worth noting that NPs in themselves are not easily categorised in terms of properties, as the physical size of a drug can greatly affect the drug's effect when compared to a smaller or larger particle of the same makeup (Oberdörster, Oberdörster and Oberdörster, 2005). As nanoparticles can be any number of particles within the scale of 1-100 nm, the term nanoparticle is in itself broad, thus leading to a difficulty of clear and defining chemical and physical properties (Ju-Nam and Lead, 2008).

In other words, variations in size and shape can have unpredictable effects on the physical and chemical properties of nanomaterials: a substance that is non-toxic at 50 nm may be

toxic at 1 nm or *vice versa* (Resnik and Tinkle, 2007). Because their properties are dependent on their microenvironment, nanomaterials may change in size or shape inside an organism. A 100 nm particle could disintegrate into 1 nm particles, or 1 nm particles could aggregate into a 100 nm particle (Resnik and Tinkle, 2007).

By limiting size in the definition of nanotechnology to the 1–100 nm range, numerous materials and devices are excluded, in particular with regards to the pharmaceutical and agricultural fields, in which nanomaterials of 100 nm to 300 nm are considered of most interest with regards to oral delivery due to the toxicity issues that arise from smaller sizes (Umerska *et al.*, 2012; Andreani *et al.*, 2014; Koppolu *et al.*, 2014; Sakai-Kato *et al.*, 2014). The driving force for the size restriction of the definition of nanoparticles is one of regulation, and therefore, in the following sections, a broader definition of nanoscale shall be considered.

2.6 Food Grade delivery systems

Nanoparticles in a size range of 100-300 nm have attracted a lot of attention as drug delivery nanocarriers and have shown remarkable therapeutic potential when formulated into different delivery systems, depending on the nature of the bioactive, release rate and compatibility with the carrier (Almeida and Souto, 2007; Sarvaiya and Agrawal, 2015). Most commonly used nanoparticle carrier systems are magnetic, dendritic, polymeric, solid-lipid liposomal, all of which exhibit different properties that are used in drug delivery. There are two ways in which nanoparticles can be made: by "bottom-up" and “top-down” approaches (Thiruvengadathan *et al.*, 2013; Diaz Fernandez *et al.*, 2014; McClements, 2015) represented in Figure 2.2.

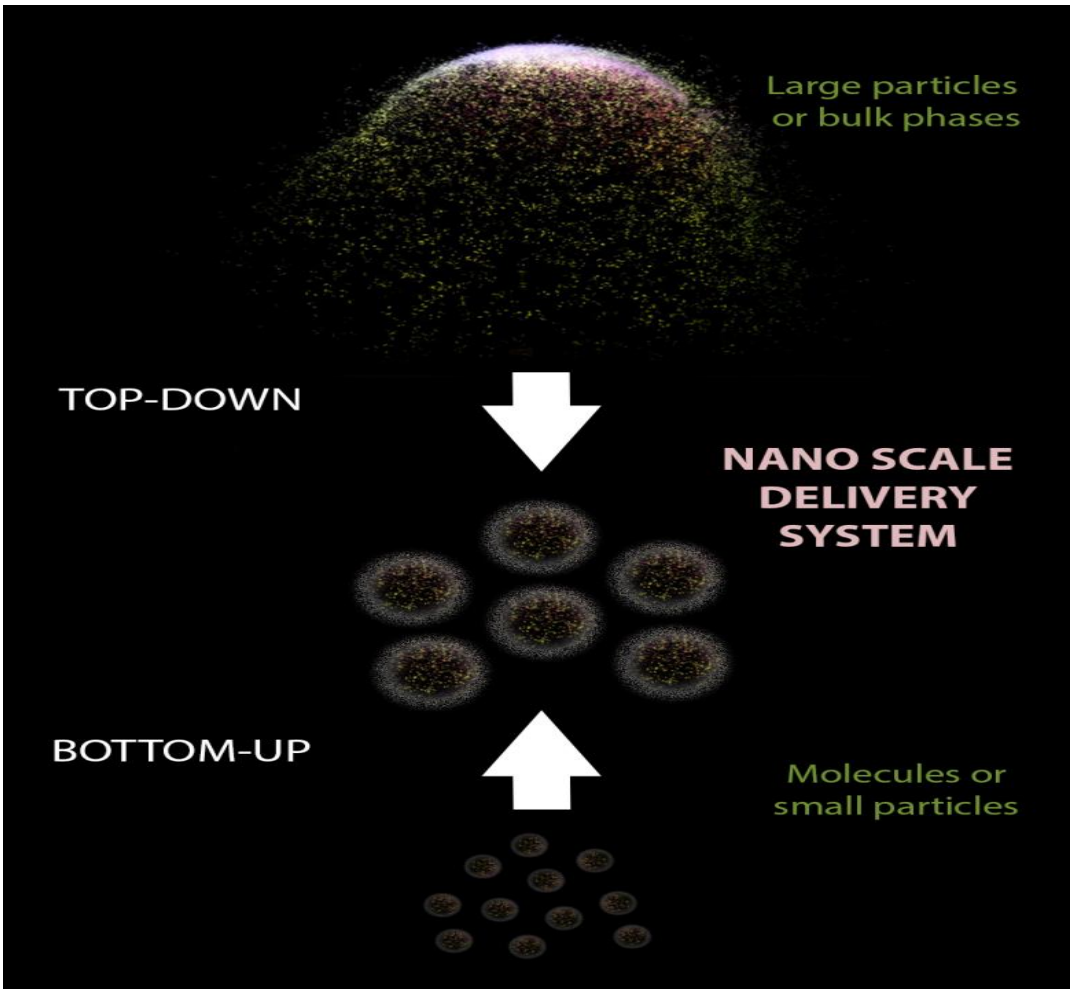

Figure 2.2 Schematic representation of top-down and bottom-up techniques used to produce nano-delivery systems.

In a “bottom-up” approach, materials and devices are built from molecular components which come together chemically by principles of molecular recognition (Chan and Kwok, 2011). On the other hand, the "top-down" approach entails the construction of nano-products from larger entities without atomic-level control (Acosta, 2009). Food grades, for example, are used to classify products according to certain quality characteristics. To establish an oral delivery system, all substances used which pass through the oral route should be classified as safe.

By instigating a pharmacological approach in order to develop food grade delivery systems, products can be potentially produced which possess the ability to protect a given

bioactive during processing and storage stages, whilst allowing for controlled delivery of the therapeutic at its target site (Lawton, 2002; Zhang *et al.*, 2015). It is generally accepted that food grade delivery systems can be classified in a wide variety of ways. However, most commonly, size and the main nutritional component are used when classifying systems (Benshitrit *et al.*, 2012).

With regards to size classification, this is considered an important means of assessment due to the behaviours of compounds on a scalar level. A given system's functionality can generally be linked to the availability of the bioactive to the body according to size (Kumari, Yadav and Yadav, 2010). By changing size of the encapsulating vehicle of a molecule, the rate of its release, its solubility and it retention at a given target site can be tuned (Mohanraj and Chen, 2007), enabling the optimisation of a formulation in order to achieve specified results. An alternative, common way of classifying these delivery systems is *via* their main nutritional component (Benshitrit *et al.*, 2012). Such food grade delivery systems can be divided into three groups: Protein-based delivery, Lipid-based delivery and Carbohydrate-based delivery (Benshitrit *et al.*, 2012). These systems provide a wide array of potential in addition to some limitations and shall be discussed in the following sections.

2.7 Protein-based nano-delivery systems

Food biopolymers, specifically food proteins, are commonly used to formulate bioactives because of their high nutritional value, biodegradability, non-antigenicity, excellent water binding capacity, cost efficient and GRAS nature (Benshitrit *et al.*, 2012; Elzoghby, Samy and Elgindy, 2012). It is also possible to exploit the delivery of bioactives over a wide range of platforms due to their physical and physicochemical diversity attributable to the

multiple functional groups present in the primary sequence of polypeptides (Chen, Remondetto and Subirade, 2006). With this in mind, it is possible to modulate protein carrier interactions with therapeutic agents and produce three dimensional networks allowing for a host of possibilities, for example, the reversible binding of active molecules to a given target site (Chen, Remondetto and Subirade, 2006). Additionally, studies have shown that the generation of bioactive peptides *via* enzymatic degradation *in vivo* can subsequently elicit a number of physiological effects, leading to an advantage regarding acceptability of protein carrier employment for drug delivery (Li-Chan, 2015).

Proteins can be sourced from bacterial, fungal, plant and animal origin, with the latter two utilised as a food grade delivery system not only because of their cost effectiveness but also because they enable excellent delivery of both hydrophilic and hydrophobic bioactives (Elzoghby, Samy and Elgindy, 2012). The preparation methods that can be employed in order to produce protein based carriers has also been cited as a major advantage of this particular delivery vehicle (Chen, Remondetto and Subirade, 2006). Techniques such as gelation, emulsification, extrusion, spray drying and coacervation are commonly used to produce delivery systems such as hydrogels, hydrocolloids, micelles, nano-assemblies, films and micro and nanoparticles (Ibrahim 2015; Zhang *et al*. 2014; Park *et al*. 2013,Yang *et al*., 2014). Common protein carriers investigated from animal sources are gelatine, collagen, casein, elastin, albumin and whey proteins, and from plant sources are soy glycinin, wheat gliadin and zein (Kimura *et al*. 2014; Song *et al*. 2009; Xiao *et al*. 2011; Nägele *et al*. 1991).

Nanoparticulate protein carriers from vegetal origin have garnered interest in the field due to their potential advantages over their animal derived counterparts (Ezpeleta *et al*., 1996; Lai and Guo, 2011; Elzoghby, Samy and Elgindy, 2012) It is hypothesised that, by

exploiting the low solubility and high hydrophobicity characteristics of these particular proteins, it is possible to negate the need for further chemical and/or physical treatments of the nanoparticles in order to harden them (Ezpeleta *et al.*, 1996). As an alternative to hydrophilic animal protein carriers such as albumin and casein, hydrophobic plant proteins such as gliadin and zein have been investigated for their ability to increase the amount of bioactive entrapped within a given carrier system in addition to their ability to improve the controlled release of target bioactives (Ezpeleta *et al.*, 1996; Xijun *et al.*, 2014; Zhang *et al.*, 2015). Moreover, they are less expensive to produce, and satisfactory supplies can be assured due to the nature of their growth and harvest processes. Plant proteins can also be regarded as a safer therapeutic delivery system due to the reduced risk of spread of disease associated with animal origin compounds, for example, bovine spongiform encephalitis (Elzoghby, Samy and Elgindy, 2012). An example of a plant derived protein carrier that has begun garnering much interest for nutrient delivery is Zein (Lawton, 2002; Paliwal and Palakurthi, 2014).

Zein is a class of alcohol soluble prolamine storage proteins found in corn (Esen, 1987). It is extracted from the endosperm of corn kernels, where it is predominantly present (Larkins *et al.*, 1984; Dombrinkkurtzman and Bietz, 1993), during corn wet milling processes. It exists as a mixture of proteins, of varying molecular weights and can be categorized by sequence homology and solubility into four main classes known as: α-zein (19 and 22 kDa), β-zein (14k Da), γ-zein (16 and 27 kDa) and δ-zein (10 kDa) (Esen, 1987). The most abundant of these, α-zein, accounts for 70-80% of the total mass fraction of zein, whilst, γ-zein, the second most abundant, accounts for 10-20% (Wilson, 1991). All groups of zein possess a fairly abundant amount of neutral and hydrophobic amino acids (AA) (e.g. proline) with a more moderate amount of polar AA residues such as serine (Zhang *et al.*, 2015). In addition, what differentiates zein from most other proteins

is that it contains negligible amounts of lysine and tryptophan, as well as low amounts of arginine and histidine residues (Zhang *et al.*, 2015). It is this inherent AA composition that lends to zein proteins unique solubility properties, whereby it is insoluble in pure water and alcohol but soluble in aqueous alcohol and alkaline solutions as well as acetic acid and acetone (Lawton, 2002).

As zein has been GRAS approved by the United States Food and Drug Administration as a pharmaceutical drug excipient since 1985 (Accessdata.fda.gov, 2014), it has been proposed as a nanodrug delivery vehicle (Paliwal and Palakurthi, 2014). It has been shown to possess the ability to improve the colloidal stability and encapsulation efficiency of bioactive components in addition to tailoring of their release profile (Zhang *et al.*, 2015). In studies conducted by Luo *et al.* 2010, zein was used to coat chitosan nanoparticles loaded with selenite and was shown to not only increase the encapsulation efficiency of the mineral from 60% to 96% but also protected the drug from the harsh conditions of the GI tract. This allowed for a slower sustained release of selenite at the intestinal target site, reducing the release of selenite from 85% in the first 4 hrs to 30% (Luo *et al.*, 2010). Zein has also been used to successfully deliver fat soluble compounds due to its high hydrophobicity (Zhong, Tian and Zivanovic, 2009).

2.8 Lipid-based nano-delivery systems

It is sometimes important to deliver lipophilic bioactives in a more edible form. For example, fatty acids such as conjugated linoleic acid and butyric acid have shown potential health benefits for Coronary Heart Disease (Haug, Hostmark and Harstad, 2007). In order to do so, lipid-based delivery systems have been shown to be a promising approach. These lipophilic components may be a diverse range of substances, including

bioactive lipids, vaccines, flavors, antimicrobials, antioxidants, and drugs (H du Plessis *et al.*, 2014).

It is advantageous for lipid bioactives to be encapsulated in a liquid form, which has shown to increase their palatability, desirability, and bioactivity due to the differing molecular, physicochemical and psychological properties (McClements, Decker and Weiss, 2007). Consequently, all of these differing properties of each lipid bioactive need to be addressed to produce the optimal formulation and effect. The most commonly used lipophilic nutraceuticals investigated recently are fatty acids (ω-3 fatty acids, conjugated linoleic acid, butyric acid), carotenoids (β-carotene, lycopene, lutein, zeaxanthin), antioxidants (tocopherols, flavonoids, polyphenols) and phytosterols (stigmasterol, β-sitosterol, campesterol) (Pol and Patravale, 2009; Puri *et al.*, 2009; Bassaganya-Riera and Hontecillas, 2010; Leong *et al.*, 2011; Song *et al.*, 2011).

The principle used to formulate a lipid based delivery system is emulsification, as oil in water (O/W) microemulsions, liposomes, multilayer emulsions, filled hydrogel particles, or solid lipid nanoparticles (Spernath and Aserin, 2006; Iglesias *et al.*, 2013; Han *et al.*, 2014). Phospholipid-based microemulsions (ME) use food-grade ingredients, soybean oil and soybean lecithin, to replace ethyl oleate and purified lecithin (Patel, Schmid and Lawrence, 2006). However, the formation of multiphase colloidal dispersions into nanoscale droplets enables the production of nanoemulsions (NE).

NE (also known as submicron emulsions) can be prepared by the physical shear induced by rupturing of one liquid within another immiscible liquid (Mukherjee, Ray and Thakur, 2009). NE have interesting properties compared to their micro sized counterparts in that they have the ability to remain stable in diluted water without a change to their relative size distribution (Gutiérrez *et al.*, 2008). Consequently, the droplet sizes in

nanoemulsions allow for optically transparent formulations due to their scalar size being smaller than visible wavelengths. Microparticles, on the other hand, usually show multiple scattering of visible light resulting in formulations with opaque appearances (McClements 2012). With this in mind, it is fair to conclude that NE may be more advantageous for nutrient delivery in commercial food products, for example, beverages, in that they will allow for no discernible change in photoreception sensory properties of the product (Fathi, Mozafari and Mohebbi, 2012).

An example of a lipid based nutraceutical carrier system that has begun garnering interest for nutrient delivery is Solid Lipid NPs (Almeida and Souto, 2007; Harde, Das and Jain, 2011; Fathi, Mozafari and Mohebbi, 2012). Solid Lipid NPs (SLNs) have the ability to solubilize lipophilic molecules and generally exist as spherical particles ranging from 10–1000 nm (Almeida and Souto, 2007). They contain a solid or semi-solid lipid core matrix and are typically stabilized by surfactants (Kalepu, Manthina and Padavala, 2013). When compared to other lipid based carries such as nanoemulsions and liposomes, SLNs have been shown to possess some distinct advantages over their alternative counterparts (Fathi, Mozafari and Mohebbi, 2012). For example, they have been shown to offer robust protection against GI tract degradation due to the reduction in crystalline mobility of the lipid structure, particularly beneficial for the delivery of bioactive peptides which are susceptible to enzymatic and or acidic degradation in the GI environment (Almeida and Souto, 2007; Ting *et al.*, 2014).

In addition, SLNs have the ability to provide controlled release profiles of a given bioactive due to the intrinsically slow degradation rate of the crystalline lipid core. These advantages have been shown to improve the pharmacokinetic profiles of bioactives delivered via SLNs, typically resulting in slow evolution of peak therapeutic responses

and more stable plasma concentration trends in comparison to lipid-lipid emulsion systems (Ting *et al.*, 2014).

There are many ways in which SLNs can be produced (Chattopadhyay *et al.*, 2007; Mehnert and Mäder, 2012; Nabi-Meibodi *et al.*, 2013). Typically, on the laboratory scale, SLNs can be simply prepared by the emulsification-evaporation and subsequent sonication methods (Fathi, Mozafari and Mohebbi, 2012). Usually, the oil phase is mixed with organic solvents, emulsifiers and bioactive(s) in order to form a coarse emulsion known as the pre-emulsion (PE). After combining, the PE is then subjected to sonication for a specified amount of time, at a temperature above the melting point of the lipid carrier. The SLNs are then finally produced upon addition of the hot PE to cold surfactant containing water, under constant mixing, in order to allow for solvent evaporation (Fathi, Mozafari and Mohebbi, 2012).

Previously, it has been shown that SLNs size may remain stable in aqueous dispersions for 12-36 months (Mehnert, 2001). Nevertheless, SLNs may become unstable and increase in size during storage and, as a result lyophilisation, has been proposed as a technique to be employed in order to avoid the sample becoming physically and/or chemically unstable (Fathi, Mozafari and Mohebbi, 2012). It is important to note that, although freeze drying has been shown to increase physicochemical stability, there is a possibility that the SLNs may acquire changes in their osmolarity and zeta potential (known as the freezing out effect) resulting in instability of the sample (Abdelwahed *et al.*, 2006; Fathi, Mozafari and Mohebbi, 2012; Soares *et al.*, 2013). With this in mind, cryoprotective agents such as trehalose (Augustin and Hemar, 2009) and glucose (Soares *et al.*, 2013) have been recommended as formulation components due to their ability to

reduce the osmotic activity of water and also to prompt the frozen sample to favour the glassy state (Hauser and Strauss, 1988; Mehnert, 2001).

Spray drying is another technique that has been used in order to increase the stability of SLNs as an alternative to lyophilisation. It does, however, have some disadvantages over freeze drying due to the fact that the SLNs may aggregate upon exposure to the high temperatures and shear forces imposed during the process (Freitas and Müller, 1998). To overcome the obstacles encountered during spray drying, it is recommended to use lipids with melting points greater than 70°C (Mehnert, 2001).

Studies by Wang *et al.* (2013) involving SLNs used in the delivery of nutrients, include the encapsulation of Curcumin (CUR) (a hydrophobic polyphenol present in the rhizomes of Curcuma longa) and the evaluation of its effects *in vitro* and *in vivo*, whereby CUR-loaded SLNs (SLN-curcumin) showed a significantly higher anti-cancer efficiency on A549 lung cancer cell lines and xenografts in mouse models. SLN-CUR was shown to reduce tumour volume by 65.3% compared with a 19.5% of reduction when using CUR in its native form. In addition, in 2014, Pandita *et al*. incorporated resveratrol, a bioactive polyphenolic phytoalexin found in common foods such as grapes, peanuts, and red wine into SLNs (Pandita *et al.*, 2014). This bioactive has been shown to provide a range of health benefits such as cancer prevention (Savouret and Quesne, 2002), increased immune cell function (Falchetti *et al.*, 2001) and increased fertility (Özcan *et al.*, 2015). In the study by Pandita *et al*., the formulation of resveratrol into SLNs produced a significant 8 fold improvement in the oral BA of the drug as compared to the native drug suspension (Pandita *et al.*, 2014).

2.9 Carbohydrate-based nano- delivery systems

Carbohydrate-based delivery systems are widely used in the nutraceutical and pharmaceutical industry for targeted and controlled release (Sunasee *et al.*, 2014). These are classified as mono, oligo and polysaccharides. Mono and oligosaccharides are often used as constituents of the encapsulating matrix (Benshitrit *et al.*, 2012), polysaccharides most often being used as the carrier component due to their massive molecular structure and thus ability for greater bioactive entrapment (Fathi, Martín and McClements, 2014).

Polysaccharides exist as natural polymers of monosaccharaides, varying in type, distribution, number and bonding of the monomers in the chain (Fathi, Martín and McClements, 2014). They can be derived from animal, algal, microbial and protein sources and are typically subdivided into three groups: neutral, anionic and cationic (Daniel-da-Silva and Trindade, 2011). Polysaccharide examples include starch & cellulose (neutral), alginate & xanthan gum (anionic) and chitosan (cationic) for which the magnitude of electrical charge depends on the pH relative to the pKa (Liu *et al.*, 2008). For example, anionic polysaccharides are neutral at pH values below their pKa value but negative above, whereas cationic polysaccharides tend to be neutral at pH values above their pKa value but positive below (Kumari, Yadav and Yadav, 2010).

Alginate is an example of an anionically charged polysaccharide that has been used for NP production. It is composed of 1,4-linked-β-d-mannuronic acid and α-l-guluronic acid residues, exhibits a propensity for gelation upon exposure to proper conditions and has been shown to be both biocompatible and non-toxic (Josef, Zilberman and Bianco-Peled, 2010).When being formulated as a nano-carrier system, alginate is cross-linked with a divalent ion such as calcium chloride and magnesium chloride, the former being the most

employed counter ion for complexing alginate-based nanoparticles (Alg-NPs). Alg-NPs have been applied to deliver drugs and nutraceuticals such as insulin (Sarmento *et al.*, 2006) and vitamin D_3 (Sun *et al.*, 2012).

Various modifications have been explored to date, in order to improve the functionality of these carbohydrate-based delivery systems. For example, hydrophobically modified starch was used to increase water solubility and *in vitro* anti-carcinogenic activity of CURNPs (Ha *et al.*, 2012). Mahjub *et al.* (2014) used N-aryl derivatives of chitosan for insulin nanoparticles to produce a permanent positive charge causing the polymer to be soluble in wide range of pH values.

The type of environmental and solution conditions present within a particular food is often important for selecting the most appropriate polysaccharide building blocks, in order to provide protection and targeted/controlled delivery (Cushen *et al.*, 2012). Carbohydrate-based delivery systems have proven useful not only in the oral delivery route but in topical delivery too. For example, Calcium alginate was chosen to design the delivery system of *L. plantarum* as a polymer widely used in burn wound treatment due to its haemostatic, gel-forming and granulation-encouraging properties (Brachkova, Duarte and Pinto, 2012). More specifically, polysaccharides appear to be the most promising materials in the preparation of nanometric carriers. In fact, over the past few years, these systems have emerged as potential carriers for delivering agents across a variety of different routes, such as nasal (Amidi *et al.*, 2006), oral (El-Shabouri, 2002) and pulmonary (Al-Qadi, Grenha and Remuñán-López, 2011).

2.10 Polysaccharide Nanoparticles for nutrient delivery

Due to their biocompatible and biodegradable nature, polysaccharide based delivery systems have found many uses in industrial applications (Fathi, Martín and McClements, 2014). Part of the reason they have attracted the attention of both industrial and academic institutions is the fact that it is possible to modify polysaccharides to exhibit requisite properties. Unlike lipid carriers, carbohydrate based carriers possess the ability to interact with a wide array of both hydrophobic and hydrophilic bioactives (Joye, Davidov-Pardo and McClements, 2014). This is due to the presence of functional groups that allow for complex formation with bioactives via electrostatic interactions, both hydrophobic and ionic in nature (Rinaudo, 2006b).

Another important aspect of polymeric materials that is particularly engaging to the industrial researcher is the robustness the compound can exhibit under high temperatures (Fathi, Martín and McClements, 2014). This is particularly useful from a manufacturing standpoint, as polysaccharides can then also be used as a protective coat during processing steps (Jang and Lee, 2008). In contrast to their protein and lipid counterparts, polysaccharide systems are unlikely to become denatured or melt due to their high temperature stability. Moreover, naturally occurring polysaccharides are considered safe and already have found wide usage as food ingredients (Blanshard and Mitchell, 2013). In fact, their functional attributes are generally custom-made by their biological origins, isolation methods or physical and/or chemical modifications (Fathi, Martín and McClements, 2014), which lends to them being viewed as an ideal carrier for nutraceuticals (Hans and Lowman, 2002). For example, non-ionic Pullulan can be modified by hydrophobic molecules such as curcumin. This was evidenced by studies conducted by Yuan *et al.* (2014) that showed self-assembled NPs could be synthesized

from Glycyrrhetic Acid-Modified Pullulans with varying molecular weight and/or degree of substitution and exhibited increased solubilization, stabilization, and controlled delivery of CUR when compared to its native form (Yuan *et al.*, 2014).

Similarly, Dextran, a neutral, water soluble and bio-friendly polysaccharide, has proven a useful tool in the field of nano-medicine, being chosen by a lot of researchers as biomaterial in the preparation of nanosystems. For example studies conducted by Susa *et al*. (2009) showed that nanoparticles loaded with doxorubicin showed increased apoptosis compared to free doxorubicin on both wild type and the MDR osteosarcoma cells *in vitro* by drug accumulation in the nucleus.

2.11 Chitosan-based delivery systems

An emerging polymeric nutraceutical carrier that has received attention for nutrient delivery is chitosan (Cs) NPs (Luo *et al.*, 2010; Akhtar, Rizvi and Kar, 2012; Chen *et al.*, 2013; Fathi, Martín and McClements, 2014; Sarvaiya and Agrawal, 2015). Chitosan is a linear polysaccharide, prepared by N-deacetylation of chitin (Figure 2.3). It is positively charged, biocompatible, non-immunogenic, nontoxic, pH responsive and biodegradable, making it a choice as a component of oral drug delivery systems and attractive for biomedical and drug delivery applications (Agnihotri, Mallikarjuna and Aminabhavi, 2004; Bezerra *et al.*, 2008; Saini *et al.*, 2014). Given that chitosan has a GRAS status, this potentially can be translated to applications of delivery of nutraceuticals (Kean and Thanou, 2010). Chitosan has been extensively used in a number of areas in medicine, for example in tissue engineering (Suh and Matthew, 2000), bioimaging (Agrawal, Strijkers and Nicolay, 2010), wound-healing and drug delivery formulations (films, hydrogel

system and particulate system) (Agnihotri, Mallikarjuna and Aminabhavi, 2004; Jayakumar *et al.*, 2010).

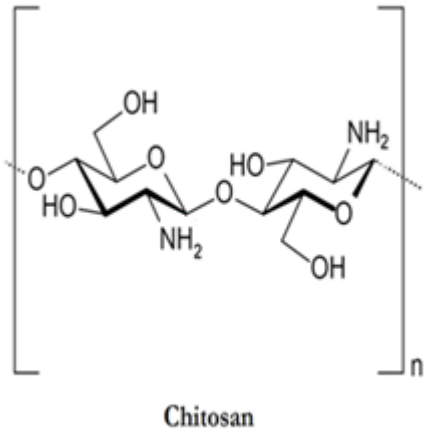

Figure 2.3 Chemical structure of chitosan.

Chitosan has an isoelectric point of 6.5 and at this pKa value it exhibits its lowest solubility, as the net charge is 0. Chitosan salts are soluble in water, the solubility depending on the degree of deacetylation and the pH of the solution.

The degree of chitosan deacetylation (DD) from chitin signifies the percentage of deacetylated primary amine groups along the molecular chain, which can determine the positive charge density when chitosan is dissolved in acidic conditions. The higher the DD, the more soluble the chitosan will be at acidic conditions (Hejazi and Amiji, 2003) and subsequently the more it will exhibit its muco-adhesive properties in the GI tract (Ting *et al.*, 2014).

Chitosan with a low degree of deacetylation (<40%) is soluble up to a pH of 9, whereas highly deacetylated chitosan (>85%) is soluble only up to a pH of 6.5 (Rinaudo, 2006a). A high degree of deacetylation more readily allows ionization of Cs as increasing the degree of deacetylation increases the viscosity and results in an extended conformation with a more flexible chain because of the charge repulsion in the molecule (Kumirska *et*

al., 2010). Hence, chitosan with a high degree of deacetylation is commonly used for drug delivery research. Table 2.6 summaries the main chemical and biological properties of chitosan.

Table 2.6 Chemical and Biological Properties of Chitosan (Adapted from Hejazi and Amiji 2003).

Chemical and Biological Properties of Chitosan	
Chemical Properties	**Biological Properties**
Cationic polyamine	Biocompatible
High charge density	Natural Polymer
Forms gels with polyanions	Biodegradable
Amiable to chemical modification	Spermicidal
Reactive amino/hydroxyl groups	Anticancerogen, Anticholesteromic
Swelling properties	Mucoadhesive
High mol wgt linear polyelectrolyte	Safe and non-toxic
Chelates certain transitional metals	Hemostatic, bacteriostatic,

2.12 Regulations surrounding nanomaterial safety

Nano-engineered particles have been used to enhance the drug delivery of actives, but due to the small sizes, increased surface area and reactive nature of the nano materials, the effectiveness and safety is a key consideration in Nanomedicine and even though the successful implementation of nanotechnology is pertinent for the growth of the global economy, there is also a need to consider the possible environmental health and safety impact for nanoparticles that could lead to hazardous biological outcomes (Martirosyan and Schneider, 2014).

The FDA (Food and Drug Administration) is one of the main regulatory nanotechnology bodies in the US and collaborates with the National Nanotechnology Initiative (NNI). In Europe, the Institute for Health and Consumer Protection (IHCP) is the main regulatory body actively involved in research into nanomaterials safety, identification and detection. For both agencies, their key goal is to deal with questions about the potential effects on health and the environment with particular emphasis on the risks and benefits to the public. With regards to foods, the European Food Safety Authority (EFSA) works closely with the IHCP to examine the behaviour of engineered nanomaterials in foods and to validate methods of characterisation.

Following a report by the European Nanoforum, a food product is considered a "Nanofood when nanoparticles and nanotechnology techniques or tools are applied during cultivation, production, processing or packaging of the food, not intending to produce atomically modified food or food produced by nanomachines" (Joseph and Morrison, 2006). Due to the increasing use of nanomaterials in foods, recent EU legislation (No 1169/2011) on novel foods has introduced obligatory labelling of nanomaterials on packaging (European Parliament, 2011).

2.13 Uptake of nanoparticles and potential toxicity

Micro- and nano-particles have been shown to permeate through GI barriers, with the latter estimated to have a 15-250 times higher absorption (Fröhlich and Roblegg, 2012). Ingestion, inhalation and dermal absorption are the main physiological routes in which NPs can enter the body, consequently resulting in the potential ability to distribute themselves to a given organ over several exposure points (Smolkova *et al.*, 2015).

Absorption, Distribution, Metabolism and Elimination (ADME) are the characteristics that effect the extent of NP exposure to a given system (Hagens *et al.*, 2007).

Previous investigations have shown that the uptake of NPs is low in healthy oro-gastrointestinal mucous. However, the level of absorption varies dependent upon type of GI cell, for example absorption is higher in the lumen in comparison to the oral cavity (Roblegg *et al.*, 2012). Epithelial barriers allow for the separation of NPs from the blood and as a result translocation of NPs into secondary organs can occur due to their ability to reach the connective tissue that is present beneath the epithelial layer surrounding the intestines (Smolkova *et al.*, 2015). For example, previous studies have found that titanium oxide (TiO_2) NPs when acutely exposed to both *ex vivo* and *in vivo* systems, possessed the ability to pass through both the follicle-associated epithelium (composed of enterocytes and microfold cells) and regular intestinal epithelium (mucous secreting cells) becoming localized in the tissues situated below both epithelial layers (Brun *et al.*, 2014). Other studies have indicated that accumulation of TiO_2 inside epithelial lining can give rise to detrimental outcomes such as inflammation and may be involved in inflammatory bowel disease pathogenesis (Lomer, Thompson and Powell, 2002; Nogueira *et al.*, 2012).

The surface properties and size of ingested NPs are affected by several environmental factors such as pH, ionic strength, protein, sugar and lipid content that are naturally present in foods such as the mucus of the saliva (Roblegg *et al.*, 2012). In addition, upon NP entrance to the system, interactions can occur between plasma proteins, platelets, peripheral blood cells as well as with the organelles and DNA of the cells (Smolkova *et al.*, 2015). Due to some NPs low excretion rate, it is plausible to suggest that more often than not, long term dose exposures occur. In spite of the fact that NP penetration into the

body is low, toxicity screening is based predominantly on high dose, short exposures (Oberdörster, 2010). This lends to acute toxicity issues being reported whilst minor changes resulting from long term accumulation in a given system go unidentified.

NPs derived from occurring nontoxic substances in the body (i.e. protein and carbohydrates) should pose less of a risk to the body than inorganic nano-delivery systems. However, the effects from the increased bioavailability of these compounds may have significant consequences on the body and must be considered also. In addition, alterations in protein and carbohydrate structure have been shown to potentially increase the allergenicity of said molecules (Říhová, 2007; Dobrovolskaia *et al.*, 2008).

Regarding the increased bioavailability of compounds when delivered in a nano-enabled format, currently safe upper levels and recommended daily allowances (RDAs) only consider the delivery of essential nutrients in their macromolecule form (Chaudhry and Castle, 2011). The use of nanotechnology to deliver these compounds may have implications when estimating a given value (Food Safety Authority of Ireland, 2006; Bouwmeester *et al.*, 2009). Conversely, inherently toxic materials (for instance some inorganic particulate metals) produced in a nano format and introduced to an environment in which it can solubilise may give rise to greater exhibited toxicity than organic forms; in fact several studies have exhibited that this may be the case in which many NPs have shown greater reactivity in *in silico* and/or *in vitro* models (Papageorgiou *et al.*, 2007; Singh *et al.*, 2007; Puzyn *et al.*, 2011).

Due to the complexity of accessing the penetration and biological effects of ingested NPs on the body it can be difficult to ascertain which chemical or physical properties can be exploited for commercial use whilst avoiding potential toxicity effects on cells and tissues (Singh *et al.*, 2007). For example, properties such as physical dimensions and surface

charge determine a particles ability to penetrate an organ or cell, in addition to the likelihood that it will be uptaken and phagocytosed by leucocytes (Owens and Peppas, 2006). Retention time of particles, together with their solubility is another facet that needs consideration, as it is well documented that increased residence time of particles at cell membrane surfaces give rise to greater toxic reactions and damage (Dowling *et al.*, 2004; Nel *et al.*, 2009).

Particle interactions represent another specific caveat that deems consideration. For example, particle contact with endogenous compounds present in the body or food matrix give rise to biomolecule coronas that may assist the absorption of novel entities into the small bowel lumen (Lomer, Thompson and Powell, 2002; Nel *et al.*, 2009). These considerations must be kept in mind when assessing the effects of using NPs for food or supplementation purposes with the intent to increase bioavailability. However, to date, there is limited information available on ADME and toxic properties of NPs, leading to recommendations to consider each NP formulation on a "case by case" basis (SCENIHR, 2007). For example, Cs NPs are insoluble yet ultimately biodegradable; they will breakdown to their substituent counterparts at a rate dependent on their physicochemical properties (Xu and Du, 2003). In contrast TiO_2 NPs lack the ability to be broken down in the body and thus have been shown to accumulate in the RES of the liver and spleen (Elgrabli *et al.*, 2015).

It is important to note that humans have been exposed to NPs throughout evolution, and there is even evidence that we have adapted strategies to benefit from dietary and physiological use of NPs in the gut (Powell *et al.*, 2010). In addition, many foods are already comprised of compounds such as proteins, carbohydrates and fats which exist in a range of sizes, at present outspreading from macromolecules to the nano scale (Food

Safety Authority of Ireland, 2006). Generally, food ingested in macro scale format is subsequently digested to the nano scale in order to exploit the energy contained in the molecule for body gains. For example, it has been shown that nanoparticulate ferritin may be utilised by gut epithelial cells as a source of dietary iron post endocytosis (Pan *et al.*, 2009). With this in mind, it is fair to state that nanoparticulates cannot be considered inherently safe or toxic. They do, however, need to be assessed such that their molecular structure, biological environment, degree of exposure and host acceptability are understood and consequently assigned a potential hazard risk value accordingly (Food Safety Authority of Ireland, 2006).

2.14 Conclusion and future directions

There is growing emphasis on health and welfare derived from food, which is being driven by demographic and social factors, such as larger emphasis on healthy living in industrial societies, the ageing of the population within the developed world in addition to the increasing prevalence of sickness and diseases related to high-fat and high cholesterol foods in rising and industrial economies (Verbeke, 2005; Annunziata and Vecchio, 2013). Innovation in food merchandise has capitalised on these trends to develop the growing marketplace for practical and/or health enhancing foods. Matching specific foods or food decisions with an individual's exact health desires appears to be the way forward for the nutrition and food business future.

Whilst it is recognised that the application of nanotechnology to nutrient delivery can give rise to several challenges within safety, ethical and regulatory perspectives (Bouwmeester *et al.*, 2009), it is important to keep in mind the major scope of potential benefits it can offer to both consumers and manufacturers alike. At this moment in time,

the long-term effects of nanomaterial exposure to human health remains largely unknown. However, by ensuring enhanced knowledge is acquired during the realisation of NP incorporation into food products it is possible to ensure consumer acceptance remains in favour of this highly promising technology (Ravichandran, 2010).

With regards to global economic effects anticipated as a result of nano-enabled nutraceuticals being applied in food product markets, undoubtedly nations who are able to develop products that deliver smarter and healthier foods whilst maintaining increased food production at cost effective margins can expect to profit in the economic long term. If regulated correctly, the sustainability of nanomaterials in foods, alongside the potential health and environmental benefits of the more efficient delivery of nutraceuticals, can be expected to hugely impact the future direction of the food industry (Ravichandran, 2010). With this in mind, it is of importance to ensure that human and environmental concerns are addressed and subsequently not compromised as new products hit the market. In order to assure this approach is embodied, the rate at which nanotechnology is introduced into food products should be sufficiently reduced in order to allow for potential risks to be identified and rectified prior to successful implementation on the food market.

Special attention should also be given to public opinion regarding the use of nanotechnology in foods in order to mitigate negative consumer responses such that was seen upon the introduction of genetically modified foods (Costa-Font, Gil and Traill, 2008; Hudson, Caplanova and Novak, 2015). As with any new technology, it is pertinent that the potential benefits and risks are thoroughly discussed in addition to appropriate labelling and regulation guidelines, in order to safeguard increased consumer acceptability.

2.15 References

Abbas, K. A. *et al.* (2009) 'The recent advances in the nanotechnology and its applications in food processing: A review', *Journal of Food, Agriculture & Environment*, 7(3&4), pp. 14–17.

Abdelwahed, W. *et al.* (2006) 'Freeze-drying of nanoparticles: Formulation, process and storage considerations', *Advanced Drug Delivery Reviews*, 58(15), pp. 1688–1713.

Accessdata.fda.gov (2014) *CFR - Code of Federal Regulations Title 21, United States Food and Drug Administration*. Available at: www.accessdata.fda.gov/scripts/cdrh/cfdocs/cfcfr/CFRSearch.cfm?fr=184.1984 (Accessed: 10 June 2015).

Acosta, E. (2009) 'Bioavailability of nanoparticles in nutrient and nutraceutical delivery', *Current Opinion in Colloid & Interface Science*, 14(1), pp. 3–15.

Aditya, N. P. *et al.* (2015) 'Co-delivery of hydrophobic curcumin and hydrophilic catechin by a water-in-oil-in-water double emulsion', *Food Chemistry*, 173, pp. 7–13.

Adjonu, R. *et al.* (2014) 'Whey protein peptides as components of nanoemulsions: A review of emulsifying and biological functionalities', *Journal of Food Engineering*, 122, pp. 15–27.

Agnihotri, S. A., Mallikarjuna, N. N. and Aminabhavi, T. M. (2004) 'Recent advances on chitosan-based micro- and nanoparticles in drug delivery', *Journal of Controlled Release*, pp. 5–28.

Agrawal, P., Strijkers, G. J. and Nicolay, K. (2010) 'Chitosan-based systems for molecular imaging.', *Advanced Drug Delivery Reviews*, 62(1), pp. 42–58.

Agrawal, U. *et al.* (2014) 'Is nanotechnology a boon for oral drug delivery?', *Drug Discovery Today*, 19(10), pp. 1530–46.

Akhtar, F., Rizvi, M. M. A. and Kar, S. K. (2012) 'Oral delivery of curcumin bound to chitosan nanoparticles cured Plasmodium yoelii infected mice.', *Biotechnology Advances*, 30 (1), 310–20.

Al-Qadi, S., Grenha, A. and Remuñán-López, C. (2011) 'Microspheres loaded with polysaccharide nanoparticles for pulmonary delivery: Preparation, structure and surface analysis', *Carbohydrate Polymers*, 86(1), pp. 25–34.

Almeida, A. J. and Souto, E. (2007) ‘Solid lipid nanoparticles as a drug delivery system for peptides and proteins.’, *Advanced Drug Delivery Reviews*, 59(6), pp. 478–90.

Amidi, M. *et al.* (2006) ‘Preparation and characterization of protein-loaded N-trimethyl chitosan nanoparticles as nasal delivery system.’, *Journal of Controlled Release* 111(1–2), pp. 107–16.

Anal, A. K. and Singh, H. (2007) ‘Recent advances in microencapsulation of probiotics for industrial applications and targeted delivery’, *Trends in Food Science and Technology*, 18(5), pp. 240–251.

Anarjan, N. *et al.* (2010) ‘Effect of processing conditions on physicochemical properties of astaxanthin nanodispersions’, *Food Chemistry*, 123(2), pp. 477–483.

Andreani, T. *et al.* (2014) ‘Preparation and characterization of PEG-coated silica nanoparticles for oral insulin delivery’, *International Journal of Pharmaceutics*, 473(1–2), pp. 627–635.

Annunziata, A. and Vecchio, R. (2013) ‘Consumer perception of functional foods: A conjoint analysis with probiotics’, *Food Quality and Preference*, 28(1), pp. 348–355.

Arnault, I. and Auger, J. (2006) ‘Seleno-compounds in garlic and onion.’, *Journal of Chromatography. A*, 1112(1–2), pp. 23–30.

Augustin, M. A. and Hemar, Y. (2009) ‘Nano- and micro-structured assemblies for encapsulation of food ingredients.’, *Chemical Society Reviews*, 38(4), pp. 902–912.

Augustin, M. A. and Sanguansri, L. (2015) ‘Challenges and Solutions to Incorporation of Nutraceuticals in Foods’, *Annual Review of Food Science and Technology*, 6(1), pp. 463–477.

Bassaganya-Riera, J. and Hontecillas, R. (2010) ‘Dietary conjugated linoleic acid and n-3 polyunsaturated fatty acids in inflammatory bowel disease.’, *Current Opinion in Clinical Nutrition and Metabolic Care*, 13(5), pp. 569–573.

BCC research (2015) *Global Market for Nutraceuticals Projected to Reach $241.1 Billion by 2019, Growing at 7% CAGR*. Available at: http://www.bccresearch.com/pressroom/fod/global-market-for-nutraceuticals-projected-to-reach-$241.1-billion-by-2019 (Accessed: 2 June 2015).

Benshitrit, R. C. *et al.* (2012) ‘Development of oral food-grade delivery systems: Current knowledge and future challenges’, *Food & Function*, 3(1), p. 10.

Bezerra, M. A. *et al.* (2008) 'Response surface methodology (RSM) as a tool for optimization in analytical chemistry.', *Talanta*, 76(5), pp. 965–77.

Blanshard, J. M. V. and Mitchell, J. R. (2013) *Polysaccharides in Food*. Elsevier.

Blasco, C. and Picó, Y. (2011) 'Determining nanomaterials in food', *TrAC Trends in Analytical Chemistry*, 30(1), pp. 84–99.

Blondeau, N. (2015) 'The nutraceutical potential of omega-3 alpha-linolenic acid in reducing the consequences of stroke', *Biochimie*, pp. 1–7.

Bonifácio, B. V. *et al.* (2014) 'Nanotechnology-based drug delivery systems and herbal medicines: a review', *International Journal of Nanomedicine*, 9, pp. 1–15.

Bouwmeester, H. *et al.* (2009) 'Review of health safety aspects of nanotechnologies in food production', *Regulatory Toxicology and Pharmacology*, 53(1), pp. 52–62.

Brachkova, M. I., Duarte, A. and Pinto, J. F. (2012) 'Alginate Films Containing Viable Lactobacillus Plantarum: Preparation and In Vitro Evaluation', *AAPS PharmSciTech*, pp. 357–363.

Braithwaite, M. C. *et al.* (2014) 'Nutraceutical-based therapeutics and formulation strategies augmenting their efficiency to complement modern medicine: An overview', *Journal of Functional Foods*, pp. 82–99.

Brouns, F. (2002) 'Soya isoflavones: a new and promising ingredient for the health foods sector', *Food Research International*, 35(2–3), pp. 187–193.

Brown, K. M. and Arthur, J. R. (2001) 'Selenium, selenoproteins and human health: a review.', *Public Health Nutrition*, 4(2B), pp. 593–599.

Brun, E. *et al.* (2014) 'Titanium dioxide nanoparticle impact and translocation through ex vivo, in vivo and in vitro gut epithelia.', *Particle and Fibre Toxicology*, 11(1), p. 13.

Chan, H.-K. and Kwok, P. C. L. (2011) 'Production methods for nanodrug particles using the bottom-up approach.', *Advanced Drug Delivery Reviews*, 63(6), pp. 406–16.

Chattopadhyay, P. *et al.* (2007) 'Production of solid lipid nanoparticle suspensions using supercritical fluid extraction of emulsions (SFEE) for pulmonary delivery using the AERx system.', *Advanced Drug Delivery Reviews*, 59(6), pp. 444–53.

Chaudhry, Q. and Castle, L. (2011) 'Food applications of nanotechnologies: An overview of opportunities and challenges for developing countries', *Trends in Food Science & Technology*, 22(11), pp. 595–603.

Chen, H. and Yada, R. (2011) 'Nanotechnologies in agriculture: New tools for sustainable development', *Trends in Food Science & Technology*, 22(11), pp. 585–594.

Chen, L., Remondetto, G. E. and Subirade, M. (2006) 'Food protein-based materials as nutraceutical delivery systems', *Trends in Food Science and Technology*, 17(5), pp. 272–283.

Chen, M. C. *et al.* (2013) 'Recent advances in chitosan-based nanoparticles for oral delivery of macromolecules', *Advanced Drug Delivery Reviews*, pp. 865–879.

Chen, Z. *et al.* (2010) 'Comparative pharmacokinetics and bioavailability studies of quercetin, kaempferol and isorhamnetin after oral administration of Ginkgo biloba extracts, Ginkgo biloba extract phospholipid complexes and Ginkgo biloba extract solid dispersions in rats.', *Fitoterapia*, 81(8), pp. 1045–52.

Chu, B.-S. *et al.* (2007) 'Preparation of Protein-Stabilized β-Carotene Nanodispersions by Emulsification–Evaporation Method', *Journal of the American Oil Chemists' Society*, 84(11), pp. 1053–1062.

Coimbra, M. *et al.* (2011) 'Improving solubility and chemical stability of natural compounds for medicinal use by incorporation into liposomes.', *International Journal of Pharmaceutics*, 416(2), pp. 433–42.

Coppens, P., Da Silva, M. F. and Pettman, S. (2006) 'European regulations on nutraceuticals, dietary supplements and functional foods: A framework based on safety', *Toxicology*, pp. 59–74.

Costa-Font, M., Gil, J. M. and Traill, W. B. (2008) 'Consumer acceptance, valuation of and attitudes towards genetically modified food: Review and implications for food policy', *Food Policy*, 33(2), pp. 99–111.

Couleaud, P. *et al.* (2010) 'Silica-based nanoparticles for photodynamic therapy applications.', *Nanoscale*, 2(7), pp. 1083–1095.

Cushen, M. *et al.* (2012) 'Nanotechnologies in the food industry - Recent developments, risks and regulation', *Trends in Food Science and Technology*, 24(1), pp. 30–46.

Daniel-da-Silva, A. L. and Trindade, T. (2011) 'Biofunctional composites of polysaccharides containing inorganic nanoparticles', *Advances in Nanocomposite Technology*, pp. 275–298.

Davidov-Pardo, G. and McClements, D. J. (2014) 'Resveratrol encapsulation: Designing delivery systems to overcome solubility, stability and bioavailability issues', *Trends in Food Science & Technology*, 38(2), pp. 88–103.

DeFelice, S. L. (1995) ‘The nutraceutical revolution: its impact on food industry R&D’, *Trends in Food Science & Technology*, 6(2), pp. 59–61.

Diaz Fernandez, Y. a. *et al.* (2014) ‘The Conquest of Middle-Earth: combining top-down and bottom-up nanofabrication for constructing nanoparticle based devices’, *Nanoscale*, 6(24), pp. 14605–14616.

Dickinson, A. and MacKay, D. (2014) ‘Health habits and other characteristics of dietary supplement users: a review.’, *Nutrition Journal*, 13, p. 14.

Dobrovolskaia, M. A. *et al.* (2008) ‘Preclinical studies to understand nanoparticle interaction with the immune system and its potential effects on nanoparticle biodistribution’, *Molecular Pharmaceutics*, 5(4), pp. 487–495.

Dombrinkkurtzman, M. a and Bietz, J. a (1993) ‘Zein composition in hard and soft endosperm of maize’, *Cereal Chemistry*, 70(1), pp. 105–108.

Dowling, a *et al.* (2004) ‘Nanoscience and nanotechnologies: opportunities and uncertainties’, *The Royal Society*.

Duncan, T. V (2011) ‘Applications of nanotechnology in food packaging and food safety: barrier materials, antimicrobials and sensors.’, *Journal of Colloid and Interface Science*, 363(1), pp. 1–24.

Ec.europa.eu (2011) *Definition of a nanomaterial, European Commission*. Available at: http://ec.europa.eu/environment/chemicals/nanotech/faq/definition_en.htm (Accessed: 2 June 2015).

Ec.europa.eu (2015) *EUROPA-Food Safety - Labelling & Nutrition - Food Supplements - Introduction.* Available at: http://ec.europa.eu/food/food/labellingnutrition/supplements/index_en.htm (Accessed: 2 June 2015).

El-Shabouri, M. . (2002) ‘Positively charged nanoparticles for improving the oral bioavailability of cyclosporin-A’, *International Journal of Pharmaceutics*, 249(1–2), pp. 101–108.

Elzoghby, A. O., Samy, W. M. and Elgindy, N. a. (2012) ‘Protein-based nanocarriers as promising drug and gene delivery systems’, *Journal of Controlled Release*, 161(1), pp. 38–49.

Ensign, L. M., Cone, R. and Hanes, J. (2012) 'Oral drug delivery with polymeric nanoparticles: the gastrointestinal mucus barriers', *Advanced Drug Delivery Reviews*, 64(6), pp. 557–570.

Esen, A. (1987) 'A proposed nomenclature for the alcohol-soluble proteins (zeins) of maize (Zea mays L.)', *Journal of Cereal Science*, 5(2), pp. 117–128.

Etheridge, M. L. *et al.* (2013) 'The big picture on nanomedicine: the state of investigational and approved nanomedicine products.', *Nanomedicine : Nanotechnology, Biology, and Medicine*, 9(1), pp. 1–14.

Eufic.org (2015) *Functional foods (EUFIC)*. Available at: http://www.eufic.org/article/en/expid/basics-functional-foods (Accessed: 2 June 2015).

European Commission (2009) *Community Register on the addition of vitamins and minerals and of certain other substances to foods*. Available at: http://ec.europa.eu/food/safety/docs/labelling_nutrition-vitamins_minerals-comm_reg_en.pdf. (Accessed: 2 June 2015).

European Parliament (2006) 'Regulation (EC) No 1924/2006 of the European Parliament and of the Council of 20 December 2006 on nutrition and health claims made on foods', *Council of the European Union*. Available at: http://eur-lex.europa.eu/legal-content/EN/TXT/PDF/?uri=CELEX:32006R1924&from=EN. (Accessed: 2 June 2015).

European Parliament, C. of the E. U. (2011) 'Regulation (EU) No 1169/2011 of the European Parliament and of the Council of 25 October 2011 on the Provision of Food Information to Consumers, Amending Regulations (EC) No 1924/2006 and (EC) No 1925/2006 of the European Parliament and of the Council, an'. European Parliament, Council of the European Union Brussels, Belgium.

Ezpeleta, I. *et al.* (1996) 'Gliadin nanoparticles for the controlled release of all-trans-retinoic acid', *International Journal of Pharmaceutics*, 131(2), pp. 191–200.

Falchetti, R. *et al.* (2001) 'Effects of resveratrol on human immune cell function', *Life Sciences*, 70(1), pp. 81–96.

Fathi, M., Martín, Á. and McClements, D. J. (2014) 'Nanoencapsulation of food ingredients using carbohydrate based delivery systems', *Trends in Food Science and Technology*, 39, pp. 18–39.

Fathi, M., Mozafari, M. R. and Mohebbi, M. (2012) 'Nanoencapsulation of food ingredients using lipid based delivery systems', *Trends in Food Science & Technology*, 23(1), pp. 13–27.

Food Safety Authority of Ireland (2006) *The Relevance for Food Safety of Applications of Nanotechnology The Relevance for Food Safety of Applications of Nanotechnology*. Dublin. Available at: www.fsai.ie/WorkArea/DownloadAsset.aspx?id=7858. (Accessed: 2 June 2015).

Freitas, C. and Müller, R. H. (1998) 'Spray-drying of solid lipid nanoparticles (SLNTM)', *European Journal of Pharmaceutics and Biopharmaceutics*, 46(2), pp. 145–151.

Fröhlich, E. and Roblegg, E. (2012) 'Models for oral uptake of nanoparticles in consumer products', *Toxicology*, 291(1–3), pp. 10–17.

Fung, A., Hamid, N. and Lu, J. (2013) 'Fucoxanthin content and antioxidant properties of *Undaria pinnatifida*', *Food Chemistry*, 136(2), pp. 1055–1062.

Gökmen, V. *et al.* (2011) 'Development of functional bread containing nanoencapsulated omega-3 fatty acids', *Journal of Food Engineering*, 105(4), pp. 585–591.

Guasch-Ferré, M. *et al.* (2014) 'Olive oil intake and risk of cardiovascular disease and mortality in the PREDIMED Study.', *BMC Medicine*, 12, p. 78.

Gutiérrez, J. M. *et al.* (2008) 'Nano-emulsions: New applications and optimization of their preparation', *Current Opinion in Colloid and Interface Science*, pp. 245–251.

Gutierro, I. *et al.* (2002) 'Size dependent immune response after subcutaneous, oral and intranasal administration of BSA loaded nanospheres', *Vaccine*, 21(1–2), pp. 67–77.

Ha, E. and Zemel, M. B. (2003) 'Functional properties of whey, whey components, and essential amino acids: Mechanisms underlying health benefits for active people (Review)', *Journal of Nutritional Biochemistry*, pp. 251–258.

Ha, P. T. *et al.* (2012) 'Preparation and anti-cancer activity of polymer-encapsulated curcumin nanoparticles', *Advances in Natural Sciences: Nanoscience and Nanotechnology*, 3(3), p. 35002.

H du Plessis, L. *et al.* (2014) 'Applications of Lipid based Formulation Technologies in the Delivery of Biotechnology-based Therapeutics', *Current Pharmaceutical Biotechnology*, 15(7), pp. 659–672.

Hagens, W. I. *et al.* (2007) 'What do we (need to) know about the kinetic properties of nanoparticles in the body?', *Regulatory Toxicology and Pharmacology : RTP*, 49(3), pp. 217–29.

Han, S. B. *et al.* (2014) 'Physical characterization and in vitro skin permeation of solid lipid nanoparticles for transdermal delivery of quercetin', *International Journal of Cosmetic Science*, 36(6), pp. 588–597.

Handford, C. E. *et al.* (2014) 'Implications of nanotechnology for the agri-food industry: Opportunities, benefits and risks', *Trends in Food Science & Technology*, 40(2), pp. 226–241.

Hans, M. . and Lowman, A. . (2002) 'Biodegradable nanoparticles for drug delivery and targeting', *Current Opinion in Solid State and Materials Science*, 6(4), pp. 319–327.

Harde, H., Das, M. and Jain, S. (2011) 'Solid lipid nanoparticles: an oral bioavailability enhancer vehicle', *Expert Opinion on Drug Delivery*, 8(11), pp. 1407–1424.

Hasler, C. M. (2000) 'The changing face of functional foods', *Journal of the American College of Nutrition*, 19(sup5), p. 499S–506S.

Haug, A., Hostmark, A. T. and Harstad, O. M. (2007) 'Bovine milk in human nutrition–a review', *Lipids Health Dis*, 6(25), pp. 1–16.

Hauser, H. and Strauss, G. (1988) 'Stabilization of Small, Unilamellar Phospholipid Vesicles by Sucrose during Freezing And Dehydration', *Biotechnological Applications of Lipid Microstructures SE - 7*, pp. 71–80.

Heitbrink, W. A., Lo, L.-M. and Dunn, K. H. (2015) 'Exposure controls for nanomaterials at three manufacturing sites', *Journal of Occupational and Environmental Hygiene*, 12(1), pp. 16–28.

Hejazi, R. and Amiji, M. (2003) 'Chitosan-based gastrointestinal delivery systems', *Journal of Controlled Release*, pp. 151–165.

Helson, L. (2013) 'Curcumin (diferuloylmethane) delivery methods: A review.', *Biofactors*, 39(1), pp. 21–26.

Huang, Q., Yu, H. and Ru, Q. (2010) 'Bioavailability and Delivery of Nutraceuticals Using Nanotechnology', *Journal of Food Science*, 75(1), pp. R50–R57.

Hudson, J., Caplanova, A. and Novak, M. (2015) 'Public attitudes to GM foods. The balancing of risks and gains.', *Appetite*, 92, pp. 303–313.

Ibrahim, S. a (2015) 'Spray-on transdermal drug delivery systems', *Expert Opinion on Drug Delivery*, 12(2), pp. 195–205.

Iglesias, G. R. *et al.* (2013) 'Lipid transfer in oil-in-water isasome emulsions: Influence of arrested dynamics of the emulsion droplets entrapped in a hydrogel', *Langmuir*, 29(50), pp. 15496–15502.

Institute of Medicine (US) Food Forum (2009) *Nanotechnology in Food Products: Workshop Summary*, *National Academies Press (US)*. Available at: http://www.ncbi.nlm.nih.gov/books/NBK32737/ (Accessed: 6 June 2015).

Jadeja, R. N. *et al.* (2010) 'Pomegranate (Punica granatum L.) juice supplementation attenuates isoproterenol-induced cardiac necrosis in rats', *Cardiovascular Toxicology*, 10(3), pp. 174–180.

Jang, K.-I. and Lee, H. G. (2008) 'Stability of Chitosan Nanoparticles for l-Ascorbic Acid during Heat Treatment in Aqueous Solution', *Journal of Agricultural and Food Chemistry*, 56(6), pp. 1936–1941.

Jayakumar, R. *et al.* (2010) 'Biomedical applications of chitin and chitosan based nanomaterials - A short review', *Carbohydrate Polymers*, 82(2), pp. 227–232.

Jelen, P. (2010) 'Bioactive Components in Milk and Dairy Products', *International Dairy Journal*, 20(8), p. 560.

De Jong, W. H. and Borm, P. J. A. (2008) 'Drug delivery and nanoparticles: Applications and hazards', *International Journal of Nanomedicine*, 3(2), pp. 133–149.

Josef, E., Zilberman, M. and Bianco-Peled, H. (2010) 'Composite alginate hydrogels: An innovative approach for the controlled release of hydrophobic drugs.', *Acta Biomaterialia*, 6(12), pp. 4642–9.

Joseph, T. and Morrison, M. (2006) 'Nanotechnology in agriculture and food. Institute of Nanotechnology, Report, Nanoforum Organization, European Nanotechnology Gateway'.

Joye, I. J., Davidov-Pardo, G. and McClements, D. J. (2014) 'Nanotechnology for increased micronutrient bioavailability', *Trends in Food Science & Technology*, 40(2), pp. 168–182.

JRC Science Hub (2015) *Human Exposure - JRC Science Hub - European Commission.* Available at: https://ec.europa.eu/jrc/en/research-topic/human-exposure (Accessed: 2 June 2015).

Ju-Nam, Y. and Lead, J. R. (2008) 'Manufactured nanoparticles: an overview of their chemistry, interactions and potential environmental implications.', *The Science of the Total Environment*, 400(1–3), pp. 396–414.

Kalepu, S., Manthina, M. and Padavala, V. (2013) 'Oral lipid-based drug delivery systems – an overview', *Acta Pharmaceutica Sinica B*, 3(6), pp. 361–372.

Kalra, E. (2003) 'Nutraceutical-definition and introduction', *AAPS PharmSci*, 5(3), pp. 27–28.

Kean, T. and Thanou, M. (2010) 'Biodegradation, biodistribution and toxicity of chitosan', *Advanced Drug Delivery Reviews*, pp. 3–11.

Kimura, A. *et al.* (2014) 'Gelatin Hydrogel as a Carrier of Recombinant Human Fibroblast Growth Factor-2 During Rat Mandibular Distraction', *Journal of Oral and Maxillofacial Surgery*, 72(10), pp. 2015–2031.

Kocbek, P. *et al.* (2007) 'Targeting cancer cells using PLGA nanoparticles surface modified with monoclonal antibody.', *Journal of Controlled Release*, 120(1–2), pp. 18–26.

Koppolu, B. P. *et al.* (2014) 'Controlling chitosan-based encapsulation for protein and vaccine delivery', *Biomaterials*, 35(14), pp. 4382–4389.

Kroon, J. *et al.* (2014) 'Liposomal nanomedicines in the treatment of prostate cancer', *Cancer Treatment Reviews*, 40(4), pp. 578–584.

Kuan, C.-Y. *et al.* (2012) 'Nanotech: Propensity in Foods and Bioactives', *Critical Reviews in Food Science and Nutrition*, pp. 55–71.

Kumari, A., Yadav, S. K. and Yadav, S. C. (2010) 'Biodegradable polymeric nanoparticles based drug delivery systems.', *Colloids and Surfaces. B, Biointerfaces*, 75(1), pp. 1–18.

Kumirska, J. *et al.* (2010) 'Application of spectroscopic methods for structural analysis of chitin and chitosan', *Marine Drugs*, 8(5), pp. 1567–1636.

Kwon, I. C. (2008) 'Chitosan-based nanoparticles for cancer therapy; tumor specificity and enhanced therapeutic efficacy in tumor-bearing mice', *Journal of Controlled Release*, 132(3), pp. e69–e70.

Lagos, J. B. *et al.* (2015) 'Recent patents on the application of bioactive compounds in food: A short review', *Current Opinion in Food Science*.

Lai, L. F. and Guo, H. X. (2011) 'Preparation of new 5-fluorouracil-loaded zein nanoparticles for liver targeting', *International Journal of Pharmaceutics*, 404(1–2), pp. 317–323.

Larkins, B. A. *et al.* (1984) 'The zein proteins of maize endosperm', *Trends in Biochemical Sciences*, 9(7), pp. 306–308.

Lawton, J. W. (2002) 'Zein: A History of Processing and Use', *Cereal Chemistry Journal*. Scientific Societies, 79(1), pp. 1–18.

Lee, B. K., Yun, Y. H. and Park, K. (2015) 'Smart nanoparticles for drug delivery: Boundaries and opportunities', *Chemical Engineering Science*, 125, pp. 158–164.

Leong, W. F. *et al.* (2011) 'Preparation and characterisation of water-soluble phytosterol nanodispersions', *Food Chemistry*, 129(1), pp. 77–83.

Li-Chan, E. C. (2015) 'Bioactive peptides and protein hydrolysates: research trends and challenges for application as nutraceuticals and functional food ingredients', *Current Opinion in Food Science*, 1, pp. 28–37.

Liang, L. *et al.* (2013) 'Pharmacokinetics, tissue distribution and excretion study of resveratrol and its prodrug 3,5,4'-tri-O-acetylresveratrol in rats.', *Phytomedicine : International Journal of Phytotherapy and Phytopharmacology*, 20(6), pp. 558–63.

Liu, R. H. (2007) 'Whole grain phytochemicals and health', *Journal of Cereal Science*, 46(3), pp. 207–219.

Liu, Z. *et al.* (2008) 'Polysaccharides-based nanoparticles as drug delivery systems.', *Advanced Drug Delivery Reviews*, 60(15), pp. 1650–62.

Lomer, M. C. E., Thompson, R. P. H. and Powell, J. J. (2002) 'Fine and ultrafine particles of the diet: influence on the mucosal immune response and association with Crohn's disease', *Proceedings of the Nutrition Society*, 61(1), pp. 123–130.

Luo, Y. *et al.* (2010) 'Preparation, characterization and evaluation of selenite-loaded chitosan/TPP nanoparticles with or without zein coating', *Carbohydrate Polymers*, 82(3), pp. 942–951.

Luo, Y. (2014). 'Nutrient delivery systems: the future strategy for chronic diseases', *Austin J Nutri Food Sci*, 2(9), pp.2-4.

Luo, Y., Teng, Z. and Wang, Q. (2012) 'Development of Zein Nanoparticles Coated with Carboxymethyl Chitosan for Encapsulation and Controlled Release of Vitamin D3', *Journal of Agricultural and Food Chemistry*, 60(3), pp. 836–843.

Maeda, H. *et al.* (2000) 'Tumor vascular permeability and the EPR effect in macromolecular therapeutics: A review', *Journal of Controlled Release*, pp. 271–284.

Mahjub, R. *et al.* (2014) 'Lyophilized insulin nanoparticles prepared from quaternized N-aryl derivatives of chitosan as a new strategy for oral delivery of insulin: in vitro, ex vivo and in vivo characterizations', *Drug Development and Industrial Pharmacy*, 40(12), pp. 1645–1659.

Mann, F. M. (2015) 'Identification and Analysis of Bioactive Components of Fruit and Vegetable Products', *Journal of Chemical Education*, 92(5), pp. 892–895.

Martirosyan, A. and Schneider, Y.-J. (2014) 'Engineered nanomaterials in food: implications for food safety and consumer health.', *International Journal of Environmental Research and Public Health*, 11(6), pp. 5720–50.

McClements, D. J. (2012) *Encapsulation Technologies and Delivery Systems for Food Ingredients and Nutraceuticals*, Elsevier.

McClements, D. J. (2012) 'Nanoemulsions versus microemulsions: terminology, differences, and similarities', *Soft Matter*, 8(6), pp. 1719–1729.

McClements, D. J. (2015) 'Enhancing nutraceutical bioavailability through food matrix design', *Current Opinion in Food Science*, 4, pp. 1–6.

McClements, D. J., Decker, E. a. and Weiss, J. (2007) 'Emulsion-based delivery systems for lipophilic bioactive components', *Journal of Food Science*, 72(8), pp. 109–124.

McClements, D. J. and Li, Y. (2010) 'Structured emulsion-based delivery systems: Controlling the digestion and release of lipophilic food components', *Advances in Colloid and Interface Science*, 159(2), pp. 213–228.

Mehnert, W. (2001) 'Solid lipid nanoparticles Production, characterization and applications', *Advanced Drug Delivery Reviews*, 47(2–3), pp. 165–196.

Mehnert, W. and Mäder, K. (2012) 'Solid lipid nanoparticles', *Advanced Drug Delivery Reviews*, 64, pp. 83–101.

Miele, E. *et al.* (2009) 'Albumin-bound formulation of paclitaxel (Abraxane® ABI-007) in the treatment of breast cancer', *International Journal of Nanomedicine*, pp. 99–105.

Mishra, N. *et al.* (2012) 'Phyto–vesicles: conduit between conventional and novel drug delivery system', *Asian Pacific Journal of Tropical Biomedicine*, 2(3), pp. S1728–S1734.

Mohanraj, V. J. and Chen, Y. (2007) 'Nanoparticles - A review', *Tropical Journal of Pharmaceutical Research*, 5(1), pp. 561–573.

Molina, V. *et al.* (2012) 'Soybean-based functional food with vitamin B12-producing lactic acid bacteria', *Journal of Functional Foods*, pp. 831–836.

Moncada-Pazos, A. *et al.* (2011) 'The nutraceutical flavonoid luteolin inhibits ADAMTS-4 and ADAMTS-5 aggrecanase activities', *Journal of Molecular Medicine*, 89(6), pp. 611–619.

Mukherjee, S., Ray, S. and Thakur, R. S. (2009) 'Solid Lipid Nanoparticles: A Modern Formulation Approach in Drug Delivery System', *Indian Journal of Pharmaceutical Sciences*, 71(4), pp. 349–358.

Mukhopadhyay, P. *et al.* (2013) 'Oral insulin delivery by self-assembled chitosan nanoparticles: in vitro and in vivo studies in diabetic animal model.', *Materials Science & Engineering. C, Materials for Biological Applications*, 33(1), pp. 376–82.

Mulholland, P. J. *et al.* (2001) 'Pre-clinical and clinical study of QC12, a water-soluble, pro-drug of quercetin', *Annals of Oncology* , 12(2), pp. 245–248.

Ngele, R., Belitz, H.-D. and Wieser, H. (1991) 'Analysis of food and feed via partial sequences of characteristic protein components (Leitpeptide). 1. Isolation and identification of wheat-specific peptides from chymotryptic hydrolyzates of gliadin', *Zeitschrift fr Lebensmittel-Untersuchung und -Forschung*, pp. 415–421.

Nabi-Meibodi, M. *et al.* (2013) 'Optimized double emulsion-solvent evaporation process for production of solid lipid nanoparticles containing baclofene as a lipid insoluble drug', *Journal of Drug Delivery Science and Technology*, 23(3), pp. 225–230.

Nair, H. B. *et al.* (2010) 'Delivery of antiinflammatory nutraceuticals by nanoparticles for the prevention and treatment of cancer.', *Biochemical Pharmacology*, 80(12), pp. 1833–43.

Nel, A. E. *et al.* (2009) 'Understanding biophysicochemical interactions at the nano–bio interface', *Nature Materials*, 8(7), pp. 543–557.

Neves, A. R. *et al.* (1999) 'Resveratrol in Medicinal Chemistry: a Critical Review', *Food Chemistry*, 47(10), pp. 4456–4461.

Nobs, L. *et al.* (2004) 'Poly(lactic acid) nanoparticles labeled with biologically active Neutravidin for active targeting.', *European Journal of Pharmaceutics and Biopharmaceutics*, 58(3), pp. 483–90.

Nogueira, C. M. *et al.* (2012) 'Titanium dioxide induced inflammation in the small intestine', *World Journal of Gastroenterology : WJG*, 18(34), pp. 4729–4735.

Nordeen, S. K. *et al.* (2013) 'Endocrine Disrupting Activities of the Flavonoid Nutraceuticals Luteolin and Quercetin', *Hormones and Cancer*, 4(5), pp. 293–300.

Oberdörster, G. *et al.* (2005) 'Principles for characterizing the potential human health effects from exposure to nanomaterials: elements of a screening strategy.', *Particle and Fibre Toxicology*, 2, p. 8.

Oberdörster, G. (2010) 'Safety assessment for nanotechnology and nanomedicine: concepts of nanotoxicology', *Journal of Internal Medicine*, 267(1), pp. 89–105.

Oberdörster, G., Oberdörster, E. and Oberdörster, J. (2005) 'Nanotoxicology: An Emerging Discipline Evolving from Studies of Ultrafine Particles', *Environmental Health Perspectives*, 113(7), pp. 823–839.

Onoue, S. *et al.* (2012) 'Novel solid self-emulsifying drug delivery system of coenzyme Q_{10} with improved photochemical and pharmacokinetic behaviors.', *European Journal of Pharmaceutical Sciences*, 46(5), pp. 492–9.

Owens, D. E. and Peppas, N. A. (2006) 'Opsonization, biodistribution, and pharmacokinetics of polymeric nanoparticles', *International Journal of Pharmaceutics*, 307(1), pp. 93–102.

Özcan, P. *et al.* (2015) 'Protective effect of resveratrol against oxidative damage to ovarian reserve in female sprague–dawley rats', *Reproductive BioMedicine Online*, 31(3), pp.404-410.

Paliwal, R. and Palakurthi, S. (2014) 'Zein in controlled drug delivery and tissue engineering.', *Journal of Controlled Release*, 189, pp. 108–22.

Pan, Y.-H. *et al.* (2009) '3D morphology of the human hepatic ferritin mineral core: new evidence for a subunit structure revealed by single particle analysis of HAADF-STEM images', *Journal of Structural Biology*, 166(1), pp. 22–31.

Pandita, D. *et al.* (2014) 'Solid lipid nanoparticles enhance oral bioavailability of resveratrol, a natural polyphenol', *Food Research International*, 62, pp. 1165–1174.

Papageorgiou, I. *et al.* (2007) 'The effect of nano-and micron-sized particles of cobalt–

chromium alloy on human fibroblasts in vitro', *Biomaterials*, 28(19), pp. 2946–2958.

Park, J. S. *et al.* (2013) 'Poly(N-isopropylacrylamide-co-acrylic acid) nanogels for tracing and delivering genes to human mesenchymal stem cells', *Biomaterials*, 34(34), pp. 8819–8834.

Patel, A., Cholkar, K. and Mitra, A. K. (2014) 'Recent developments in protein and peptide parenteral delivery approaches', *Therapeutic Delivery*, 5(3), pp. 337–365.

Patel, N., Schmid, U. and Lawrence, M. J. (2006) 'Phospholipid-based microemulsions suitable for use in foods', *Journal of Agricultural and Food Chemistry*, 54(20), pp. 7817–7824.

Pérez-Esteve, É. *et al.* (2015) 'Mesoporous Silica-Based Supports for the Controlled and Targeted Release of Bioactive Molecules in the Gastrointestinal Tract', *Journal of Food Science*, 80(11), pp. E2504–E2516.

Pol, A. and Patravale, V. (2009) 'Novel lipid based systems for improved topical delivery of antioxidants', *Household and Personal Care Today*, 4, pp. 5–8.

Powell, J. J. *et al.* (2010) 'Origin and fate of dietary nanoparticles and microparticles in the gastrointestinal tract', *Journal of Autoimmunity*, 34(3), pp. J226–J233.

Puri, A. *et al.* (2009) 'Lipid-based nanoparticles as pharmaceutical drug carriers: from concepts to clinic.', *Critical Reviews in Therapeutic Drug Carrier Systems*, 26(6), pp. 523–580.

Puzyn, T. *et al.* (2011) 'Using nano-QSAR to predict the cytotoxicity of metal oxide nanoparticles', *Nature Nanotechnology*, 6(3), pp. 175–178.

Rashidi, L. and Khosravi-Darani, K. (2011) 'The Applications of Nanotechnology in Food Industry', *Critical Reviews in Food Science and Nutrition*, 51(8), pp. 723–730.

Ravichandran, R. (2010) 'Nanotechnology applications in food and food processing: Innovative green approaches, opportunities and uncertainties for global market', *International Journal of Green Nanotechnology: Physics and Chemistry*, 1(2), pp. P72–P96.

Resnik, D. B. and Tinkle, S. S. (2007) 'Ethics in Nanomedicine', *Nanomedicine*, 2(3), pp. 345–350.

Říhová, B. (2007) 'Biocompatibility and immunocompatibility of water-soluble polymers based on HPMA', *Composites Part B: Engineering*, 38(3), pp. 386–397.

Rinaudo, M. (2006a) ‘Chitin and chitosan: Properties and applications’, *Progress in Polymer Science*, 31(7), pp. 603–632.

Rinaudo, M. (2006b) ‘Non-covalent interactions in polysaccharide systems’, *Macromolecular Bioscience*, 6(8), pp. 590–610.

Rizzo, M. *et al.* (2013) ‘Effects of Chitosan on Plasma Lipids and Lipoproteins: A 4-Month Prospective Pilot Study.’, *Angiology*, 65(6), pp.538-542.

Roberts, L. M. *et al.* (2013) ‘A randomised controlled trial of a probiotic “functional food” in the management of irritable bowel syndrome.’, *BMC gastroenterology*, 13(1), p. 45.

Roblegg, E. *et al.* (2012) ‘Evaluation of a physiological in vitro system to study the transport of nanoparticles through the buccal mucosa’, *Nanotoxicology*, 6(4), pp. 399–413.

Ron, N. *et al.* (2010) ‘Beta-lactoglobulin–polysaccharide complexes as nanovehicles for hydrophobic nutraceuticals in non-fat foods and clear beverages’, *International Dairy Journal*, 20(10), pp. 686–693.

Saini, D. *et al.* (2014) ‘Formulation, development and optimization of raloxifene-loaded chitosan nanoparticles for treatment of osteoporosis’, *Drug Delivery*, pp. 1–14.

Sakai-Kato, K. *et al.* (2014) ‘Physicochemical properties and in vitro intestinal permeability properties and intestinal cell toxicity of silica particles, performed in simulated gastrointestinal fluids’, *Biochimica et Biophysica Acta - General Subjects*, 1840(3), pp. 1171–1180.

Sarmento, B. *et al.* (2006) ‘Development and Comparison of Different Nanoparticulate Polyelectrolyte Complexes as Insulin Carriers’, *International Journal of Peptide Research and Therapeutics*, 12(2), pp. 131–138.

Sarvaiya, J. and Agrawal, Y. K. (2015) ‘Chitosan as a suitable nanocarrier material for anti-Alzheimer drug delivery’, *International Journal of Biological Macromolecules*, 72, pp. 454–465.

Sastry, S. V., Nyshadham, J. R. and Fix, J. A. (2000) ‘Recent technological advances in oral drug delivery – a review’, *Pharmaceutical Science & Technology Today*, 3(4), pp. 138–145.

Savouret, J. . and Quesne, M. (2002) ‘Resveratrol and cancer: a review’, *Biomedicine & Pharmacotherapy*, 56(2), pp. 84–87.

Scientific Committee on Emerging and Newly Identified Health Risks. (2007) ‘Opinion on the appropriateness of the risk assessment methodology in accordance with the technical

guidance documents for new and existing substances for assessing the risk of nanomaterials'

Scrinis, G. and Lyons, K. (2007) 'The emerging nano-corporate paradigm: nanotechnology and the transformation of nature, food and agri-food systems', *International Journal of Sociology of Food and Agriculture*, 15(2), pp. 22–44.

Seelinger, G. *et al.* (2008) 'Anti-carcinogenic effects of the flavonoid luteolin', *Molecules*, pp. 2628–2651.

Sharma, B. *et al.* (2009) 'Effects of guggulsterone isolated from Commiphora mukul in high fat diet induced diabetic rats.', *Food and Chemical Toxicology*, 47(10), pp. 2631–9.

Shoji, Y. and Nakashima, H. (2004) 'Nutraceutics and delivery systems.', *Journal of Drug Targeting*, 12(6), pp. 385–391.

Simopoulos, A. P. (2002) 'Omega-3 fatty acids in inflammation and autoimmune diseases.', *Journal of the American College of Nutrition*, 21(6), pp. 495–505.

Singh, R. and Lillard, J. W. (2009) 'Nanoparticle-based targeted drug delivery.', *Experimental and Molecular Pathology*, 86(3), pp. 215–23.

Singh, S. *et al.* (2007) 'Endocytosis, oxidative stress and IL-8 expression in human lung epithelial cells upon treatment with fine and ultrafine TiO 2: role of the specific surface area and of surface methylation of the particles', *Toxicology and Applied Pharmacology*, 222(2), pp. 141–151.

Smolkova, B. *et al.* (2015) 'Nanoparticles in food. Epigenetic changes induced by nanomaterials and possible impact on health', *Food and Chemical Toxicology*, 77, pp. 64–73.

Soares, S. *et al.* (2013) 'Effect of freeze-drying, cryoprotectants and storage conditions on the stability of secondary structure of insulin-loaded solid lipid nanoparticles.', *International Journal of Pharmaceutics*, 456(2), pp. 370–81.

Song, F. *et al.* (2009) 'Genipin-crosslinked casein hydrogels for controlled drug delivery', *International Journal of Pharmaceutics*, 373(1–2), pp. 41–47.

Song, L. L. *et al.* (2011) 'β-carotene radical cation addition to green tea polyphenols. Mechanism of antioxidant antagonism in peroxidizing liposomes', *Journal of Agricultural and Food Chemistry*, 59(23), pp. 12643–12651.

Song, W. O. *et al.* (2007) 'Soy isoflavones as safe functional ingredients.', *Journal of Medicinal Food*, 10(4), pp. 571–580.

De Souza, V. R. *et al.* (2014) 'Determination of the bioactive compounds, antioxidant activity and chemical composition of Brazilian blackberry, red raspberry, strawberry, blueberry and sweet cherry fruits.', *Food Chemistry*, 156, pp. 362–8.

Sozer, N. and Kokini, J. L. (2009) 'Nanotechnology and its applications in the food sector.', *Trends in Biotechnology*, 27(2), pp. 82–9.

Spernath, A. and Aserin, A. (2006) 'Microemulsions as carriers for drugs and nutraceuticals', *Advances in Colloid and Interface Science*, pp. 47–64.

Srinivas, P. R. *et al.* (2010) 'Nanotechnology research: applications in nutritional sciences.', *The Journal of Nutrition*, 140(1), pp. 119–24.

Suh, J.-K. F. and Matthew, H. W. T. (2000) 'Application of chitosan-based polysaccharide biomaterials in cartilage tissue engineering: a review', *Biomaterials*, 21(24), pp. 2589–2598.

Sun, F. *et al.* (2012) 'Nanoparticles Based on Hydrophobic Alginate Derivative as Nutraceutical Delivery Vehicle: Vitamin D3 Loading', *Artificial Cells, Blood Substitutes, and Biotechnology*, 40(1–2), pp. 113–119.

Sunasee, R. *et al.* (2014) 'Therapeutic potential of carbohydrate-based polymeric and nanoparticle systems.', *Expert Opinion on Drug Delivery*, 11(6), pp. 867–84.

Susa, M. *et al.* (2009) 'Doxorubicin loaded polymeric nanoparticulate delivery system to overcome drug resistance in osteosarcoma', *BMC cancer*, 9(1), p. 399.

Thilakarathna, S. H. and Rupasinghe, H. P. V. (2012) 'Anti-atherosclerotic effects of fruit bioactive compounds: A review of current scientific evidence', *Canadian Journal of Plant Science*, 92(3), pp. 407–419.

Thiruvengadathan, R. *et al.* (2013) 'Nanomaterial processing using self-assembly-bottom-up chemical and biological approaches.', *Reports on Progress in Physics*, 76(6), p. 66501.

Thomas, T. *et al.* (2013) 'Design and In vitro Validation of Multivalent Dendrimer Methotrexates as a Folate-targeting Anticancer Therapeutic', *Current Pharmaceutical Design*, 19(37), pp. 6594–6605.

Ting, Y. *et al.* (2014) 'Common delivery systems for enhancing in vivo bioavailability and biological efficacy of nutraceuticals', *Journal of Functional Foods*, 7, pp. 112–128.

Ubbink, J. and Krüger, J. (2006) 'Physical approaches for the delivery of active ingredients in foods', *Trends in Food Science and Technology*, 17(5), pp. 244–254.

Umerska, A. *et al.* (2012) 'Exploring the assembly process and properties of novel

crosslinker-free hyaluronate-based polyelectrolyte complex nanocarriers', *International Journal of Pharmaceutics*, 436(1–2), pp. 75–87.

Velikov, K. P. and Pelan, E. (2008) 'Colloidal delivery systems for micronutrients and nutraceuticals', *Soft Matter*, p. 1964.

Verbeke, W. (2005) 'Consumer acceptance of functional foods: socio-demographic, cognitive and attitudinal determinants', *Food Quality and Preference*, 16(1), pp. 45–57.

Wacker, M. G. (2014) 'Nanotherapeutics - Product development along the nanomaterial discussion', *Journal of Pharmaceutical Sciences*, pp. 777–784.

Wahajuddin and Arora, S. (2012) 'Superparamagnetic iron oxide nanoparticles: Magnetic nanoplatforms as drug carriers', *International Journal of Nanomedicine*, pp. 3445–3471.

Wang, P. *et al.* (2013) 'The formulation and delivery of curcumin with solid lipid nanoparticles for the treatment of non-small cell lung cancer both in vitro and in vivo.', *Materials science & engineering. C, Materials for Biological Applications*, 33(8), pp. 4802–8.

Wang, S. *et al.* (2014) 'Application of nanotechnology in improving bioavailability and bioactivity of diet-derived phytochemicals', *Journal of Nutritional Biochemistry*, 25(4), pp. 363–376.

Wilson, C. M. (1991) 'Multiple Zeins from Maize Endosperms Characterized by Reversed-Phase High Performance Liquid Chromatography', *Plant Physiology* , 95(3), pp. 777–786.

Xiao, D., Davidson, P. M. and Zhong, Q. (2011) 'Spray-dried zein capsules with coencapsulated nisin and thymol as antimicrobial delivery system for enhanced antilisterial properties', *Journal of Agricultural and Food Chemistry*, 59(13), pp. 7393–7404.

Xijun, L. *et al.* (2014) 'Effects of Protein in Wheat Flour on Retrogradation of Wheat Starch', *Journal of Food Science*, 79(8), pp. C1505–C1511.

Xu, Y. and Du, Y. (2003) 'Effect of molecular structure of chitosan on protein delivery properties of chitosan nanoparticles', *International Journal of Pharmaceutics*, 250(1), pp. 215–226.

Yang, L. *et al.* (2004) 'Comparison of extraction methods for quantitation of methionine and selenomethionine in yeast by species specific isotope dilution gas chromatography-mass spectrometry', *Journal of Chromatography A*, 1055(1–2), pp. 177–184.

Yao, M., McClements, D. J. and Xiao, H. (2015) 'Improving oral bioavailability of

nutraceuticals by engineered nanoparticle-based delivery systems', *Current Opinion in Food Science*, 2, pp. 14–19.

Yoon, H. Y. *et al.* (2014) 'Glycol chitosan nanoparticles as specialized cancer therapeutic vehicles: Sequential delivery of doxorubicin and Bcl-2 siRNA', *Scientific Reports*, 4, p. 6878.

Yuan, R. *et al.* (2014) 'Self-Assembled Nanoparticles of Glycyrrhetic Acid-Modified Pullulan as a Novel Carrier of Curcumin', *Molecules*, 19(9), pp. 13305–13318.

Zhang, L. *et al.* (2014) 'Imprinted-like biopolymeric micelles as efficient nanovehicles for curcumin delivery', *Colloids and Surfaces B: Biointerfaces*, 123, pp. 15–22.

Zhang, Y. *et al.* (2015) 'Zein-based films and their usage for controlled delivery: Origin, classes and current landscape', *Journal of Controlled Release*, 206(2699), pp. 206–219.

Zhong, Q., Tian, H. and Zivanovic, S. (2009) 'Encapsulation of fish oil in solid zein particles by liquid-liquid dispersion', *Journal of Food Processing and Preservation*, 33(2), pp. 255–270.

Zhou, H. *et al.* (2014) 'Fumagillin Prodrug Nanotherapy Suppresses Macrophage Inflammatory Response via Endothelial Nitric Oxide', *ACS Nano*, 8(7), pp. 7305–7317.

Zhou, Y. *et al.* (2015) 'In vivo anti-apoptosis activity of novel berberine-loaded chitosan nanoparticles effectively ameliorates osteoarthritis.', *International Immunopharmacology*, 28(1), pp. 34–43.

3 RESEARCH METHODOLOGY

3.1 Design of experiments: Response Surface Methodology

Response surface methodology (RSM) is an empirical modelling approach for defining the relationship between various process parameters and responses with various desired criteria and searching the significance of these process parameters on the coupled responses. Originally developed by Box & Wilson (1952), RSM is based on the fit of mathematical models (linear, square polynomial functions and others) to experimental results produced from a designed experiment and the verification of the model obtained by means of statistical techniques. In situations where several variables may influence system properties, RSM is a useful technique to employ as it allows for the relationships between a given response and independent variables (or factors) to be identified and optimised (Anderson and Whitcomb, 2005). RSM is a more efficient approach to experimentation than one factor at a time (OFAT) experiments due to the fact that it:

1. Reduces the number of experimental runs typically required to gather the same information as OFAT, thus reducing resource requirements.
2. Is useful in detecting interaction amongst variables that would not be typically identified during OFAT experiments.
3. Improves the prediction of a response through use of gathered information from a larger space.

Two of the most commonly applied RSM designs for process optimisation are the CCD and BBD (Dayal *et al.*, 2005; Singh, Chakkal and Ahuja, 2006; Varshosaz, Tabbakhian and Mohammadi, 2010; Anarjan *et al.*, 2011; Nabi-Meibodi *et al.*, 2013; Maleki Dizaj *et al.*, 2015). Both methods require the user to supply minimum and maximum values for each factor that defines the experimental domain to be investigated during the optimisation procedure (Ferreira *et al.*, 2007). The combinations of the different factor

levels used to perform the actual experiments are subjected to multivariate optimisation by employing the following steps (Ferreira *et al.*, 2007).

1. Run experiments in random order to mitigate bias
2. Fit a full polynomial regression model on the obtained data.
3. Identify the significant terms via analysis of variance (ANOVA).
4. Assess the R^2 or R^2 adjusted to determine how well the constructed model explains variation (ideally as close to 1 as possible).
5. Ensure that there is no evidence of lack of fit for the produced model of the representative data.
6. Construct an objective function either with the individual response or the linear combination of all the responses (Desirability function)
7. Examine contour and surface plots and perform canonical analysis in order to identify optimum variable conditions.

CCD considers 5 levels of factors with three different design points: edge points as in two-level designs (±1), star points at (±α), that take care of quadratic effects and centre points (α) that allow for the estimation of error (Bezerra *et al.*, 2008). CCD designs provide predictions over the entire design space, although, when factor levels are at extreme points in the design, loss of information may occur (Singh, Chakkal and Ahuja, 2006).

BBD is an independent quadratic design approach in which factor combinations are considered at 3 levels: the midpoints of edges of the process space and the centre. The primary advantage is in addressing the issue of where the experimental boundaries should be, and in particular to avoiding treatment combinations that are extreme (Sivamani and Baskar, 2015). As the design avoids extreme experiment points, a reduced number of experimental runs is required for BBDs than that of CCDs. However, it should be

emphasised that the vertices of the cube are not covered by the design, and therefore, prediction at these points is an extrapolation and should be avoided (Zolgharnein, Shahmoradi and Ghasemi, 2013)

3.1.1 Nanoparticle characterisation

As discussed in chapter 1 (section 1.2), to ensure activity of a bioactive within a NP oral delivery system, it is recommended to achieve specific physicochemical properties such as a NP size of 100-500 nm, PDI $\leq$ 0.5 and ZP $\geq$ 30 mV (des Rieux *et al.*, 2006). In this work, these properties were measured using the following methodologies.

3.1.2 Particle Size and Zeta Potential Characterisation using DLS

A powerful technique employed for the sizing of NPs and their and characterisation in the liquid phase is DLS, in which a laser beam is passed through the NPs (in suspension) and is scattered by the particles. DLS measures random Brownian motion, whereby the smaller the particle, the more rapidly it moves, the viscosity of the solution also playing a role in the analysis. Fundamentally, the Stokes-Einstein equation allows us to link Brownian motion with the NP size, by measuring the time dependant fluctuations in the scattering intensity, allowing for determination of the translational diffusion coefficient (D), and subsequently the hydrodynamic radius (Uskoković, 2012). The ZP of NPs can be indirectly detected with DLS based on electrophoretic mobility of particles and calculated by the application of the Henry equation. This provides information of the colloidal stability of the nanoparticles (Malvern Instruments Ltd., 2007).

In Chapters 4, 5, 6 & 8, freshly prepared NP solutions were analysed. The mean particle size and PDI of the NP formulations were determined by DLS. The ZP values were

measured with the use of laser Doppler velocimetry (LDV). Both DLS and LDV analysis were performed in triplicate at 25 °C with a Zetasizer Nano series Nano-ZS ZEN3600, fitted with a 633 nm laser (Malvern Instruments Ltd., UK), using a folded capillary cuvette (Folded capillary cell-DTS1060, Malvern, UK). The values presented herein were acquired from three separate experiments, each of which included three replicates, N=3.

3.1.3 Scanning electron microscopy (SEM)

SEM produces images of a sample by scanning it with a focused beam of electrons. Different types of electron signals, emitted at or near the specimen surface, arise as a consequence of interactions between the sample and the electron beam that scans across the sample surface. These electronic signals are then collected, processed, and eventually translated as pixels on a monitor to form an image of the specimen's surface topography that appears three dimensional (Carter *et al.*, 2015). SEM can achieve a resolution of up to 1 nm. Specimens can be observed in high vacuum, in low vacuum, in wet conditions (in environmental SEM), and at a wide range of cryogenic or elevated temperatures (Stokes, 2003).

In this work (Chapters 4, 5, 6 & 8), NP morphology was evaluated by SEM (Hitachi, SU6600 FESEM, USA), at an accelerating voltage of 20 kV, using the secondary electron detector. The fresh NP solutions were spin coated onto Si wafers, dried at room temperature and then sputter coated with 4 nm Au/Pd prior to imaging (Mukhopadhyay *et al.*, 2013).

3.1.4 Encapsulation efficiency

Encapsulation efficiency (EE%), refers to the percentage amount of a given bioactive entrapped within a colloidal system, after the formulation process (Koppolu *et al.*, 2014). Personal communication with various industrial stakeholders in this project set the target of EE% to be ≥ 80%.

In this work (Chapters 5, 6 & 8), the EE% of organic Se entrapped within the produced NPs was determined by the separation and quantification of Se left in the supernatant. This was performed by ultracentrifugation of the loaded NPs at 3000 rpm, 4 °C for 30 min. Unentrapped Se in the supernatant was then quantified by reverse phase high performance liquid chromatography (RP-HPLC), as previously described (Ward, Connolly and Murphy, 2012) with the following modifications. Samples were analysed with a Waters 2998 HPLC and Photodiode Array Detector, (Waters, USA), using a Poroshell 120, EC-C8 column, 3.0 x 100 mm, 2.7 μm, (Agilent Technologies, UK). Isocratic elution was carried out at a flow rate of 0.4 mL/min, column temperature 45.0 ± 5.0 °C with a mobile phase of water/methanol/trifluoroacetic acid (97.9:2.0:0.1). Samples were monitored according to their UV absorbance at 218 nm. The encapsulation efficiency was calculated according to Equation 3.1 (Xu and Du, 2003):

$$EE\% = \frac{Total\ amount\ of\ Se\ Met - Free\ amount\ of\ SeMet}{Total\ amount\ of\ SeMet}\ X\ 100$$

(Equation 3.1)

3.2 Nanoparticle *in vitro* assessment

3.2.1 Cytotoxicity

The cytotoxicity of a specific material or carrier for a specific *in vivo* application is initially accessed via *in vitro* testing. In this work, a commonly employed cytotoxicity assay which employs a tetrazolium salt, MTS (3-(4,5-dimethylthiazol-2-yl)-5-(3-carboxymethoxyphenyl)-2-(4-sulfophenyl)-2H-tetrazolium), was used.

This assay is based on the reduction of MTS tetrazolium compound by viable cells to generate a coloured soluble formazan product. This conversion is due to NAD(P)H-dependent dehydrogenase enzymes in metabolically active cells. The formazan dye produced by viable cells can be quantified by measuring the absorbance at 490-500 nm. MTS is a derivative of the more commonly employed MTT (3-(4,5-dimethylthiazol-2-yl)-2,5-diphenyltetrazolium bromide) test, which produces a dye within cells with functioning mitochondrial activity. The MTS assay has the advantage that the reagent is added directly into the cell culture media without the intermittent steps which are required in the routine MTT assay (Malich, Markovic and Winder, 1997).

Generally, it is accepted that an early indication of cellular damage is related to the reduction of cellular metabolic activity (Rodrigues *et al*. 2012). Regardless of whether one uses MTS or MTT, both indicate mitochondrial activity dysfunction, which can be used to detect disrupted cell function (Rodrigues *et al*. 2012). The higher the assay response, the higher the amount of metabolically active cells, which indicates higher cell viability.

Cytotoxicity was assessed using human cell lines: Caco-2 (derived from continuous cells of heterogeneous human epithelial colorectal adenocarcinoma) and HepG2 (derived from, human hepatocellular carcinoma), to assess whether the NPs formed would be suitable for oral delivery.

In Chapters 5, 6 & 8, Caco-2 and HepG2, were seeded at a cell density of 2 x 10^4 cells/well and cultured on 96 well plates in Dulbecco's Modified Eagle Medium (DMEM) and Eagle's Minimum Essential Medium (EMEM), respectively, supplemented with 10% foetal bovine serum, 1% L-glutamine, 1% penicillin-streptomycin and 1% non-essential amino acids at 37°C in a humidified incubator with 5% CO_2 and 95% O_2. The assay was carried out using 4 h exposure times for the test compounds on Caco-2 cells (Neves *et al.*, 2016) and 72 h on HepG2 cells (Gleeson *et al.*, 2015), using Triton X-100™ (0.05%) as a positive control. The time points were selected to mimic *in vivo* conditions for each cell type. The concentrations of the test compounds applied were 25, 50 and 100 uM. After exposure, treatments were removed and replaced with MTS (3-(4,5-dimethylthiazol-2-yl)-5-(3-carboxymethoxyphenyl)-2-(4-sulfophenyl)-2H-tetrazolium). Optical density (OD) was measured at 490 nm using a microplate reader (TECAN GENios, Grodig, Austria). Each value measured was normalised against untreated control and calculated from three separate experiments, each of which included six replicates.

3.2.2 Accelerated stability studies

The principle aim of accelerated stability testing is to provide reasonable assurance that the product will remain at an acceptable level of fitness/quality throughout its timespan in the market place (Bajaj *et al.*, 2012). Broadly speaking, real-time, retained sample, cyclic temperature and acceleration, are the four categories into which stability testing procedures fall (Bhagyashree *et al.*, 2015). In the latter, the product is subjected to

elevated temperatures and/or humidity well above ambient values, to determine the temperature at which product failure (i.e. degradation) will occur.

The Arrhenius equation, upon which the interpretation of accelerated stability testing is based, allows for the determination of the activation energy and consequently, the ability to extrapolate the degradation rate of a product at lower temperatures (i.e. ambient, refrigerated etc.). In this instance, the data acquired can then be used to project the shelf life of the product in a much shorter time than that of real time assessments (Ema, 2003). This is a beneficial approach to stability testing, as it results in a greatly reduced product development schedule and provides a good indication of the temperature sensitivity of the product.

In this work (Chapters 5, 6 & 8), NPs were stored at accelerated conditions: 60°C for 720min, 70°C for 300min and 80°C for 120min (Danish *et al.*, 2017). The particle size, PDI and ZP were measured over different time intervals, to determine the degree of degradation. The temperature dependence of the kinetic parameters of organic Se-loaded NPs stability was measured by calculating the observed rate constants.

This was plotted in an Arrhenius representation and apparent activation energy, E_a and reaction rate, k_{ref} were calculated according to Equation 3.2:

$$\boldsymbol{C(t) = Co + e^{ln(k) - \frac{Ea}{R}\left(\frac{1}{T} - \frac{1}{T_{ref}}\right)t}}$$

(Equation 3.2)

where C(t) is the property (particle size, PDI or ZP) at time t, Co is the initial property conditions, k is the apparent zero order reaction constant, E_a is the energy of activation, R is the universal gas constant, T is the temperature of the experiment (K) and T_{ref} is the reference temperature (343 K).

3.2.3 *In vitro* controlled release studies

In vitro techniques are advantageous for modelling potential interactions between NPs and the *in vivo* environment of the GI tract. Simulated gastric fluid and membrane analysis models enable assessment of *in vivo* environments without the use of human cell lines. The site of target for Se is in the jejunum, in the small intestine. Therefore, it is important to bypass the acidic stomach environment. Three basic mechanisms that are typically applied to describe the release of drugs from polymeric particles, are swelling/erosion, diffusion, and degradation (Liechty *et al.*, 2010).

In this work (Chapters 5, 6 & 8), the total cumulative release of organic Se (SeMet, $SeCys_2$ or MSC) from the zein coated NPs was carried out using a dialysis bag diffusion technique (Hosseinzadeh *et al.*, 2012) over 6 hr (Calderon *et al*., 2013; Yoon *et al*., 2014). Freeze dried Se loaded NPs were suspended in 5 mL H_2O and probe sonicated (Branson Ultrasonics; Ultrasonic processor VCX-750W, Wilmington, North Carolina, USA) at 35 % amplitude for 30 s with 5 s intervals and placed into a Float-A-Lyzer®G2 dialysis membrane with a pore size of 25 kDa (Spectrum Laboratories, USA). The sample was placed into 40 mL of simulated gastric fluid (SGF) or simulated intestinal fluid (SIF), specified according to the British Pharmacopoeia (Pharmacopoeia, 2016). SGF was composed of 0.1 M HCL and SIF was composed of 1 volume of 0.2 M trisodium phosphate dodecahydrate and 3 volumes of 0.1 M HCL (adjusted to pH 6.8), without enzymes (British Pharmacopoeia Commission, 2016). Samples were placed in a thermostatic shaker at 37 ºC and agitated at 100 rpm. At predetermined time points, 1mL of release fluid was analysed and replaced with simulated fluid to maintain sink conditions.

Se release was measured by RP-HPLC (section 3.2.3), whereby Equation 3.3 was used to determine the % drug release;

$$\boldsymbol{Drug_{rel}}\,\% = \frac{\boldsymbol{D(t)}}{\boldsymbol{D(l)}} * \mathbf{100}$$

(Equation 3.3)

where $\boldsymbol{Drug_{rel}}$ is the percentage of SeMet released, D(*l*) represents the concentration of drug loaded and D(t) represents the amount of drug released at time t, respectively.

3.3 Chitin/Chitosan characterisation

In Chapter 7, several techniques were employed in the characterisation of chitin (CT), chitosan (Cs) and trimethyl chitosan (TMC) produced during this project, as detailed in the following subsections.

3.3.1 Fourier Transform Infrared spectroscopy– Quantitative analysis

In the infrared (IR) region of the electromagnetic spectrum, all covalent compounds have the capability to absorb frequencies of electromagnetic radiation. Fourier Transform Infrared spectroscopy (FTIR) is a useful technique for identifying functional groups within a molecule as it identifies these groups based on the stretching and/or bending of their bonds rather than on any given property of the atoms themselves. The wavenumber unit (cm^{-1}) in the IR energy spectrum represents the inverse of wavelength and is proportional to frequency, typically extending from 4000-400 cm^{-1} (Pretsch *et al.*, 2000). This scale is directly proportional to energy, whereby a higher bond energy corresponds to a higher wavenumber. Compounds with unsymmetrical bond stretching (such as NH_2, OH and C=O) are particularly suited for this type of analysis, attributable to the increased energy required to vibrate the bond and increased intensity resultant from the change of

dipole moment when the bond is stretched (Duarte *et al.*, 2002) and as such this was employed for the quantitative analysis of CT and Cs extracted in this work (Chapter 7).

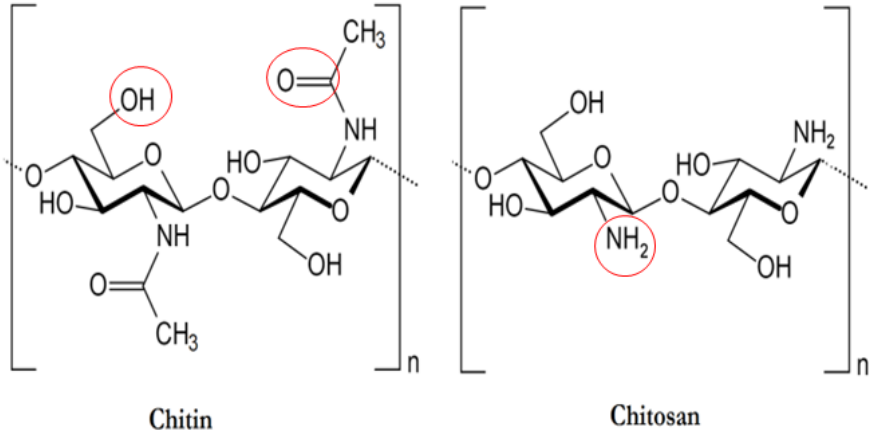

Figure 3.1 Functional groups present in chitin and chitosan structures, particularly sensitive to IR analysis.

3.3.2 Gel permeation chromatography - MW determination

MW is an important physical property of Cs and is typically determined via viscosity measurements or gel permeation chromatography (Baxter *et al*. 2005; Zielinska *et al*. 2014). GPC is a useful technique for determination of the molecular weight of polymers where analytes are separated based on the size or hydrodynamic volume (radius of gyration) of the analytes. Smaller analytes tend to be retained in the column longer than larger molecules, owing to their ability to enter the pores present within the column packing. This contrasts with other chromatographic techniques (e.g. HPLC), which depend upon chemical interactions between the columns surface chemistry (stationary phase) and the analyte of interest during separation. Polymers can be defined according to a number of conventions for molecular weight, including the number average molecular weight (Mn), the weight average molecular weight (Mw), the size average molecular weight (Mz), or the viscosity molecular weight (Mv). GPC allows for the

determination of PDI as well as Mv and, based the concentration of molecules on a weight/volume basis, the Mn, Mw, and Mz can be determined (Agilent Technologies Inc., 2015). Essentially, what GPC truly measures is the molecular volume and shape function as defined by the intrinsic viscosity. If comparable standards are used, this relative data can be used to determine molecular weights within ± 5% accuracy.

3.3.3 Nuclear magnetic resonance -NMR

Nuclear magnetic resonance (NMR) techniques, such as proton NMR (^{1}H NMR) and carbon NMR (^{13}C NMR) have been developed and employed to determine: the degree of acetylation (DA%) of CT (Heux *et al.*, 2000); degree of deacetylation (DDA%) of Cs (Lavertu *et al.*, 2003) and the degree of quaternisation (DQ %) of TMC (Verheul *et al.*, 2008). CT is effectively insoluble in most solvents and, as such, solid-state NMR spectroscopy is suitable tool to analyse its structure, as it mitigates the requirement for solubilisation. Figure 3.2 displays a typical ^{13}C-NMR spectra of CT which exhibits eight main peaks, whereby the peaks at 175 and 25 ppm are assigned to the carbonyl and methyl carbons, respectively, and the peaks at 103, 82, 74, 72, 59 and 55 ppm were ascribable to the resonances of C1, C4, C5, C3, C6, and C2 on the N-acetyl-D-glucosamine unit of CT, respectively (Heux *et al.*, 2000).

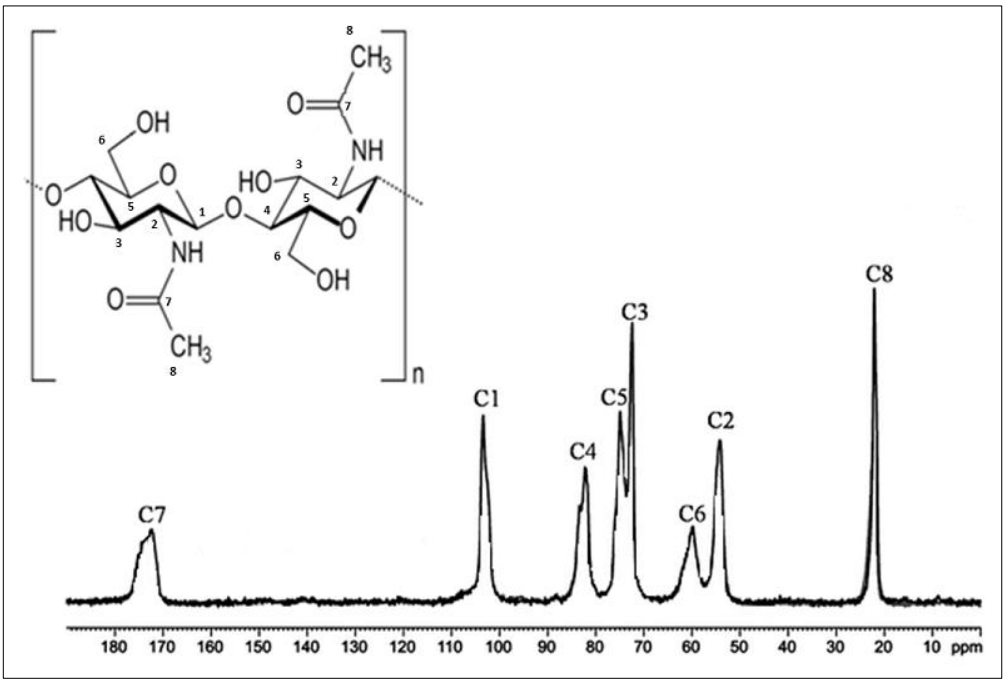

Figure 3.2 Chemical structure of chitin and ^{13}C-NMR chemical shifts associated to each carbon (adapted from Duan *et al.*, 2013).

The DA% of the CT can then be calculated using the relative integrals of methyl or carbonyl groups related to the carbon integrals of the polysaccharidic backbone (Equation 3.4,) (Heux *et al.*, 2000)**.**

$$DA = \frac{AUC_{25\,ppm}}{AUC_{175ppm}} \times 100$$

(Equation 3.4)

Several methods have been established in order to determine the DDA% of Cs, namely FTIR (Beil *et al*. 2012), potentiometric titration (Jiang *et al.* 2003), UV-Visible spectrophotometry (Wu & Zivanovic 2008) and ^{1}H-NMR spectroscopy (Lavertu *et al*. 2003; Hirai *et al*. 1991), the latter being considered the "gold standard" analytical methodology for DDA% analysis due to the lack of requirement for a calibration curve or reference sample of known DDA% (Kasaai 2010, Bellich *et al.*, 2016).

A typical ^{1}H-NMR spectra of Cs, outlining its structure and characteristic functional groups, is represented in Figure 3.3 (Kumirska *et al.*, 2011). C-H linkages are produced, via the six hydrogen and seven carbon atoms present on each unit residue. Likewise, due to the presence of four hydroxyl groups in each unit residue, O-H linkages are established (Rinaudo, 2006; Kumirska *et al.*, 2011) also. The characteristics of these unique bond environments result in each proton possessing its own unique chemical shift. Essentially, the ^{1}H-NMR spectrum of Cs reflects a superposition of the individual unit residues which become marginally modified due to their linkages to one another (Kasaai, 2010).

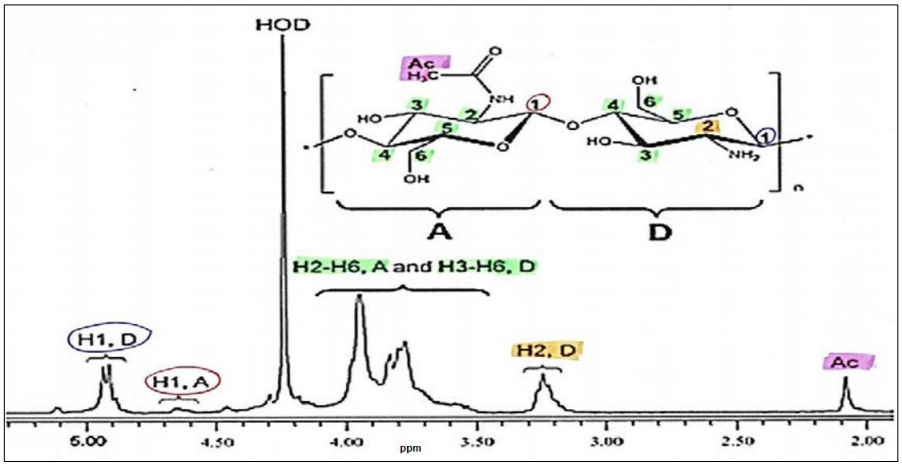

Figure 3.3 Chemical structure of chitosan and ^{1}H-NMR chemical shifts associated to each hydrogen (adapted from Weinhold *et al*. 2009).

The DDA% can then be calculated using Equation 3.5 (Lavertu *et al*. 2003):

$$\boldsymbol{DDA}\ (\%) = \frac{(\mathbf{1} - (\frac{\mathbf{1}}{\mathbf{3}}\boldsymbol{HAc})}{(\frac{\mathbf{1}}{\mathbf{6}}\boldsymbol{H26})} \times \mathbf{100}$$

(Equation 3.5)

where HAc corresponds to the methyl protons of the acetyl group and H26 represents the signal from protons H2, H3, H4, H5, H6, H6 of both monomers, through use of the integral peak intensity values (Lavertu *et al*. 2003).

Synthesis of TMC entails the methylation of the amino groups in the C-2 position of Cs to form quaternary amino groups (with fixed positive charges) on the repeating units of the TMC polymer chain (Figure 3.4 A) (Sieval, *et al*, 1998). There is also some degree of methylation on the 3 and 6 hydroxyl groups of the Cs polymer and partial quaternisation on the amine unit that can reduce the aqueous solubility of the product (Figure 3.4 B) (Verheul *et al.*, 2008).

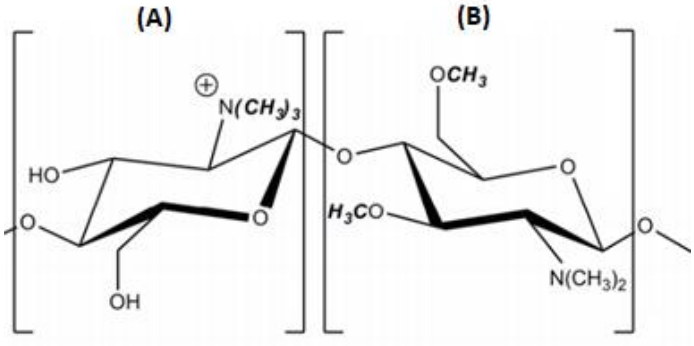

Figure 3.4 Chemical structure of TMC. TMC can vary in degree of quaternisation (A), and O-methylation (B). The various substitutions are randomly distributed throughout the polymer and mono and di-methylation (incomplete quaternisation) may occur on the amine unit also (B) (Verheul *et al.*, 2008).

Figure 3.5 shows the typical structure and characteristic functional groups of TMC as observed in ^{1}H-NMR spectra. The degree of quaternisation (% DQ) and O-methylation (OMe) can then be calculated using the following equations (Zarifpour, 2013):

$$\boldsymbol{DQ = \frac{[(CH_3)_3]}{[H]} \times \frac{1}{9} \times 100\%}$$

(Equation 3.6)

$$\boldsymbol{OMe = \frac{[(CH_3)]}{[H]} \times \frac{1}{3} \times 100\%}$$

(Equation 3.7)

where DQ is the degree of quaternisation, in mole percentage of free amine, $[(CH_3)_3]$ is the integral of chemical shift of the hydrogens of trimethyl amino groups at 3.3 ppm,

[(CH_3)] the methylated hydroxyl groups at either 3.4 (OMe-6) or 3.5 (OMe-3) ppm and [H] is the integral of H-1 peaks between 4.7 and 5.7 ppm, related to hydrogen atoms bound to carbon 1 of the chitosan molecule, which is taken as the reference signal.

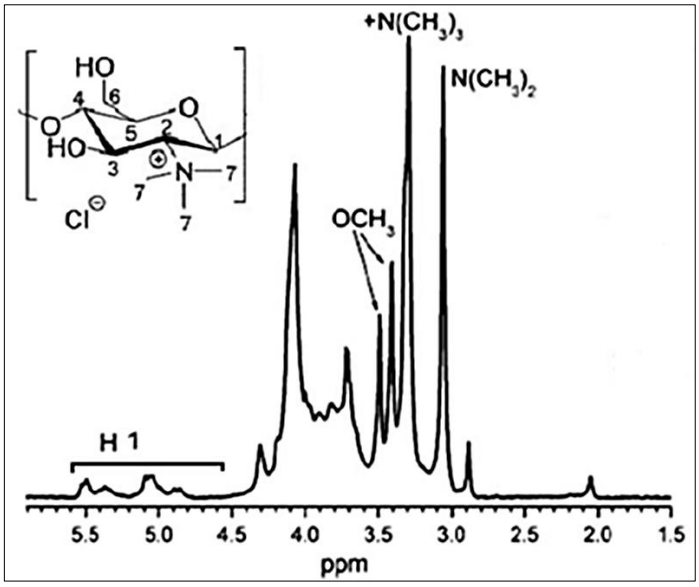

Figure 3.5 Chemical structure of TMC and ^{1}H-NMR chemical shifts associated to each hydrogen (adapted from Verheul *et al.*, 2008).

3.4 TEER-Permeation enhancement

Cs extracted from *A. bisporus* was assessed as an intestinal permeation enhancer using Caco-2 monolayers via an electrical method known as transepithelial electrical resistance (TEER, $\Omega\,cm^2$). TEER is measured across the monolayers using an EVOM® voltammeter with a chopstick-type electrode (EVOM®, WPI, UK). It allows for the assessment of transport of a molecule through tight junction (TJ) pores (paracellular route) (Hidalgo, 2001). Hydrophilic molecules must rely on transport between adjacent cells through the paracellular pathway, unless they are substrates for membrane transporters and so are not likely to transverse lipid rich cell membranes (Upadhyay, 2014). A schematic representation of paracellular and transcellular transport is shown in Figure 1.2.

In essence, the cell membrane can be thought of as an electrical insulator, in which the lipophilic components that constitute the cell membrane are responsible for maintenance of the membrane's electrical potential, in addition to inhibiting the movement of water. The tight junctions (TJs), on the other hand, possess open pores that allow the passage of water and ions through fluid filled routes and as such can be considered as electrical conductance pathways. An electrical potential difference, which is measurable as electrical resistance, is created due to the TJs of the monolayers of epithelial cells restricting the movement of ions (Anderson and Van Itallie, 2009). With a decrease in TEER, in conjunction with an increased ionic conductance, an increase in paracellular permeability of ions across a monolayer is indicated rather than transcellular permeability. Even in the presence of ion channels, significantly lower resistance and concordantly higher conductance to ion flow is seen in the paracellular space, as opposed to the cell membranes.

TEER has been applied to study the permeation enhancing effects of compounds such as polyacrylic acid, polycarbophil and Cs, over recent years (Aungst, 2000; Liu *et al.*, 2008; Maher, Mrsny and Brayden, 2016). The latter has been shown to exhibit a reversible time and dose dependant decrease in TEER values in Caco-2 cells, indicating its ability to open the TJs (Ranaldi *et al.*, 2002). The effect of Cs on TJs was confirmed by increasing the permeation coefficient of mannitol when applied in conjunction with 0.1-0.5 w/v % Cs solution for 60 min, compared to cells treated with mannitol in the absence of Cs (Dodane, Khan and Merwin, 1999). Additionally, observations by Sonaje *et al.* (2012) have also suggested that the opening of TJs by Cs at 0.2 mg/mL is transient and reversible in Caco-2 cell monolayers, further indicating it as an effective permeation enhancer.

It has been shown that specific MWs of Cs significantly influence its permeation

enhancement (Chae, Jang and Nah, 2005). For example, studies by Opanasopit *et al*. 2007, showed that, as the MW of Cs is increased from 20 to 460 kDa, the reduction in TEER significantly decreased in the order: 20 < 45 < 200 < 460 kDa, observed in Caco-2 cell lines.

3.5 Selenium speciation

As the bioavailability of Se is highly dependent on its speciation, organic formats are typically sought after when proposing a health supplement (Rayman, 2000). Typically, Se is supplemented with SeMet, produced from *Saccharomyces cerevisiae*, a strain of yeast which, when cultivated with minimal S in the presence of inorganic Se, possesses the ability to accumulate up to 1400 µg SeMet per g of dried sample (Suhajda *et al.*, 2000). The high yield of Se from selenised yeast is one of the main factors for its employment. However, an alternative source of Se has been investigated in recent years, the edible mushroom *A. bisporus*.

The Irish mushroom industry produces in the region of 200,000 tonnes of spent mushroom substrate (SMS) every year (Teagasc Mushroom Stakeholder Consultative Group, 2013). Naturally, *A. bisporus*, contains an average of >1 µg Se/g dw (Savic *et al.*, 2012). However, when cultivated in substrates containing Se in either inorganic or organic forms, they exhibit much higher concentrations, ranging from 354 ± 0.19 to 707 ± 37.3 µg of Se per g of dried sample (Gergely *et al.*, 2006; Savic *et al.*, 2012). Previous studies conducted in DIT identified high levels of $SeCys_2$ (≈60 µg/g) in *A. bisporus* samples supplied by Monaghan mushrooms (Vozza, 2013). However, identification of the source and total Se content in the fruiting bodies was beyond the scope of the research, at that time. Regardless, the levels of $SeCys_2$ alone reflected Se fortification had occurred

during cultivation and that these Irish mushrooms may potentially offer an alternative source of Se to *S. cerevisiae.*

In order to use Se species sourced from *A. bisporus* in the NP formulation, it is first necessary to isolate fractions of Se from the fruiting bodies of the mushrooms and identify the species present. However, to date, no robust method for complete extraction and analysis of Se from food sources has been developed (Thiry *et al.*, 2012). Careful optimisation of extraction procedures is an essential requirement for Se speciation analysis of solid samples, in order to achieve high extraction efficiencies that also mitigate interconversion of the original species present (Dumont, Vanhaecke and Cornelis, 2006). It is generally recognised that a single step extraction is insufficient for Se liberation due to the varied matrix associations of Se in real samples (Pyrzyńska, 1996). For example, hot water extraction has been employed as a Se leaching solution for three edible wild mushroom species (*Macrolepiota procera, Lepista luscina* and *Boletus luridus*). However, it was shown that merely 47% of the total Se content present in the sample (present in water soluble proteins) could be recovered (Huerta, Sánchez and Sanz-Medel, 2005).

As many Se species are protein bound, several authors have utilised strong acids in extraction procedures, in order to increase liberation of Se from various matrices (Casiot *et al.*, 1999; Wrobel *et al.*, 2003). Additionally, proteolytic enzymes have been employed for extracting SeAAs incorporated into proteins due to their ability to cleave peptide bonds (Montes-Bayón *et al.*, 2006). Also, inorganic forms of Se have been found to become entrapped physically or chemically into cell walls and as such, acids and non-proteolytic enzymes such as driselase have been used in Se extraction (Infante, Hearn and Catterick, 2005).

In this work, Se species were extracted from Se supplemented *A. bisporus* samples, using protease enzymes, under microwave energy following the procedure detailed by (Ward, Connolly and Murphy, 2012). Once optimised, the entire procedure was subjected to a validation protocol, based on approved guidelines (EMEA, 1995), to assess its suitability for routine work.

3.5.1 HPLC-DAD

High Performance Liquid Chromatography (HPLC) is a powerful technique for separating complex mixtures and quantitating their components. HPLC equipment can be as simple as a specialised pump, a means of permitting sample injection, a specialised column and a suitable detector. In this work, a HPLC system coupled with a diode array detector (DAD) was employed for Se species quantification. A DAD detects the absorption in the UV to visible region of the spectrum. While a UV-VIS detector has only one sample-side light-receiving section, a beneficial feature of a DAD is that it has multiple (1024) photodiodes to obtain information over a wide range of wavelengths at one time. DADs differ from conventional UV-VIS detectors in that, light from the lamps is shone directly onto the flow cell, light that passes through the flow cell is dispersed by the diffraction grating, and the amount of the dispersed light is estimated for each wavelength in the DAD (Figure 3.6).

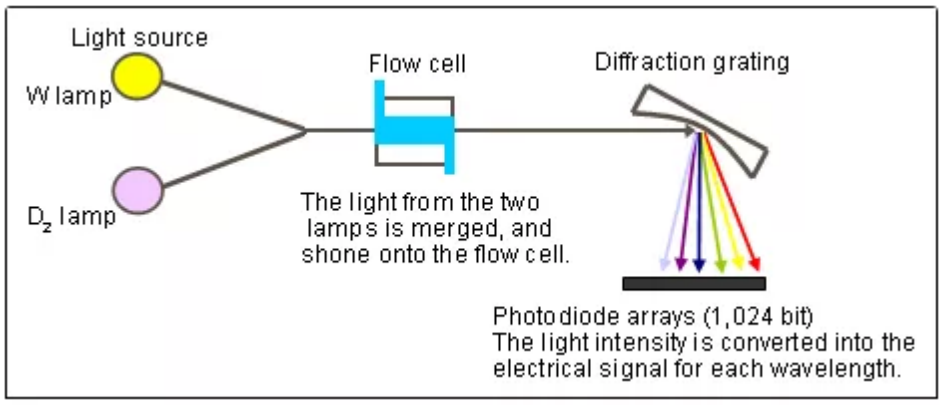

Figure 3.6 Schematic representation of a DAD optical system (picture acquired from www.crawfordscientific.com).

3.6 Summary

This chapter has presented the experimental techniques used throughout this thesis and provided relevant information and theory about each of the techniques employed. Experimental procedures were described, with specifications and parameters used given for each relevant procedure replicated throughout this thesis. The following chapter (4) will present the results of the optimisation and the characterisation of unloaded chitosan NPs that were formulated to ascertain formulation constituents and quantities that were requisite to hit target physicochemical and morphological properties. Finally, the specific detail on the applications of each technique will be described in the experimental section of the subsequent chapters (5, 6, 7 & 8), which are presented in the form of papers.

3.7 References

Agilent Technologies Inc. (2015) 'An Introduction to Gel Permeation Chromatography and Size Exclusion Chromatography', *Primer*, pp. 1–32. Available at: https://www.agilent.com/cs/library/primers/Public/5990-6969EN GPC SEC Chrom Guide.pdf. (Accessed: 10 Jan 2018).

Anarjan, N. *et al.* (2011) 'Effect of processing conditions on physicochemical properties of sodium caseinate-stabilized astaxanthin nanodispersions', *LWT - Food Science and Technology*, 44(7), pp. 1658–1665.

Anderson, J. M. and Van Itallie, C. M. (2009) 'Physiology and function of the tight junction', *Cold Spring Harbor Perspectives in Biology*, 1(2), p. a002584.

Anderson, M. J. and Whitcomb, P. J. (2005) *RSM simplified: optimizing processes using response surface methods for design of experiments*. Productivity press.

Aungst, B. J. (2000) 'Intestinal permeation enhancers', *Journal of Pharmaceutical Sciences*, 89(4), pp. 429–442.

Bajaj, S. *et al.* (2012) 'Stability Testing of Pharmaceutical Products', *Journal of Applied Pharmaceutical Science*, 2(2012), pp. 129–138.

Bellich, B. *et al.* (2016) '"The good, the bad and the ugly" of chitosans', *Marine Drugs*, 14(5), p. 99.

Bezerra, M. A. *et al.* (2008) 'Response surface methodology (RSM) as a tool for optimization in analytical chemistry.', *Talanta*, 76(5), pp. 965–77.

Bhagyashree, P. *et al.* (2015) 'Recent trends in stability testing of pharmaceutical products: A review', *Research Journal of Pharmaceutical, Biological and Chemical Sciences*, 6(1), pp. 1557–1569.

British Pharmacopoeia Commission (2016) *British Pharmacopoeia: Appendix XII B. Dissolution*. London: TSO.

Calderon L. *et al.* (2013) 'Nano and microparticulate chitosan-based systems for antiviral topical delivery', *European Journal of Pharmaceutical Sciences*, 48, pp. 216–222.

Carter, M. *et al.* (2015) 'Microscopy', in *Guide to Research Techniques in Neuroscience*, pp. 117–144.

Casiot, C. *et al.* (1999) 'Sample preparation and HPLC separation approaches to speciation analysis of selenium in yeast by ICP-MS', *Journal of Analytical Atomic Spectrometry*, 14(4), pp. 645–650.

Chae, S. Y., Jang, M.-K. and Nah, J.-W. (2005) 'Influence of molecular weight on oral absorption of water soluble chitosans', *Journal of Controlled Release*, 102(2), pp. 383–394.

Danish, M. K. *et al.* (2017) 'Formulation, Characterization and Stability Assessment of a Food-Derived Tripeptide, Leucine-Lysine-Proline Loaded Chitosan Nanoparticles', *Journal of Food Science*, 82(9), pp. 2094–2104.

Dayal, P. *et al.* (2005) 'Box-Behnken experimental design in the development of a nasal drug delivery system of model drug hydroxyurea: characterization of viscosity, in vitro drug release, droplet size, and dynamic surface tension.', *AAPS PharmSciTech*, 6(4), pp. E573–E585.

Dodane, V., Khan, M. A. and Merwin, J. R. (1999) 'Effect of chitosan on epithelial permeability and structure', *International Journal of Pharmaceutics*, 182(1), pp. 21–32.

Duan, B. *et al.* (2013) 'High strength films with gas-barrier fabricated from chitin solution dissolved at low temperature', *Journal of Materials Chemistry A*, 1(5), pp. 1867–1874.

Duarte, M. L. *et al.* (2002) 'An optimised method to determine the degree of acetylation of chitin and chitosan by FTIR spectroscopy', *International Journal of Biological Macromolecules*, 31(1), pp. 1–8.

Dumont, E., Vanhaecke, F. and Cornelis, R. (2006) 'Selenium speciation from food source to metabolites: a critical review', *Analytical and Bioanalytical Chemistry*, 385(7), pp. 1304–1323.

EMA (2003) 'European Medicines Agency', *ICH-Stability Testing of new Drug Substances and Products*, pp. 1–20.

EMEA (1995) 'Validation of analytical procedures: definitions and methodology', *ICH Harmonised Tripartite Guideline*, 20(121), p. 278.

Ferreira, S. L. C. *et al.* (2007) 'Statistical designs and response surface techniques for the optimization of chromatographic systems', *Journal of Chromatography A*, 1158(1), pp. 2–14.

Gergely, V. *et al.* (2006) 'Selenium speciation in Agaricus bisporus and Lentinula edodes mushroom proteins using multi-dimensional chromatography coupled to inductively coupled plasma mass spectrometry', *Journal of Chromatography A*, 1101(1–2), pp. 94–102.

Gleeson, J. P. *et al.* (2015) 'Stability, toxicity and intestinal permeation enhancement of two food-derived antihypertensive tripeptides, Ile-Pro-Pro and Leu-Lys-Pro. TL - 71', *Peptides*, 71 VN-r, pp. 1–7.

Gleeson, J. P., Ryan, S. M. and Brayden, D. J. (2016) 'Oral delivery strategies for nutraceuticals: Delivery vehicles and absorption enhancers', *Trends in Food Science & Technology*, 53, pp. 90–101.

Heux, L. *et al.* (2000) 'Solid state NMR for determination of degree of acetylation of chitin and chitosan.' *Biomacromolecules*, 1(4), pp.746-751.

Hidalgo, I. J. (2001) 'Assessing the absorption of new pharmaceuticals', *Current Topics in Medicinal Chemistry*, 1(5), pp. 385–401.

Hosseinzadeh, H. *et al.* (2012) 'Chitosan-Pluronic nanoparticles as oral delivery of anticancer gemcitabine: Preparation and in vitro study', *International Journal of Nanomedicine*, 7, pp. 1851–1863.

Huerta, V. D., Sánchez, M. L. F. and Sanz-Medel, A. (2005) 'Qualitative and quantitative speciation analysis of water soluble selenium in three edible wild mushrooms species by liquid chromatography using post-column isotope dilution ICP–MS', *Analytica Chimica Acta*, 538(1), pp. 99–105.

Infante, H. G., Hearn, R. and Catterick, T. (2005) 'Current mass spectrometry strategies for selenium speciation in dietary sources of high-selenium', *Analytical and Bioanalytical chemistry*, 382(4), pp. 957–967.

Kasaai, M. R. (2010) 'Determination of the degree of N-acetylation for chitin and chitosan by various NMR spectroscopy techniques: A review', *Carbohydrate Polymers*, 79(4), pp. 801–810.

Koppolu, B. P. *et al.* (2014) 'Controlling chitosan-based encapsulation for protein and vaccine delivery', *Biomaterials*, 35(14), pp. 4382–4389.

Kumirska, J. *et al.* (2011) 'Biomedical Activity of Chitin/Chitosan Based Materials—Influence of Physicochemical Properties Apart from Molecular Weight and Degree of N-Acetylation', *Polymers*, 3(4), pp. 1875–1901.

Lavertu, M. *et al.* (2003) 'A validated 1H NMR method for the determination of the degree of deacetylation of chitosan', *Journal of Pharmaceutical and Biomedical Analysis*, 32(6), pp. 1149–1158.

Liechty, W. B. *et al.* (2010) 'Polymers for Drug Delivery Systems', *Annual Review of Chemical and Biomolecular Engineering*, 1, pp. 149–173.

Liu, Z. *et al.* (2008) 'Polysaccharides-based nanoparticles as drug delivery systems.', *Advanced Drug Delivery Reviews*, 60(15), pp. 1650–62.

Maher, S., Mrsny, R. J. and Brayden, D. J. (2016) 'Intestinal Permeation Enhancers for Oral Peptide Delivery', *Advanced Drug Delivery Reviews*, 106, pp.277-319.

Maleki Dizaj, S. *et al.* (2015) 'Box-Behnken experimental design for preparation and optimization of ciprofloxacin hydrochloride-loaded CaCO3 nanoparticles', *Journal of Drug Delivery Science and Technology*, 29, pp. 125–131.

Malich, G., Markovic, B. and Winder, C. (1997) 'The sensitivity and specificity of the MTS tetrazolium assay for detecting the in vitro cytotoxicity of 20 chemicals using human cell lines', *Toxicology*, 124(3), pp. 179–192.

Montes-Bayón, M. *et al.* (2006) 'Evaluation of different sample extraction strategies for selenium determination in selenium-enriched plants (Alliumsativum and Brassicajuncea) and Se speciation by HPLC-ICP-MS', *Talanta*, 68(4), pp. 1287–1293.

Mukhopadhyay, P. *et al.* (2013) 'Oral insulin delivery by self-assembled chitosan nanoparticles: in vitro and in vivo studies in diabetic animal model.', *Materials science & engineering. C, Materials for Biological Applications*, 33(1), pp. 376–82.

Nabi-Meibodi, M. *et al.* (2013) 'Optimized double emulsion-solvent evaporation process for production of solid lipid nanoparticles containing baclofene as a lipid insoluble drug', *Journal of Drug Delivery Science and Technology*, 23(3), pp. 225–230.

Neves, A. R. *et al.* (2016) 'Nanoscale delivery of resveratrol towards enhancement of supplements and nutraceuticals', *Nutrients*, 8(3), p. 131.

Opanasopit, P. *et al.* (2007) ‘Effect of salt forms and molecular weight of chitosans on in vitro permeability enhancement in intestinal epithelial cells (Caco-2)’, *Pharmaceutical Development and Technology*, 12(5), pp. 447–455.

Pharmacopoeia, B. (2016) ‘British Pharmacopoeia Commission: London’. UK.

Pretsch, E. *et al.* (2000) *Structure Determination of Organic Compounds*. Springer.

Pyrzyńska, K. (1996) ‘Speciation analysis of some organic selenium compounds. A review’, *Analyst*, 121(8), p. 77R–83R.

Ranaldi, G. *et al.* (2002) ‘The effect of chitosan and other polycations on tight junction permeability in the human intestinal Caco-2 cell line’, *The Journal of Nutritional Biochemistry*, 13(3), pp. 157–167.

Rayman, M. P. (2000) ‘The importance of selenium to human health.’, *Lancet*, 356(9225), pp. 233–241.

des Rieux, A. *et al.* (2006) ‘Nanoparticles as potential oral delivery systems of proteins and vaccines: a mechanistic approach’, *Journal of Controlled Release*, 116(1), pp. 1–27.

Rinaudo, M. (2006) ‘Chitin and chitosan: Properties and applications’, *Progress in Polymer Science*, 31(7), pp. 603–632.

Savic, M. *et al.* (2012) ‘The fungistatic activity of organic selenium and its application to the production of cultivated mushrooms Agaricus bisporus and Pleurotus spp.’, *Archives of Biological Sciences*, 64(4), pp. 1455–1463.

Sieval, A. B. *et al.* (1998) ‘Preparation and NMR characterization of highly substitutedN-trimethyl chitosan chloride’, *Carbohydrate Polymers*, 36(2–3), pp. 157–165.

Singh, B., Chakkal, S. K. and Ahuja, N. (2006) ‘Formulation and optimization of controlled release mucoadhesive tablets of atenolol using response surface methodology.’, *AAPS PharmSciTech*, 7(1), p. E3.

Sivamani, S. and Baskar, R. (2015) ‘Optimization of bioethanol production from cassava peel using statistical experimental design’, *Environmental Progress & Sustainable Energy*, 34(2), pp. 567–574.

Sonaje, K. *et al.* (2012) ‘Opening of epithelial tight junctions and enhancement of paracellular permeation by chitosan: microscopic, ultrastructural, and computed-tomographic observations’, *Molecular Pharmaceutics*, 9(5), pp. 1271–1279.

Stokes, D. J. (2003) ‘Recent advances in electron imaging, image interpretation and applications: environmental scanning electron microscopy’, *Philosophical Transactions of the Royal Society of London Series a-Mathematical Physical and Engineering Sciences*, 361(1813), pp. 2771–2787.

Suhajda, A. *et al.* (2000) ‘Preparation of selenium yeasts I. Preparation of selenium-enriched Saccharomyces cerevisiae’, *Journal of Trace Elements in Medicine and Biology*, 14(1), pp. 43–47.

Teagasc Mushroom Stakeholder Consultative Group (2013) ‘Mushroom Sector Development Plan to 2020’, pp. 16, 14. Available at: http://www.teagasc.ie/publications/2013/2916/Mushroom_ Conference_ Proceedings_web.pdf. (Accessed: 10 Jan 2018)

Thiry, C. *et al.* (2012) ‘Current knowledge in species-related bioavailability of selenium in food’, *Food Chemistry*, 130(4), pp. 767–784.

Uskoković, V. (2012) ‘Dynamic Light Scattering Based Microelectrophoresis: Main Prospects and Limitations’, *Journal of Dispersion Science and Technology*, 33(12), pp. 1762–1786.

Varshosaz, J., Tabbakhian, M. and Mohammadi, M. Y. (2010) ‘Formulation and optimization of solid lipid nanoparticles of buspirone HCl for enhancement of its oral bioavailability’, *Journal of Liposome Research*, 20(4), pp. 286–296.

Verheul, R. J. *et al.* (2008) ‘Synthesis, characterization and in vitro biological properties of O-methyl free N,N,N-trimethylated chitosan’, *Biomaterials*, 29(27), pp. 3642–3649.

Vozza, G. (2013) *Identification and quantitative analysis of selenium species present in Agaricus bisporus by gas chromatography mass spectrometry*. Dublin institute of Technology.

Ward, P., Connolly, C. and Murphy, R. (2012) ‘Accelerated Determination of Selenomethionine in Selenized Yeast: Validation of Analytical Method’, *Biological Trace Element Research*, 151(3), pp. 446–450.

Weinhold, M. X. *et al.* (2009) ‘Strategy to improve the characterization of chitosan for sustainable biomedical applications: SAR guided multi-dimensional analysis’, *Green Chemistry*, 11(4), pp. 498–509.

Wrobel, K. K. *et al.* (2003) 'Hydrolysis of proteins with methanesulfonic acid for improved HPLC-ICP-MS determination of seleno-methionine in yeast and nuts', *Analytical and Bioanalytical Chemistry*, 375(1), pp. 133–138.

Xu, Y. and Du, Y. (2003) 'Effect of molecular structure of chitosan on protein delivery properties of chitosan nanoparticles', *International Journal of Pharmaceutics*, 250(1), pp. 215–226.

Yoon, H. Y. *et al.* (2014) 'Glycol chitosan nanoparticles as specialized cancer therapeutic vehicles: Sequential delivery of doxorubicin and Bcl-2 siRNA', *Scientific Reports*, 4, p. 6878.

Zielinska, K., Shostenko, a. G. and Truszkowski, S. (2014) 'Analysis of chitosan by gel permeation chromatography', *High Energy Chemistry*, 48(2), pp. 72–75.

Zolgharnein, J., Shahmoradi, A. and Ghasemi, J. B. (2013) 'Comparative study of Box–Behnken, central composite, and Doehlert matrix for multivariate optimization of Pb (II) adsorption onto Robinia tree leaves', *Journal of Chemometrics*, 27(1–2), pp. 12–20.

4 FORMULATION AND CHARACTERISATION OF UNLOADED CHITOSAN NANOPARTICLES

4.1 Introduction

Cs is a linear polysaccharide, prepared by N-deacetylation of chitin, the second most abundant biopolymer in nature (next to cellulose) (Prochazkova, Vårum and Ostgaard, 1999). Cs holds a unique positive charge when dissolved in acid media (owing to the primary amines present on its backbone), is biocompatible, non-immunogenic, nontoxic and biodegradable, making it a choice component for oral drug delivery systems and attractive for biomedical applications (Agnihotri, Mallikarjuna and Aminabhavi, 2004; Bezerra *et al.*, 2008; Saini *et al.*, 2014). Cs nanoparticles (NPs) are emerging polymeric bioactive carriers that have received attention for nutrient delivery (Luo *et al.*, 2010; Akhtar, Rizvi and Kar, 2012; Chen *et al.*, 2013; Fathi, Martín and McClements, 2014; Sarvaiya and Agrawal, 2015).

Specifically, Cs NPs can be made using a variety of techniques, such as complex coacervation (Diop *et al.*, 2015), co-precipitation (Bhattarai *et al.*, 2006), polyelectrolyte complexation (Kouchak and Azarpanah, 2015), solvent evaporation (Nagpal, Singh and Mishra, 2010), emulsification solvent diffusion (Fathi, Martín and McClements, 2014), micro-emulsion (El-Shabouri, 2002) and ionotropic gelation (IG) (Yan *et al.*, 2012; Ramasamy *et al.*, 2014; Wu *et al.*, 2014). The latter has been considered more favourable for the stability of the cargo, owing to the ease with which the NPs can be produced under mild operating conditions (room temperature, low stirring rates) and mild solvents (dilute acids and bases) (Koppolu *et al.*, 2014).

This research work has used the IG technique for the preparation of Cs NPs, by ionically cross-linking Cs with a counter ion sodium tripolyphosphate (TPP) (Sureshkumar *et al.*, 2010). IG is based on the interaction between the negatively

charged phosphate groups of TPP and the positively charged amino groups of Cs Figure 4.1. When the concentrations of the cationic polymer Cs and oppositely charged anionic polyelectrolytes are at appropriate pH values to induce sufficient protonation/ionisation charge, electrostatic crosslinking can occur resulting in the generation of NPs (Calvo *et al.*, 1997).

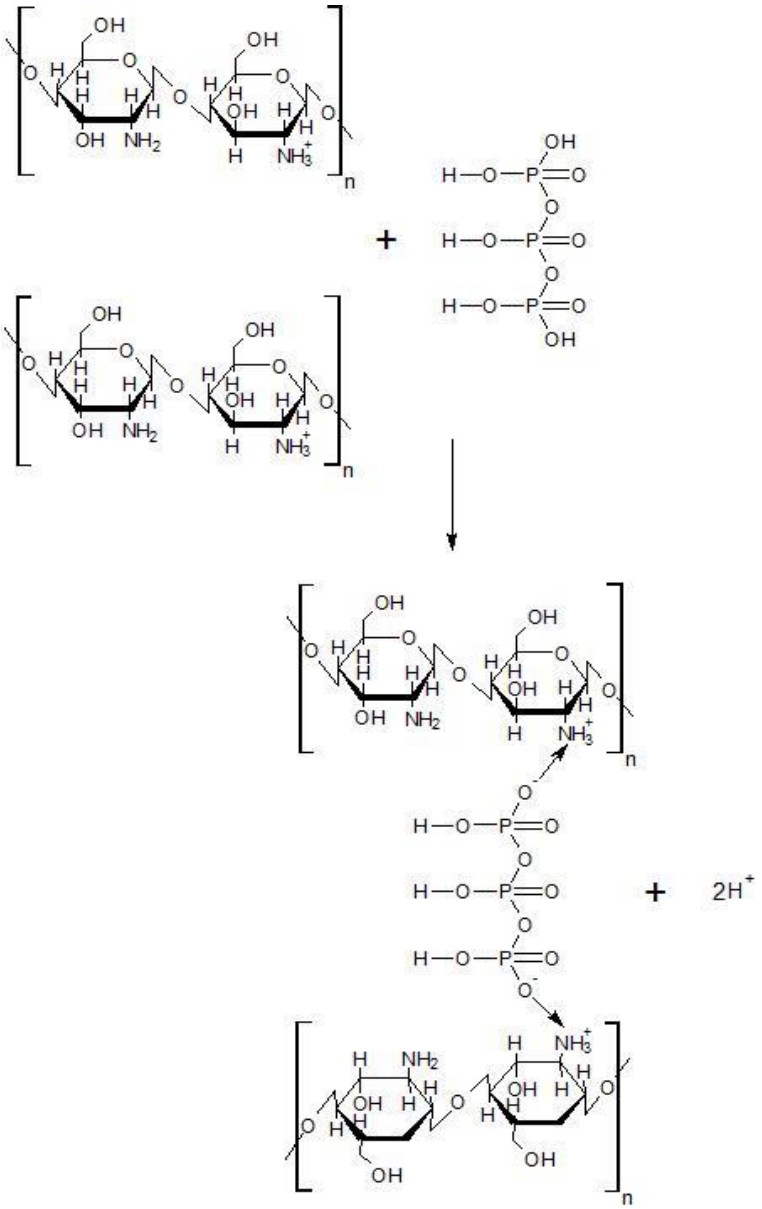

Figure 4.1 Schematic representation of cross-linking between Cs and TPP (adapted from Sureshkumar *et al.* (2010)).

There are several process variables known to affect the properties of Cs NPs produced via the IG technique, the most commonly studied being:

1. The pKa of Cs itself and the target BA to be encapsulated (modulated through the formulation media pH) (Fonte *et al.*, 2014)
2. The mass ratio of Cs to its oppositely charged crosslinker/counter ion (Gupta and Karar, 2011)
3. The stirring rate and stabilisation time the formulation is subjected to during the crosslinking process (Grenha, 2012)
4. The DDA and MW of the Cs used (Aktaş *et al.*, 2005)

Research studies, regarding the encapsulation of bioactive nutrients within a Cs based NP delivery system, include the binding of curcumin (CUR) onto Cs NPs through passive diffusion, which produced a significant 3 fold reduction in the plasma concentration of *Plasmodium yoelii* infected mice, compared to the rapidly metabolised intact CUR drug (Akhtar, Rizvi and Kar, 2012). In another study, the oral administration of Cs insulin loaded Cs NPs formed via the complex coacervation method, was shown to be effective in lowering the blood glucose level of alloxan-induced diabetic mice, showing promising effects as a potential insulin carrier system in animal models (Mukhopadhyay *et al.*, 2013). In 2008, Kwon, showed successful systemic administration of the anticancer drug, paclitaxel, encapsulated in Cs NPs in SCC7 tumour-bearing mice, resulting in sensitive tumour-detection ability, ultimately leading to simultaneous early-stage cancer diagnosis, drug delivery, and therapy (Kwon, 2008).

It is worth noting that the success of these NPs applicability strongly depends on the physicochemical properties of the produced NPs, such as particle size, ZP and PDI

(des Rieux *et al.*, 2006). Despite the simplicity of IG, controlling the process for the reproducible, systematic, production and prediction of NP size, ZP and PDI is a difficult task, attributable to the large number of aforementioned variables that can affect the final product (Landriscina, 2015). Successful translation of NPs from bench to bedside, depends on overcoming obstacles in terms of scalability and reproducibility (Dong *et al.*, 2013). Consequently, several attempts have been made to optimise this methods outcome, for example, the variations in Cs molecular weight, Cs concentration, Cs to TPP weight ratio and solution pH value have been investigated for their effects on NP size, ZP and PDI (Pan *et al.*, 2002; Jonassen, Kjøniksen and Hiorth, 2012; Rampino *et al.*, 2013; Kleine-Brueggeney *et al.*, 2015). Often these studies employ a OFAT approach for NP process optimisation and, although useful in preliminary screening of factors and/or identification of the working ranges for these factors, limited knowledge of the process can be gained by this approach. In contrast, statistically designed experiments that vary several factors simultaneously are more efficient when studying two or more factors aiming for optimisation (Ferreira *et al.*, 2007). RSM is a collection of mathematical and statistical techniques for designing experiments, that: evaluates the relative significance of several independent variables and their interactions, allows for building of regression models and determines the optimum conditions for desirable responses, minimising the number of experiments (Anarjan *et al.*, 2011; Xue *et al.*, 2015). While OFAT experiments are more commonly adopted in the literature, designed experiments offer several advantages over the OFAT counterparts (Politis *et al.*, 2017):

- First, RSM reduces the number of experimental runs typically required to gather the same information as OFAT, thus reducing resource requirements.

- Second, RSM is useful in detecting interdependencies of variables that would not be typically identified during OFAT experiments
- Third, RSM improves the prediction of a response through use of gathered information from a larger parameter space (Abdel-Hafez, Hathout and Sammour, 2014).
- Fourth, RSM provides an iterative approach to experimental design where the previous knowledge will contribute to the design specification of the next experiment.

Recently, RSM experimental designs such as the Central composite and Box–Behnken have been investigated for NP formulation optimisation (Hao *et al.*, 2012; De Carvalho *et al.*, 2013; Zolgharnein, Shahmoradi and Ghasemi, 2013). The CCD is a suitable approach to understand the effects of formulation variables (independent factors) and the interactions between factors on the responses (dependent factors). Commonly employed CCDs take factors at five levels (two-level factorial design points, axial or star points, and centre points), resulting in a fully rotatable design (Hao *et al.*, 2012).

In this work, the mass ratios of Cs:TPP ranging from 4:1-27.5:1 were selected for investigation, as these high and low levels were identified from previous preliminary studies as feasible ranges for Cs NP production (Khalid, 2014). Further investigation of these variables allowed for supplementary information on the characteristics of Cs NP formation and their dependency on the Cs and TPP interaction. Overlaid contour plots were used for optimisation purposes to produce NPs at a targeted diameter of 200-300 nm. The formulated NPs were characterised by DLS, SEM and FTIR spectroscopy.

4.2 Materials and Methods

4.2.1 Materials

The Cs compound PROTASAN™ UP (CL113) was purchased from NovaMatrix, FMC Corporations, Norway. Sodium tripolyphosphate, technical grade, 85%, sodium acetate anhydrous, for molecular biology, ≥99%, acetic acid, ACS reagent, ≥99.7 were obtained from Sigma Aldrich, Ireland. Ultrapure water was obtained from a Milli-Q (Millipore Corporation, USA) water purification system and was used for all aqueous solution preparations throughout.

4.2.2 Central composite design

CCD (Bulmer, Margaritis and Xenocostas, 2012) was used to (i) determine the optimum concentration ratio of Cs to cross linker, TPP and (ii), produce NPs with the optimum physicochemical properties recommended for oral delivery (~300 nm particle size, PDI < 0.5 and ZP > 30 mV). DoE software (Minitab™ 17, Pennsylvania, USA) produced a two factor design with 5 levels. Centre points were replicated 5 times in order to estimate the experimental error and curvature associated with the design. The formulation variables, concentration of CL113 (mg/mL) and concentration of TPP (mg/mL), in addition to their high and low levels were identified from previous preliminary studies (Khalid, 2014).

A second order polynomial model (Equation 4.1) was used to approximate the response surface:

$$\boldsymbol{Ri = b_0 + b_1A + b_2B + b_{11}A^2 + b_{22}B^2 + b_{12}AB + \varepsilon}$$

(Equation 4.1)

where R_i is the measure of the response associated with each factor level combination, b_0 is an intercept, $b_1 \ldots b_{22}$ are the regression coefficients, A and B are the independent variables, and A^2, B^2 and AB denote the quadratic terms and interactive term respectively and ε the error term. The responses selected were size, PDI and ZP with the following criteria of minimise, minimise, and maximise adopted respectively. The translation of coded levels into the actual variables natural units of measurement (concentration (mg/mL) of CL113 and TPP) are denoted in Table 4.1.

In this experiment, the desirability function was created to give equal weight to particle size, PDI and ZP, with EE% not included.

Table 4.1 Variables and levels employed in the CCD design (α=1.414)

Coded level	-α	-1	0	1	+α
A: CL113 (mg/mL)	1.10	1.20	1.45	1.70	1.80
B: TPP (mg/mL)	0.04	0.10	0.25	0.40	0.46

4.2.3 Preparation of unloaded Cs:TPP NPs

Cs solution (10 mg/mL) was prepared by adding 100 mg of CL113 to 10 mL of sodium acetate-acetic acid buffer (pH 3) and stirring at 700 rpm for 4 hrs. Once fully dissolved, the Cs solution was then filtered through a 0.22 μm syringe filter (Millex Millipore) and diluted to experimental requirements with pH 3 buffer. Cs:TPP NPs were then formed according to the ionotropic gelation process (Calvo *et al.*, 1997) with slight modifications. Aqueous TPP solution (10 mg/mL) was prepared and

diluted with H_2O to experimental requirements and subsequently added *via* burette droplet addition to the Cs solution. The NPs formed were then left to stabilise for a further 30 min whilst the stirring speed of the solution was maintained at 700 rpm.

After stabilisation, NPs were then transferred to a 20 kDa MWCO (Vivaspin 20, Sartorius) centrifugal filter and isolated by centrifugation at 3000 rpm for 30 min. Filtered H_2O (equivalent in volume to the recovered supernatant) was then added to the purified NPs and the suspension was subsequently sonicated at 35 % amplitude for 30 s with 5 s pulse intervals. Physicochemical properties of the NPs (size, PDI and ZP) were then determined using a Malvern Zetasizer NanoZS (Worcestershire, UK), under the conditions described in Chapter 3, Section 3.2.1.

4.2.4 Fourier transform infrared spectroscopy (FTIR)

FTIR spectra of CL113, TPP and Cs:TPP NPs were acquired via a Spotlight 400 series spectrometer (Perkin Elmer, USA), using the attenuated total reflectance spectroscopy method (ATR-FTIR), in the range of 650-4000 cm^{-1}. Prior to analysis, NP samples were lyophilised using a FreeZone 6 L bench top freeze dry system (Labconco, USA) at -40 °C for 20 hrs. The dried solids were then placed on the ATR crystal prism (ZnSe), and 32 scans were acquired at 4 cm^{-1} resolution with background subtraction (Vongchan *et al.*, 2011).

4.2.5 Morphology assessment of formulated NPs- SEM

SEM analysis was used to ascertain the morphology of the formed CS:TPP NPs, under conditions described in Chapter 3, Section 3.2.2.

4.3 Results and Discussion

4.3.1 CCD

The observed values for all 13 experiments encompassed by the CCD are presented in Table 4.2. Minimum and maximum values obtained for particle size, PDI, and ZP were (194, 850 nm), (0.396, 0.799) and (24, 47.3 mV) respectively.

Table 4.2 CCD design matrix and corresponding results for dependant variables.

Batch	A:CL113 (mg/mL)	B:TPP (mg/mL)	Size (nm)	PDI	ZP (mV)
1	1.10	0.25	233	0.500	34.0
2	1.45	0.46	203	0.420	24.3
3	1.45	0.25	186	0.412	52.5
4	1.45	0.25	194	0.421	47.3
5	1.45	0.25	194	0.406	44.1
6	1.45	0.04	850	0.723	31.0
7	1.80	0.25	274	0.396	38.5
8	1.45	0.25	189	0.535	41.5
9	1.20	0.40	199	0.430	24.0
10	1.20	0.10	608	0.799	28.0
11	1.70	0.10	661	0.543	29.0
12	1.45	0.25	220	0.461	40.0
13	1.70	0.40	233	0.411	27.0

The significance of independent variables and their interactions was assessed by statistical software (Minitab™,17) to generate regression models. Through bidirectional elimination (testing at each step for variables to be included or excluded), non-significant terms were removed from the model in order to calculate regression equations with significant terms only (Wang *et al.*, 2013). The calculated regression coefficients and standard errors for size, PDI and ZP of the reduced models are shown in Table 4.3, in which coefficients related to the independent variables with significant

t-values ($p \leq 0.05$) were used. Higher significant effects of the independent variable on the response are indicated by a lower p-value.

As discussed in Chapter 3 (Section 3.3), RSM allows for the construction of a mathematical model to identify the optimum level of each factor to produce a target response (Reddy *et al.*, 2017). As such, the application of CCD to map the response (particle size (nm), PDI and ZP (mV)) over the experimental domain studied, was used to identify and tune an optimal formulation with desirable properties (des Rieux *et al.*, 2006) for oral delivery and is explored in the following section.

Regarding the size of the NPs, the model shows that two linear [concentration of CL113 (A) and TPP (B)] and two quadratic [(AA) (BB)], terms were significant ($p < 0.05$). Size was mostly affected by the quadratic effects of the B*B term, whereby a positive correlation was observed such that, at minimum and upper levels of B, size increased. It is also worth noting that, the linear term of B showed a negative coefficient, indicating that B has a negative effect on size until a turning point is reached, after which the B*B term has a positive impact on size. This is in agreement with the contour plot (Figure 4.2, B) and findings by Calvo *et al*. (1997), which showed that intermediate concentrations (ratio of Cs:TPP of 5:1) of TPP gave rise to smaller NPs compared to lower and higher concentrations. Additionally, they found that formation of NPs was only possible at specific concentrations of Cs and TPP, with a maximum concentration of 3 mg/mL and 0.75 mg/mL respectively (Calvo *et al.*, 1997).

Table 4.3 The normalised estimated regression coefficients and standard errors, for size, PDI and ZP of the reduced models. All parameters statistically significant ($p<0.05$).

Estimated regression Coefficients for size (nm)		
Term	**Coef**	**SE Coef**
Constant	196.83	9.79
A: CL113 mg/mL	25.4	10.9
B: TPP mg/mL	-307.9	10.9
A^2: CL113 mg/mL*CL113 mg/ml	72.6	16.5
B^2: TPP mg/mL*TPP mg/mL	345.6	16.5
Model summary	$\mathbf{R_2}$ = 99.36 %	$\boldsymbol{R^2_{adj}}$=99.04 %
Estimated regression Coefficients for PDI		
Term	**Coef**	**SE Coef**
Constant	0.4532	0.0167
A: CL113 mg/mL	-0.0743	0.0230
B: TPP mg/mL	-0.1635	0.0230
B^2: TPP mg/mL*TPP mg/mL	0.1399	0.0345
A*B: CL113 mg/mL*TPP mg/mL	0.1161	0.0452
Model summary	$\mathbf{R_2}$ = 91.32 %	$\boldsymbol{R^2_{adj}}$= 86.98 %
Estimated regression Coefficients for ZP (mV)		
Term	**Coef**	**SE Coef**
Constant	45.10	1.91
A:CL113 mg/mL	1.82	2.13
B:TPP mg/mL	-2.72	2.13
A^2: CL113 mg/mL*CL113 mg/ml	-11.22	3.22
B^2: TPP mg/mL*TPP mg/mL	-19.77	3.22
Model summary	$\mathbf{R_2}$ = 85.62 %	$\boldsymbol{R^2_{adj}}$= 78.44 %

As PDI reflects the NP size distribution (whereby samples with a wider range of particle sizes have higher PDI values and vice versa), it is highly desirable that NP formulations consist of monodisperse populations, to ensure that the system can deliver its cargo over a sustained period of time (Nagpal, Singh and Mishra, 2010). Table 4.3 shows that PDI was mostly affected by the linear effect of B (TPP concentration mg/mL), i.e. PDI decreases as B increases one unit from median levels.

Consequently, the quadratic terms of B*B showed a positive correlation, signifying that PDI increases at upper and lower levels of B. This agrees with the contour plot (Figure 4.2, C). This finding supports the work of other authors that observed the free primary amino groups of Cs decreasing upon the addition of TPP, indicating the formation of monodisperse Cs:TPP via anionic and cation linkages of both polyelectrolytes (Masarudin *et al.*, 2015).

In terms of ZP, the two quadratic terms [(A*A), (B*B)] were found to have a negative effect on ZP, whereas the linear terms were shown to have a positive effect on ZP. Table 4.3 shows the quadratic effect of TPP on the highest effect on ZP, indicating that, at concentrations above and below median levels, a decrease in ZP is observed. The positive correlation observed for the linear term of B indicates that, at one unit above median level, ZP is increased signifying curvature in the model and a maximum value for ZP can be achieved at this level. Figure 4.2A indicates that the optimum value (maximum) for ZP can be found within the range of variables studied: ≈ 1.5 mg/mL Cs to 0.25 mg/mL TPP (Ratio 6:1). This is in agreement with other authors' findings, as several studies investigating the optimum ratio of Cs to TPP have indicated that a ratios of 4:1 – 8:1 give rise to the most stable NP complexes (Pan *et al.*, 2002; Kouchak and Azarpanah, 2015), attributable to sufficient quantities of TPP that allow for the formation of crosslinked NPs, yet are not in an excess of that which would result in complete neutralisation of the cationic charge on the free primary free amines of Cs (Huang, Cai and Lapitsky, 2015)

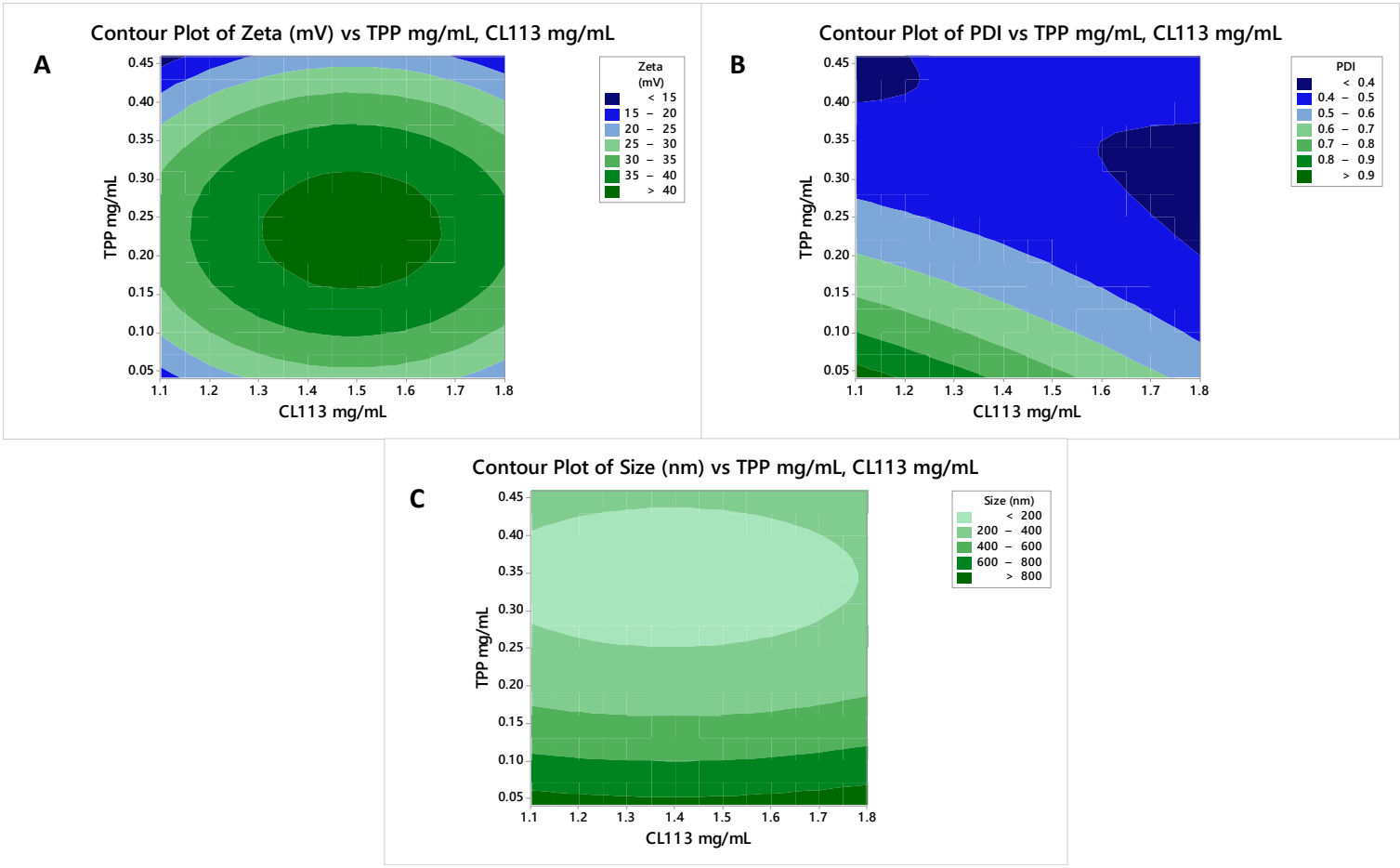

Figure 4.2 Contour plots for Zeta potential (mV) (A), PDI (B), and size (nm) (C) vs TPP (mg/mL), CL113 (mg/mL)

4.3.2 Optimisation of CL113 and TPP concentrations for Cs:TPP NP formation

Overlaid contour plots for the fitted polynomials predicting the change of PDI, ZP and particle size with Cs and TPP concentration were employed in order to identify optimum conditions for the formulation, whereby NPs with sizes between 200-300 nm, PDI <0.5 and ZP >30 mV could be produced. Figure 4.3 details the results and shows that increasing concentrations of Cs ≈ 1.68-1.8 mg/mL and intermediate TPP concentrations ≈ 0.20-0.37 mg/mL give rise to a region in which NP target properties can be achieved.

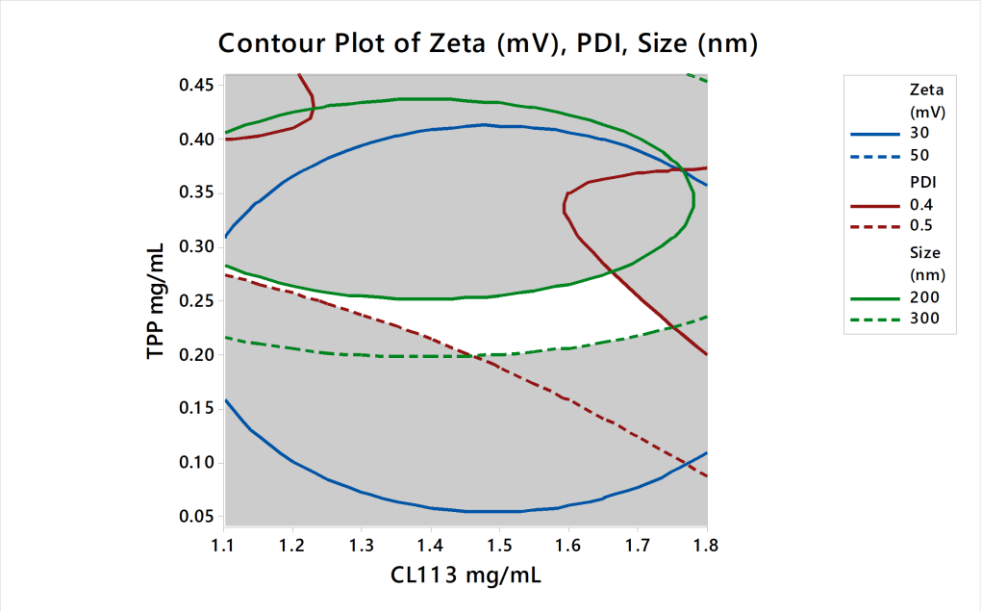

Figure 4.3 Overlapped contour plots for the fitted polynomials predicting the change of PDI, Zeta potential and particle size with Cs and TPP concentration. The feasible zone with PDI< 0.5, Zeta< 30 (mV) and Size> 200 (nm) is indicated in white.

By employing the constructed models from the CCD evaluation, response optimisation could be used to establish an optimum NP formulation. In this approach, the value of each response for a given combination of controllable factors is first translated to a number between zero and one, known as individual desirability (Bezerra *et al.*, 2008). An optimal minimum (size (nm)), minimum (PDI) and maximum (ZP (mV)) forecast has been

obtained with the present models and is presented in Figure 4.4, indicating that when the variable settings of CL113 mg/mL and TPP mg/mL are set at ratio ≈ 6:1 (1.53 mg/mL and 0.27 mg/mL respectively), NPs with the desired properties are produced. The 95% confidence interval ranges that these conditions would produce are presented in Table 4.4. This is in agreement with previous authors' findings (Janes, Calvo and Alonso, 2001; Antoniou *et al.*, 2015).

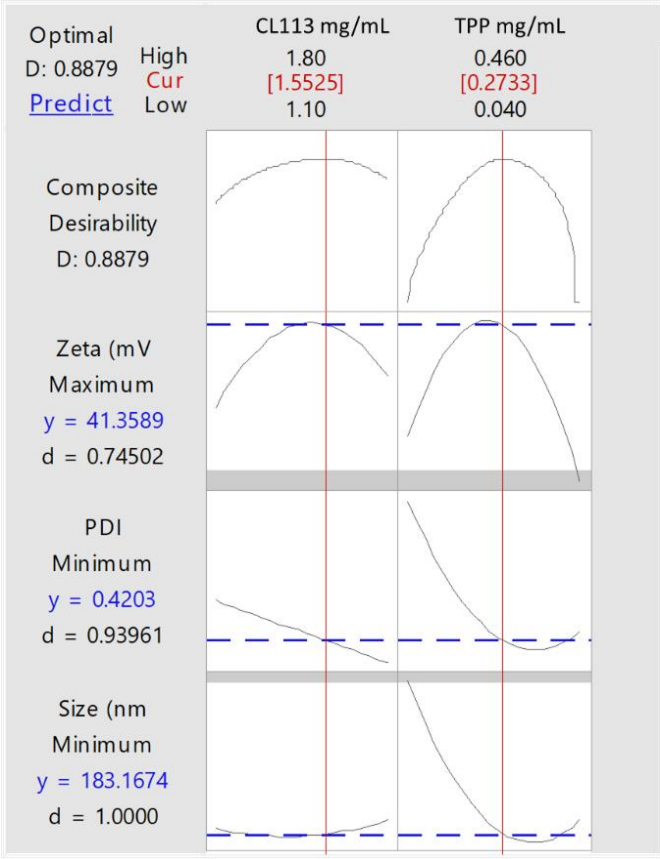

Figure 4.4 Desirability profiles for the optimisation problem, maximising the Zeta potential and minimising particle size and PDI of the particles.

To verify the validity of the proposed models, n = 4 replicates of the optimised formulation was prepared, and each experimental response was compared with the predicted one. Table 4.4 shows the validation results of the model, whereby NPs presented sizes of 161.3 ± 43 nm, PDI of 0.391 ± 0.022, ZP of 41.5 ± 3.1. No statistically significant values ($p>0.05$) for predicted and measured responses (Size, PDI and ZP) were

observed, indicating that the models fit the data satisfactorily. Lastly, by employing a CCD, many additional experiments (in addition to time consuming laborious laboratory studies) were eliminated in comparison to a OFAT approach.

Table 4.4 95% confidence intervals of the particle characteristics that optimal conditions would produce under the present experimental conditions of uncertainty.

Response	Fit	SE fit	95% CI
Size	181.5	9.6	(159.4, 236.6)
PDI	0.4247	0.0175	(0.3843, 0.4651)
ZP	44.5	1.9	(40.2,48.8)

4.3.3 Characterisation of unloaded Cs:TPP NPs - FTIR

Figure 4.5 shows the FTIR spectra of (A) TPP, (B) Cs and (C) Cs:TPP NPs and the characteristic peaks associated with TPP and Cs are presented in Table 4.5.

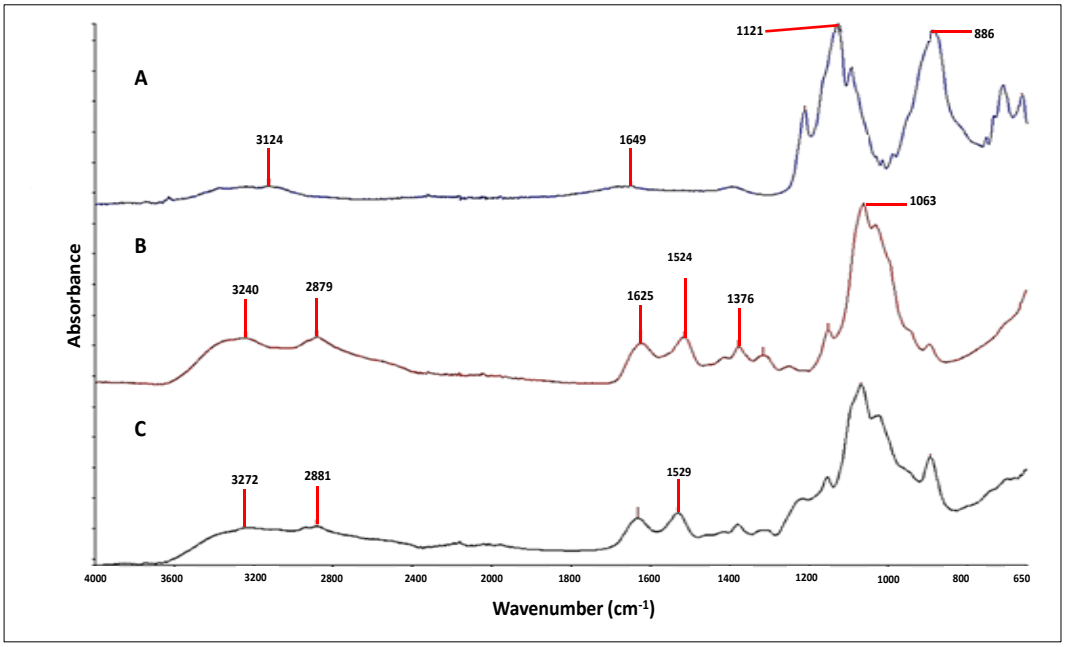

Figure 4.5 FTIR spectra of (A) TPP, (B) Cs and (C) Cs:TPP NPs. N=3.

By observing the intermolecular interaction of Cs:TPP NPs via FTIR (Figure 4.5, C), it can be seen that the spectrum is different to that of the Cs matrix. If interaction between the Cs and TPP has occurred, it will lead to frequency shifts or splitting in absorption

peaks (Gan *et al.*, 2005). For example, the peaks at 1514 cm^{-1} in the Cs spectrum have been shifted to 1529 cm^{-1}, indicating electrostatic interaction between the phosphate groups of TPP and the amino groups present in the Cs NP matrix (Papadimitriou *et al.*, 2008). Additionally, the broadening and the reduced absorbance of the peak at 3272 cm^{-1} indicate hydrogen bonding has been enhanced (Luo *et al.*, 2010). The crosslinked Cs also showed a peak for P = O at 1155 cm^{-1}.

Table 4.5 FTIR analysis of characteristic peaks associated with TPP and Cs.

TPP		
Bond	Wavelength (cm^{-1})	Reference
P=O	1121, 886	(Bhumkar and Pokharkar, 2006)
Chitosan		
Bond	Wavelength (cm^{-1})	Reference
NH Stretch / OH in pyranose ring	3240	(Luo *et al.*, 2010; Mohammed, Williams and Tverezovskaya, 2013)
CH_2 in CH_2OH group	2879	
C=O in $NHCOCH_3$ group (amide I)	1625	
NH_2 in $NHCOCH_3$ group (amide II)	1514	
CH_3 in $NHCOCH_3$ group	1376	
C-O-C (glycosidic linkage)	1063	

4.3.4 Scanning electron microscopy (SEM)

Figure 4.6 shows the SEM image of unloaded Cs:TPP NPs. Spherical, monodisperse particles were observed and the particle size of the NPs after spin coating was in good agreement with the DLS measurements taken on the freshly prepared NPs.

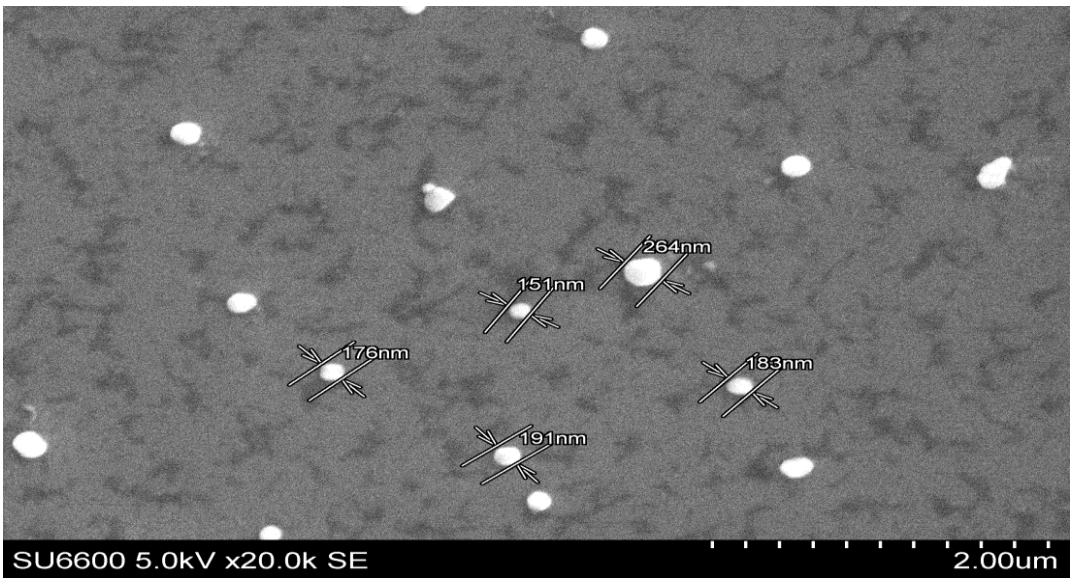

Figure 4.6 SEM image of unloaded Cs:TPP NPs.

4.4 Conclusion

In this work, Cs:TPP NPs have been produced via ionotropic gelation. As one of the most influential variables that dominates the size, PDI, ZP and morphology of ionotropic formed Cs NPs has been established to be Cs:TPP mass ratios (Almalik *et al.*, 2013), a CCD statistical design was employed to generate a mathematical model that identified the optimum ratio of Cs:TPP for NPs with properties reported to be beneficial for oral drug delivery (des Rieux *et al.*, 2006). The results of the CCD design identified that, at approximate concentrations of Cs (1.68 - 1.8 mg/mL) and intermediate concentrations of TPP (0.20 - 0.37 mg/mL), a feasible region was produced in which NP target properties could be achieved. The physicochemical properties of the NPs produced from the validation of the CCD study were assessed by DLS, showing that, under optimum conditions of Cs:TPP (6:1), NPs with sizes of 161 ± 43 nm, PDI of 0.39 ± 0.02, ZP of 42 ± 3 could be produced. Evidence for the formation of NPs via ionotropic gelation was acquired *via* FTIR analysis, through identification of key functional groups on Cs and TPP and identifying their shifts in the crosslinked matrices. The morphology of the NPs was then assessed by SEM analysis, showing that spheroidal, well distributed particles were formed. The findings provide an overview to produce Cs NPs with desirable physicochemical properties for successful use in drug delivery.

4.5 References

Abdel-Hafez, S. M., Hathout, R. M. and Sammour, O. A. (2014) 'Towards better modeling of chitosan nanoparticles production: Screening different factors and comparing two experimental designs', *International Journal of Biological Macromolecules*, 64, pp. 334–340.

Agnihotri, S. A., Mallikarjuna, N. N. and Aminabhavi, T. M. (2004) 'Recent advances on chitosan-based micro- and nanoparticles in drug delivery', *Journal of Controlled Release*, pp. 5–28.

Akhtar, F., Rizvi, M. M. A. and Kar, S. K. (2012) 'Oral delivery of curcumin bound to chitosan nanoparticles cured Plasmodium yoelii infected mice.', *Biotechnology Advances*, 30 (1), pp. 310–20.

Aktaş, Y. *et al.* (2005) 'Preparation and in vitro evaluation of chitosan nanoparticles containing a caspase inhibitor', in *International Journal of Pharmaceutics*, pp. 378–383.

Almalik, A. *et al.* (2013) 'Hyaluronic acid-coated chitosan nanoparticles: Molecular weight-dependent effects on morphology and hyaluronic acid presentation', *Journal of Controlled Release*, 172(3), pp. 1142–1150.

Anarjan, N. *et al.* (2011) 'Effect of processing conditions on physicochemical properties of sodium caseinate-stabilized astaxanthin nanodispersions', *LWT - Food Science and Technology*, 44(7), pp. 1658–1665.

Antoniou, J. *et al.* (2015) 'Physicochemical and morphological properties of size-controlled chitosan–tripolyphosphate nanoparticles', *Colloids and Surfaces A: Physicochemical and Engineering Aspects*, 465, pp. 137–146.

Bezerra, M. A. *et al.* (2008) 'Response surface methodology (RSM) as a tool for optimization in analytical chemistry.', *Talanta*, 76(5), pp. 965–77.

Bhattarai, N. *et al.* (2006) 'Chitosan and lactic acid-grafted chitosan nanoparticles as carriers for prolonged drug delivery', *International Journal of Nanomedicine*, 1(2), p. 181.

Bhumkar, D. R. and Pokharkar, V. B. (2006) ‘Studies on effect of pH on cross-linking of chitosan with sodium tripolyphosphate: a technical note’, *AAPS Pharmscitech*, 7(2), pp. E138–E143.

Bulmer, C., Margaritis, A. and Xenocostas, A. (2012) ‘Production and characterization of novel chitosan nanoparticles for controlled release of rHu-Erythropoietin’, *Biochemical Engineering Journal*, 68, pp. 61–69.

Calvo, P. *et al.* (1997) ‘Novel hydrophilic chitosan-polyethylene oxide nanoparticles as protein carriers’, *Journal of Applied Polymer Science*, 63(1), pp. 125–132.

Chen, M. C. *et al.* (2013) ‘Recent advances in chitosan-based nanoparticles for oral delivery of macromolecules’, *Advanced Drug Delivery Reviews*, pp. 865–879.

De Carvalho, S. M. *et al.* (2013) ‘Optimization of α-tocopherol loaded solid lipid nanoparticles by central composite design’, *Industrial Crops and Products*, 49, pp. 278–285.

Diop, M. *et al.* (2015) ‘Design, characterisation, and bioefficiency of insulin-chitosan nanoparticles after stabilisation by freeze-drying or cross-linking’, *International Journal of Pharmaceutics*, 491(1–2), pp. 402–408.

Dong, Y. et al. (2013) ‘Scalable ionic gelation synthesis of chitosan nanoparticles for drug delivery in static mixers’, *Carbohydrate Polymers*, 94(2), pp. 940–945.

El-Shabouri, M. . (2002) ‘Positively charged nanoparticles for improving the oral bioavailability of cyclosporin-A’, *International Journal of Pharmaceutics*, 249(1–2), pp. 101–108.

Fathi, M., Martín, Á. and McClements, D. J. (2014) ‘Nanoencapsulation of food ingredients using carbohydrate based delivery systems’, *Trends in Food Science and Technology*, 39, pp. 18–39.

Ferreira, S. L. C. *et al.* (2007) ‘Statistical designs and response surface techniques for the optimization of chromatographic systems’, *Journal of Chromatography A*, 1158(1), pp. 2–14.

Fonte, P. *et al.* (2014) ‘Polymer-based nanoparticles for oral insulin delivery: Revisited approaches’, *Biotechnology Advances*, 33(6), pp. 1342–1354.

Gan, Q. *et al.* (2005) ‘Modulation of surface charge, particle size and morphological properties of chitosan–TPP nanoparticles intended for gene delivery’, *Colloids and Surfaces B: Biointerfaces*, 44(2), pp. 65–73.

Grenha, A. (2012) ‘Chitosan nanoparticles: a survey of preparation methods’, *Journal of Drug Targeting*, 20(4), pp. 291–300.

Gupta, V. K. and Karar, P. K. (2011) ‘Optimization of Process Variables for the Preparation of Chitosan - Alginate Nanoparticles’, *International Journal of Pharmacy and Pharmaceutical Sciences*, 3, pp. 3–5.

Hao, J. *et al.* (2012) ‘Development and optimization of baicalin-loaded solid lipid nanoparticles prepared by coacervation method using central composite design’, *European Journal of Pharmaceutical Sciences*, 47(2), pp. 497–505.

Huang, Y., Cai, Y. and Lapitsky, Y. (2015) ‘Factors affecting the stability of chitosan/tripolyphosphate micro- and nanogels: resolving the opposing findings’, *Journal of Materials Chemistry B*, 3(29), pp. 5957–5970.

Janes, K. A., Calvo, P. and Alonso, M. J. (2001) ‘Polysaccharide colloidal particles as delivery systems for macromolecules’, *Advanced Drug Delivery Reviews*, 47(1), pp. 83–97.

Jonassen, H., Kjøniksen, A. L. and Hiorth, M. (2012) ‘Effects of ionic strength on the size and compactness of chitosan nanoparticles’, *Colloid and Polymer Science*, 290(10), pp. 919–929.

Khalid, M. (2014) *Formulation and characterisation of food derived peptides into a nanoparticle oral drug delivery system using a Design of Experiment (DOE) approach*. Dublin Institute of Technology.

Kleine-Brueggeney, H. *et al.* (2015) ‘A rational approach towards the design of chitosan-based nanoparticles obtained by ionotropic gelation’, *Colloids and Surfaces B: Biointerfaces*., 135, pp. 99–108.

Koppolu, B. P. *et al.* (2014) ‘Controlling chitosan-based encapsulation for protein and vaccine delivery’, *Biomaterials*, 35(14), pp. 4382–4389.

Kouchak, M. and Azarpanah, A. (2015) ‘Preparation and inVitro Evaluation of Chitosan Nanoparticles Containing Diclofenac Using the Ion-Gelation Method’, *Jundishapur Journal of Natural Pharmaceutical Products*, 10(2).

Kwon, I. C. (2008) ‘Chitosan-based nanoparticles for cancer therapy; tumor specificity and enhanced therapeutic efficacy in tumor-bearing mice’, *Journal of Controlled Release*, 132(3), pp. e69–e70.

Landriscina, A. (2015) ‘Biodegradable chitosan nanoparticles in drug delivery for infectious disease’, *Nanomedicine*, 10, pp. 1609–1619.

Luo, Y. *et al.* (2010) 'Preparation, characterization and evaluation of selenite-loaded chitosan/TPP nanoparticles with or without zein coating', *Carbohydrate Polymers*, 82(3), pp. 942–951.

Masarudin, M. J. *et al.* (2015) 'Factors determining the stability, size distribution, and cellular accumulation of small, monodisperse chitosan nanoparticles as candidate vectors for anticancer drug delivery: Application to the passive encapsulation of [14C]-doxorubicin', *Nanotechnology, Science and Applications*, 8, pp. 67–80.

Mohammed, M. H., Williams, P. a. and Tverezovskaya, O. (2013) 'Extraction of chitin from prawn shells and conversion to low molecular mass chitosan', *Food Hydrocolloids*, 31(2), pp. 166–171.

Mukhopadhyay, P. *et al.* (2013) 'Oral insulin delivery by self-assembled chitosan nanoparticles: in vitro and in vivo studies in diabetic animal model.', *Materials Science & Engineering. C, Materials for Biological Applications*, 33(1), pp. 376–82.

Nagpal, K., Singh, S. K. and Mishra, D. N. (2010) 'Chitosan Nanoparticles: A Promising System in Novel Drug Delivery', *Chemical & Pharmaceutical Bulletin*, 58(11), pp. 1423–1430.

Pan, Y. *et al.* (2002) 'Bioadhesive polysaccharide in protein delivery system: Chitosan nanoparticles improve the intestinal absorption of insulin in vivo', *International Journal of Pharmaceutics*, 249(1–2), pp. 139–147.

Papadimitriou, S. *et al.* (2008) 'Chitosan nanoparticles loaded with dorzolamide and pramipexole', *Carbohydrate Polymers*, 73(1), pp. 44–54.

Politis, S. N. *et al.* (2017) 'Design of experiments (DoE) in pharmaceutical development', *Drug Development and Industrial Pharmacy*, 43(6), pp. 889–901.

Prochazkova, S., Vårum, K. M. and Ostgaard, K. (1999) 'Quantitative determination of chitosans by ninhydrin', *Carbohydrate Polymers*, 38(2), pp. 115–122.

Ramasamy, T. *et al.* (2014) 'Chitosan-based polyelectrolyte complexes as potential nanoparticulate carriers: Physicochemical and biological characterization', *Pharmaceutical Research*, 31(5), pp. 1302–1314.

Rampino, A. *et al.* (2013) 'Chitosan nanoparticles: Preparation, size evolution and stability', *International Journal of Pharmaceutics*, 455(1), pp. 219–228.

Reddy, Y. *et al.* (2017) 'Formulation and Optimization of Extended Release Matrix Tablets of Losartan Potassium Using Response Surface Methodology (RSM)', *Journal of*

Pharmaceutical Research International, 19(5), pp. 1–12.

des Rieux, A. *et al.* (2006) 'Nanoparticles as potential oral delivery systems of proteins and vaccines: a mechanistic approach', *Journal of Controlled Release*, 116(1), pp. 1–27.

Saini, D. *et al.* (2014) 'Formulation, development and optimization of raloxifene-loaded chitosan nanoparticles for treatment of osteoporosis', *Drug Delivery*, (0), pp. 1–14.

Sarvaiya, J. and Agrawal, Y. K. (2015) 'Chitosan as a suitable nanocarrier material for anti-Alzheimer drug delivery', *International Journal of Biological Macromolecules*, 72, pp. 454–465.

Sureshkumar, M. K. *et al.* (2010) 'Adsorption of uranium from aqueous solution using chitosan-tripolyphosphate (CTPP) beads', *Journal of Hazardous Materials*, 184(1–3), pp. 65–72.

Vongchan, P. *et al.* (2011) 'N, N, N-Trimethyl chitosan nanoparticles for the delivery of monoclonal antibodies against hepatocellular carcinoma cells', *Carbohydrate Polymers*, 85(1), pp. 215–220.

Wang, M. *et al.* (2013) 'A comparison of approaches to stepwise regression for global sensitivity analysis used with evolutionary optimization', in *Proceedings of the BS2013, 13th Conference of International Building Performance Simulation Association*, pp. 26–28.

Wu, H. *et al.* (2014) 'Emulsion cross-linked chitosan/nanohydroxyapatite microspheres for controlled release of alendronate', *Journal of Materials Science: Materials in Medicine*, 25(12), pp. 2649–2658.

Xue, M. *et al.* (2015) 'Development of chitosan nanoparticles as drug delivery system for a prototype capsid inhibitor', *International Journal of Pharmaceutics*, 495(2), pp. 771–782.

Yan, H. *et al.* (2012) 'Preparation of chitosan/poly (acrylic acid) magnetic composite microspheres and applications in the removal of copper (II) ions from aqueous solutions', *Journal of Hazardous Materials*, 229, pp. 371–380.

Zolgharnein, J., Shahmoradi, A. and Ghasemi, J. B. (2013) 'Comparative study of Box–Behnken, central composite, and Doehlert matrix for multivariate optimization of Pb (II) adsorption onto Robinia tree leaves', *Journal of Chemometrics*, 27(1–2), pp. 12–20.

5 APPLICATION OF BOX-BEHNKEN EXPERIMENTAL DESIGN FOR THE FORMULATION AND OPTIMISATION OF SELENOMETHIONINE-LOADED CHITOSAN NANOPARTICLES COATED WITH ZEIN FOR ORAL DELIVERY

The work presented in this chapter is reproduced from:

Vozza, G., Khalid, M.D, Byrne, H. J., Ryan, S and Frias, J. (2018). Application of Box-Behnken experimental design for the formulation and optimisation of selenomethionine-loaded chitosan nanoparticles coated with zein for oral delivery. Submitted to the International Journal of Pharmaceutics (IJP) on 25.03.2018.

Vozza, G., was the primary author, Khalid, M.D., helped develop the formulation process and Byrne, H. J., Frias, J. and Ryan S contributed to layout, design and proofing.

Numbering of Sections, Figures and Tables has been adapted to the thesis format.

Abstract

Selenomethionine is an essential amino acid with a narrow therapeutic index and susceptibility to oxidation. Here it was encapsulated into a nanoparticle composed of chitosan cross-linked with tripolyphosphate for oral delivery. The formulation was optimised using a three-factor Box-Behnken experimental design. The chitosan:tripolyphosphate ratio, chitosan solvent pH, and drug load concentration were independently varied. The dependent variables studied were encapsulation efficiency, particle size, polydispersity index (PDI) and zeta potential (ZP). For optimisation, encapsulation efficiency and zeta potential were maximised, particle diameter was set to 300 nm and PDI was minimised. A 0.15mg/mL concentration of selenomethionine, chitosan solvent pH of 3, and chitosan:tripolyphosphate ratio of 6:1 yielded optimum nanoparticles of size 187±58nm, PDI 0.24±0.01, ZP 36±6mV, and encapsulation efficiency of 39±3%. Encapsulation efficiency was doubled to 80±1.5% by varying pH of the ionotropic solution components and by subsequent coating of the NPs with zein, increasing NP diameter to 377±47nm, whilst retaining PDI and ZP values. Selenomethionine-entrapped nanoparticles were not cytotoxic to intestinal and liver cell lines. Accelerated thermal stability studies indicated good stability of the nanoparticles under normal storage conditions. In simulated gastrointestinal and intestinal fluid conditions, 60% cumulative release was obtained over 6 hours.

Keywords

chitosan, zein, selenomethionine, nanoparticles, Box-Behnken design, oral delivery.

Abbreviations

BBD, Box-Behnken design; **CL113**, PROTASAN™ UP; **Cs**, Chitosan; **DLS**, dynamic light scattering; **EE%**, Encapsulation efficiency; **GRAS**, Generally recognised as safe; **LDV**, laser doppler velocimetry; **MSC**, methylselenocysteine; **NP**, nanoparticle; **PDI**, Polydispersity; **pI**, Isoelectric point; **SeCys**, selenocysteine; **SeMet**, Selenomethionine; **TPP**, Tripolyphosphate; **ZP**, Zeta potential.

5.1 Introduction

Selenium is an essential micronutrient in human and animal nutrition (Rayman, 2000), that exists in a wide array of different formats, both organic and inorganic, better known as speciation. Selenomethionine (SeMet), the selenium analogue of methionine, is the predominant form of organic Se found in foods from the *Brassica* and *Allium* families (Reilly *et al.*, 2014). SeMet is used for oral supplementation due to its capacity to be non-specifically incorporated into body proteins in place of methionine (Rayman, Infante and Sargent, 2008). The potential health benefits of selenium are dependent on its chemical species, and several studies have suggested a possible role in cancer prevention (Nie *et al.*, 2016), increased immunological status (Narayan *et al.*, 2015) and increased fertility (Shanmugam *et al.*, 2015). SeMet may also to have a number of benefits regarding oncology treatments due to its modulation of the therapeutic efficacy and selectivity of anticancer drugs (Evans, Khairuddin and Jameson, 2017), capacity to provide protection of normal tissues from the toxicities associated with chemotherapy and radiation treatments, in addition to enhancing their anti-tumour effects (Chintala *et al.*, 2012; Mix *et al.*, 2015; Panchuk *et al.*, 2016). It

may also have some potential in degenerative disease by decreasing oxidative stress of small molecule antioxidants used as a buffer for free radicals in brain tissue (Song *et al.*, 2014; Reddy *et al.*, 2017). However, the oral delivery of SeMet can be challenging due to the distinctive electronegativity and atomic radius of the selenium atom (i.e. larger radius and lower electronegativity than sulphur,) that makes it easier for low valence state Se compounds to be more readily oxidised compared to their sulphur counter parts (Xu, Cao and Zhang, 2013). SeMet is readily oxidised (Davies, 2016) and, even though it is less toxic than inorganic selenium (Se), it still has a low therapeutic index (Takahashi, Suzuki and Ogra, 2017). Oral delivery formulations of SeMet therefore need to consider the balance between doses that exert beneficial effects and those which may potentially be toxic.

Inorganic Se species such as selenite (SeO_3^{2-}) and elemental selenium (Se_0), together with methylseleninic acid, have been formulated to nano-enabled delivery systems which exhibited improved bioactivity with reduced cytotoxicity *in vitro* (Zhang, Wang and Xu, 2008; Forootanfar *et al.*, 2014; Loeschner *et al.*, 2014). Nanoparticles (NPs) can be more biologically active due to their enhanced surface area per mass compared with larger-sized particles of the same chemistry (Oberdörster *et al.*, 2005). By using NPs as a drug delivery vehicle, it might be possible to enhance a range of characteristics for a given bioactive, including increased protection and stability (Nair *et al.*, 2010) and suitability to increase bioavailability by non-parenteral routes of administration including oral, pulmonary and topical applications (Helson, 2013).

The natural polymer chitosan (Cs) is a mucopolysaccharide, closely related to cellulose and obtained by deacetylation of the compound chitin, predominantly found in the exoskeletons of crustaceans (Nagpal, Singh and Mishra, 2010). Cs has been used for the development and formulation of nanoparticles by ionotropic gelation due

to its physicochemical and biological beneficial properties (H. Zhang *et al.*, 2015; Mohammed *et al.*, 2017). Benefits include improved adherence to mucosal surfaces, increased drug residence time (Ryan *et al.*, 2012), and protection of the bioactive drug from intestinal proteases (Ryan *et al.*, 2013; Amaro *et al.*, 2015). In acidic medium, Cs can be dissolved, due to protonation of the amine residues present in the polymer backbone. Ionotropic gelation allows for the formation of NPs from Cs via crosslinking with oppositely-charged electrolytes under mild conditions in which amino acids and peptides will remain reasonably stable (Janes, Calvo and Alonso, 2001; Wang *et al.*, 2011; Chen *et al.*, 2013).

Zein a GRAS approved prolamine-rich protein derived from maize, has been used in the formulation and coating of peptide oral delivery systems (Y. Zhang *et al.*, 2015), to increase encapsulation efficiency (Luo and Wang, 2014) and improve the control of gastric release of labile bioactives (Luo *et al.*, 2010; Paliwal and Palakurthi, 2014). By exploiting the physical interactions between protein and polysaccharide (in this instance zein and Cs), it is possible to improve and broaden the physical and chemical stability properties of the NP delivery systems (Benshitrit *et al.*, 2012). However, the formulation, characterisation and development of these multi-component systems can be more challenging than single component systems and as such, it is important to comprehensively optimise the formulation process. To the best of our knowledge, there are currently no reports which describe the formulation of biological Se species such as SeMet into a NP delivery system. The potential optimisation of this formulation could be significant, given that SeMet more effectively increases human and animal selenium levels and is less toxic than inorganic Se (Garousi, 2015).

In situations where several variables may influence system properties, a useful technique to identify the relationships between a given response and independent

variables (or factors) and optimise the system, is Response Surface Methodology (RSM) (Anderson and Whitcomb, 2005). RSM is a more efficient approach to experimentation than one factor at a time (OFAT) experiments since it: 1) reduces the number of experimental runs typically required to gather the same information as OFAT, thus reducing resource requirements, 2) is useful in detecting interdependencies of variables that would not be typically identified during OFAT experiments and 3) improves the prediction of a response through use of gathered information from a larger parameter space. The Box-Behnken design (BBD) is an RSM for process optimisation with an independent quadratic design where factor combinations are considered at 3 levels: the midpoints of edges of the process space and the centre (Traynor *et al.*, 2013; Zolgharnein, Shahmoradi and Ghasemi, 2013). After polynomial models for each of the different responses in a study have been completed, a desirability function may be constructed in order to estimate minima or maxima, provided such optima are within the design space (Bezerra *et al.*, 2008).

In this study, SeMet was formulated into nanoparticles consisting of Cs and zein using ionotropic gelation. After evaluating the main variables which affect encapsulation efficiency, particle size and drug loading, a systematic approach (RSM) was used to optimise the formulation of nanoparticles suitable for oral delivery. A three-level, three-factor BBD was utilised to build polynomial models for the three responses and a desirability function was then constructed to optimise the system. Optimised SeMet NPs were prepared based on the predicted optimum levels of the independent variables of the factorial design. To ensure stability of the optimised formulation after lyophilisation, a cryoprotectant (trehalose) was also included (Danish *et al.*, 2017a). The physicochemical properties, storage stability, cytotoxicity, and the release profile in a simulated intestinal buffer were assessed.

5.2 Materials and Methods

5.2.1 Materials

The chitosan PROTASAN™ UP (CL113) was purchased from NovaMatrix, FMC Corporations, Norway. DL-selenomethionine, D(+)-Trehalose dihydrate, and zein, of ≥99% purity, were obtained from ACROS Organics™, Fisher Scientific, Ireland. Ultra-pure water 18mΩcm^{-1} was obtained from a Millipore simplicity 185 model instrument, UK, and was used for all aqueous solution preparations throughout. All other reagents, chemicals and solvents were of analytical grade from Sigma Aldrich, Ireland.

5.2.2 Optimisation of nanoparticle formulation physicochemical properties

A BBD was used to optimise the formulation and EE% of SeMet into the nanoparticle. Selected physicochemical properties for oral delivery for the NPs were particle size ~300 nm, PDI < 0.5 and ZP > 30 mV (des Rieux *et al.*, 2006). A three level, three factor BBD (Zhao *et al.*, 2013; Maleki Dizaj *et al.*, 2015) of 15 random order experiments was designed using Minitab™ 17 (Pennsylvania, USA). The 3 independent variables were, (X_1) the pH of the Cs solvent - the isoelectric point (pI) of SeMet, (pH-pI) (X_2), the load concentration of SeMet and (X_3) the ratio of Cs:TPP, while (Y_1) Particle size, (Y_2) PDI, (Y_3) ZP and (Y_4) EE% were the dependent variables. The variable ranges (Table 5.1) were based on an exploratory study.

Each dependant variable was independently assessed by linear regression using a 2nd degree polynomial model with 1st order interactions (Equation 5.1).

$$Y_i = b_0 + b_1X_1 + b_2X_2 + b_3X_3 + b_{12}X_1X_2 + b_{13}X_1X_3 + b_{23}X_2X_3 + b_{11}X_1^2 + b_{22}X_2^2 + b_{33}X_3^2+\varepsilon$$

(Equation 5.1)

where Y_i is the measure of the response associated with each factor level combination, b_0 is an intercept, b_1-b_{33} are the regression coefficients, X_1-X_3 are the coded independent variables and the X_iX_j and X_i^2 ($_{i,j}$ = 1, 2, 3) denote the interactive and quadratic terms, respectively. The linear regression and the significance ($p<0.05$) test of independent variables and their interactions was assessed by statistical software (Minitab™,17) to generate regression models. Through bidirectional elimination (testing at each step for variables to be included or excluded), non-significant terms were removed from the model in order to calculate regression equations with significant terms only (Wang *et al.*, 2013). Desirability functions to optimise all responses were built the weighted geometric mean of individual desirabilities presented in Table 5.1.

Table 5.1 Variables and levels employed in the BBD with desirability function for optimisation of nanoparticle formulation.

Factor (Independent variables)	**Levels used, (Actual coded)**		
X_1 = pH of the Cs solvent – the pI of SeMet (pH-pI)	0.5	1.5	2.5
X_2 = SeMet concentration (mg/mL)	0.05	0.15	0.25
X_3 = ratio of Cs:TPP	4:1	6:1	8:1
Dependent Variables	**Composite desirability**		
Y_1= Size (nm)	Target of 300nm		
Y_2 = PDI	Minimise		
Y_3 = ZP (mV)	Maximise		
Y_4 = Encapsulation efficiency (EE%)	Maximise		

Response surface plots, statistical testing of the linear models and identification of optimum formulations *via* feasibility and grid searches was performed to study the optimal area (Barrentine, 1999). Finally, repetitions (N=4) of the optimal point found were conducted experimentally to validate the study.

5.2.3 Preparation of SeMet loaded Cs:TPP nanoparticles

SeMet-entrapped NPs were produced using a modified ionic gelation method (Calvo *et al.*, 1997). Briefly, Cs was dissolved in buffered pH medium (3, 4 or 5 pH) at a concentration of 3 mg/mL and filtered through a 0.22 μm syringe filter (Millex Millipore, UK) to remove undissolved Cs. A known amount of SeMet was then added to the Cs solution prior to crosslinking to obtain a final load concentration 0.05, 0.150 or 0.250 mg/mL. TPP was added dropwise to the solution under stirring at 700 rpm and room temperature to yield final mass ratios of Cs:TPP NPs of 4:1, 6:1 or 8:1. All of these experimental parameters (pH, concentrations and ratios) were prepared according to the BBD design. The NP suspension was stirred at 700 rpm for 30 min at room temperature for further crosslinking. After stabilisation, NPs were then

transferred to a 30 kDa molecular weight cut off (Vivaspin 20, Sartorius) centrifugal filter and isolated by centrifugation at 3000 rpm for 30 min. Filtered H_2O (equivalent in volume to the recovered supernatant) was then added to the isolated NPs and sonicated at 35 % amplitude for 30 s with 5 s pulse intervals. Physicochemical properties of the NPs were then determined as per Section 2.4, using a Malvern Zetasizer NanoZS (Worcestershire, UK) and the supernatant was retained for EE% determination as outlined in Section 2.7. The optimised formulation has a mass ratio 6:1 (Cs:TPP), Cs media (pH 5), and a final SeMet load concentration of 0.15 mg/mL.

5.2.4 Increase of Ionisation/Protonation states to increase EE% - Formulation I

After optimising the general physicochemical properties via BBD (Section 2.2), the ionic gelation component preparation procedure was modified with the aim of increasing the EE%. Formulation I was produced as described in Section 2.3 with one exception: SeMet and TPP were dissolved and diluted with NaOH (0.01 M) prior to crosslinking. The rationale for the pH adjustment was to induce higher electrostatic interactions (i.e. maximise the cationic component of Cs and the anionic component of SeMet) between SeMet and Cs during the crosslinking process.

5.2.5 Coating NPs with zein to increase EE%

NPs were prepared as per formulation I (ratio 6:1 (Cs:TPP), Cs media (pH 3), TPP/SeMet NaOH solution (pH 11) and a final load concentration of 0.15 mg/mL), with the following modifications: after the NPs had stabilised, 8 mL of absolute EtOH were added dropwise to the formulation whilst the stirring speed of the solution was maintained at 700 rpm for 30 min at room temperature. Zein (10 mg/mL dissolved in

80 % EtOH and filtered) was added dropwise to yield zein:Cs mass ratios of 0.5:1, 1:1 and 2:1, stabilised at 700 rpm for 30 min and isolated as per Section 2.3. The NP formulations were then concentrated under vacuum (175 mbar) at 40 °C until EtOH was completely removed. To ensure stability of the optimised formulation after lyophilisation, 10 mL of the cryoprotectant trehalose 5 % w/v in H_2O was added to each formulation and lyophilised for 36 hr (Danish *et al.*, 2017a).

5.2.6 Particle size, PDI and surface charge

Freshly prepared NP solutions were used for physicochemical analysis (Luo *et al.*, 2010). The mean particle size and PDI of the NP formulations were determined by dynamic light scattering (DLS). The ZP values were measured with the use of laser doppler velocimetry (LDV). Both DLS and LDV analysis were performed in triplicate at 25 °C with a Zetasizer Nano series Nano-ZS ZEN3600 fitted with a 633 nm laser (Malvern Instruments Ltd., UK), using a folded capillary cuvette (Folded capillary cell-DTS1060, Malvern, UK). The values presented herein were acquired from three separate experiments, each of which included three replicates; N=3.

5.2.7 Scanning electron microscopy (SEM)

NP morphology was evaluated by scanning electron microscopy (SEM) (Hitachi, SU6600 FESEM, USA), at an accelerating voltage of 20 kV, unless otherwise stated, using the secondary electron detector. The fresh NP solutions were then spin coated onto Si wafers, dried at room temperature and then sputter coated with 4 nm Au/Pd prior to imaging (Mukhopadhyay *et al.*, 2013).

5.2.8 Fourier transform infrared spectroscopy (FTIR)

FTIR spectra of CL113, TPP, Cs:TPP NPs, SeMet and SeMet loaded Cs:TPP NPs were acquired via a Spotlight 400 series spectrometer (Perkin Elmer, USA), using the attenuated total reflectance spectroscopy method (ATR-FTIR), in the range of 650-4000 cm^{-1}. Prior to analysis, NP samples were lyophilised using a FreeZone 6 L bench top freeze dry system (Labconco, USA) at -40 °C for 20 hr. The dried solids were then placed on the ATR crystal prism (ZnSe), and 32 scans were acquired at 4 cm^{-1} resolution with background subtraction (Vongchan *et al.*, 2011).

5.2.9 Encapsulation efficiency of SeMet in Cs:TPP nanoparticles

The EE% of SeMet in the NPs was determined by the separation and quantification of SeMet left in the supernatant. This was performed by ultracentrifugation at 3000 rpm, 4 °C for 30 min. SeMet in the supernatant was quantified by reverse phase high performance liquid chromatography (RP-HPLC), as previously described (Ward, Connolly and Murphy, 2012) with the following modifications. Samples were analysed with a Waters 2998 HPLC and Photodiode Array Detector, (Waters, USA), using a Poroshell 120, EC-C8 column, 3.0 x 100 mm, 2.7 µm, (Agilent Technologies, UK). Isocratic elution was carried out at a flow rate of 0.4 mL/min, column temperature 45.0 ± 5.0 °C with a mobile phase of water/methanol/trifluoroacetic acid (97.9:2.0:0.1). Samples were monitored according to their UV absorbance at 218 nm. The encapsulation efficiency was calculated by Equation 5.2 (Xu and Du, 2003):

$$EE\% = \frac{Total\ amount\ of\ Se\ Met - Free\ amount\ of\ SeMet}{Total\ amount\ of\ SeMet}\ X\ 100$$

(Equation 5.2)

5.2.10 MTS assay

The potential cytotoxicity of pure SeMet, SeMet loaded NPs and unloaded NPs (coated with zein) were examined on Caco-2 human epithelial cells, and HepG2 human liver hepatocellular cells. Both cell lines are routinely employed to assess the potential toxicity of orally delivered compounds (Gleeson *et al*., 2015; Brayden *et al*., 2015). Caco-2 and HepG2 cells, were seeded at a density of 2 x 10^4 cells/well and cultured on 96 well plates in Dulbecco's Modified Eagle Medium (DMEM) and Eagle's Minimum Essential Medium (EMEM) respectively, supplemented with 10 % foetal bovine serum, 1 % L-glutamine, 1 % penicillin-streptomycin and 1 % non-essential amino acids at 37 °C in a humidified incubator with 5 % CO_2 and 95 % O_2. Time points were selected with the intention to mimic *in vivo* conditions for each cell type. As the maximum time NPs will be exposed to the intestine, a 4 hr exposure time was used in Caco-2 cell lines (Neves *et al.,* 2016), to mimic the liver, a 72-h exposure time was used for HepG2 cell lines (Brayden, Gleeson and Walsh, 2014). Triton X-100™ (0.05%) was used as a positive control. The concentrations of the test compounds applied were 25, 50 and 100 uM. After exposure, treatments were removed and replaced with MTS (3-(4,5-dimethylthiazol-2-yl)-5-(3-carboxymethoxyphenyl)-2-(4-sulfophenyl)-2H-tetrazolium). Optical density (OD) was measured at 490 nm using a microplate reader (TECAN GENios, Grodig, Austria). Each value presented was normalised against untreated control and calculated from three separate experiments, each of which included six replicates.

5.2.11 Accelerated stability analysis

NPs were suspended at a concentration of 0.1 mg/mL, in aqueous KCl solution (10 mM) and stored at accelerated conditions: 60 °C for 720 min, 70 °C for 300 min and 80 °C for 120 min (Danish *et al.*, 2017b). The particle size, PDI and zeta potential were measured using the Nanosizer ZS (Malvern Instruments Ltd, UK) over time intervals to determine the degree of degradation. The generated data was then analysed via R software (R Core Team, 2016). The temperature dependence of the kinetic parameters of SeMet-loaded NPs stability was measured by calculating the observed rate constants. This was plotted in an Arrhenius representation and apparent activation energy, E_a and reaction rate constant, k_{ref} were calculated according to Equation 5.3:

$$\boldsymbol{P = Po + e^{ln(k) - \frac{Ea}{R}(\frac{1}{T} - \frac{1}{T_{ref}})} t}$$

(Equation 5.3)

where P is the property (particle size, PDI or ZP) at time t, Po is the initial property conditions, k is the apparent zero order reaction constant, E_a is the energy of activation, R is the universal gas constant, T is the temperature of the experiment in Kelvin (K) and T_{ref} is the reference temperature (343 K).

5.2.12 *In vitro* controlled release studies

SeMet release from the NPs was carried out using a dialysis bag diffusion technique (Hosseinzadeh *et al.*, 2012) over 6 hr (Calderon L. *et al.*, 2013; Yoon *et al.*, 2014). Freeze dried SeMet loaded NPs were suspended in 5 mL H_2O and sonicated at 35 % amplitude for 30 s with 5 s intervals and placed into a Float-A-Lyzer®G2 dialysis membrane with a pore size of 25 kDa (Spectrum Laboratories, USA). The sample was

placed into 40 mL of simulated gastric fluid (SGF) or simulated intestinal fluid (SIF) specified according to the British Pharmacopoeia (Pharmacopoeia, 2016). SGF was composed of 0.1 M HCL and SIF was composed of 1 volume of 0.2 M trisodium phosphate dodecahydrate and 3 volumes of 0.1 M HCL (adjusted to pH 6.8), without enzymes (British Pharmacopoeia Commission, 2016). Samples were placed in a thermostatic shaker at 37 ºC and agitated at 100 rpm. At predetermined time points, 1 mL of release fluid was analysed and replaced with simulated fluid to maintain sink conditions.

SeMet release was measured by RP-HPLC (Section 5.2.9). Equation 5.4 was used to determine the % drug release:

$$\boldsymbol{Drug_{rel}}\,\% = \frac{\boldsymbol{C(t)}}{\boldsymbol{C(l)}} * \mathbf{100}$$

(Equation 5.4)

where $Drug_{rel}$ is the percentage of SeMet released, C(*l*) represents the concentration of drug loaded and C(t) represents the amount of drug released at time t, respectively.

5.3 Results and Discussion

5.3.1 Response Surface Modelling – Box Behnken design

The observed values for all 15 experiments described by the BBD yielded minimum and maximum values for Size (Y_1) (152, 318 nm), PDI (Y_2) (0.218, 0.554), ZP (Y_3) (26.0, 42.7 mV) and EE% (Y_4) of, (24.7, 41.4 %). The reduced models resulting from the analysis are presented in Table 5.2. Response Y_1 showed no significant terms in the model, suggesting that there was no evidence in the sample population that could prove the association of the independent variables with particle size. This finding is unsurprising, as the NPs produced in this study fell within a narrow target region (152, 318 nm) and the regions of interest chosen in this study (e.g. Cs:TPP 4:1-8:1, pH 3-5), to produce the Cs NPs, have been well established for yielding particle sizes within 100-400 nm range (Hassani *et al.*, 2015; Sipoli *et al.*, 2015; Mohammed *et al.*, 2017).

Responses Y_2-Y_4 (PDI, ZP and EE% respectively) all showed a curvature with regards to X_1-X_3, as quadratic or interactive effects of some independent variables were statistically significant in all the models.

Table 5.2 Normalised variable estimated coefficients (Coef) with associated standard error (SE Coef.) and unnormalised reduced regression equations for Y_2-Y_4.

Y_2 (PDI)			**Y_3 (ZP)**			**Y_4 (EE%)**		
Term	**Coef**	**SE Coef**	**Term**	**Coef**	**SE Coef**	**Term**	**Coef**	**SE Coef**
Constant	0.3083	0.0063	Constant	35.534	0.293	Constant	31.731	0.814
X_1 (pH-pI)	0.0515	0.0039	X_1 (pH-pI)	6.405	0.300	X_1 (pH-pI)	6.113	0.599
X_2 (SeMet (mg/mL))	0.0084	0.0039	X_2 (SeMet (mg/mL))	-	-	X_2 (SeMet (mg/mL))	-	-
X_3 (Ratio of Cs:TPP)	0.0521	0.0039	X_3 (Ratio of Cs:TPP)	1.245	0.300	X_3 (Ratio of Cs:TPP)	0.487	0.599
X_1*X_1	-0.0613	0.0057	X_1*X_1	-	-	X_1*X_1	3.821	0.879
X_2*X_2	0.1040	0.0057	X_2*X_2	-	-	X_2*X_2	-	-
X_3*X_3	0.0645	0.0057	X_3*X_3	-2.626	0.419	X_3*X_3	-3.529	0.879
X_1*X_2	-0.0175	0.0054	X_1*X_2	-	-	X_1*X_2	-	-
X_1*X_3	0.0165	0.0054	X_1*X_3	-	-	X_1*X_3	-	-
X_2*X_3	-0.0402	0.0054	X_2*X_3	-	-	X_2*X_3	-	-
R^2adjusted	98.66%		**R^2adjusted**	98.65%		**R^2adjusted**	90.82%	
Equation 5.5	$Y_2 = 0.592 + 0.212\ X_1 - 1.565\ X_2 - 0.1495\ X_3 - 0.06\ X_1$*$X_1$ $+ 10.40\ X_2$*X_2 $+0.01611\ X_3$*$X_3 - 0.175\ X_1$*X_2 $+0.00825\ X_1$*$X_3 - 0.2012\ X_2$*X_3		**Equation 5.6**	$Y_3 = -1.21 + 6.405\ X_1 + 8.49\ X_3 - 0.6588\ X_3$*$X_3$		**Equation 5.7**	$Y_4 = -2.06 + 5.35\ X_1 + 10.83\ X_3 + 3.821\ X_1$*$X_1$ $- 0.882\ X_3$*X_3	

In Table 5.2 (Equation 5.5), PDI was mostly affected by the quadratic effects of X_2*X_2, which showed a positive correlation such that, at -1 and +1 levels of X_2, the PDI increased. It is also worth noting that the linear term of X_2 showed a negative coefficient, indicating that X_2 has a negative effect on PDI until a turning point is reached, whereafter X_2*X_2 has a positive impact on PDI. Similar findings were reported by Masarudin *et al.*, (2015), who found that ratios of Cs:TPP less than 3:1 and greater than 12:1, resulted in a significant increase of the formed NPs PDI values (>0.75). Additionally, they found that the NPs produced at ratios between (median levels) the aforementioned upper and lower bounds resulted in NPs with PDI values ranging from 0.15-0.32. A contour plot based on the regression model is presented in Figure 5.1(A) and highlights this, showing that, at medium load concentrations of 0.15 mg/mL and medium/low ratios of Cs:TPP (4.75:1 to 5.5:1), a minimum value for PDI

can be achieved. Conversely, as the concentration of TPP passes median levels PDI increases, which may be attributable to TPP inducing cross-linking between the nanoparticles and thus the presence of smaller aggregates within the solution (Hu *et al.*, 2008; Antoniou *et al.*, 2015a). Furthermore, the reduction of PDI as the concentration of TPP approaches median levels, has been shown to relate with the increased availability of TPP molecules to interact with the free amino groups of Cs, thus allowing for additional incorporation of the anion within the NP Cs chains (Huang and Lapitsky, 2017). Although PDI can be minimised at these particular levels, it is worth noting that the PDI values for all formulations fell within optimum values for oral delivery (Wong, Al-Salami and Dass, 2017).

The results presented in Table 5.2 (Equation 5.6) show that ZP was not affected by X_2, although it was affected by X_1 (pH-pI) and X_3 (Cs:TPP), indicating that the pH of the formulation medium and the electrostatic forces between the ionizable groups of Cs and TPP determine the net charge of the produced particles. It is likely that this is a direct consequence of the binding between the anionic phosphate groups of TPP with the positively charged amino acid moieties of Cs (Rampino *et al.*, 2013), for example, a positive correlation was observed, such that ZP increased with increasing ratios. In addition, X_1 also showed a prominent effect on ZP, whereby an increase in ZP is observed as X_1 increases. The contour plot representing the reduced regression model (Figure 5.1(B)), demonstrates that low X_1 levels (pH 5 - 4.2) and low ratios of Cs:TPP (4.0/4.5:1) are the areas where NPs of ZP <30mV were obtained (with a minimum of 27 mV). As X_1 increases (approximately pH 3.5), an increment in ZP was observed and maximum values of >39 mV are achieved between X_3 (ratio) of 4.5:1 - 7.5:1. This is in agreement with previous studies by Antoniou *et al.*, (2015), that showed at Cs: TPP mass ratios of 7:1, the ZP of the produced NPs decreased

almost linearly with increasing pH of the formulation medium. As it has been shown that high ZP (either negative or positive), requires higher energy for bringing two particles in contact with each other (Dora *et al.*, 2010), this pH-responsive behaviour can be attributed to the protonation of the primary amino groups present on the Cs chain, resulting in an increase of electron density and repulsion forces between the crosslinked Cs chains (Lai and Guo, 2011). For example, at pH 3.5, the charge interaction between these two molecules becomes strong enough, and stable Cs NPs are obtained. At pH approaching the pI of Cs, reduced availability of protonated amine residues ($-NH_3^+$) present on the Cs polymer backbone chain results in a lower surface charge of the formed NPs (Huang, Cai and Lapitsky, 2015).

EE% was not affected by load concentration (X_2) but was mostly affected by the pH of the Cs media (pH-pI (X_1)) (Table 5.2, Equation 5.7), demonstrating the notable effect of SeMet loading with the charge of both polyelectrolytes (Cs and TPP) and their subsequent interaction during the crosslinking process. As can be seen, a negative correlation was observed, indicating that, as X_1 increases, the EE% decreases, most likely attributable to the reduced protonation of the primary amines present on Cs (Umerska, Corrigan and Tajber, 2014). It is also worth noting that the quadratic term X_1*X_1 showed a positive coefficient, indicating X_1 had a negative effect on EE% until a turning point was reached, where after X_1 had a positive impact on EE%. He *et al.*, (2017), reported that by exploiting the ionic nature of insulin through modulation of the formulation media, the EE% of insulin into Cs:TPP NPs could be significantly enhanced, going from 37 to 94 %. This is evident in the contour plot produced by the regression model (Figure 5.1(C)) showing that, at maximum X_1 levels (approximately 2.5 unit distance from pI of SeMet) and minimum to median/high ratios of Cs:TPP (4:1 - 7.5:1), maximum EE% (>40 %) can be achieved,

indicating that pH plays a significant role in the EE%. These findings agree with those of other research groups (Janes, Calvo and Alonso, 2001; Antoniou *et al.*, 2015b), that reported a strategy to increase ionisable proteins (such as bovine serum albumin (BSA) and insulin) EE% (>80%) within a Cs NP matrix, by dissolving the load protein at a pH above its isoelectric point. By doing this, deprotonation of the hydroxy groups present on the load cargo occurs, inducing a predominantly negative state and thus has a higher affinity to Cs and increased EE%. Several other studies have mirrored these findings, showing that the electrostatic interactions between the acidic groups present on insulin and the amino groups of Cs play a role in the association of insulin to the Cs-NPs by mediation of the ionic interaction between both macromolecules (Pan *et al.*, 2002; Mattu, Li and Ciardelli, 2013).

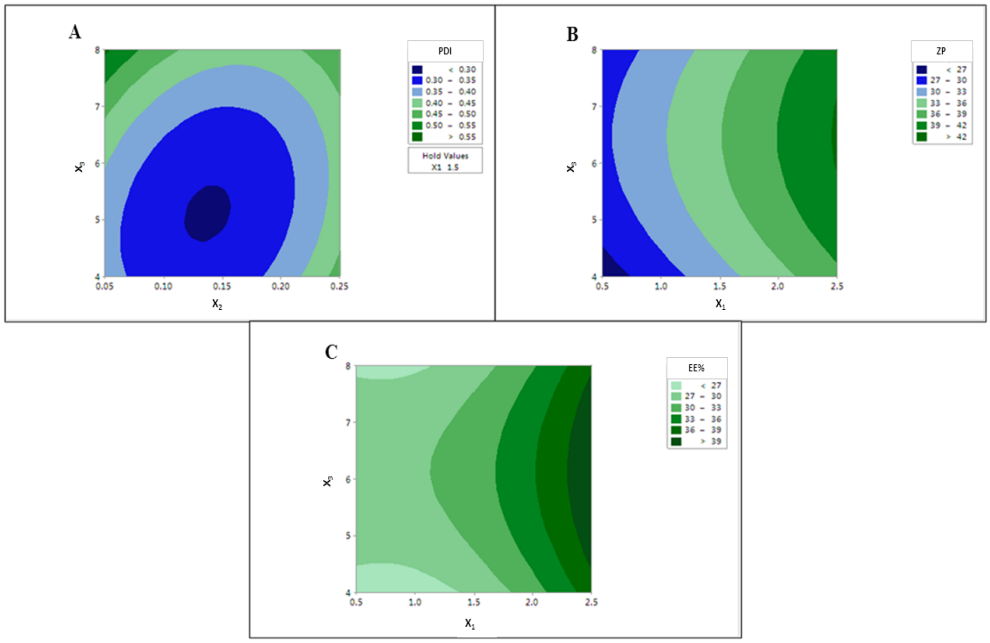

Figure 5.1 Contour Plot of (A) PDI against ratio of Cs:TPP (X_3) and SeMet (mg/mL) (X_2), with pH-pI (X_1) held at median level (1.5), (B) ZP against pH-pI (X_1) and the ratio of Cs:TPP (X_3) and (C) EE% against pH-pI (X_1) vs ratio of Cs:TPP (X_3) for the RSM models presented in Table 5.2.

5.3.2 Optimisation

Employing the models constructed with the BBD evaluation in Table 5.2, response optimisation was employed in order to establish a formulation strategy to yield NPs with minimum PDI values, ZP of ≥30 mV and maximum EE% (des Rieux *et al.*, 2006). As the range of NP sizes within all experimental runs fell within recommended target values for oral delivery, this response was excluded from the optimisation analysis.

Figure 5.2 shows the optimisation plot of the desired responses and indicates that, when the variable settings of X_1, X_2 and X_3 are fixed at 2.5 (pH-pI), 0.15 (mg/mL) and 6 (Cs:TPP), respectively, NPs with the desired properties can be produced. Additionally, the 95 % confidence interval ranges of the predicted NP properties that these conditions would produce are presented in Table 5.3.

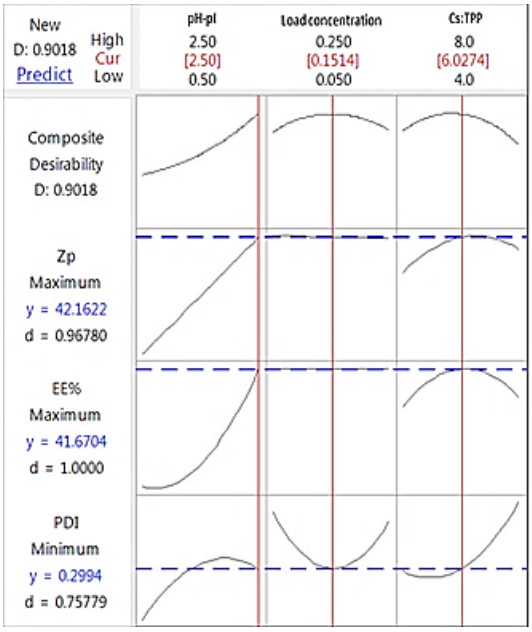

Figure 5.2 Desirability profiles for optimisation of the formulation parameters; X_1 (pH-pI), X_2 (load concentration) and X_3 (Ratio of Cs:TPP) - maximising ZP and EE%, whilst minimising PDI.

To verify the validity of the proposed models, n = 4 replicates of the optimised formulation were prepared, and each experimental response was compared with the predicted one. Table 5.3 shows the validation results of the model, whereby NPs presented sizes of 187 ± 58 nm, PDI of 0.284 ± 0.044, ZP of 39.7 ± 2.6 mV and a max EE% of 39 ± 3 %.

Table 5.3 95% confidence interval for particle characteristics that optimal conditions would produce under the present experimental conditions of uncertainty.

Response	Fit	95 % CI	Actual values
Y_2 (PDI)	0.299 ± 0.007	(0.282, 0.317)	0.284 ± 0.044
Y_3 (mV)	42.2 ± 2.0	(41.6, 42.7)	39.7 ± 2.6
Y_4 (EE%)	41.7 ± 1.0	(39.5, 43.8)	39 ± 3

No statistically significant values ($p>0.05$) for predicted and measured responses (Y_2-Y_4) were observed, indicating that the models fit the data satisfactorily and has adequate precision for the prediction of NP ZP, PDI and EE% in the chosen space of independent variables (in the domain of levels chosen for the independent variables). Additionally, several consuming and laborious laboratory studies were eliminated in this study by using the BBD, rather than a OFAT approach.

5.3.3 EE% optimisation I: protonation and ionisation

The results from the BBD were promising in terms of the NPs produced and their physicochemical properties. However, even when optimised, EE% remained low at approximately 40 %. A second study was undertaken with the aim of maximising the EE%, by controlling the ionisation process, given that this property primarily influenced the encapsulation efficiency in the desirability profile (Figure 5.2). In the previous BBD, it was noted that the highest EE% of SeMet within Cs:TPP NPs was obtained when the pH of the Cs medium was maintained at pH 3 and the SeMet load

was dissolved within it prior to crosslinking. The fundamentals of ionotropic gelation exploit the opposing charges between the protonated amine residues found on the glucosamine residue unit of Cs against the deprotonated hydroxyl groups on TPP (Janes, Calvo and Alonso, 2001). In order to increase the EE%, a modulation of the ionisation state of SeMet was achieved by dissolving it (and TPP) in a basic solution prior to crosslinking with Cs. The rationale for this approach is the observation that the pKa for the acid moiety of SeMet is pH 2.6, whereas the pKa for the basic moiety is at pH 8.9 (Foulkes, 2003) and as such, further electrostatic interactions can be induced at time of complexation (Qi *et al.*, 2010). The effect of dissolving the TPP and SeMet in 0.01 M NaOH (pH 12) rather than H_2O prior to crosslinking in the optimised formulation (ratio Cs:TPP 6:1, SeMet load concentration of 0.15 mg/mL and Cs medium pH of 3) was investigated, as a means to elicit greater interaction between Cs and SeMet and subsequently increase EE%. N= 3.

By altering the pH of the formulation, the EE% increased from 39 ± 3 % to 66 ± 1 %, whilst the physicochemical properties of the NPs remained within the target range for oral delivery (Table 5.4) (des Rieux *et al.*, 2006). This was most likely attributed to the electrostatic interactions between the now further ionised TPP and SeMet groups and protonated amine residues found on the glucosamine unit of Cs. This is consistent with the work by Pan *et al.*, (2014) which showed curcumin (CUR) successful encapsulation (>90%) into casein NPs, through deprotonation of CUR at pH 12, enabling for its re-association and thus subsequent encapsulation into the NP matrix.

Table 5.4 Size, PDI, ZP and EE% results for formulation I. N=3.

SeMet NPs Ratio 6:1, SeMet in NaOH (0.15 mg/mL load conc.), Cs in pH 3			
SIZE (nm)	PDI	ZP (mV)	EE (%)
227 ± 17	0.448 ± 0.049	32 ± 1	66 ± 4

5.3.4 Improved Encapsulation Efficiency using zein

The results from the first EE% optimisation study (Table 5.4) were promising, in terms of increasing EE% in addition to maintaining the desired NP physicochemical properties. Nevertheless, the maximum EE% obtained by modifying the pH remained at 66 ± 4 %. Therefore, a subsequent step, involving the coating of the optimised NPs with zein (at varying zein:Cs mass ratios), was pursued as a means to increase the encapsulation efficiency of SeMet into the Cs: TPP NPs.

As shown in Table 5.5, as the ratio of zein in the formulation increased, the EE% improved. At 0.5:1, zein:Cs, the average EE% achieved was 75 % and approximately 5 % increments in EE% were observed with subsequent increments of zein:Cs. The physicochemical properties of the NPs (PDI and ZP) were still within the target range for oral delivery for formulations with zein:Cs ratios ≤1:1, although an increase in NP size was observed upon increasing zein concentrations. At a ratio of 2:1, zein:Cs, the physicochemical properties of the NPs were less than ideal, as large particle sizes (721 nm average) and high PDI values (0.783) were yielded, most likely as a consequence of a denser and thicker coating (Luo *et al.*, 2010) provided by the partial deposition of the negatively charged protein on the particle surface, thus reducing the total net charge and inducing particle swelling (Rampino *et al.*, 2013). For example, as the zein concentration increases, so does the viscosity of the dispersion, which can affect the nucleation process leading to the production of larger sized NPs (Zhong and Jin, 2009). Similar results have been observed by others, whereby, an increase in zein concentration led to an increase in particle size of 6,7-dihydroxycoumarin loaded zein NPs (Podaralla and Perumal, 2012) or alpha-tocopherol loaded zein NPs, stabilised with Cs (Luo, Teng and Wang, 2012). Lastly, the ZP of this formulation was the

lowest observed (average of + 6 mV), which may be attributed to the increasing zein concentration, causing increased masking of the free positively charged amino groups of Cs (Krauland and Alonso, 2007). It is also possible that agglomeration occurred as a result of the reduced electrostatic repulsion between the NPs in suspension (Liu and Gao, 2009).

Table 5.5 Physiochemical results for SeMet loaded NPs (Ratio 6:1, SeMet in NaOH (0.15 mg/mL load), Cs in pH 3) coated with zein. Size, PDI, ZP and EE% are presented for each NP using different mass ratio combinations of zein and Cs. N=3.

Zein:Cs	Size (nm)	PDI	ZP (mV)	EE (%)
0.5:1	319 ± 19	0.221 ± 0.040	27 ± 6	74 ± 1
1:1	377 ± 47	0.325 ± 0.136	35 ± 6	81 ± 1
2:1	721 ± 108	0.783 ± 0.281	6 ± 4	85 ± 1

5.3.5 Characterisation Fourier transform infrared spectroscopy (FTIR)

Figure 5.3 shows the FTIR spectra of (A) zein, (B) TPP, (C) Cs, (D) SeMet:Cs:TPP NPs and (E) SeMet:Cs:TPP:zein NPs. The zein spectrum (Figure 5.3, A) shows characteristic peaks at 3289, 2929, 1644, 1515 and 1233 cm^{-1} corresponding to NH stretching vibrations, CH stretching, amide I (C=O stretch), amide II (C-N and C-N-H/ in plane bending) and amide III respectively (Podaralla and Perumal, 2012). Characteristic peaks for the phosphate ion (P=O) in TPP (Figure 5.3, B) were observed at 1121 cm^{-1} and 886 cm^{-1}, respectively (Rampino *et al.*, 2013). Cs spectra (Figure 5.3, C) showed characteristic peaks at 3240, 2879, 1625, 1514, 1376 and 1063 cm^{-1}. corresponding to NH Stretch / OH in pyranose ring, CH_2 in CH_2OH group, C=O in $NHCOCH_3$ group (amide I), NH_2 in $NHCOCH_3$ group (amide II), CH_3 in $NHCOCH_3$ group and C-O-C (glycosidic linkage) respectively (Luo *et al.*, 2010; Mohammed, Williams and Tverezovskaya, 2013).

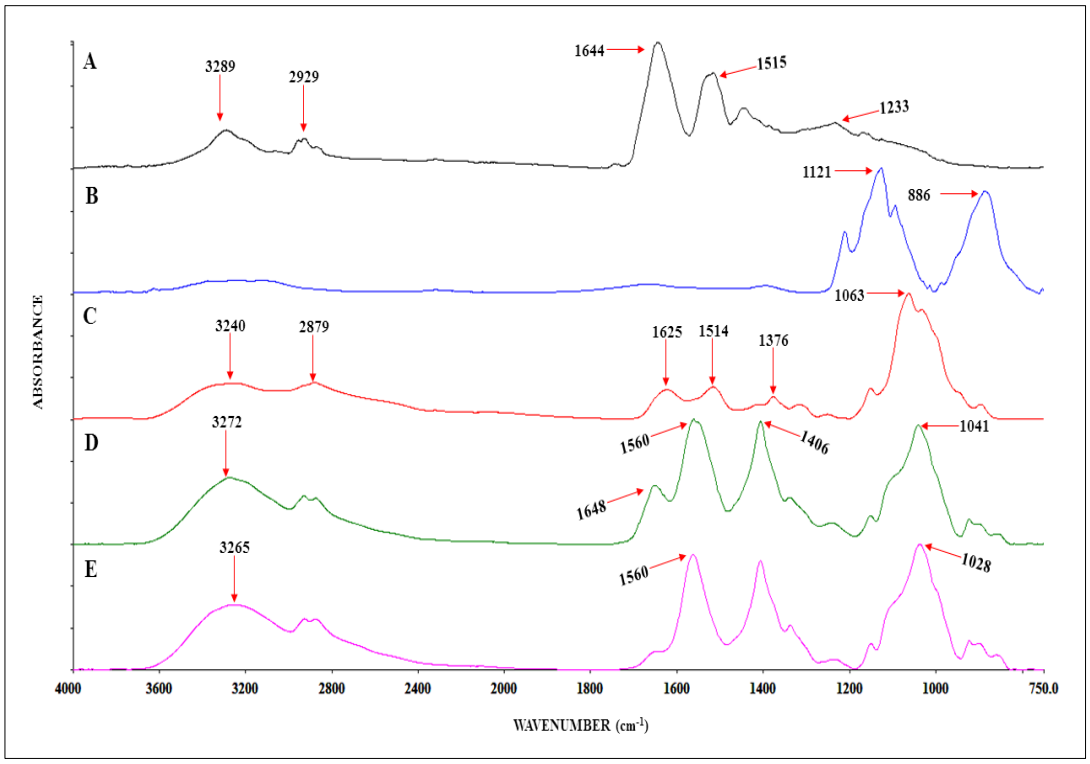

Figure 5.3 FTIR spectra of (A) zein, (B) TPP, (C) Cs, (D) SeMet:Cs:TPP NPs and (E) SeMet:Cs:TPP:zein NPs. Spectra are offset for clarity.

The FTIR spectrum of SeMet:Cs:TPP NPs (Figure 5.3, D) is different to that of the Cs matrix, as a result of intermolecular interactions of the constituent components. If interaction between the Cs and TPP had occurred, it will lead to frequency shifts or splitting in absorption peaks (Gan *et al.*, 2005). For example, the peaks at 1514 cm^{-1} in the Cs spectrum have been shifted to 1560 cm^{-1}, indicating electrostatic interaction between the phosphate groups of TPP and the amino groups present in the Cs NP matrix (Papadimitriou *et al.*, 2008). Additionally, the broadening and the increased absorbance of the peak at 3272 cm^{-1} indicate hydrogen bonding has been enhanced (Luo *et al.*, 2010). The band observed at 1644 cm^{-1} in the zein FTIR spectrum (assigned to N-H bond), has been shifted to 1648 cm^{-1} in the zein/Cs NPs spectrum (Figure 5.3, A and E respectively), indicating an interaction among the zein and Cs chains, possibly through hydrogen bonding among the amino groups present on both

Cs and zein chains (Müller *et al.*, 2011). Another indication of Cs:zein interaction arises from the amide III bands at 1406 cm^{-1}, not visible in the zein spectrum, but now visible in the zein/Cs NPs (Figure 5.3, A and E respectively) spectrum, most likely as a result of the C-N stretching and out of plane N-H deformation being highly sensitive to structural changes (Sessa, Mohamed and Byars, 2008).

Lastly, the formation of zein/Cs NPs (E) is also characterised by the appearance of a band at 1041 cm^{-1} (assigned to C-O-C (glycosidic linkage)), which was observed in Cs/SeMet NPs (D) at 1028 cm^{-1} but not observed in the zein spectrum (A), supporting the presence of Cs within the NP matrix (Figure 5.3) (Müller *et al.*, 2011). The crosslinked Cs also showed a peak for P = O at 1151 cm^{-1} (Bhumkar and Pokharkar, 2006), further indicating electrostatic interaction between Cs and TPP (Figure 5.3, E). No significant SeMet peaks in either Cs/TPP/SeMet or Cs/TPP/SeMet/zein NPs spectra were observed, most likely due to the fact, that only 0.07 % of the dried formulation is contributed by SeMet and it is consequently masked by the other formulation components.

5.3.6 Scanning electron microscopy

Figure 5.4 shows the SEM images of uncoated and zein coated Se loaded NPs. The particle size of the NPs after spin coating was in good agreement with the DLS measurements taken on the freshly prepared NPs. Spherical, well distributed particles for both coated and uncoated SeMet loaded NPs were observed. However, it is interesting to note that the zein coated NPs displayed a smoother surface than that of the uncoated. This may be attributed to the use of the acetic acid buffer used during the formulation process, as similar results have been observed in spin-cast zein films prepared from an aqueous ethanol solvent compared to an acetic acid solution,

indicating that a rough and hydrophilic surface was acquired for the former, whilst the zein film produced from an acetic acid solution appeared to be smooth, featureless and more hydrophobic (Shi, Kokini and Huang, 2009; Y. Zhang *et al.*, 2015).

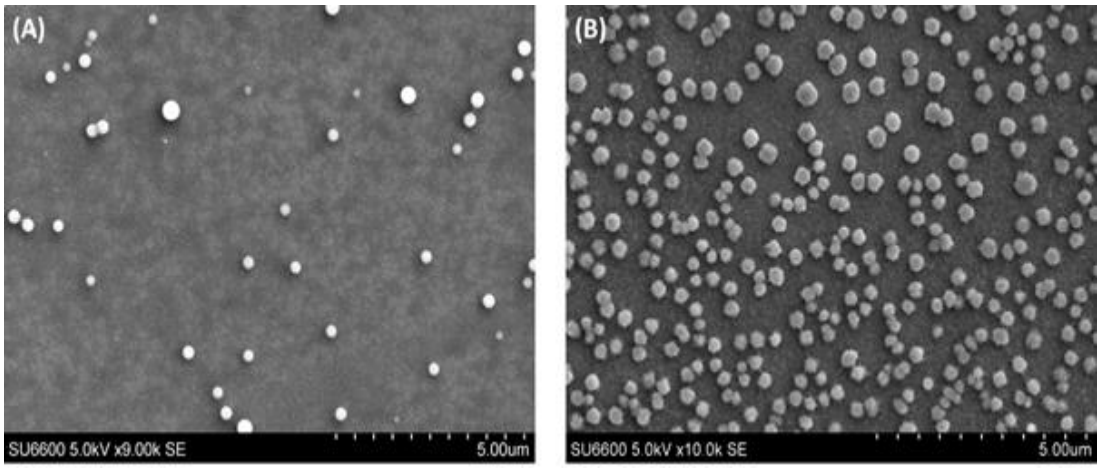

Figure 5.4 SEM image of (A) SeMet:Cs:TPP NPs and (B) SeMet:Cs:TPP NPs coated with zein.

5.3.7 Accelerated stability analysis of SeMet-loaded NPs coated with zein

The principle aim of accelerated stability testing is to provide reasonable assurance that a pharmaceutical or food consumable will remain at an acceptable level of quality throughout its timespan in the market place (Waterman and Adami, 2005; Bajaj *et al.*, 2012). Real-time, retained sample, cyclic temperature and acceleration, are the four categories into which stability testing procedures fall (Bhagyashree *et al.*, 2015). In the latter, the product is subjected to elevated temperatures and/or humidity well above ambient values, to determine the temperature at which product failure (i.e. degradation) will occur.

The Arrhenius equation, upon which the interpretation of accelerated stability testing is based, allows for the determination of the activation energy and consequently, the

degradation rate of a product at lower temperatures (i.e. ambient, refrigerated etc.). In this instance, the data acquired can then be used to project the shelf life of the product in a much shorter time than that of real time assessments (Ali *et al.*, 2013; Bhagyashree *et al.*, 2015). This is a beneficial approach to stability testing, as it results in a greatly reduced product development schedule.

Figure 5.5 shows the kinetic behaviour of the NP properties: size (A), PDI (B) and ZP (C) at temperatures ranging from 60-80 °C. The stability of the NPs decreased with increasing temperature. Little change was detected for all properties at 60 °C, over the course of 720 min, whereas a more pronounced increment in size and PDI and a decrease in ZP was observed at 70 °C after 300 min. At 80 °C, destabilisation of the NP complexes was evident across all properties, whereby size increased from approximately 300 nm to > 800 nm, PDI from approximately 0.2 to >0.9 and ZP reduced from approximately 32 mV to < 18 mV, indicating that aggregation of the NPs had occurred (Wu, Zhang and Watanabe, 2011).

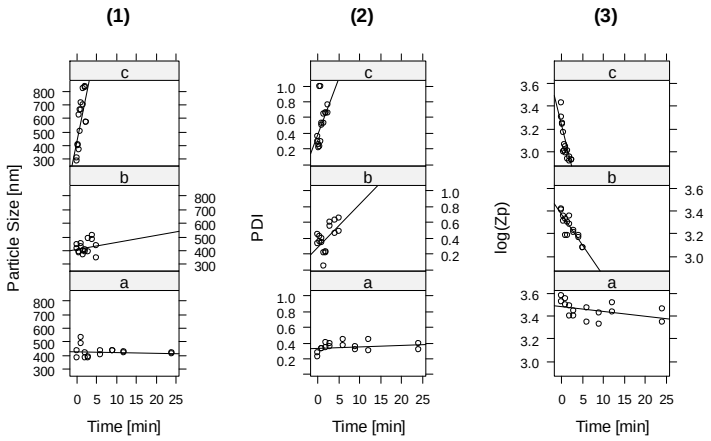

Figure 5.5 (1) Particle size, (2) PDI and (3) ZP analysis of SeMet loaded NPs exposed to (a) 80 °C, (b) 70 °C and (c) 60 °C, over time periods of 120, 300 and 720 min, respectively. N=3.

The one-step nonlinear regression analysis of the kinetic experiments shows that particle size and PDI fit to a zero-order kinetic behaviour, with an Arrhenius dependence of ln (k_{ref}@70 °C) = 1.66 ± 9.44 min^{-1} and Ea = 452.57 ± 570.59 kJ/mol for size, and a ln (k_{ref}@70 °C) = 0.029 ± 0.014 min^{-1}, and an Ea = 182.31 ± 42.64 kJ/mol for PDI respectively. In terms of ZP, an apparent first order mechanism fits the data better than that of an apparent zero order model, with an Arrhenius dependence of ln (k_{ref}@70 °C) = 0.038 ± 0.010 min^{-1} and Ea = 205.71 ± 25.65 kJ/mol. Additionally, as can be seen in Figure 5.6, a linear correlation is evident between 1/T and ln k, indicating that the formulations will be stable under normal storage conditions. This was expected, as previous reports have shown that zein coatings can increase the colloidal stability of iron phosphate NPs (Van Leeuwen, Velikov and Kegel, 2014) and, when stabilised with Cs, results in high thermal resistance of the NPs over prolonged periods of time (Luo *et al.*, 2013).

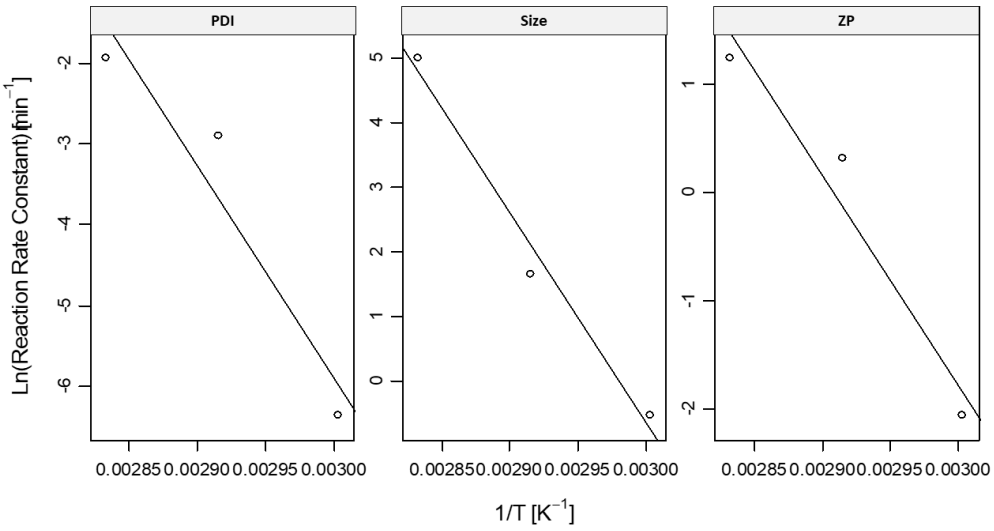

Figure 5.6 Arrhenius plots for the (A) ZP, (B) PDI and (C) size accelerated studies of SeMet loaded NPs. N=3.

5.3.8 Cytotoxicity assessment of SeMet-loaded NPs

The potential cytotoxicity of SeMet in its native form and unloaded or SeMet loaded NPs coated with zein, at different test concentrations (25, 50 and 100 uM), were examined on Caco-2 human epithelial cells, and HepG2 human liver hepatocellular cells, using the MTS assay. As the NPs will become exposed to the intestinal epithelia following oral delivery (leading to its facilitated transport and uptake), time points were selected with the intention to mimic *in vivo* conditions for each cell type, to assess the potential cytotoxicity of the formulated NPs (Gleeson *et al*., 2015; Brayden *et al*., 2015). Caco-2 cells were exposed for 4h (Figure 5.7(A)) and HepG2 cells for 72h (Figure 5.7(B)). In Caco-2 exposures, no cytotoxicity was observed for unloaded or SeMet loaded NPs, in comparison to the negative control, across all tested concentrations. For HepG2 exposures, no cytotoxicity was observed for unloaded or SeMet loaded NPs coated with zein. Additionally, the lower concentrations (25 and 50 uM) of native SeMet showed no cytotoxicity to either cell line, whereas a reduction in HepG2 cell viability (Figure 5.7(B)) for native SeMet, at the 100 uM test concentration, was observed (approx. 66% cell viability).

Similar results were observed by Takahashi, Suzuki and Ogra, 2017, whereby SeMet showed no significant change on the viability of Caco-2 cell lines, although it did show marginal toxicity to HepG2 cells at concentrations > 80 ug/mL after prolonged exposure (48 hr). This finding is also in agreement with other works that showed SeMet toxicity occurred at concentrations ≥40 uM in various hepatoma cell lines (Kajander *et al.,* 1991). It has previously been shown that Cs nanoparticles can enhance the delivery of inorganic Se compounds whilst reducing its toxicity (C. Zhang *et al.*, 2015).

In this work, SeMet loaded NPs elicited no significant reduction in viability of either cell line at equivalent concentration (100 uM), indicating that, by encapsulating SeMet within the Cs NP matrix, the cytotoxic effects of pure SeMet, can be reduced.

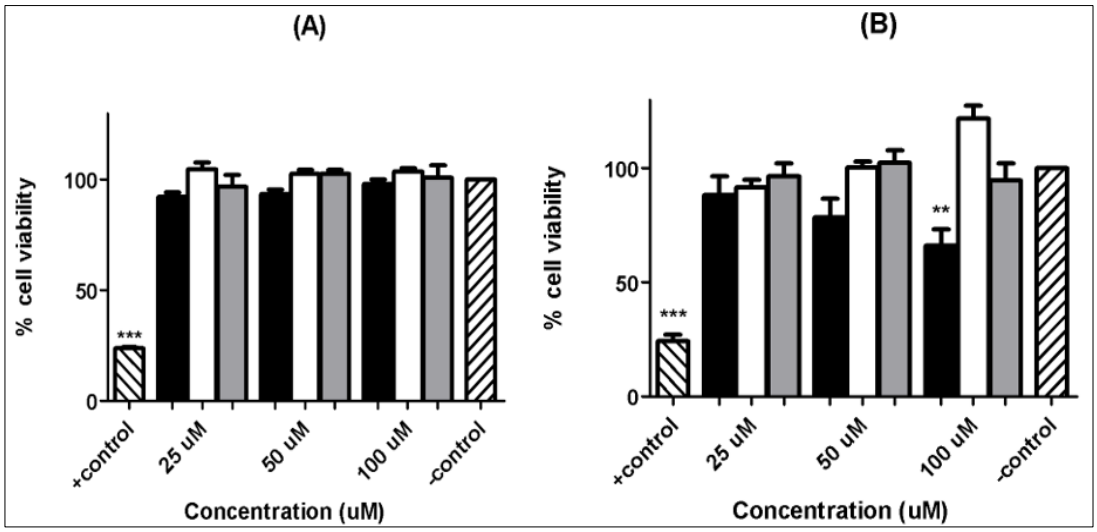

Figure 5.7: Cytotoxicity assessment of ■ SeMet, ▭ unloaded NPs with zein coating and ▭ SeMet loaded NPs with zein coating, exposed for (a) 4h in Caco-2 cell lines and (b) 72h in HepG2 cell line at SeMet equivalent concentrations (25 uM, 50 uM and 100 uM). Triton™ X-100 (0.05%) was used as positive control and percentage (%) of MTS converted was compared to untreated control. 1-Way ANOVA with Dunnetts's post-test *** $p < 0.001$, ** $p < 0.01$, Each value presented was normalised against untreated control and calculated from three separate experiments, each of which included six replicates. N=3.

5.3.9 *In vitro* release studies

In vitro techniques are advantageous for modelling potential interactions between NPs and the *in vivo* environment of the GI tract. Simulated gastric fluid and membrane analysis models enable assessment of *in vivo* environments without the use of human cell lines (Gamboa and Leong, 2013). Figure 5.8 shows the cumulative release profile of SeMet loaded NPs coated with zein, after subjection to 2 hr in an SGF environment (pH 1.2) representative of the stomach, followed by a compartmental change to SIF (pH 6.8), representative of the intestine, for 4 hr. As can be seen, 25±1 % of SeMet was released after 2 hr in SGF, followed by 33 ±3 % in SIF for 4 hr. No significant difference in the release profile of SeMet loaded NPs without zein coating was observed (data not shown). However, it was necessary to keep zein in the formulation due to the increase in EE (≥ 80 %).

The target site of absorption of SeMet is the jejunum, in the small intestine. Therefore, it is important to withstand the acidic environment of the stomach. Three basic mechanisms that are typically applied to describe the release of drugs from polymeric particles, are swelling/erosion, diffusion, and degradation (Liechty *et al.*, 2010). In this work, the total cumulative release of SeMet from the zein coated NPs, after 6 hr in simulated gastrointestinal tract environments, was 58 %, indicating that degradation of the NP was slow and thus the mechanism may be diffusion/relaxation oriented. As such, the release kinetics of SeMet NPs, under the SGF and SIF sequential controlled release experiments, were fitted using the following diffusive models derived from swellable systems (Siepmann and Peppas, 2011; Danish *et al.*, 2017a).

For the SGF:

$$\frac{M_t}{M_\infty} = ks_1 * \sqrt{time} + ks_2 * time$$

(Equation 5.8)

where M_t is the diffused mass at a given time, M_∞ is the asymptotic diffused mass at infinite time, and ks_1 and ks_2 are the diffusive and relaxation rate constants respectively.

For the SIF:

$$\frac{M_t}{M_\infty} - \frac{M_{120}}{M_\infty} = ki_1 * (\sqrt{time - 120}) + ki_2 * (time - 120)$$

(Equation 5.9)

where M_{120} is the predicted diffused mass at the time of changing from SGF to SIF (120 min), ki_1 and ki_2 are diffusive and relaxation rate constants.

Table 5.6 Swellable model parameters for kinetic release studies SeMet NPs. ks represents the stomach compartment and ki the intestinal compartment, divided into diffusion and relaxation mechanisms ($_1$ and $_2$). All parameters listed where statistically significant, *P < 0.05.

Parameters	Estimate	Std. Error	t-value
Ks_2	0.17082	0.04092	4.175
Ki_1	0.69145	0.33863	2.042
Ki_2	0.10817	0.02105	5.140
R^2_{adj}		**0.984**	

Table 5.6 presents the fitted values for the rate constants in SGF (ks) and SIF (ki) for SeMet NPs, with ks_1, representing a diffusion mechanism and ks_2 a relaxation mechanism (Equation 5.8, 5.9). In terms of the stomach compartment (SGF, pH 1.2), no statistically significant ks_1 parameter was found, indicating that the primary mechanism for release in the stomach was via relaxation, i.e. slower release,

approaching zero-order kinetics. After 2 hr subjected to the SGF environment, a compartmental change was employed to mimic the movement of the NPs to the intestinal environment (SIF, pH 6.8), whereupon a combination of diffusion (ki_1) and relaxation (ki_2) mechanisms were observed ($p<0.05$). Overall, the model employed (Equation 5.8, 5.9) predicted the experimental data well, with an R^2adj >0.98. These results were expected, as polysaccharides generally undergo solvent penetration, swelling and chain disentanglement and relaxation, resulting in their ultimate dissolution (Fu and Kao, 2010). Additionally, this result is in agreement with previous studies, reporting a diffusion and zero order kinetic profile for IPP and LKP loaded Cs NPs, coated with zein (Danish *et al.*, 2017a) and that of other researchers, who observed that zein proved to be a good coating for NPs, whereby, the stronger the interaction of the load material (in this instance phenolic monoterpenes) with that of the wall material (zein) was evidenced by its controlled release over time (da Rosa *et al.*, 2015).

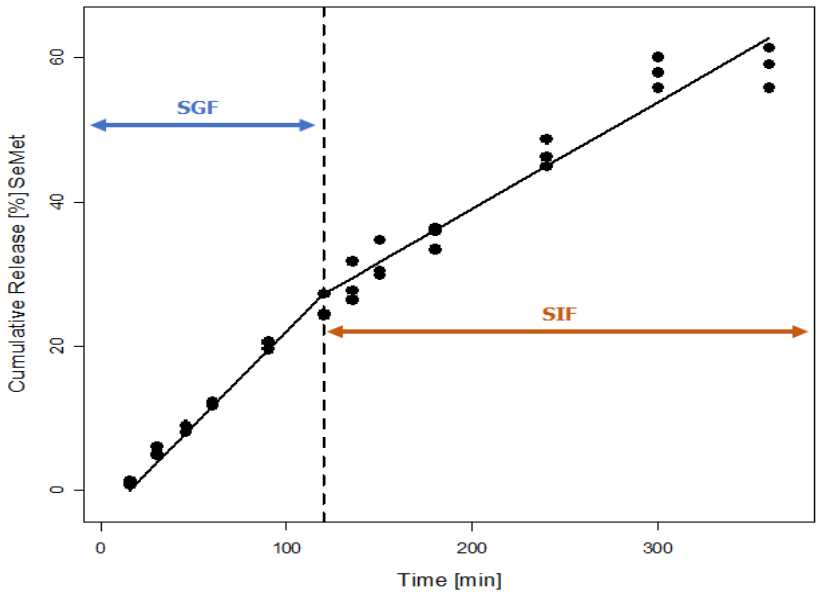

Figure 5.8 Release kinetics of SeMet NPs coated with zein after 2 hr in SGF (pH 1.2) and 4 hr in SIF (pH 6.8). The continuous line indicates the model prediction.

5.4 Conclusion

In this study, SeMet-loaded Cs NPs were produced via ionotropic gelation. BBD was used to identify optimum formulation variables that would result in NPs with physicochemical properties thought to be suitable for oral delivery. BBD highlighted the optimum conditions for NP production, although EE% remained relatively low. By varying the formulation media pH, increased electrostatic interaction between the crosslinking polyelectrolytes and drug were achieved, resulting in an increase in EE%. Coating the NPs at a 1:1 mass ratio of Cs:zein, resulted in NPs with a doubled EE accompanied by an increase in diameter. These NPs were then characterised *via* FTIR analysis, which identified the presence of key functional groups of the native components and identifying shifts in the crosslinked matrixes. SEM analysis showed that spherical, well distributed particles were observed. MTS cytotoxicity studies showed no decrease in cellular viability in either Caco-2 or HepG2 cell after 4 and 72 hr exposures, respectively. Accelerated thermal stability of the loaded NPs indicated good stability under normal storage conditions. Lastly, after 6 hr exposure to simulated intestinal buffers, the release profile of the formulation showed that $\leq 60\%$ of the drug had been released. These findings infer that encapsulation of SeMet into a NP delivery system comprising food-derived components reveals an oral administration approach for this molecule.

5.5 References

Ali, M. S. *et al.* (2013) 'Accelerated stability testing of a clobetasol propionate-loaded nanoemulsion as per ICH guidelines', *Scientia Pharmaceutica*, 81(4), pp. 1089–1100.

Amaro, M. I. *et al.* (2015) 'Formulation, stability and pharmacokinetics of sugar-based salmon calcitonin-loaded nanoporous/nanoparticulate microparticles (NPMPs) for inhalation', *International Journal of Pharmaceutics*, 483(1–2), pp. 6–18.

Anderson, M. J. and Whitcomb, P. J. (2005) *RSM simplified: optimizing processes using response surface methods for design of experiments*. Productivity press.

Antoniou, J. *et al.* (2015a) 'Physicochemical and morphological properties of size-controlled chitosan-tripolyphosphate nanoparticles', *Colloids and Surfaces A: Physicochemical and Engineering Aspects*, 465, pp. 137–146.

Antoniou, J. *et al.* (2015b) 'Physicochemical and morphological properties of size-controlled chitosan–tripolyphosphate nanoparticles', *Colloids and Surfaces A: Physicochemical and Engineering Aspects*, 465, pp. 137–146.

Bajaj, S. *et al.* (2012) 'Stability Testing of Pharmaceutical Products', *Journal of Applied Pharmaceutical Science*, 2(2012), pp. 129–138.

Barrentine, L. B. (1999) *An Introduction to Design of Experiments: a Simplified Approach*. ASQ Quality Press.

Benshitrit, R. C. *et al.* (2012) 'Development of oral food-grade delivery systems: Current knowledge and future challenges', *Food & Function*, 3(1), p. 10.

Bezerra, M. A. *et al.* (2008) 'Response surface methodology (RSM) as a tool for optimization in analytical chemistry.', *Talanta*, 76(5), pp. 965–77.

Bhagyashree, P. *et al.* (2015) 'Recent trends in stability testing of pharmaceutical products: A review', *Research Journal of Pharmaceutical, Biological and Chemical Sciences*, 6(1), pp. 1557–1569.

Bhumkar, D. R. and Pokharkar, V. B. (2006) 'Studies on effect of pH on cross-linking of chitosan with sodium tripolyphosphate: a technical note', *AAPS Pharmscitech*, 7(2), pp. E138–E143.

Brayden, D. J., Gleeson, J. and Walsh, E. G. (2014) 'A head-to-head multi-parametric high content analysis of a series of medium chain fatty acid intestinal permeation

enhancers in Caco-2 cells', *European Journal of Pharmaceutics and Biopharmaceutics*, 88(3), pp. 830–839.

Brayden, D. J., Cryan, S.-A., *et al.* (2015) 'High-content analysis for drug delivery and nanoparticle applications', *Drug Discovery Today*, 20(8), pp. 942–957.

Brayden, D. J., Maher, S., *et al.* (2015) 'Sodium caprate-induced increases in intestinal permeability and epithelial damage are prevented by misoprostol', *European Journal of Pharmaceutics and Biopharmaceutics*, 94, pp. 194–206.

British Pharmacopoeia Commission (2016) *British Pharmacopoeia: Appendix XII B. Dissolution*. London: TSO.

Calderon L. *et al.* (2013) 'Nano and microparticulate chitosan-based systems for antiviral topical delivery', *European Journal of Pharmaceutical Sciences*, 48, pp. 216–222.

Calvo, P. *et al.* (1997) 'Novel hydrophilic chitosan-polyethylene oxide nanoparticles as protein carriers', *Journal of Applied Polymer Science*, 63(1), pp. 125–132.

Chen, M. C. *et al.* (2013) 'Recent advances in chitosan-based nanoparticles for oral delivery of macromolecules', *Advanced Drug Delivery Reviews*, pp. 865–879.

Chintala, S. *et al.* (2012) 'Prolyl hydroxylase 2 dependent and Von-Hippel-Lindau independent degradation of Hypoxia-inducible factor 1 and 2 alpha by selenium in clear cell renal cell carcinoma leads to tumor growth inhibition', *BMC Cancer*, 12(1), p. 293.

Danish, M. K. *et al.* (2017a) 'Comparative study of the structural and physicochemical properties of two food derived antihypertensive tri-peptides, Isoleucine-Proline-Proline and Leucine-Lysine-Proline encapsulated into a chitosan based nanoparticle system', *Innovative Food Science & Emerging Technologies*, 44, pp. 139–148.

Danish, M. K. *et al.* (2017b) 'Formulation, Characterization and Stability Assessment of a Food-Derived Tripeptide, Leucine-Lysine-Proline Loaded Chitosan Nanoparticles', *Journal of Food Science*, 82(9), pp. 2094–2104.

Davies, M. J. (2016) 'Protein oxidation and peroxidation', *Biochemical Journal*, 473(7), pp. 805–825.

Dora, C. P. *et al.* (2010) 'Development and characterization of nanoparticles of glibenclamide by solvent displacement method', *Acta Poloniae Pharmaceutica - Drug Research*, 67(3), pp. 283–290.

Evans, S. O., Khairuddin, P. F. and Jameson, M. B. (2017) 'Optimising Selenium for Modulation of Cancer Treatments', *Anticancer Research*, 37(12), pp. 6497–6509.

Forootanfar, H. *et al.* (2014) 'Antioxidant and cytotoxic effect of biologically synthesized selenium nanoparticles in comparison to selenium dioxide', *Journal of Trace Elements in Medicine and Biology*, 28(1), pp. 75–79.

Foulkes, M. E. (2003) 'Screening Methods for Semi-quantitative Speciation Analysis', *Handbook of Elemental Speciation: Techniques and Methodology*. John Wiley & Sons, Ltd.

Fu, Y. and Kao, W. J. (2010) 'Drug Release Kinetics and Transport Mechanisms of Non-degradable and Degradable Polymeric Delivery Systems', *Expert Opinion on Drug Delivery*, 7(4), pp. 429–444.

Gamboa, J. M. and Leong, K. W. (2013) 'In vitro and in vivo models for the study of oral delivery of nanoparticles', *Advanced Drug Delivery Reviews*, 65(6), pp. 800–810.

Gan, Q. *et al.* (2005) 'Modulation of surface charge, particle size and morphological properties of chitosan–TPP nanoparticles intended for gene delivery', *Colloids and Surfaces B: Biointerfaces*, 44(2), pp. 65–73.

Garousi, F. (2015) 'The toxicity of different selenium forms and compounds – Review', *Acta Agraria Debreceniensis*, 64, pp. 33–38.

Gleeson, J. P. *et al.* (2015) 'Stability, toxicity and intestinal permeation enhancement of two food-derived antihypertensive tripeptides, Ile-Pro-Pro and Leu-Lys-Pro', *Peptides*, 71, pp. 1–7.

Hassani, S. *et al.* (2015) 'Preparation of chitosan–TPP nanoparticles using microengineered membranes–Effect of parameters and encapsulation of tacrine', *Colloids and Surfaces A: Physicochemical and Engineering Aspects*, 482, pp. 34–43.

He, Z. *et al.* (2017) 'Scalable fabrication of size-controlled chitosan nanoparticles for oral delivery of insulin', *Biomaterials*, 130, pp. 28–41.

Helson, L. (2013) 'Curcumin (diferuloylmethane) delivery methods: A review.', *Biofactors*, 39(1), pp. 21–26.

Hosseinzadeh, H. *et al.* (2012) 'Chitosan-Pluronic nanoparticles as oral delivery of anticancer gemcitabine: Preparation and in vitro study', *International Journal of Nanomedicine*, 7, pp. 1851–1863.

Hu, B. *et al.* (2008) 'Optimization of fabrication parameters to produce chitosan−tripolyphosphate nanoparticles for delivery of tea catechins', *Journal of Agricultural and Food Chemistry*, 56(16), pp. 7451–7458.

Huang, Y., Cai, Y. and Lapitsky, Y. (2015) 'Factors affecting the stability of chitosan/tripolyphosphate micro- and nanogels: resolving the opposing findings', *Journal of Materials Chemistry B*, 3(29), pp. 5957–5970.

Huang, Y. and Lapitsky, Y. (2017) 'On the kinetics of chitosan/tripolyphosphate micro- and nanogel aggregation and their effects on particle polydispersity', *Journal of Colloid and Interface Science*, 486, pp. 27–37.

Janes, K. A., Calvo, P. and Alonso, M. J. (2001) 'Polysaccharide colloidal particles as delivery systems for macromolecules', *Advanced Drug Delivery Reviews*, 47(1), pp. 83–97.

Kajander, E. O. *et al.* (1991) 'Metabolism, cellular actions, and cytotoxicity of selenomethionine in cultured cells', *Biological Trace Element Research*, 28(1), pp. 57–68.

Krauland, A. H. and Alonso, M. J. (2007) 'Chitosan/cyclodextrin nanoparticles as macromolecular drug delivery system', *International Journal of Pharmaceutics*, 340(1), pp. 134–142.

Lai, L. F. and Guo, H. X. (2011) 'Preparation of new 5-fluorouracil-loaded zein nanoparticles for liver targeting', *International Journal of Pharmaceutics*, 404(1–2), pp. 317–323.

Van Leeuwen, Y. M. M., Velikov, K. P. P. and Kegel, W. K. K. (2014) 'Colloidal stability and chemical reactivity of complex colloids containing Fe3+', *Food Chemistry*, 155, pp. 161–166.

Liechty, W. B. *et al.* (2010) 'Polymers for Drug Delivery Systems', *Annual Review of Chemical and Biomolecular Engineering*, 1, pp. 149–173.

Liu, H. and Gao, C. (2009) 'Preparation and properties of ionically cross-linked chitosan nanoparticles', *Polymers for Advanced Technologies*, 20(7), pp. 613–619.

Loeschner, K. *et al.* (2014) 'Absorption, distribution, metabolism and excretion of selenium following oral administration of elemental selenium nanoparticles or selenite in rats', *Metallomics*, 6(2), pp. 330–337.

Luo, Y. *et al.* (2010) 'Preparation, characterization and evaluation of selenite-loaded chitosan/TPP nanoparticles with or without zein coating', *Carbohydrate Polymers*, 82(3), pp. 942–951.

Luo, Y. *et al.* (2013) 'Encapsulation of indole-3-carbinol and 3,3′-diindolylmethane in zein/carboxymethyl chitosan nanoparticles with controlled release property and improved stability', *Food Chemistry*, 139(1–4), pp. 224–230.

Luo, Y., Teng, Z. and Wang, Q. (2012) 'Development of Zein Nanoparticles Coated with Carboxymethyl Chitosan for Encapsulation and Controlled Release of Vitamin D3', *Journal of Agricultural and Food Chemistry*, 60(3), pp. 836–843.

Luo, Y. and Wang, Q. (2014) 'Zein-based micro- and nano-particles for drug and nutrient delivery: A review', *Journal of Applied Polymer Science*, 131(16), pp. 1–12.

Maleki Dizaj, S. *et al.* (2015) 'Box-Behnken experimental design for preparation and optimization of ciprofloxacin hydrochloride-loaded CaCO3 nanoparticles', *Journal of Drug Delivery Science and Technology*, 29, pp. 125–131.

Masarudin, M. J. *et al.* (2015) 'Factors determining the stability, size distribution, and cellular accumulation of small, monodisperse chitosan nanoparticles as candidate vectors for anticancer drug delivery: Application to the passive encapsulation of [14C]-doxorubicin', *Nanotechnology, Science and Applications*, 8, pp. 67–80.

Mattu, C., Li, R. and Ciardelli, G. (2013) 'Chitosan nanoparticles as therapeutic protein nanocarriers: The effect of ph on particle formation and encapsulation efficiency', *Polymer Composites*, 34(9), pp. 1538–1545.

Mix, M. *et al.* (2015) 'Effects of selenomethionine on acute toxicities from concurrent chemoradiation for inoperable stage III non-small cell lung cancer', *World Journal of Clinical Oncology*, 6(5), pp. 156–165.

Mohammed, M. A. *et al.* (2017) 'An overview of chitosan nanoparticles and its application in non-parenteral drug delivery', *Pharmaceutics*, 9(4).

Mohammed, M. H., Williams, P. a. and Tverezovskaya, O. (2013) 'Extraction of chitin from prawn shells and conversion to low molecular mass chitosan', *Food Hydrocolloids*, 31(2), pp. 166–171.

Mukhopadhyay, P. *et al.* (2013) 'Oral insulin delivery by self-assembled chitosan nanoparticles: in vitro and in vivo studies in diabetic animal model.', *Materials Science & Engineering. C, Materials for Biological Applications*, 33(1), pp. 376–82.

Müller, V. *et al.* (2011) 'Preparation and characterization of zein and zein-chitosan microspheres with great prospective of application in controlled drug release', *Journal of Nanomaterials*, pp. 10.

Nagpal, K., Singh, S. K. and Mishra, D. N. (2010) 'Chitosan Nanoparticles: A Promising System in Novel Drug Delivery', *Chemical & Pharmaceutical Bulletin*, 58(11), pp. 1423–1430.

Nair, H. B. *et al.* (2010) 'Delivery of anti-inflammatory nutraceuticals by nanoparticles for the prevention and treatment of cancer.', *Biochemical Pharmacology*, 80(12), pp. 1833–43.

Narayan, V. *et al.* (2015) 'Epigenetic regulation of inflammatory gene expression in macrophages by selenium', *The Journal of Nutritional Biochemistry*, 26(2), pp. 138–145.

Neves, A. R. *et al.* (2016) 'Nanoscale delivery of resveratrol towards enhancement of supplements and nutraceuticals', *Nutrients*, 8(3), p. 131.

Nie, T. *et al.* (2016) 'Facile synthesis of highly uniform selenium nanoparticles using glucose as the reductant and surface decorator to induce cancer cell apoptosis', *Journal of Materials Chemistry B*, 4(13), pp. 2351–2358.

Oberdörster, G. *et al.* (2005) 'Principles for characterizing the potential human health effects from exposure to nanomaterials: elements of a screening strategy.', *Particle and Fibre Toxicology*, 2, p. 8.

Paliwal, R. and Palakurthi, S. (2014) 'Zein in controlled drug delivery and tissue engineering.', *Journal of Controlled Release*, 189, pp. 108–22.

Pan, Y. *et al.* (2002) 'Bioadhesive polysaccharide in protein delivery system: Chitosan nanoparticles improve the intestinal absorption of insulin in vivo', *International Journal of Pharmaceutics*, 249(1–2), pp. 139–147.

Panchuk, R. R. *et al.* (2016) 'Antioxidants selenomethionine and D-pantethine decrease the negative side effects of doxorubicin in NL/Ly lymphoma-bearing mice.', *Croatian Medical Journal*, 57(2), pp. 180–92.

Papadimitriou, S. *et al.* (2008) 'Chitosan nanoparticles loaded with dorzolamide and pramipexole', *Carbohydrate Polymers*, 73(1), pp. 44–54.

Pharmacopoeia, B. (2016) 'British Pharmacopoeia Commission: London'. UK.

Podaralla, S. and Perumal, O. (2012) 'Influence of formulation factors on the preparation of zein nanoparticles', *AAPS Pharmscitech*, 13(3), pp. 919–927.

Qi, J. *et al.* (2010) 'Nanoparticles with dextran/chitosan shell and BSA/chitosan core-Doxorubicin loading and delivery', *International Journal of Pharmaceutics*, 393(1–2), pp. 177–185.

Rampino, A. *et al.* (2013) 'Chitosan nanoparticles: Preparation, size evolution and stability', *International Journal of Pharmaceutics*, 455(1), pp. 219–228.

Rayman, M. P. (2000) 'The importance of selenium to human health.', *Lancet*, 356(9225), pp. 233–241.

Rayman, M. P., Infante, H. G. and Sargent, M. (2008) 'Food-chain selenium and human health: spotlight on speciation.', *The British Journal of Nutrition*, 100(2), pp. 238–253.

Reddy, V. S. *et al.* (2017) 'A systematic review and meta-analysis of the circulatory, erythrocellular and CSF selenium levels in Alzheimer's disease: A metal meta-analysis (AMMA study-I)', *Journal of Trace Elements in Medicine and Biology*, 42, pp. 68–75.

Reilly, K. *et al.* (2014) 'A note on the effectiveness of selenium supplementation of Irish-grown Allium crops', *Irish Journal of Agricultural and Food Research*, pp. 91–99.

des Rieux, A. *et al.* (2006) 'Nanoparticles as potential oral delivery systems of proteins and vaccines: a mechanistic approach', *Journal of Controlled Release*, 116(1), pp. 1–27.

da Rosa, C. G. *et al.* (2015) 'Characterization and evaluation of physicochemical and antimicrobial properties of zein nanoparticles loaded with phenolics monoterpenes', *Colloids and Surfaces A: Physicochemical and Engineering Aspects*, 481, pp. 337–344.

Ryan, K. B. *et al.* (2012) 'Nanostructures overcoming the intestinal barrier: drug delivery strategies', *Nanostructured Biomaterials for Overcoming Biological Barriers*, (22), p. 63.

Ryan, S. M. *et al.* (2013) 'An intra-articular salmon calcitonin-based nanocomplex reduces experimental inflammatory arthritis', *Journal of Controlled Release*, 167(2), pp. 120–129.

Sessa, D. J., Mohamed, A. and Byars, J. A. (2008) 'Chemistry and physical properties of melt-processed and solution-cross-linked corn zein', *Journal of Agricultural and Food Chemistry*, 56(16), pp. 7067–7075.

Shanmugam, M. *et al.* (2015) 'Dietary organic zinc and selenium supplementation improves semen quality and fertility in layer breeders', *The Indian Journal of Animal Sciences*, 85(2).

Shi, K., Kokini, J. L. and Huang, Q. (2009) 'Engineering zein films with controlled surface morphology and hydrophilicity', *Journal of Agricultural and Food Chemistry*, 57(6), pp. 2186–2192.

Siepmann, J. and Peppas, N. A. (2011) 'Higuchi equation: Derivation, applications, use and misuse', *International Journal of Pharmaceutics*, pp. 6–12.

Sipoli, C. C. *et al.* (2015) 'Scalable production of highly concentrated chitosan/TPP nanoparticles in different pHs and evaluation of the in vitro transfection efficiency', *Biochemical Engineering Journal*, 94, pp. 65–73.

Song, G. *et al.* (2014) "Selenomethionine ameliorates cognitive decline, reduces tau hyperphosphorylation, and reverses synaptic deficit in the triple transgenic mouse model of alzheimer"s disease', *Journal of Alzheimer's Disease*, 41(1), pp. 85–99.

Takahashi, K., Suzuki, N. and Ogra, Y. (2017) 'Bioavailability comparison of nine bioselenocompounds in vitro and in vivo', *International Journal of Molecular Sciences*, 18(3), pp. 1–11.

Umerska, A., Corrigan, O. I. and Tajber, L. (2014) 'Intermolecular interactions between salmon calcitonin, hyaluronate, and chitosan and their impact on the process of formation and properties of peptide-loaded nanoparticles', *International Journal of Pharmaceutics*, 477(1), pp. 102–112.

Vongchan, P. *et al.* (2011) 'N, N, N-Trimethyl chitosan nanoparticles for the delivery of monoclonal antibodies against hepatocellular carcinoma cells', *Carbohydrate Polymers*, 85(1), pp. 215–220.

Wang, J. J. *et al.* (2011) 'Recent advances of chitosan nanoparticles as drug carriers.', *International Journal of Nanomedicine*, pp. 765–774.

Wang, M. *et al.* (2013) 'A comparison of approaches to stepwise regression for global sensitivity analysis used with evolutionary optimization', in *Proceedings of the BS2013*, pp. 26–28.

Ward, P., Connolly, C. and Murphy, R. (2012) 'Accelerated Determination of Selenomethionine in Selenized Yeast: Validation of Analytical Method', *Biological Trace Element Research*, 151(3), pp. 446–450.

Waterman, K. C. and Adami, R. C. (2005) 'Accelerated aging: prediction of chemical stability of pharmaceuticals', *International Journal of Pharmaceutics*, 293(1–2), pp. 101–125.

Wong, C. Y., Al-Salami, H. and Dass, C. R. (2017) 'The role of chitosan on oral delivery of peptide-loaded nanoparticle formulation', *Journal of Drug Targeting*, 0(0), pp. 1–12.

Wu, L., Zhang, J. and Watanabe, W. (2011) 'Physical and chemical stability of drug nanoparticles', *Advanced Drug Delivery Reviews*, 63(6), pp. 456–469.

Xu, H., Cao, W. and Zhang, X. (2013) 'Selenium-containing polymers: promising biomaterials for controlled release and enzyme mimics', *Accounts of Chemical Research*, 46(7), pp. 1647–1658.

Yoon, H. Y. *et al.* (2014) 'Glycol chitosan nanoparticles as specialized cancer therapeutic vehicles: Sequential delivery of doxorubicin and Bcl-2 siRNA', *Scientific Reports*, 4, p. 6878.

Zhang, C. *et al.* (2015) 'Synthesis, characterization, and controlled release of selenium nanoparticles stabilized by chitosan of different molecular weights', *Carbohydrate Polymers*, 134, pp. 158–166.

Zhang, H. *et al.* (2015) 'Preparation and physicochemical properties of chitosan broadleaf holly leaf nanoparticles', *International Journal of Pharmaceutics*, 479(1), pp. 212–218.

Zhang, J., Wang, X. and Xu, T. (2008) 'Elemental selenium at nano size (Nano-Se) as a potential chemopreventive agent with reduced risk of selenium toxicity: comparison with se-methylselenocysteine in mice', *Toxicological Sciences*, 101(1), pp. 22–31.

Zhang, Y. *et al.* (2015) 'Zein-based films and their usage for controlled delivery: Origin, classes and current landscape', *Journal of Controlled Release*, 206(2699), pp. 206–219.

Zhao, L. *et al.* (2013) 'Preparation of biocompatible carboxymethyl chitosan nanoparticles for delivery of antibiotic drug', *BioMed Research International*, pp. 1–8.

Zhong, Q. and Jin, M. (2009) 'Zein nanoparticles produced by liquid–liquid dispersion', *Food Hydrocolloids*, 23(8), pp. 2380–2387.

Zolgharnein, J., Shahmoradi, A. and Ghasemi, J. B. (2013) 'Comparative study of Box–Behnken, central composite, and Doehlert matrix for multivariate optimization of Pb (II) adsorption onto Robinia tree leaves', *Journal of Chemometrics*, 27(1–2), pp. 12–20.

6 FORMULATION, CHARACTERISATION, AND *IN VITRO* EVALUATION OF METHYLSELENOCYSTEINE AND SELENOCYSTINE LOADED CHITOSAN NANOPARTICLES-COATED WITH ZEIN

The work presented in this chapter is reproduced from:

Vozza, G., Khalid, M.D, Byrne, H. J., Ryan, S and Frias, J. (2018). Formulation, characterisation, and *in vitro* evaluation of methylselenocysteine and selenocystine loaded chitosan nanoparticles-coated with zein. Ready for submission to the Journal of Food Hydrocolloids.

Vozza, G. was the primary author, Khalid, M.D. helped develop the formulation process and Byrne, H. J., Frias, J. and Ryan S. contributed to layout, design and proofing.

Numbering of Sections, Figures and Tables has been adapted to the thesis format.

Abstract

Organic forms of selenium, an essential micronutrient, such as selenoamino acids (SeAAs), have been shown to possess antioxidant and anticancer properties. However, their bioavailability is low, and they may be toxic above the recommended nutritional intake level, and thus improved, targeted oral delivery methods are desirable. In this work, the SeAAs, Methylselenocysteine (MSC) and selenocystine ($SeCys_2$) were encapsulated into nanoparticles (NPs) using the mucoadhesive polymer chitosan (Cs), via ionotropic gelation with tripolyphosphate (TPP) and the NPs produced were then coated with zein (a maize derived prolamine rich protein). Optimum NP physicochemical properties for oral delivery were obtained at a 6:1 ratio of Cs:TPP, with a 1:0.75 mass ratio of Cs:zein coating (diameter ~260nm, polydispersity index ~0.2, zeta potential >30mV). SEM analysis showed that spheroidal, well distributed particles were obtained. Encapsulation Efficiencies of 80.7% and 78.9% were achieved, respectively, for MSC an $SeCys_2$ loaded NPs. Cytotoxicity studies of MSC loaded NPs showed no decrease in cellular viability in either Caco-2 (intestine) or HepG2 (liver) cells after 4 and 72 hr exposures. For $SeCys_2$ loaded NPs, although no cytotoxicity was observed in Caco-2 cells after 4 hr, a significant reduction in cytotoxicity was observed, compared to pure $SeCys_2$, across all test concentrations in HepG2 after 72 hr exposure. Accelerated thermal stability testing of both loaded NPs indicated good stability under normal storage conditions. Lastly, after 6 hr exposure to simulated gastrointestinal tract environments, the sustained release profile of the formulation showed that 62 ± 8 % and 69 ± 4% of MSC and $SeCys_2$, had been released from the NPs respectively.

Keywords Selenium, selenocystine, methylselenocysteine, chitosan, zein nanoparticles, stability, 3-(4,5-dimethylthiazol-2-yl)-5-(3-carboxymethoxyphenyl)-2-(4-sulfophenyl)-2H-tetrazolium (MTS), controlled release.

Abbreviations

Se, selenium; **SeAAs**, selenoamino acids; **$SeCys_2$**, selenocystine; **MSC**, methylselenocysteine; **BA**, bioactive; **Cs**, chitosan; **TPP**, tripolyphosphate; **GIT**, gastrointestinal tract; **GRAS**, generally recognised as safe; **NP**, nanoparticle, **DLS**, dynamic light scattering; **PDI**, polydispersity index; **ZP**, zetapotential; **EE%** encapsulation efficiency

6.1 Introduction

In recent years, interest in preventative public health has increased through the emergence of nutraceuticals, bioactive (BA) food compounds, shown to offer a wide variety of physiological benefits in addition to reduced disease risks (Lagos *et al.*, 2015). By incorporating BA compounds (such as minerals or peptides) into food systems, a potentially simple means of ameliorating the risk of disease, and the subsequent development of an innovative functional food, can be achieved (Cencic and Chingwaru, 2010). Unfortunately, the ability for such products to affect disease prevention is highly dependent on the bioavailability and stability of these BA compounds (Tavano *et al.*, 2014). Given that a substantial amount of BA molecules remain poorly available via oral administration, due to various factors such as, a lack of stability in the environmental conditions encountered in food processes (temperature, oxygen, light) and in the gastrointestinal tract (GIT) (pH, enzymes, presence of other nutrients), a short gastric residence time of the dosage form, and a

low permeability and/or solubility within the gut, all presenting a major formulation challenge (Chen, Remondetto and Subirade, 2006).

Over the past few decades, encapsulation systems have been developed and employed to overcome these limitations, based to their potential to more effectively deliver BA agents to a selected target site of action (Vozza *et al.*, 2016). Although several synthetic polymers have been employed for use in various delivery applications in the pharmaceutical industry, they are not suitable for deployment within the food industry unless they have a generally recognised as safe (GRAS) status. Nanoparticle (NP) delivery systems can offer an added advantage to the delivery of BA compounds, as they possess a higher mobility and cellular uptake compared to systems of larger size. As an illustration, He *et al.*, (2012) found that particles 300 nm in size or less are ideal for oral drug delivery since they are preferentially internalized by both enterocytes and M cells and demonstrate higher intestinal transport compared to larger sized particles. Etheridge *et al*. (2013) observed that the effect of particle size on cellular intake can also be influenced by the constituent material and the particle geometry, a consequence of reduced intestinal clearance mechanisms and an increase in the mass to surface ratio interaction with the biological support.

Chitosan (Cs), a polysaccharide derived from chitin, the second most abundant biopolymer (next to cellulose) in nature, has gained increasing popularity for numerous biomedical applications and more specifically for use in NP deliver systems (Kumari, Yadav and Yadav, 2010; Rodrigues *et al.*, 2012; Mohammed *et al.*, 2017) Given the combination of its GRAS approved status and its well documented biodegradable, biocompatible, and mucoadhesive properties, it is unsurprising that this compound has been targeted for use in the delivery of BA cargos (Hejazi and Amiji, 2003; Kumirska *et al.*, 2011; Anitha *et al.*, 2014). Due to the presence of

primary amine groups in the Cs backbone, it can readily become protonated and thus solubilised in acidic media, offering the ability to be cross linked with negatively charged polyelectrolytes and under relatively mild reaction conditions, a technique known as ionotropic gelation (Janes, Calvo and Alonso, 2001). Recent reports have indicated the capacity of Cs NPs to improve the bioavailability of nutraceuticals such as tea derived phenols, that are soluble yet poorly absorbed, through opening of tight junctions and/or direct uptake by epithelial cells via endocytosis (Liang *et al.*, 2017). However, the oral administration of BA molecules contained within a Cs:NP matrix remains a challenge, due to its lack of stability in the low pH media typically found in the GIT (pH 1.2), in which rapid dissociation and thus degradation can lead to the destruction of sensitive nutraceutical cargo (Yan *et al.*, 2012).

Surface coating of Cs NPs has been proposed to confer increased protection to BA's as they pass through the GIT after oral consumption (Luo and Wang, 2014). Zein, a GRAS approved prolamine rich protein derived from maize, has been employed for the coating of Cs:NP oral delivery systems in recent years due to its ability to increase the encapsulation efficiency (EE%) of BAs and to improve their controlled release in the GIT (Luo *et al.*, 2010; Luo and Wang, 2014; Paliwal and Palakurthi, 2014). This coating strategy harnesses both the protein (zein) and polysaccharide (Cs) properties in a combined NP delivery system in which a broader range of physical, chemical and colloidal stability can be achieved (Benshitrit *et al.*, 2012).

Selenium (Se), is an essential micronutrient in human and animal nutrition (Rayman, 2000) that exists in a wide array of different forms, both organic and inorganic. Selenite and selenate salts are the most common inorganic forms, whereas selenoamino acids (SeAAs), such as selenocystine ($SeCys_2$), selenomethionine (SeMet), and methylselenocysteine (MSC) are the most commonly found forms in

foods from the *Agaricus, Brassica* and *Allium* families (Montes-Bayón *et al.*, 2006; Maseko *et al.*, 2013; Reilly *et al.*, 2014). Although essential, Se possesses a low therapeutic index in which there is a fine line between beneficial and toxic doses. Generally, organic Se shows a greater bioavailability than that of the inorganic forms, in addition to showing a higher threshold for toxicity (Amoako, Uden and Tyson, 2009). Health benefits of MSC and $SeCys_2$ have been linked to the body's endogenous antioxidant defence system, protecting cellular components such as cell membranes, lipids, lipoproteins and DNA from oxidative damage by free radicals, reactive oxygen and reactive nitrogen species (Ponnampalam *et al.*, 2009). As oxidative damage is linked to the development of cardiovascular and neurodegenerative diseases as well as cancers, several experimental *in vivo* studies of the effects of administration of Se compounds have been undertaken (Valko *et al.*, 2007; Lobo *et al.*, 2010; de Souza *et al.*, 2014). $SeCys_2$ has been shown to reduce tobacco-derived nitrosamine-induced lung tumour growth and enhance hepatic chemoprotective enzyme activities in mice (Fan *et al.*, 2013), whereas MSC has been shown to offer selective protection against organ specific toxicity induced by clinically active antitumor agents, cisplatin, oxaliplatin, and irinotecan in rat models (Cao *et al.*, 2014).

However, organometals such as MSC and $SeCys_2$ are readily oxidised (Wasowicz *et al.*, 2003; Davies, 2016) and although less toxic than inorganic Se, the adequate physiological range between deficient and excess doses is narrow, being one order of magnitude (0.1–1.0 µg/g diet) in experimental animals (Takahashi, Suzuki and Ogra, 2017). Additionally, the site of target for SeAAs is the jejunum, in the small intestine (Cousins and Liuzzi, 2018). Therefore, it is important that the composition of the formulation offers a sufficient ability to withstand the acidic environment of the stomach whilst retaining the stability of the cargo. As such, the potential optimisation

of the delivery of these compounds in a NP formulation could be significant, given that both these organic species can more effectively increase both human and animal selenium levels and are less toxic than inorganic selenium (Garousi, 2015).

This study builds directly on previous work (Vozza *et al*., 2018, Chapter 5) in which the production of Cs:TPP NPs via ionotropic gelation, using selenomethionine (SeMet) as a prototype encapsulant, was investigated. In that study, a Design of Experiments (DoE) approach was employed to establish optimum formulation conditions that would produce SeMet loaded NPs suitable for oral delivery. The conditions of mass ratio 6:1 (Cs:TPP), with TPP dissolved in NaOH (0.1 M) and Cs dissolved in acetate buffer (pH 3) prior to crosslinking, produced NPs with physicochemical properties (Size ~ 300 nm, PDI <0.5 and ZP >30 mV) suitable for oral delivery (des Rieux *et al.*, 2006). By coating the NPs with zein, the encapsulation efficiency (EE%) was significantly improved from < 65% to >80%. In this work, the optimised formulation conditions, as previously identified by DoE, were employed to encapsulate $SeCys_2$ and MSC, based on the rationale that $SeCys_2$ (with a pKa of 4.7 (Lacourciere and Stadtman, 1999)), and MSC (with a pKa of 4.9 (Mishra, Priyadarsini and Mohan, 2007)), contain comparably ionisable groups to SeMet. As such, it was hypothesised that by employing the previously established DoE parameters to the current Cs:TPP NP formulation of MSC and $SeCys_2$, similar formulations (e.g. physicochemical properties and EE%) as those achieved for the SeMet loaded NPs could be produced. Once prepared, the cryoprotectant trehalose was employed, to ensure stability of the optimised formulations after lyophilisation (Danish, 2017a). NPs were then extensively assessed for their physicochemical properties, morphology, thermal stability, cytotoxicity and *in vitro* controlled release, utilising the methods developed in the previous studies (Vozza *et al*., 2018, Chapter 5).

6.2 Material and Methods

6.2.1 Materials

The chitosan compound PROTASAN™ UP (CL113) was purchased from NovaMatrix, FMC Corporations, Norway. D (+) - Trehalose dihydrate, and zein, of ≥99 % purity, were obtained from ACROS Organics™, Fisher Scientific, Ireland. Seleno-DL-cystine (>98 % purity) and Se-methyl-seleno-L-cysteine (>98 % purity), were purchased from Sigma Aldrich, Ireland and LKT laboratories, UK, respectively. Ultra-pure water 18mΩcm^{-1} was obtained from a Millipore simplicity 185 model instrument, UK, and was used for all aqueous solution preparations. All other reagents, chemicals and solvents were of analytical grade, from Sigma Aldrich, Ireland.

6.2.2 Formulation of MSC and $SeCys_2$ loaded Cs NPs – coated with zein

Cs:TPP NPs were formed according to (Vozza *et al*, 2018, Chapter 5) with the following modifications. Aqueous TPP solution (3 mg/mL) was prepared in NaOH (0.01 M), with a Se species ($SeCys_2$ or MSC) concentration of 400 ug/mL. Subsequently, this mixture was added in equal volumetric proportions to CL113 solution (3 mg/mL) via burette droplet addition. The NPs formed were then left to stabilise for a further 30 min whilst the stirring speed of the solution was maintained at 700 rpm. Once the NPs had stabilised, absolute EtOH (8 mL) was added dropwise to the formulation whilst the stirring speed of the solution was maintained (700 rpm,

30 min). Filtered Zein (2 mL, 5.625 mg/mL), dissolved in aqueous EtOH (80% v/v), was then added dropwise to the solution to yield Zein:Cs NPs of mass ratio 0.75:1. All formulations were left to stabilise at 700 rpm for 30 min, then transferred to a 20 kDa MWCO (Vivaspin 20, Sartorius) centrifugal filter and isolated by centrifugation at 3000 rpm for 30 min. Filtered EtOH (80% v/v) (equivalent in volume to the recovered supernatant) was then added to the purified NPs and subsequently sonicated at 35% amplitude for 30 s with 5 s pulse intervals. The NP formulations were then concentrated under vacuum (175 mbar) at 40 °C until EtOH was completely removed. To ensure stability of the optimised formulation after lyophilisation, 10 mL of the cryoprotectant trehalose 5 % w/v in H_2O were added to each formulation and they were lyophilised for 36 hr (Danish, 2017a).

6.2.3 Physicochemical characterisation of MSC and $SeCys_2$ loaded Cs NPs coated with zein

Dynamic light scattering (DLS) was used to determine the mean particle size and polydispersity index (PDI) of the NP formulations. Laser doppler velocimetry (LDV) was used to measure the zeta potential (ZP). Both DLS and LDV analysis were performed with a Zetasizer Nano series Nano-ZS ZEN3600 fitted with a 633 nm laser (Malvern Instruments Ltd., UK), using a folded capillary cuvette (Folded capillary cell-DTS1060, Malvern, UK), at 25 °C. The values presented herein were acquired from three separate experiments, each of which included three replicates. N=3 (Chapter 3, Section 3.2.1).

6.2.4 Scanning electron microscopy (SEM)

SEM analysis was used to visualise the morphology of the NPs formed' at an accelerating voltage of 20 kV, using a secondary electron detector (Hitachi, SU6600 FESEM, USA). NP solutions were spin coated onto Si wafers, dried at room temperature and then sputter coated with 4 nm Au/Pd prior to imaging (Mukhopadhyay *et al.*, 2013), (Chapter 3, Section 3.2.2).

6.2.5 Encapsulation efficiency (EE%)

The EE% of Se (MSC or $SeCys_2$) in the NPs was determined by the separation and quantification of Se left in the supernatant. This was performed after ultracentrifugation of the formed NPs (3000 rpm, 4 °C, 30 min). Reverse phase high performance liquid chromatography (RP-HPLC), was employed to quantify unencapsulated Se in the supernatant, as previously described (Ward, Connolly and Murphy, 2012) with the following modifications. Samples were analysed with a Waters 2998 HPLC coupled to a Photodiode Array Detector, (Waters, USA), using a Pursuit 5 C18, 250 x 4.6 mm column, (Agilent Technologies, UK). Isocratic elution was carried out at a flow rate of 0.8 mL/min, column temperature 45.0 ± 5.0 °C with a mobile phase of water/methanol/trifluoroacetic acid (97.9:2.0:0.1). Samples were monitored according to their UV absorbance at 218 nm. The encapsulation efficiency was calculated using Equation 6.1 (Xu and Du, 2003), (Chapter 3, Section 3.2.3):

$$EE\% = \frac{Total\ amount\ of\ Se\ Met - Free\ amount\ of\ SeMet}{Total\ amount\ of\ SeMet}\ X\ 100$$

(Equation 6.1)

6.2.6 Cellular viability assay (MTS)

The potential cytotoxicity of the different SeAA (MSC and $SeCys_2$) loaded NPs, coated with zein, were examined on Caco-2 human epithelial cells, and HepG2 human liver hepatocellular cells, using the MTS (3-(4,5-dimethylthiazol-2-yl)-5-(3-carboxymethoxyphenyl)-2-(4-sulfophenyl)-2H-tetrazolium) assay. Caco-2 and HepG2, were seeded at a cell density of 2 x 10^4 cells/well and cultured on 96 well plates in Dulbecco's Modified Eagle Medium (DMEM) and Eagle's Minimum Essential Medium (EMEM) respectively, supplemented with 10% foetal bovine serum, 1% L-glutamine, 1% penicillin-streptomycin and 1% non-essential amino acids at 37°C in a humidified incubator with 5% CO_2 and 95% O_2. The assay was carried out using 4 h exposure times for the test compounds on Caco-2 cells (Neves *et al.*, 2016) and 72 h on HepG2 cells (Gleeson *et al.*, 2015), using Triton X-100™ (0.05%) as a positive control. The time points were selected to mimic *in vivo* conditions for each cell type. The concentrations of the test compounds applied were 25, 50 and 100 uM. After exposure, treatments were removed and replaced with MTS. Optical density (OD) was measured at 490 nm using a microplate reader (TECAN GENios, Grodig, Austria). Each value presented was normalised to that of untreated control and calculated from three separate experiments, each of which included six replicates (Chapter 3, Section 3.3.1).

6.2.7 Stability studies

Accelerated stability studies of MSC and $SeCys_2$ loaded NPs, were conducted to determine the change in physicochemical properties (particle size, PDI and ZP) stored at accelerated conditions: 60°C for 720min, 70°C for 300min and 80°C for 120min

(Danish, 2017a). In brief, aqueous KCl solution (10 mM) was used to suspend the NPs at a concentration of 0.1 mg/mL and the degree of degradation was measured using the Nanosizer ZS (Malvern Instruments Ltd, UK) over different time intervals. R software (R Core Team, 2016) was used to analyse the generated data.

The temperatures dependence of the kinetic parameters of MSC or $SeCys_2$ loaded NPs stability were measured by calculating the observed rate constants. This was plotted in an Arrhenius representation and apparent activation energy, E_a and reaction rate, k_{ref} were calculated according to Equation 6.2:

$$C = Co + e^{ln(k) - \frac{Ea}{R}\left(\frac{1}{T} - \frac{1}{T_{ref}}\right)t}$$

(Equation 6.2)

where C is the property (particle size, PDI or zeta potential) at time t, Co is the initial property conditions, k is the apparent zero order reaction constant, E_a is the energy of activation, R is the universal gas constant, T is the temperature of the experiment (K) and T_{ref} is the reference temperature (343 K), (Chapter 3, Section 3.3.2.).

6.2.8 Release studies

In vitro release studies of MSC and $SeCys_2$ from the NPs were conducted using a dialysis bag diffusion technique (Hosseinzadeh *et al.*, 2012) over 12 hr (Calderon *et al*., 2013; Yoon *et al*., 2014). In brief, freeze dried loaded (MSC or $SeCys_2$) NPs were suspended in H_2O (5 mL) and probe sonicated (Branson Ultrasonics; Ultrasonic processor VCX-750W, USA) at 35 % amplitude for 30 s with 5 s intervals and placed into a Float-A-Lyzer®G2 dialysis membrane (DM) with a pore size of 25 kDa (Spectrum Laboratories, USA). The DM was then placed into 40 mL of simulated gastric fluid (SGF) for 2 hr, followed by a compartmental change to simulated

intestinal fluid (SIF) for 4 hr. The composition of SGF was 0.1 M HCl and SIF comprised of a 3:1 mixture of 0.2 M trisodium phosphate dodecahydrate and 0.1 M HCl (adjusted to pH 6.8), without enzymes (British Pharmacopoeia Commission, 2016). Samples were then placed in a thermostatic shaker (37 ºC, 100 rpm) and, at 7 equidistant predetermined time points, release fluid was removed (1 mL) and replaced with fresh simulated fluid to maintain sink conditions.

The % of drug (MSC or $SeCys_2$) released was measured by RP-HPLC (Section 6.1). Equation 6.3 was used to determine the % drug release:

$$\boldsymbol{Drug_{rel}}\,\% = \frac{\boldsymbol{D(t)}}{\boldsymbol{D(l)}} * \mathbf{100}$$

(Equation 6.3)

where $Drug_{rel}$ % is the percentage of drug released, D(*l*) represents the concentration of drug loaded and D(t) represents the amount of drug released at time t, respectively (Chapter 3, Section 3.3.3.).

6.3 Results and Discussion

6.3.1 Particle size, PDI and Zeta potential and EE%

The Se species (MSC or $SeCys_2$) used to load the NPs did not have a significant effect on any of the NP properties (size (nm), PDI, ZP (mV) and EE (%) as shown in Table 6.1. The effects of zein and zein:Cs ratio on particle characteristics and Se species EE% are also presented in Table 6.1.

Table 6.1 Physicochemical analysis of SeAA loaded Cs NPs, coated with zein, at mass ratios of 1:1 and 1:0.75 (Cs:zein).

Zein:Cs 1:1				
Se Species	**Size (nm)**	**PDI**	**ZP (mV)**	**EE%**
$SeCys_2$	335.2 ± 34.5	0.346 ± 0.070	23.8 ± 2.6	82.1± 1.2
MSC	333.6 ± 15.8	0.374± 0.054	23.0±3.4	83.2 ± 2.5
Zein:Cs 0.75:1				
Se Species	**Size (nm)**	**PDI**	**ZP (mV)**	**EE%**
$SeCys_2$	262.1 ± 11.1	0.243 ± 0.061	31.5 ± 1.0	78.9 ± 1.5
MSC	271.2 ± 21.4	0.211 ± 0.148	32.2 ± 1.3	80.7 ± 0.7
Zein:Cs 0:1				
Se Species	**Size (nm)**	**PDI**	**ZP (mV)**	**EE%**
$SeCys_2$	205.9 ± 14.3	0.271 ± 0.042	36.6 ± 2.0	61.9 ± 2.8
MSC	226.5 ± 40.1	0.280± 0.034	38.6 ± 2.4	61.5 ± 1.0

Zein was shown to significantly increase NP size (nm) and EE (%), in a linear fashion with respect to increasing mass ratio to Cs (Figure 6.1). For example, it was observed that the average size of MSC or $SeCys_2$ loaded Cs NPs, before zein coating, increased from 227 ± 40 (weight ratio of 0:1), to 334 ± 16 (weight ratio of 1:1) and 206 ± 14 (weight ratio of 0:1), to 352 ± 35 nm (weight ratio of 1:1), respectively.

Similar observations were made by Zhang *et al.* (2014) where zein to sodium caseinate (SC) mass ratios of 1:0.625–1:1.25, resulted in an increase in particle size from 176.85±1.06 nm to 204.75± 1.62 nm, most likely a consequence of NP coating. Additionally, this finding may be due to the larger size of zein (relative to TPP), and is consistent with our previous observations for SeMet loaded Cs NPs coated with zein (Vozza *et al.*, 2018, Chapter 5) and that of others, whereby, an increase in zein concentration led to an increase in particle size of 6,7-dihydroxycoumarin loaded zein NPs (Podaralla and Perumal, 2012) or alpha-tocopherol loaded zein NPs, stabilised with Cs (Luo *et al.*, 2011), evidenced by a denser and thicker coating of zein around the Cs NP.

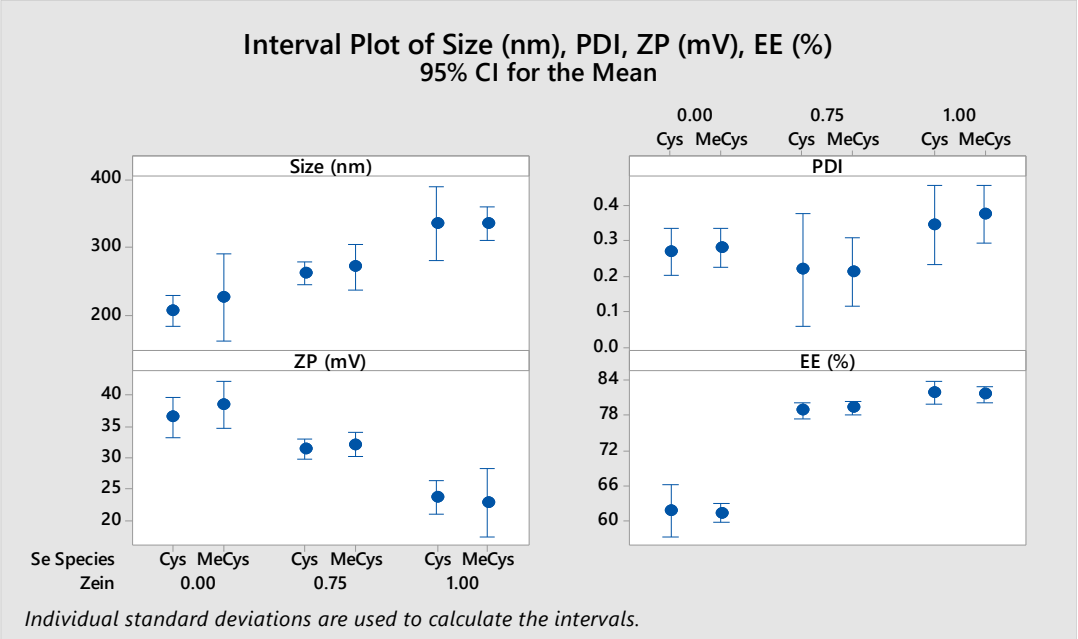

Figure 6.1 Interval plot showing the effect of Se Species and Cs:zein mass ratios on NP physicochemical properties (Size (nm), PDI, ZP (mV) and EE (%).

PDI reflects the particle size distribution of dispersions, ranging from homogenous (0.0) to heterogeneous (1.0) (Win and Feng, 2005). For a NP formulation to be orally active, it is generally recognised that PDI values should be no greater than 0.5 (Avadi *et al.*, 2010). In this work, The PDI of the formulations (with or without zein coating)

remained below 0.4 and neither Se species nor addition of zein significantly affected the size distribution of the NPs formed, indicating that they could be suitable for oral delivery (des Rieux *et al.*, 2006).

Additionally, to establish an industrially viable delivery system, it is recommended that a high degree of the drug cargo be encapsulated within the NP complex (> 80 %) (Sinead Bleiel, AnaBio Technologies Ltd, private communication). As can be seen in Table 6.1, the Se loaded Cs NPs, showed a higher EE (> 79%) for all formulations with zein coating (0.75-1:1 mass ratio), compared to < 62% for uncoated formulations. This is most likely attributable to zein facilitating the incorporation of a higher proportion of the SeAAs into the NP matrix. In other work, bovine serum albuminin has been encapsulated within hydrophobic polymers such as poly-lactic-co-glycolic acid (PLGA) and poly-ε-caprolactone (PCL), providing evidence that EE%, can greatly depend on the interactions between the polymer (in this instance Cs), protein (zein), and organic solvent (Lamprecht *et al.*, 2000).

Conversely, an inverse relationship was observed for ZP (mV), whereby the surface charge of the NPs reduced upon increasing the zein:Cs mass ratio. This trend is conceivable, as, as the concentration of zein increases, a higher proportion of the positively charged primary amines ($-NH_3^+$) present in Cs, become neutralised during complexation with the negatively charged carboxyl (COO^-) groups of zein (Mukhopadhyay *et al.*, 2013) and thus a reduction in ZP occurs.

6.3.2 Scanning electron microscopy (SEM)

SEM provides information on both the size and morphology of nanoscale particles, factors which may influence the colloidal and chemical stability of a given NP formulation. Figure 6.2 shows the SEM images of uncoated NPs (1, A, B), zein coated, MSC (2, A, B) and $SeCys_2$ (3, A, B) loaded NPs. The uncoated NPs showed uniform spheroidal morphologies and the particle size, after spin coating, was in good agreement with that determined by DLS (Figure 6.2, (3 (A), (B)), and consistent with the works of several others (Luo *et al.*, 2011; Park, Park and Kim, 2015).

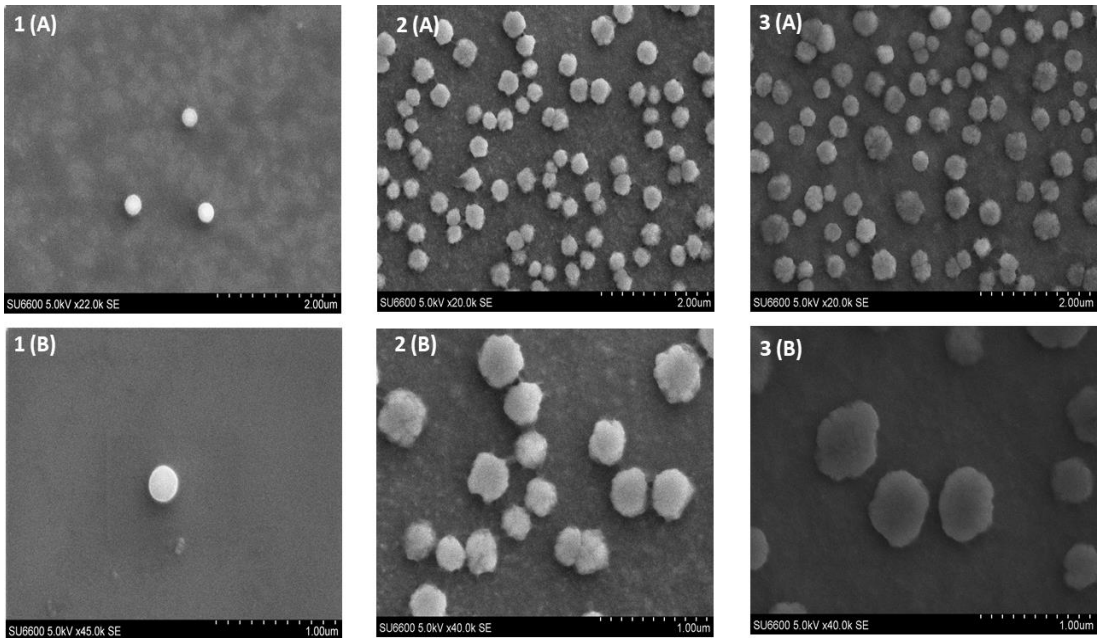

Figure 6.2 SEM images of uncoated NPs (1 (A), (B)). MSC loaded NPs - coated with zein (2 (A), (B)) and $SeCys_2$ loaded NPs - coated with zein (3 (A), (B)).

Interestingly, the NPs coated with zein showed a slightly irregular surface morphology, with a denser core and brighter shell structure (Figure 6.2 (1 (A), (B)) and 2 (A), (B)) inferring that zein produces a less dense coating when compared to Cs NPs alone. This may be attributable to the electrostatic interaction of the negatively charged carboxyl groups of zein facilitating a thin layer membrane around the positively charged amines residues of Cs (Luo *et al.*, 2011).

In terms of the particle size, comparing between SEM and DLS measurements, slightly larger sizes were observed under SEM imaging (approx. 80-120 nm larger), which may be due to the rapid evaporation of residual ethanol (present in the final suspension media) during the spin casting process and subsequent flattening of the particles on the grid (da Rosa *et al.*, 2015).

6.3.3 Stability studies

Figure 6.3 shows the kinetic behaviour of the MSC loaded NP properties: size (A), PDI (B) and ZP (C), at temperatures ranging from 60-80 °C.

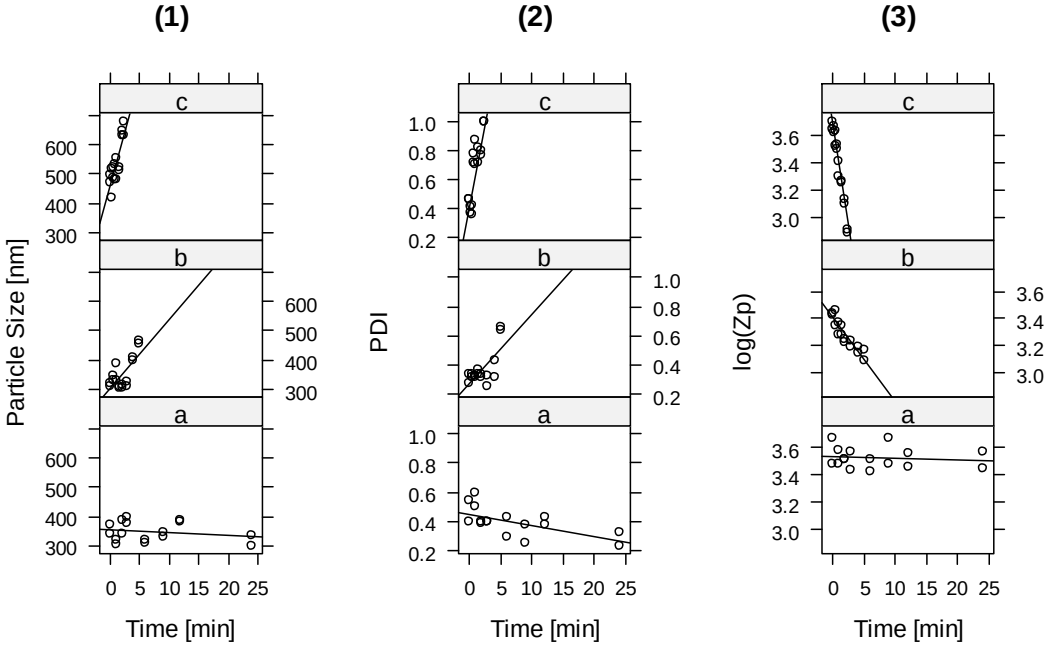

Figure 6.3(1) Particle size, (2) PDI and (3) ZP analysis of MSC loaded NPs exposed to (a) 80 °C, (b) 70 °C and (c) 60 °C, over time periods of 120, 300 and 720 min, respectively. N=3.

The stability of the NPs decreased with increasing temperature. Little change was detected for all properties at 60 °C, over the course of 720 min, whereas a more pronounced influence on size and PDI and a decrease in ZP was observed at 70 °C after 300 min. At 80 °C, destabilisation of the NP complexes was evident according

to all properties, whereby size increased from approximately 350 nm to > 700 nm, PDI from approximately 0.2 to >0.9 and ZP reduced from approximately 32 mV to < 18 mV, indicating that aggregation of the NPs had occurred (Wu, Zhang and Watanabe, 2011).

A linear relationship is evident between 1/T and ln k, indicating that the formulations three physical chemical properties follow Arrhenius law (Figure 6.4).

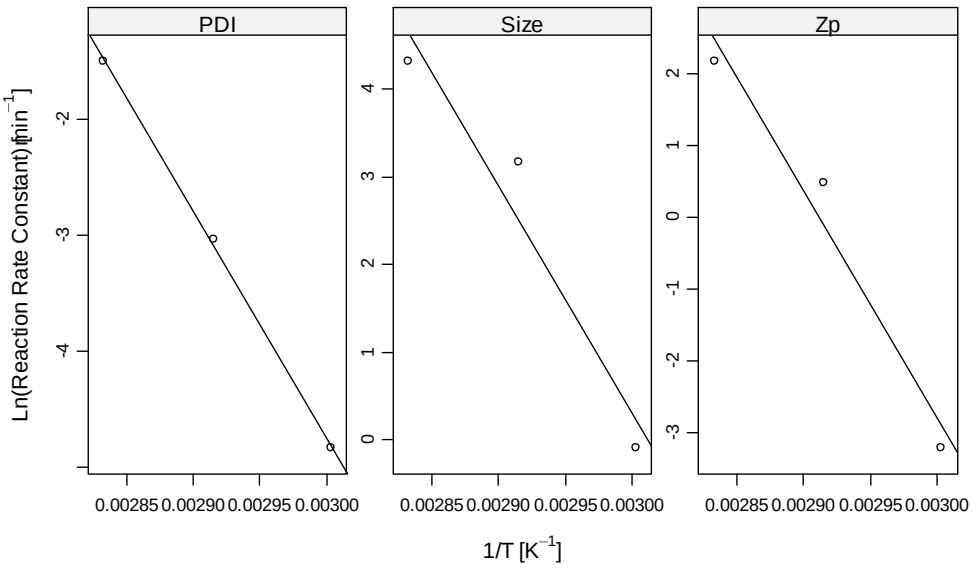

Figure 6.4 Arrhenius plots for the (A) ZP, (B) PDI and (C) size accelerated studies of MSC loaded NPs.

The one-step nonlinear regression analysis of the kinetic experiments at T_{ref} the reference temperature (70°C) shows that the particle size and PDI of MSC loaded NPs fit to a zero-order kinetic behaviour, with an Arrhenius dependence of ln (k_{ref}@70 °C) = 4.45 ± 6.28 min^{-1} and Ea = 340.32 ± 139.20 kJ/mol for size, and a ln (k_{ref}@70 °C) = 0.0112 ± 0.0124 min^{-1}, and an Ea = 314.30 ± 109.00 kJ/mol for PDI respectively (Figure 6.4). Regarding ZP, an apparent first order mechanism fits the data better than an apparent zero order model, with an Arrhenius dependence of ln (k_{ref}@70 °C) = 0.047 ± 0.011 min^{-1} and Ea = 157.25 ± 19.95 kJ/mol.

Similar kinetic behaviour was observed for the $SeCys_2$ loaded NPs properties (size (A), PDI (B) and ZP (C)) at temperatures ranging from 60-80 °C (Supplemental Figure S6.1). Again, as temperature increased destabilisation of the NPs occurred, whereby size and PDI fit to a zero-order kinetic behaviour, with an Arrhenius dependence of ln (k_{ref}@70 °C) = 5.22 ± 6.04 min^{-1} and Ea = 301.87 ± 112.99 kJ/mol for size, and a ln (k_{ref}@70 °C) = 0.0267 ± 0.0101 min^{-1}, and an Ea = 200.53 ± 34.10 kJ/mol for PDI respectively. Likewise, ZP, followed an apparent first order mechanism better than that of an apparent zero order model, with an Arrhenius dependence of ln (k_{ref}@70 °C) = 0.043 ± 0.007 min^{-1} and Ea = 175.70 ± 15.12 kJ/mol. Lastly, a linear correlation is evident between 1/T and ln k, further indicating that the formulations will be stable under normal storage conditions (Supplemental Figure S6.2).

As there was no significant difference observed between the Se species (MSC or $SeCys_2$) used to load the NPs on the formulations stability, it can be concluded that the contributing factors are determined by the Cs:zein complex rather than the specific loaded SeAA. This is expected, as the complexation of protein (in this instance zein) with polysaccharide (Cs) systems, involves non-covalent interactions that can change the interfacial behaviour and stability of food colloids (Ghosh and Bandyopadhyay, 2012).

For example, by harnessing Cs' thermal stability and combining it with zeins' aromatic side groups and double bonds, it is possible to greatly increase the stability of labile nutraceuticals against thermal degradation and oligomerization (Luo *et al.*, 2013). Zein coated tablets exhibit stronger resistance to abrasion, high humidity and high temperatures than a variety of commercial sugar-coated tablets (Zhang *et al.*,

2015). Moreover, it has been reported that the bi-layer approach for encapsulation of bioactives leads to a better control of the NP interface structure, charge, thickness and permeability, and substantially enhanced stability (Hu and McClements, 2014).

Notably, the net attractive and net repulsive strength character of protein–polysaccharide non-covalent physical interactions can vary substantially, depending primarily on environmental conditions such as pH, ionic strength, and temperature (Semenova *et al.*, 2014). In this work, the conditions (presence of salt) used to prepare the NPs, in addition to the strong bonding between the zein and Cs complex may have been a contributing factor to the enhanced stability of the formulation and is consistent with our previous observations (Vozza *et al*., 2018, Danish *et al*., 2017b).

6.3.4 Cellular viability

Se loaded NPs become exposed to the intestinal epithelia following oral delivery, leading to its facilitated transport and uptake. Therefore, the potential cytotoxicity of the different Se species were examined on Caco-2 human epithelial cells, and HepG2 human liver hepatocellular cells. Both cell lines are routinely used to assess cytotoxicity of orally delivered molecules (Gleeson *et al*., 2015; Brayden *et al*., 2015). The MTS assay was used to assess the cytotoxicity of both MSC and $SeCys_2$ in native format and within the NP formulation (loaded and unloaded), at different test concentrations (25, 50 and 100 uM).

Supplementary figures show the cytotoxicity assessment of MSC loaded NPs on Caco-2 (S6.3 (A)) and HepG2 cell lines (S6.3 (B)). In terms of Caco-2, no cytotoxicity was observed for all test formulations (native, loaded and unloaded NPs), after 4 hr exposure, in comparison to the negative control, across all tested concentrations (S6.3

(A)). The same response was observed for the HepG2 cell exposures for 72h (S6.3 (B)). These results are in accordance with the observations of Barrera *et al.*, (2013), who observed no apparent cytotoxicity on Caco-2 cells after a 72 hr exposure of MSC (0.2-100 uM) and Marschall *et al.*, (2016), who reported no obvious cytotoxicity HepG2 cells incubated with MSC (2.5-200 uM) after 48 hr exposure.

Regarding $SeCys_2$ (native, loaded and unloaded NPs), although no cytotoxicity was observed in Caco-2 cells after 4 hr exposure (Figure 6.5 (A)), a significant reduction in cell viability was observed for both native and equivalent loaded NPs across all test concentrations, with native $SeCys_2$ resulting in a reduction of $\geq 63\%$ cell viability at 50 and 100 uM test concentrations (Figure 6.5 (B)). Similar results were observed by Takahashi, Suzuki and Ogra (2017), who reported that $SeCys_2$ elicited no significant change in the viability of Caco-2 cell lines after 6 hr, although it did show significant toxicity to HepG2 cells at 100 uM, comparable to that of the inorganic form selenite, after prolonged exposure (48 hr).

Organic Se species, such as SeAAs have been reported to be less toxic than inorganic Se species and as such the high toxicity of $SeCys_2$ is quite surprising (Suzuki *et al.*, 2010; Takahashi, Suzuki and Ogra, 2017). As the toxicity of $SeCys_2$ has been shown to be comparable to that of selenite, it has been proposed by others that the cellular overload of metabolites (such as selenide moieties ($-Se^-$) and (HSe^-) produced during selenoprotein formation or excretion (Rayman, Infante and Sargent, 2008; Marschall *et al.*, 2016) is responsible for this effect. Most likely, the reduction of $SeCys_2$ to SeCys in the cell results in the generation of a highly reactive and sensitive to oxidation selenyl group (-SeH), whose relatively low pKa of 5.2 promotes the formation of ($-Se^-$) at physiological pH (Iwaoka, 2014). As can be seen in Figure 6.5

(B), the encapsulation of $SeCys_2$ within the Cs:zein NP matrix conferred protection to the HepG2 cells after 72 hr exposure, indicating that, at the tested concentrations used in this study, the cytotoxic effects of pure $SeCys_2$ can be reduced.

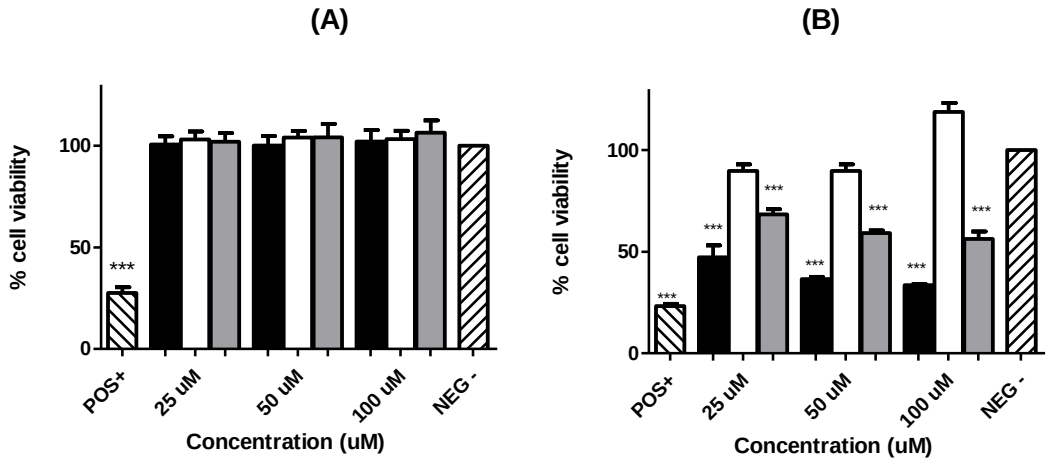

Figure 6.5 Cytotoxicity assessment of $SeCys_2$, unloaded NPs and $SeCys_2$ loaded NPs, exposed for (a) 4h in Caco2 cell lines and (b) 72h in HepG2 cell line at 25 uM, 50 uM and 100 uM concentrations. Percentage (%) of MTS converted was compared to untreated control. 1-Way ANOVA with Dunnett's post-test *** $p < 0.001$. Each value presented was normalised against untreated control and calculated from three separate experiments, each of which included six replicates. N=3.

Lastly, the unloaded NPs showed no significant effect on Caco-2 cells over the range of test concentrations, nor HepG2 at test concentrations of 25 and 50 uM. However, at 100 uM, a significant increase in cell viability was observed, indicating that the formulation elicits an enhanced proliferative effect at this concentration. This may be attributable to a combination of zein's demonstrated cytocompatibility with NIH 3T3 and human liver cells (HL-7702) in terms of cell adhesion and proliferation (Dong, Sun and Wang, 2004), and an increase in fibroblast production caused by the presence of Cs (Rajam *et al.*, 2011).

6.3.5 Release studies

Three basic mechanisms that are typically employed to describe the release of drugs from polymeric particles are, swelling/erosion, diffusion, and degradation (Liechty *et al.*, 2010). The prominence of each can depend on the conditions of the environment. Therefore, the release kinetics of MSC NPs were monitored sequentially in SGF and SIF controlled release experiments.

Figure 6.6 shows the cumulative release profile of MSC and $SeCys_2$ loaded NPs, coated with zein, after subjection to 2 hrs in an SGF environment (pH 1.2) representative of the stomach, followed by a compartmental change to SIF (pH 6.8), representative of the intestine, for 4 hrs. As can be seen, 37 ± 11 % of MSC was released from the NP after 2 hr in SGF, followed by 25 ± 8 % release in SIF for 4 hr. Regarding $SeCys_2$, 45 ± 4 % was released from the NPs after 2 hr in SGF, with a subsequent release of 24 ± 4 % after subjection to a SIF environment (4 hr).

Despite the high-water solubility of the SeAAs, there was good control of drug release in the simulated physiological environment of stomach and small intestine. On exposure to the dissolution fluids (SGF and SIF), the Cs complex will become hydrated forming a viscous gel layer that slows down further seeping-in of dissolution fluids towards the core of the NP (Miladi *et al.*, 2015). The subsequent Cs swelling under these conditions allows for the drug release to follow a diffusion oriented mechanism, which is then typically trailed by the mechanical erosion of the swollen Cs hydrogel (Mohammed *et al.*, 2017). In tandem, subsequent hydration and swelling of the system is heavily dependent upon whether or not the Cs erodes further. With this in mind, it was observed that the release of both SeAAs from the Cs:zein NPs was pH dependent, indicative of Cs solubility in acidic media (Yuan *et al.*, 2013).

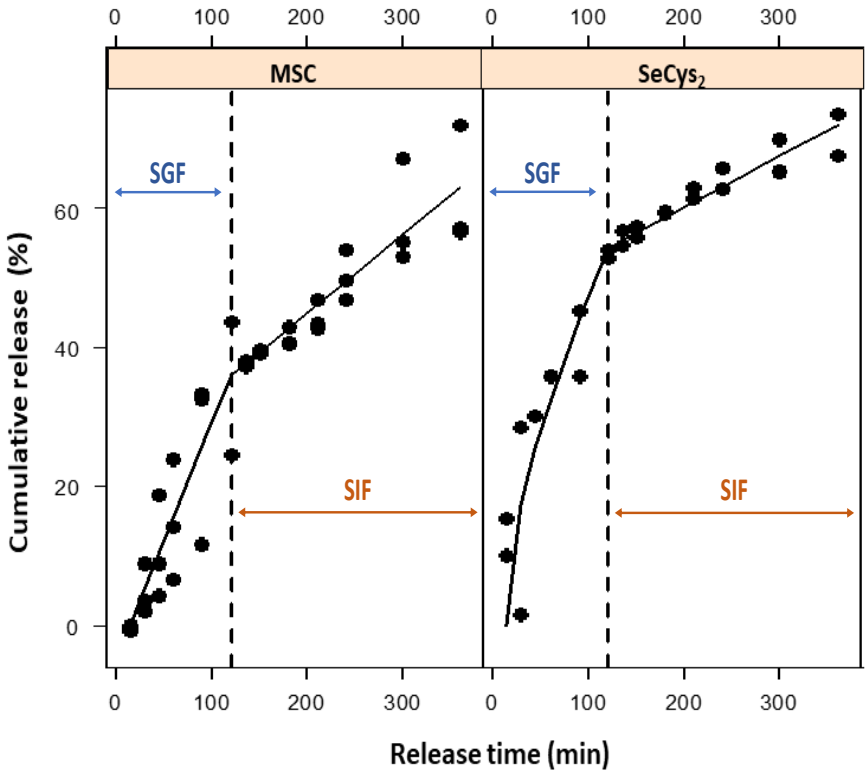

Figure 6.6 Release kinetics of MSC and SeCys2 loaded NPs, coated with zein, after 2 hr in SGF (pH 1.2) and 4 hrs in SIF (pH 6.8). Solid lines are a fit to the model of Equations 6.4 and 6.5. The continuous line indicates the model prediction.

As two different simulated fluids were used for this study, representing the pH environment in the stomach (SGF) and the jejunum target site in the intestine (SIF), their release profile was modelled using a swelling, Peppas equation (6.4) and (6.5) (Siepmann and Peppas, 2011; Danish, 2017a).

For the SGF:

$$\frac{\boldsymbol{M_t}}{\boldsymbol{M_\infty}} = \boldsymbol{ks_1} * \left(\sqrt{\boldsymbol{time}}\right) + \boldsymbol{ks_2} * \boldsymbol{time}$$

(Equation 6.4)

where M_t is the diffused mass at a given time, M_∞ is the asymptotic diffused mass at infinite time, and ks_1 and ks_2 are the diffusive and relaxation rate constants respectively.

For the SIF:

$$\frac{\boldsymbol{M_t}}{\boldsymbol{M_\infty}} - \frac{\boldsymbol{M_{120}}}{\boldsymbol{M_\infty}} = \boldsymbol{ki_1} * \left(\sqrt{\boldsymbol{time - 120}}\right) + \boldsymbol{ki_2} * (\boldsymbol{time - 120})$$

(Equation 6.5)

where M_{120} is the predicted diffused mass at the time of changing from SGF to SIF (120 min), ki_1 and ki_2 are diffusive and relaxation rate constants.

The release of $SeCys_2$ and MSC from the nanoparticles was best fitted with a combination of diffusion and relaxation mechanisms. The fits of the model are illustrated by solid lines in Figure 6.6. Table 6.2 presents the fitted values for the rate constants in SGF (ks) and SIF (ki) for both Se loaded (MSC and $SeCys_2$) NPs, divided into diffusion and relaxation mechanisms ($_1$ and $_2$) (Eq. 6.4, 6.5).

For $SeCys_2$ loaded NPs, subjected to the simulated stomach environment (SGF, pH 1.2), no statistically significant ks_1 parameter was found, indicating that the primary mechanism for release in the stomach was via relaxation, i.e. slower release, approaching zero-order kinetics. After 2 hr subjected to the SGF environment, a compartmental change was employed to mimic the movement of the $SeCys_2$ NPs to the intestinal environment (SIF, pH 6.8), whereupon a combination of diffusion (ki_1) and relaxation (ki_2) mechanisms were observed ($p<0.05$). In contrast, a combination

of ki_1 and ki_2 mechanisms in the stomach (SGF) was observed for the release of the MSC loaded NPs and no statistically significant ki_1 parameter was found for the intestinal compartment, indicating that, in the small intestine (jejunum), at pH 6.8, relaxation is the primary mechanism of release for MSC.

These findings corroborate previous studies, reporting a diffusion and zero order kinetic profile for IPP and LKP loaded Cs NPs, coated with zein (Danish *et al.*, 2017a) and that of other researchers, who observed that zein proved to be a good coating for NPs, whereby, the stronger interaction of the load material (in this instance phenolic monoterpenes) with that of the wall material (zein) was evidenced by its controlled release over time (da Rosa *et al.*, 2015).

Table 6.2 Swellable model parameters for kinetic release studies of MSC and SeCys2 loaded NPs, coated with zein. ks represents the stomach compartment and ki the intestinal compartment, divided into diffusion and relaxation mechanisms ($_1$ and $_2$). All parameters listed where statistically significant, ($*P < 0.05$).

$SeCys_2$ loaded NPs	
Coefficients	**Estimate ($min^{-1/2}$)**
ks_2	0.26±0.08
ki_1	1.86±0.28
ki_2	-0.023±0.05
MSC loaded NPs	
Coefficients	**Estimate ($min^{-1/2}$)**
ks_1	-1.65±0.75
ks_2	0.46±0.08
ki_2	0.14±0.05
$R^2_{adjusted}$	**0.95**

In terms of significant differences between the common release parameters of the two SeAAs (Ks_2 and Ki_2, Table 6.2), MSC was found to exhibit a lower release rate in SGF than $SeCys_2$, with a release of 37 ± 11 % observed for MSC vs 45 ± 4 % for $SeCys_2$. This may be attributable to a number of different factors, for example the difference in the polar surface area (PSA) between the two compounds (MSC PSA =

63.32 A^2 vs $SeCys_2$ PSA = 126.44 A^2) allowing for MSC to become more physically entrapped into the NP matrix. Additionally, the electrostatic attractions between the NP matrix and $SeCys_2$ becomes amplified at pH 1.2, whereby the $SeCys_2$ charged state predominantly exists with both amine residues going to $NH3^+$ (Rivail da Silva *et al.*, 1997; Kotrebai *et al.*, 2000), facilitating increased electrostatic repulsion with the primary amines of Cs. As other authors have observed that swelling rates, swelling capacity and release rates of drugs varying in hydrophobicity were pH dependent, because of the presence of charged groups on the drug molecules in varying pH release media (Katas, Raja and Lam, 2013; Bouman *et al.*, 2016), it is reasonable to suggest that this may be the attributing factor to the faster release observed with $SeCys_2$. No significant difference in the release profile of either MSC or $SeCys_2$ loaded NPs against those without zein coating, was observed (data not shown), indicating that the release profile is influenced by the interaction of the active with Cs:TPP and is not significantly influenced by the zein coating. This may be related to the formulation media conditions employed in this study for TPP (pH 12) prior to crosslinking with Cs, which has been shown to decrease drug release rates. For example, Ajun *et al.*, (2009) observed that aspirin's release rate from Cs NPs could be reduced from 64 to 40 % within 8 hr by increasing the basicity of the TPP media pH from 3 to 8.4, allowing for the production of high density structured NPs and consequently, the drugs slower release. Nonetheless, whether zein affected the release profile or not, it remained necessary to keep zein in the formulation to ensure an EE (≥80 %) for the encapsulated SeAAs.

Lastly, the release profile of SeMet, previously assessed in Chapter 5 (Section 5.9, Figure 5.8), was compared to those of both MSC and $SeCys_2$, SeMet was found to release in SGF at a slower rate than the other SeAAs, with a total release of 25±1 %

after 2 hr in the SGF environment, vs 37 ± 11 % and 45 ± 4 % for MSC and $SeCys_2$ respectively. Conversely, in the SIF environment SeMet was the fastest releasing SeAA, showing release of 33 ± 3 % vs 25 ± 8 for MSC and 24 ± 4 for $SeCys_2$ (Supplemental Table S6.1). From the Henderson–Hasselbalch equation it can be derived that any drug-like molecule (weak acid or base) will be predominantly ionised if the pH of the system is about two pH units higher than its pKa. *Vice versa*, at two pH units lower than its pKa the drug will be predominantly (99%) protonated. The pKas for the SeAAs are 4.66 < 4.93 < 5.53 ($SeCys_2$, MSC, SeMet) (Supplemental Table S6.1) suggesting that the observed variance in release rates is attributable to their chargeable properties and interactions with the protonated 1º amines of Cs (Makhlof, Tozuka and Takeuchi, 2011). For example, $SeCys_2$, the fastest releasing SeAA in SGF (45 ± 4%), would be the most protonated (pKa = 4.66) at pH 1.2, allowing for increased electrostatic repulsion between its two $-NH_3^+$ moieties and that of Cs, thus driving the release from both the surface and within the NP structure. Conversely, SeMet with a pKa of 5.5 showing the slowest release in SGF (25 ± 1) (Supplemental Table S6.1), would be the least protonated out of the SeAAs allowing for less repulsion between its $-NH_2$ and $-NH_3^+$ and thus a slower release in SGF. As the target site for the SeAAs is the jejunum, sufficient ability of the NP to withstand the acidic environment of the stomach is important, with the findings showing that SeMet loaded NPs are the most resistant in this instance, followed by MSC and $SeCys_2$.

6.4 Conclusion

In this study, SeAA loaded Cs NPs, were produced via ionotropic gelation. NPs with optimum properties for oral delivery were formed by coating the produced NPs at a 1:0.75 mass ratio of Cs:zein, resulting in MSC loaded NPs with sizes of 271.2 ± 21.4 nm, PDI 0.211 ± 0.061, ZP 32.2 ± 1.3, EE% of 80.7 ± 0.7 and $SeCys_2$ loaded NPs of 262.1 ± 11.1 nm, PDI 0.243 ± 0.148, ZP 31.5 ± 1.0 and EE% 78.9 ± 1.5. SEM analysis showed that spheroidal, well distributed particles were observed. MTS cytotoxicity studies on MSC loaded NPs showed no decrease in cellular viability in either Caco-2 (intestine) and HepG2 (liver) cell lines after 4 and 72 hr exposures, respectively. For $SeCys_2$ loaded NPs, no cytotoxicity was observed in Caco-2 cell lines after 4 hr, however a significant reduction in cytotoxicity was observed, when compared to pure $SeCys_2$, across all test concentrations on HepG2 after 72 hr exposure. Accelerated thermal stability of both loaded NPs indicated good stability under normal storage conditions. Lastly, after 6 hr exposure to simulated GIT environments, the sustained release profile of the formulation showed that 62 ± 8 % and 69 ± 4 of drug had been released from MSC and $SeCys_2$ loaded NPs respectively. These findings infer that, by encapsulating SeAAs into a NP delivery system, improved oral administration of this molecule may be achieved, which could be of beneficial use for the supplementation of food products with these essential nutrients.

6.5 References

Ajun, W. *et al.* (2009) 'Preparation of aspirin and probucol in combination loaded chitosan nanoparticles and in vitro release study', *Carbohydrate Polymers*, 75(4), pp. 566–574.

Amoako, P. O., Uden, P. C. and Tyson, J. F. (2009) 'Speciation of selenium dietary supplements; formation of S-(methylseleno)cysteine and other selenium compounds', *Analytica Chimica Acta*, 652(1–2), pp. 315–323.

Anitha, A. *et al.* (2014) 'Chitin and chitosan in selected biomedical applications', *Progress in Polymer Science*, 39(9), pp. 1644–1667.

Avadi, M. R. *et al.* (2010) 'Preparation and characterization of insulin nanoparticles using chitosan and Arabic gum with ionic gelation method', *Nanomedicine: Nanotechnology, Biology, and Medicine*, 6(1), pp. 58–63.

Barrera, L. N. *et al.* (2013) 'Colorectal cancer cells Caco-2 and HCT116 resist epigenetic effects of isothiocyanates and selenium in vitro', *European Journal of Nutrition*, 52(4), pp. 1327–1341.

Benshitrit, R. C. *et al.* (2012) 'Development of oral food-grade delivery systems: Current knowledge and future challenges', *Food & Function*, 3(1), p. 10.

Bouman, J. *et al.* (2016) 'Controlled Release from Zein Matrices: Interplay of Drug Hydrophobicity and pH', *Pharmaceutical Research*, 33(3), pp. 673–685.

British Pharmacopoeia Commission (2016) *British Pharmacopoeia: Appendix XII B. Dissolution*. London: TSO.

Calderon L. *et al.* (2013) 'Nano and microparticulate chitosan-based systems for antiviral topical delivery', *European Journal of Pharmaceutical Sciences*, 48, pp. 216–222.

Cao, S. *et al.* (2014) 'Se-methylselenocysteine offers selective protection against toxicity and potentiates the antitumour activity of anticancer drugs in preclinical animal models', *British Journal of Cancer*, 110(7), p. 1733.

Cencic, A. and Chingwaru, W. (2010) 'The Role of Functional Foods, Nutraceuticals, and Food Supplements in Intestinal Health', *Nutrients*, 2(6), pp. 611–625.

Chen, L., Remondetto, G. E. and Subirade, M. (2006) 'Food protein-based materials as nutraceutical delivery systems', *Trends in Food Science and Technology*, pp. 272–283.

Cousins, R. J. and Liuzzi, J. P. (2018) ‘Trace Metal Absorption and Transport’, in *Physiology of the Gastrointestinal Tract (Sixth Edition)*, pp. 1485–1498.

Danish, M. K. *et al.* (2017a) ‘Comparative study of the structural and physicochemical properties of two food derived antihypertensive tri-peptides, Isoleucine-Proline-Proline and Leucine-Lysine-Proline encapsulated into a chitosan based nanoparticle system’, *Innovative Food Science & Emerging Technologies*, 44, pp. 139–148.

Danish, M. K. *et al.* (2017b) ‘Formulation, Characterization and Stability Assessment of a Food-Derived Tripeptide, Leucine-Lysine-Proline Loaded Chitosan Nanoparticles’, *Journal of Food Science*, 82(9), pp. 2094–2104.

Davies, M. J. (2016) ‘Protein oxidation and peroxidation’, *Biochemical Journal*, 473(7), pp. 805–825.

Dong, J., Sun, Q. and Wang, J.-Y. (2004) ‘Basic study of corn protein, zein, as a biomaterial in tissue engineering, surface morphology and biocompatibility’, *Biomaterials*, 25(19), pp. 4691–4697.

Etheridge, M. L. *et al.* (2013) ‘The big picture on nanomedicine: the state of investigational and approved nanomedicine products.’, *Nanomedicine : Nanotechnology, Biology, and Medicine*, 9(1), pp. 1–14.

Fan, C. *et al.* (2013) ‘Selenocystine potentiates cancer cell apoptosis induced by 5-fluorouracil by triggering reactive oxygen species-mediated DNA damage and inactivation of the ERK pathway’, *Free Radical Biology and Medicine*, 65, pp. 305–316.

Garousi, F. (2015) ‘The toxicity of different selenium forms and compounds – Review’, *Acta Agraria Debreceniensis*, 64, pp. 33–38.

Ghosh, A. K. and Bandyopadhyay, P. (2012) ‘Polysaccharide-protein interactions and their relevance in food colloids’, *The Complex World of Polysaccharides*. InTech.

Gleeson, J. P. *et al.* (2015) ‘Stability, toxicity and intestinal permeation enhancement of two food-derived antihypertensive tripeptides, Ile-Pro-Pro and Leu-Lys-Pro’, *Peptides*, 71, pp. 1–7.

He, C. *et al.* (2012) ‘Size-dependent absorption mechanism of polymeric nanoparticles for oral delivery of protein drugs’, *Biomaterials*, 33(33), pp. 8569–8578.

Hejazi, R. and Amiji, M. (2003) ‘Chitosan-based gastrointestinal delivery systems’, *Journal of Controlled Release*, pp. 151–165.

Hosseinzadeh, H. *et al.* (2012) 'Chitosan-Pluronic nanoparticles as oral delivery of anticancer gemcitabine: Preparation and in vitro study', *International Journal of Nanomedicine*, 7, pp. 1851–1863.

Hu, K. and McClements, D. J. (2014) 'Fabrication of surfactant-stabilized zein nanoparticles: A pH modulated antisolvent precipitation method', *Food Research International*, 64, pp. 329–335.

Iwaoka, M. (2014) 'Antioxidant organoselenium molecules', *Organoselenium Chemistry: Between Synthesis and Biochemistry*. Bentham Books, pp. 361–378.

Janes, K. A., Calvo, P. and Alonso, M. J. (2001) 'Polysaccharide colloidal particles as delivery systems for macromolecules', *Advanced Drug Delivery Reviews*, 47(1), pp. 83–97.

Katas, H., Raja, M. A. G. and Lam, K. L. (2013) 'Development of chitosan nanoparticles as a stable drug delivery system for protein/siRNA', *International Journal of Biomaterials*, pp.1-9.

Kotrebai, M. *et al.* (2000) 'High-performance liquid chromatography of selenium compounds utilizing perfluorinated carboxylic acid ion-pairing agents and inductively coupled plasma and electrospray ionization mass spectrometric detection', *Journal of Chromatography A*, 866(1), pp. 51–63.

Kumari, A., Yadav, S. K. and Yadav, S. C. (2010) 'Biodegradable polymeric nanoparticles based drug delivery systems.', *Colloids and Surfaces. B, Biointerfaces*, 75(1), pp. 1–18.

Kumirska, J. *et al.* (2011) 'Biomedical Activity of Chitin/Chitosan Based Materials—Influence of Physicochemical Properties Apart from Molecular Weight and Degree of N-Acetylation', *Polymers*, 3(4), pp. 1875–1901.

Lacourciere, G. M. and Stadtman, T. C. (1999) 'Catalytic properties of selenophosphate synthetases: comparison of the selenocysteine-containing enzyme from Haemophilus influenzae with the corresponding cysteine-containing enzyme from Escherichia coli', *Proceedings of the National Academy of Sciences*, 96(1), pp. 44–48.

Lagos, J. B. *et al.* (2015) 'Recent patents on the application of bioactive compounds in food: A short review', *Current Opinion in Food Science*, 5, pp.1-7.

Lamprecht, A. *et al.* (2000) 'Influences of process parameters on nanoparticle preparation performed by a double emulsion pressure homogenization technique', *International Journal of Pharmaceutics*, 196(2), pp. 177–182.

Liang, J. *et al.* (2017) 'Applications of chitosan nanoparticles to enhance absorption and bioavailability of tea polyphenols: A review', *Food Hydrocolloids*, 69, pp. 286–292.

Liechty, W. B. *et al.* (2010) 'Polymers for Drug Delivery Systems', *Annual Review of Chemical and Biomolecular Engineering*, pp. 149–173.

Lobo, V. *et al.* (2010) 'Free radicals, antioxidants and functional foods: Impact on human health', *Pharmacognosy Reviews*, 4(8), p. 118.

Luo, Y. *et al.* (2010) 'Preparation, characterization and evaluation of selenite-loaded chitosan/TPP nanoparticles with or without zein coating', *Carbohydrate Polymers*, 82(3), pp. 942–951.

Luo, Y. *et al.* (2011) 'Preparation and characterization of zein/chitosan complex for encapsulation of a-tocopherol, and its in vitro controlled release study', *Colloids and Surfaces B: Biointerfaces*, 85(2), pp. 145–152.

Luo, Y. *et al.* (2013) 'Encapsulation of indole-3-carbinol and 3,3′-diindolylmethane in zein/carboxymethyl chitosan nanoparticles with controlled release property and improved stability', *Food Chemistry*, 139(1–4), pp. 224–230.

Luo, Y. and Wang, Q. (2014) 'Zein-based micro- and nano-particles for drug and nutrient delivery: A review', *Journal of Applied Polymer Science*, 131(16), pp. 1–12.

Makhlof, A., Tozuka, Y. and Takeuchi, H. (2011) 'Design and evaluation of novel pH-sensitive chitosan nanoparticles for oral insulin delivery', *European Journal of Pharmaceutical Sciences*, 42(5), pp. 445–451.

Marschall, T. A. *et al.* (2016) 'Differing cytotoxicity and bioavailability of selenite, methylselenocysteine, selenomethionine, selenosugar 1 and trimethylselenonium ion and their underlying metabolic transformations in human cells', *Molecular Nutrition & Food Research*, 60(12), pp. 2622–2632.

Maseko, T. *et al.* (2013) 'Chemical characterisation and speciation of organic selenium in cultivated selenium-enriched Agaricus bisporus.', *Food Chemistry*, 141(4), pp. 3681–3687.

Miladi, K. *et al.* (2015) 'Enhancement of alendronate encapsulation in chitosan nanoparticles', *Journal of Drug Delivery Science and Technology*, 30, pp. 391–396.

Mishra, B., Priyadarsini, K. I. and Mohan, H. (2007) 'Effect of pH on one-electron oxidation of selenium aminoacids', *BARC Newsletter*, 285, p. 220.

Mohammed, M. A. *et al.* (2017) 'An overview of chitosan nanoparticles and its application in non-parenteral drug delivery', *Pharmaceutics*, 9(4).

Montes-Bayón, M. *et al.* (2006) 'Evaluation of different sample extraction strategies for selenium determination in selenium-enriched plants (Allium sativum and Brassica juncea) and Se speciation by HPLC-ICP-MS', *Talanta*, 68(4), pp. 1287–1293.

Mukhopadhyay, P. *et al.* (2013) 'Oral insulin delivery by self-assembled chitosan nanoparticles: in vitro and in vivo studies in diabetic animal model.', *Materials Science & Engineering. C, Materials for Biological Applications*, 33(1), pp. 376–82.

Neves, A. R. *et al.* (2016) 'Nanoscale delivery of resveratrol towards enhancement of supplements and nutraceuticals', *Nutrients*, 8(3), p. 131.

Paliwal, R. and Palakurthi, S. (2014) 'Zein in controlled drug delivery and tissue engineering.', *Journal of Controlled Release*, 189, pp. 108–22.

Park, C. E., Park, D. J. and Kim, B. K. (2015) 'Effects of a chitosan coating on properties of retinol-encapsulated zein nanoparticles', *Food Science and Biotechnology*, 24(5), pp. 1725–1733.

Podaralla, S. and Perumal, O. (2012) 'Influence of formulation factors on the preparation of zein nanoparticles', *AAPS Pharmscitech*, 13(3), pp. 919–927.

Ponnampalam, E. *et al.* (2009) 'Nutritional strategies to increase the selenium and iron content in pork and promote human health', *Co-operative Research Centre for an Internationally Competitive Pork Industry, Pork CRC, Australian Government*.

R Core Team (2016) 'R: A Language and Environment for Statistical Computing. Vienna, Austria: R Foundation for Statistical Computing; 2014. R Foundation for Statistical Computing'.

Rajam, M. *et al.* (2011) 'Chitosan nanoparticles as a dual growth factor delivery system for tissue engineering applications', *International Journal of Pharmaceutics*, 410(1–2), pp. 145–152.

Rayman, M. P. (2000) 'The importance of selenium to human health.', *Lancet*, 356(9225), pp. 233–241.

Rayman, M. P., Infante, H. G. and Sargent, M. (2008) ‘Food-chain selenium and human health: spotlight on speciation.’, *The British Journal of Nutrition*, 100(2), pp. 238–253.

Reilly, K. *et al.* (2014) ‘A note on the effectiveness of selenium supplementation of Irish-grown *Allium* crops’, *Irish Journal of Agricultural and Food Research*, pp. 91–99.

des Rieux, A. *et al.* (2006) ‘Nanoparticles as potential oral delivery systems of proteins and vaccines: a mechanistic approach’, *Journal of Controlled Release*, 116(1), pp. 1–27.

Rivail da Silva, M. *et al.* (1997) ‘Determination of the deprotonation constants of seleno-DL-cystine and seleno-DL-methionine and implication to their separation by HPLC’, *Applied Organometallic Chemistry*, 11(1), pp. 21–30.

Rodrigues, S. *et al.* (2012) ‘Biocompatibility of chitosan carriers with application in drug delivery’, *Journal of Functional Biomaterials*, 3(3), pp. 615–641.

da Rosa, C. G. *et al.* (2015) ‘Characterization and evaluation of physicochemical and antimicrobial properties of zein nanoparticles loaded with phenolics monoterpenes’, *Colloids and Surfaces A: Physicochemical and Engineering Aspects*, 481, pp. 337–344.

Semenova, M. G. *et al.* (2014) ‘Protein–Polysaccharide Interactions and Digestion of the Complex Particles’, in *Food Structures, Digestion and Health*, pp. 169–192.

Siepmann, J. and Peppas, N. A. (2011) ‘Higuchi equation: Derivation, applications, use and misuse’, *International Journal of Pharmaceutics*, pp. 6–12.

de Souza, V. R. *et al.* (2014) ‘Determination of the bioactive compounds, antioxidant activity and chemical composition of Brazilian blackberry, red raspberry, strawberry, blueberry and sweet cherry fruits.’, *Food Chemistry*, 156, pp. 362–8.

Suzuki, M. *et al.* (2010) ‘Differential apoptotic response of human cancer cells to organoselenium compounds’, *Cancer Chemotherapy and Pharmacology*, 66(3), pp. 475–484.

Takahashi, K., Suzuki, N. and Ogra, Y. (2017) ‘Bioavailability comparison of nine bioselenocompounds in vitro and in vivo’, *International Journal of Molecular Sciences*, 18(3), pp. 1–11.

Tavano, L. *et al.* (2014) ‘Co-encapsulation of antioxidants into niosomal carriers: gastrointestinal release studies for nutraceutical applications’, *Colloids and Surfaces B: Biointerfaces*, 114, pp. 82–88.

Valko, M. *et al.* (2007) 'Free radicals and antioxidants in normal physiological functions and human disease', *The International Journal of Biochemistry & Cell Biology*, 39(1), pp. 44–84.

Vozza, G. *et al.* (2016) *Nutrition - Nutrient delivery: Nanotechnology in the Food Industry, Volume 5*. 1st edn, U. K. E. Oxford.

Ward, P., Connolly, C. and Murphy, R. (2012) 'Accelerated Determination of Selenomethionine in Selenized Yeast: Validation of Analytical Method', *Biological Trace Element Research*, 151(3), pp. 446–450.

Wasowicz, W. *et al.* (2003) 'The role of essential elements in oxidative stress', *Comments on Toxicology*, 9(1), pp. 39–48.

Win, K. Y. and Feng, S.-S. (2005) 'Effects of particle size and surface coating on cellular uptake of polymeric nanoparticles for oral delivery of anticancer drugs', *Biomaterials*, 26(15), pp. 2713–2722.

Wu, L., Zhang, J. and Watanabe, W. (2011) 'Physical and chemical stability of drug nanoparticles', *Advanced Drug Delivery Reviews*, 63(6), pp. 456–469.

Xu, Y. and Du, Y. (2003) 'Effect of molecular structure of chitosan on protein delivery properties of chitosan nanoparticles', *International Journal of Pharmaceutics*, 250(1), pp. 215–226.

Yan, H. *et al.* (2012) 'Preparation of chitosan/poly (acrylic acid) magnetic composite microspheres and applications in the removal of copper (II) ions from aqueous solutions', *Journal of Hazardous Materials*, 229, pp. 371–380.

Yoon, H. Y. *et al.* (2014) 'Glycol chitosan nanoparticles as specialized cancer therapeutic vehicles: Sequential delivery of doxorubicin and Bcl-2 siRNA', *Scientific Reports*, 4, p. 6878.

Yuan, Z. *et al.* (2013) 'Chitosan-graft-β-cyclodextrin nanoparticles as a carrier for controlled drug release', *International Journal of Pharmaceutics*, 446(1–2), pp. 191–198.

Zhang, Y. *et al.* (2014) 'Fabrication, characterization and antimicrobial activities of thymolloaded zein nanoparticles stabilized by sodium caseinate-chitosan hydrochloride double layers', *Food Chemistry*, 142, pp. 269–275.

Zhang, Y. *et al.* (2015) 'Zein-based films and their usage for controlled delivery: Origin, classes and current landscape', *Journal of Controlled Release*, 206(2699), pp. 206–219.

6.6 Supplemental Information

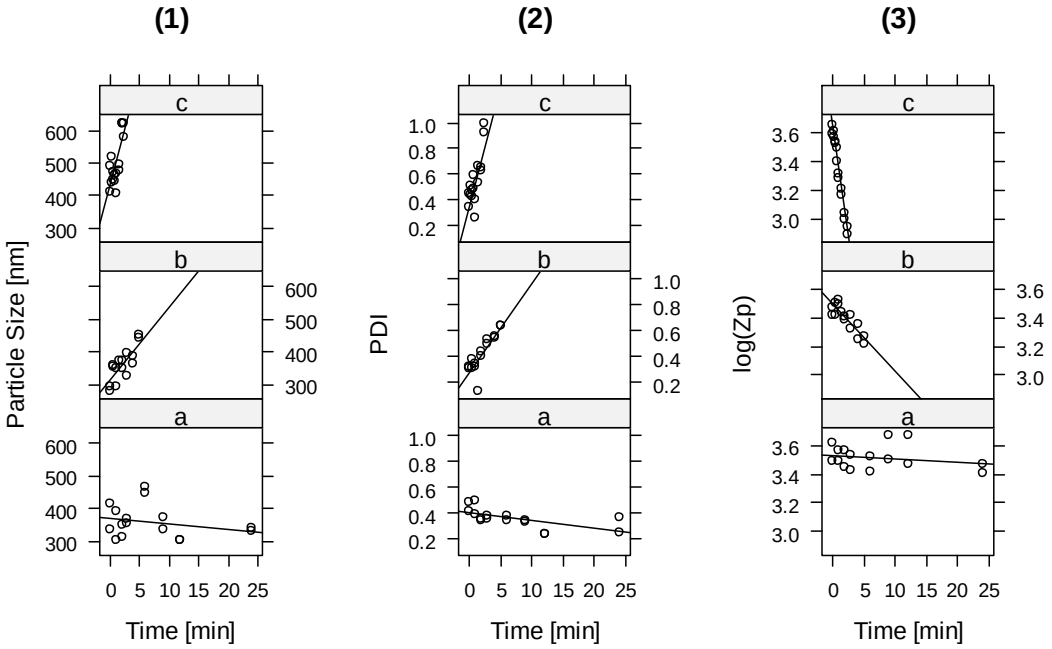

Figure S6.1(1) Particle size, (2) PDI and (3) ZP analysis of $SeCys_2$ loaded NPs exposed to (a) 80 °C, (b) 70 °C and (c) 60 °C, over time periods of 120, 300 and 720 min, respectively. N=3.

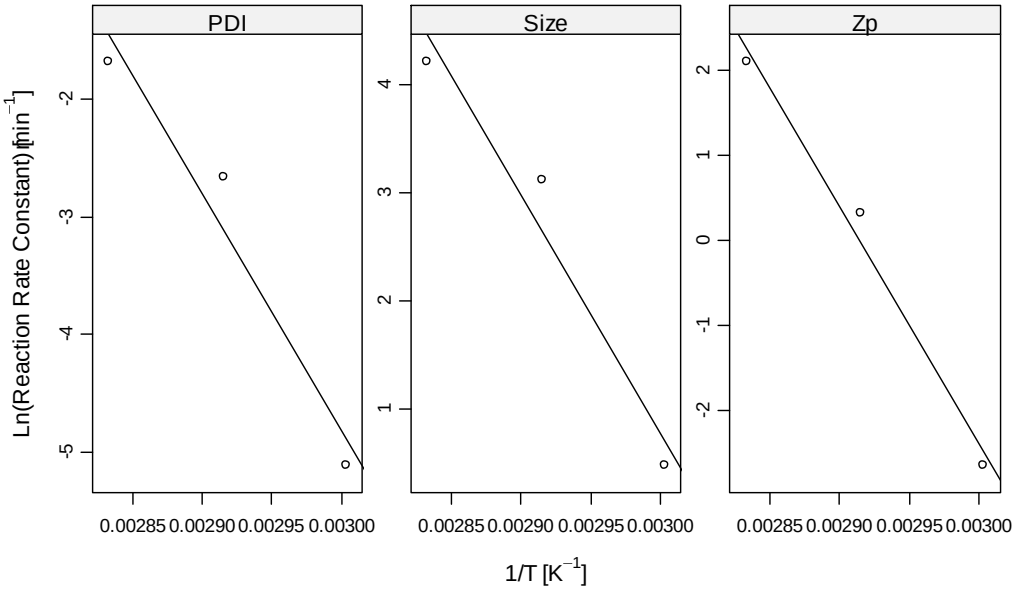

Figure S6.2 Arrhenius plots for the (A) ZP, (B) PDI and (C) size accelerated studies of $SeCys_2$ loaded NPs.

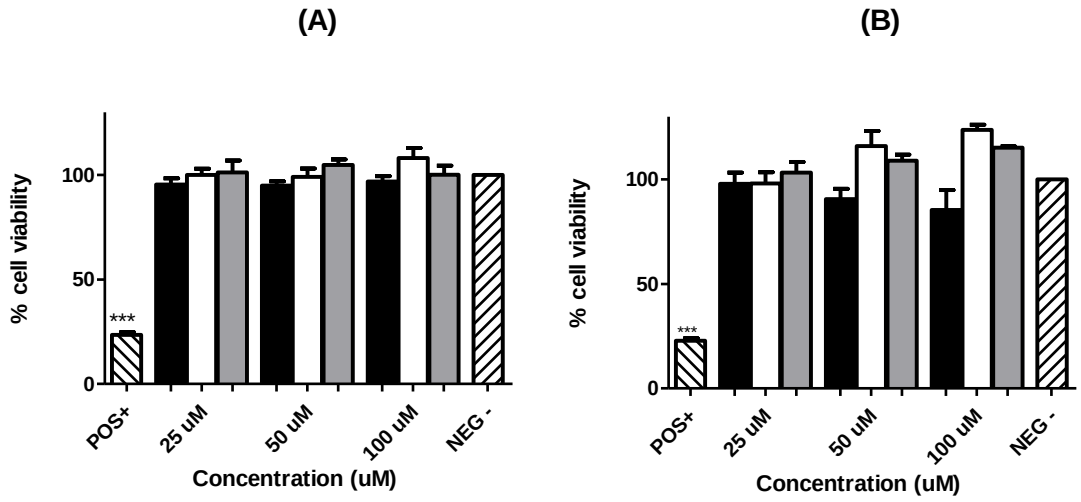

Figure S6.3 Cytotoxicity assessment of ■ MSC, ▭ unloaded NPs and ▭ MSC loaded NPs, exposed for (a) 4h in Caco2 cell lines and (b) 72h in HepG2 cell line at 25 uM, 50 uM and 100 uM concentrations. Percentage (%) of MTS converted was compared to untreated control. 1-Way ANOVA with Dunnett's post-test *** p< 0.001, ** p< 0.01, Each value presented was normalised. against untreated control and calculated from three separate experiments, each of which included six replicates. N=3.

Table S6.1 Release (%) of SeAAs in SGF and SIF.

SeAA loaded NP	% Release in SGF	% Release in SIF	% Cumulative release	pKa
SeMet	25 ± 1	33 ± 3	58 ± 2	5.53
MSC	37 ± 11	25 ± 8	62 ± 9	4.93
$SeCys_2$	45 ± 4	24 ± 4	69 ± 4	4.66

7 POTENTIAL OF MUSHROOM BY-PRODUCTS FOR NUTRIENT DELIVERY APPLICATIONS: PRODUCTION AND CHARATERISATION OF CHITIN FROM *AGARICUS BISPORUS* AND ITS DERIVATISATION TO CHITOSAN AND TRIMETHYL CHITOSAN

The work presented in this chapter is reproduced from:

Vozza, G., Vozza, E, Byrne, H. J., Ryan, S and Frias, J. (2018). Potential of mushroom by-products for drug delivery applications: Production and characterisation of chitin from *Agaricus bisporus* and its derivatisation to chitosan and trimethyl chitosan. Submitted to the Journal of Carbohydrate Polymers, May 2018.

Vozza, G., was the primary author, Vozza, E conducted the experiments in Section 7.3.8 and Byrne, H. J., Frias, J. and Ryan S contributed to layout, design and proofing.

Numbering of Sections, Figures and Tables has been adapted to the thesis format.

Abstract

In this work, chitin (CT) was extracted from *A. bisporus* using alkali reflux, yielding 6.6 ± 2.2 % of dried mushroom powder determined to be CT. The CT produced showed equivalent purity and degree of acetylation (DA%) (≈ 100%) to a commercial standard, as determined by ^{13}C NMR. The extracted CT was then derivatised to Chitosan (Cs), via microwave irradiation and conventional thermal heating methods, the optimum method for conversion being identified as microwave treatment (yield of 55 vs 33 %). The Cs produced using microwave irradiation showed equivalent purity and degree of deacetylation (DDA%) (≈86 %) to that of commercial fungal Cs and that of an ultrapure Cs typically employed for use in bioactive delivery formulations, as identified by ^{1}H-NMR and FTIR spectroscopy. The extract was then chemically modified to water soluble trimethyl chitosan (fTMC), for assessment as a permeation enhancer, showing equivalent degrees of quaternisation (≈ 44 %) with low O-methylation values (≈ 25 %), as determined by ^{1}H-NMR. Lastly, fTMC was assessed for permeation enhancing effects via the trans-epithelial electrical resistance (TEER) assay on human epithelial colorectal adenocarcinoma cell (Caco-2) monolayers, showing a time reversible reduction in TEER of ≈ 75 vs ≈ 90 against a well-established permeation enhancer, sodium caprate used as positive control. The findings indicate that *A. bisporus* can be considered as a good source of CT that can be easily isolated without aggressive treatments, subsequently deacetylated for the production of Cs and chemically modified to fTMC, supporting the proposition that these by-products have potential use for many different practical applications.

Keywords

Fungal extracts, chitin, microwave treatment, chitosan, Trimethylchitosan, permeation enhancer.

Abbreviations

CT, Chitin; **Cs**, Chitosan; **CL113**, PROTASAN™ UP; **DA%**, Degree of Acetylation; **DDA%**, Degree of Deacetylation; **TMC**, Trimethyl chitosan; **DDQ%**, Degree of quaternisation; **cTMC,** commercial TMC, **fTMC,** fungal TMC; **TEER**, trans epithelial electrical resistance assay.

7.1 Introduction

Chitin (CT) is a polysaccharide consisting of adjacent monosaccharides, 2-(acetylamino)-2-deoxy-d-glucose, bonded by glycosidic bonds in a linear or branched fashion, and is the second most abundant polymer found in nature (next to cellulose) (Rathke and Hudson, 1994). CT is insoluble in most regular solvents owing to the presence of acetyl, amino and hydroxyl groups in the polysaccharide chain, that generate hydrogen bonds (inter and intramolecular), and cause a high degree of aggregation (Pillai, Paul and Sharma, 2009). Today, CT, chitosan (Cs) and Cs are produced on a commercial scale for a variety of applications, e.g. cosmetics, pharmaceuticals, and wastewater treatment, with a market value of $2.0 billion (BCC research, 2016). However, CT insolubility affects the scaling up of the processes to produce CT-based products (Hamed, Özogul and Regenstein, 2016; Yang *et al.*, 2016; Aranaz *et al.*, 2018).

Cs is a linear, semi-crystalline polysaccharide composed of (1, 4)-2-acetamido-2-deoxy-β-D-glucan (N-acetyl D-glucosamine) and (1,4)-2-amino-2-deoxy-β-D-glucan

(D-glucosamine) units, that are not widely present in nature (Duarte *et al.*, 2002). Cs is typically produced from CT by chemical hydrolysis under severe alkaline conditions, by removing the acetyl groups from the molecular chain of CT, which results in a high degree of the chemically reactive group (NH_2) being left on the compound (Cs), thus allowing for its solubilisation in acidic aqueous solutions (Ospina Álvarez *et al.*, 2014). The ratio of N-acetyl-D-glucosamine to D-glucosamine is what determines whether the polymer can be considered Cs or CT, whereby, if more than 60% of the partially deacetylated CT exists as D-glucosamine, it is considered Cs (de Alvarenga, Pereira de Oliveira and Roberto Bellato, 2010). For Cs this ratio percent is known as the degree of deacetylation (DDA%) (whereas for CT this ratio percent is known as the degree of acetylation (DA%)) and is an important property to consider in Cs production, as it determines its solubility properties, biodegradability and immunological activity (Tolaimate *et al.*, 2000; Pillai, Paul and Sharma, 2009). A considerable amount of work on Cs and its chemically modified derivatives, for potential use in drug delivery systems, has been published over the past 20 years (Felt, Buri and Gurny, 1998; Prabaharan, 2008; Xing *et al.*, 2018). Cs, in contrast to all other polysaccharides, holds a unique cationic character, owing to the primary amino groups present on its backbone. It has been used for the development and formulation of nanoparticles for drug delivery due to properties such as controlled drug release, mucoadhesion, in situ gelation, transfection and permeation enhancement (PE) properties (Bernkop-Schnürch and Dünnhaupt, 2012; Katas, Raja and Lam, 2013; Huang, Cai and Lapitsky, 2015). In terms of drug delivery properties, it has previously been reported that Cs with a higher DDA%, has the ability to achieve higher encapsulation of bioactives, due to the increased level of functional groups present

that can complex with reactive groups on the bioactive (BA) of interest (Xu and Du, 2003).

At present, crustacean shells are considered the most convenient available source for the commercial production of CT (Hamed, Özogul and Regenstein, 2016). However, due to seasonal availability and environmental pollution, the industrial isolation of CT from this source faces some challenges. For example, calcium carbonate, proteins, lipids and pigments associated with crustacean CT requires aggressive, successive, acid (HCL), alkali (KOH) and bleaching treatments (decolourising agent) at high temperatures, for purification (Barikani *et al.*, 2014). Consequently, the final product produced can often undergo chemical changes such as the deacetylation and depolymerisation of CT thus reducing its overall quality and reproducible functionality (Kardas *et al.*, 2012). Moreover, the release of waste containing alkali and degradation products into the surrounding environment has been identified as a contributing source of environmental pollution (Kaur *et al.*, 2014). Enzymatic hydrolysis has also been reported as a method of Cs production, but it is not as commonly employed as chemical hydrolysis due to its higher cost (Kim and Rajapakse, 2005).

PROTASAN™ CL113, a commercial Cs, derived from crustacean shells and sold by NovaMatrix, FMC Corporations, has been previously promoted for its ability to encapsulate and deliver food derived bioactives such as Retinyl Palmitate (a vitamin A isomer) and possesses the following physicochemical properties: molecular weight (MW) of 110-150 kDa, DDA% ≥80 % and minimal metal contamination (Fernández-Gutiérrez *et al.*, 2015). It has also been used to slow and control the drug release profile of Triclosan (an efficient anti-malarial drug) (Maestrelli, Mura and Alonso,

2004) and salmon calcitonin (a potential osteoarthritic drug) (Ryan *et al*., 2013) owing to both its known mucoadhesive and enhancer properties and its demonstrated effectiveness in optimally controlling drug release rate. In fact, to date, much of the research involving its employment as a nanocarrier, has been of Cs of animal origin (crustaceans) (Hamed, Özogul and Regenstein, 2016). However, high batch to batch variability and climate change (David Brayden, TRANS-INT, private communication) of Cs from these sources have been reported, resulting in formulations with variable physicochemical properties and with potential for inducing allergic responses (Smets and Rüdelsheim, 2018). Hence, an alternative Cs produced, for example from edible *A. bisporus* mushrooms, could be well placed for pharmaceutical applications, particularly if available with batch to batch reproducibility and high control over its molecular characteristics, such as molecular weight and DDA%.

During white mushroom (*A. bisporus)* cultivation, by-products are generated, whereby between 5 and 20% of fruiting bodies with misshaped cups and stalks do not meet the specifications set by retailers and are not utilised for human consumption (Figure 7.1). In the USA alone, mushroom production results in nearly 50,000 metric tons of mushroom material per year, with no suitable commercial application (Philibert, Lee and Fabien, 2017). Notably, however, under mild conditions, media optimisation and green conversion of agricultural industrial wastes, CT and Cs can be obtained from mushrooms and fungi and present an alternative to other uses of this by-product (Kulshreshtha, Mathur and Bhatnagar, 2014). Extraction of CT, which the European Food Safety Authority (EFSA) approved as a food additive in 2010, can potentially offer alternative revenue with significant economic potential (Tetens, 2010).

Mariod (2016) reported that, for the isolation of CT from different marine sources, chemical treatments like deproteinisation with hot alkali (1 M NaOH at 65–100 ˚C for 1–72 hr), demineralisation with acid to eliminate calcium carbonate (0.275–2 M HCl at near 100 ˚C for 1–48 hr) and decolouration to remove pigments are necessary. The fungal approach, however, has the advantage of easy handling, harvesting and control to produce high quality Cs, through enhanced control of environmental and nutritional conditions used during cultivation (Ghormade, Pathan and Deshpande, 2017). Feofilova (2010) extensively reviewed the contributions of the structural and matrix components of fungal cell walls, such as chitin/chitosan, glucans, proteins, lipids, uronic acids, etc, reporting that, for isolation of CT, the chemical treatments used are milder than that as reported for marine sources.

Figure 7.1 Mushroom by-products and nonconforming mushroom bodies, not currently utilised for human consumption.

The most common procedure for obtaining Cs is based on the alkaline deacetylation of CT with strong alkaline solution at high temperature (Castelli *et al*., 1996), while other procedures include alkali treatment at high temperature and high pressure (autoclave) (Abdou *et al*., 2008), and enzymatic N-deacetylation (Martinou *et al*., 1995). Recently, microwave irradiation as a non-conventional energy source has received increasing attention in organic chemistry, due to its ability to accelerate reactions, provide high batch-to-batch consistency, scalability and to increase the yield of product, in comparison to conventional heating (Singh, Kumar and Sanghi, 2012). By exploiting the rapid energy transfer from the functional groups (-OH and -NH_2 groups) during dielectric heating using microwave energy, the reaction rate can be greatly enhanced, allowing for rapid breakage of covalent and glycosidic linkages between the glucosamine residues and thus faster production of Cs (Wasikiewicz and Yeates, 2013). Sagheer *et al.*, (2009) studied the production of Cs from crustacean sources using microwave irradiation and found the reaction time was significantly reduced (15 min vs 10 hr), in addition to producing Cs with DDA and MW values higher than those of Cs produced by conventional methods.

A particularly interesting application for Cs is its employment as a permeation enhancer (PE) for enhanced delivery of biopharmaceuticals, that are generally labile, large, hydrophilic and usually require parenteral administration (Boateng, Okeke and Khan, 2015). Oral delivery, considered the "gold standard" drug delivery method (in terms of patient compliance and reduced adverse effects related to injections) is an often sought-after alternative to methods such as inhalation or parenteral delivery (Gleeson, Ryan and Brayden, 2016). The limitation of delivering hydrophilic dugs orally arises from the low permeability of the epithelial barrier, as a result of which they must rely on active transport across the barrier, or passive transport between

adjacent cells through the paracellular pathway, known as tight junctions (TJs), present in the mucosal membrane (Upadhyay, 2014). Polymeric PEs, such as Cs, have been studied to enable the safe passage of drugs with low bioavailability. However, the pKa of 6.5 of Cs, and its low solubility, limits its application as a PE for mucosal surfaces when the pH is above 6.5 (Sonia and Sharma, 2011).

N-trimethyl chitosan (TMC) is a quaternary derivative of Cs, in which partial trimethylation of the primary amine results in a permanent, pH independent positive charge and thus aqueous solubility at neutral pH. The degree to which TMC can act as a PE has varied in a number of reports, partially due to differences in the physicochemical properties of the Cs precursor (Benediktsdóttir, Baldursson and Másson, 2014). The structure of TMC can vary in O-methylation, DA%, degree of trimethylation (DQ) and MW and often, the potential mechanism of action for TMC as a PE, is suggested to be a consequence of mucoadhesion, arising from charge interactions between polymer and mucosal membrane (Mourya and Inamdar, 2009). Furthermore, it has been postulated that TMC can be used for the enhancement of antigen delivery for vaccines via nasal delivery, due to the increased interaction of the antigen with the epithelial cell barrier and thus increased antigen uptake (Amidi *et al.*, 2010).

To date, a vast number of researchers have derived TMC from commercially available Cs derived from crustacean sources (Xu *et al.*, 2010). Yet, to the best of our knowledge, none have synthesised TMC from Cs of fungal origin, which presents an opportunity that may address the variations typically associated with crustacean TMC products. Fungal Cs (fCs) offers several advantages over its crustacean counterparts, owing to the highly controlled environments in which it is cultivated, year-round

growth that is not seasonally dependant and significantly less heavy metal association than that of crustaceans (Muzzarelli *et al.*, 2012). In this context, production and purification of CT from the cell walls of waste fungal mycelium, and its subsequent derivatisation to Cs and TMC, offer the advantage of being environmentally friendly with potential for a more consistent product.

As such, the aim of this study was to extract CT from the edible basidiomycete mushroom *A. bisporus* and to produce Cs with the same properties (DDA%, MW and purity) to that of PROTASAN™ UP (CL113), a commercially available fungal sourced Cs from Sigma Aldrich was also compared to the Cs produced in this work, as an additional reference check point.

Following production of fCs with a satisfactory match to CL113, a further chemical modification to TMC was performed to assess whether fungal derived TMC may offer potential use as a PE and as an alternative to crustacean derived. The permeation enhancing properties of this new fTMC were tested.

7.2 Materials and Methods

7.2.1 Materials

PROTASAN™ UP (CL113) was purchased from NovaMatrix, FMC Corporations, Norway. Commercial CT (SACT) and Cs from fungal origin (SACs) was purchased from Sigma Aldrich. Ireland. Acetic acid, ACS reagent, ≥99.7%, sodium hydroxide solution 50 wt % in H_2O, hydrochloric acid (HCL) 37 wt % in H_2O were purchased from Fisher Scientific, Ireland. All other reagents, chemicals and solvents were of analytical grade from Sigma Aldrich, Ireland. Deionised water (dH_2O) ≥18 MΩcm was obtained using Millipore Simplicity® Water Purification System and used for all manipulations unless otherwise specified.

7.2.2 Preparation of Mushroom Samples

A. bisporus samples were sourced from Tyholland Farm, Monaghan Mushrooms. Mushroom bodies were freeze-dried, ground to a powder, sieved through a 500 uM sieve and stored in a desiccator at room temperature for further analyses and extraction. Extraction of CT was preformed according to the protocol of Sagheer *et al.*, (2009), with the following modifications. Dried mushroom powder (DMP) (10 g), was suspended in NaOH (1 M, 300 mL) to give a final weight to volume ratio of 1:30. The resultant slurry was then heated in a thermostatic chamber (80 °C) and agitated at 120 rpm for 1.5 hr, thrice, to extract proteins, alkali soluble polysaccharides, and small molecules (e.g. monosaccharides, phenolics, amino acids, and salts). The slurry was then centrifuged at 5,500 rpm, for 20 min at 4 °C, to obtain alkaline insoluble

material (AIM). The supernatant was discarded and the pellet subjected to the previous digestion conditions (80 °C, 120 rpm for 1.5 hr). The AIM was then centrifuged (5500 rpm, 20 min, 4 °C) and the pellet washed to neutrality (pH 7-7.4) extensively by H_2O. Once neutral, the AIM was washed twice with boiling absolute ethanol (30 ml), resuspended in dH_2O and freeze dried for approximately 36 hr (FreeZone 6 L bench top freeze dry system (Labconco, USA)). The weight of the dried product was recorded and then it was ground to a fine powder.

7.2.2.1 Extraction of chitin from *A. bisporus*

To obtain insoluble, crude fungal CT, the AIM was refluxed in 5 % acetic acid (20 mL) for 6 h at 95 °C and then centrifuged at 10,000 rpm for 20 min at 4 °C. The resultant pellet was then washed with dH_2O and ethanol as described in 7.2.2. CT, if present, remained as an insoluble residue (crude CT), and was then freeze dried for approximately 36 hours. The weight of the dried product was recorded and then ground to a fine powder.

7.2.2.2 Chitosan preparation from crude CT

Two methods were employed to produce Cs, conventional and microwave derivatisation. For the conventional method, crude CT (250 mg) was suspended in concentrated KOH (50 mL, 45 w/v %) and heated on a boiling water bath under constant agitation for 3.5 hr. The solution was then centrifuged (10,000 rpm, 30 min, 22 °C) to obtain a pellet of Cs. The Cs pellet was then washed extensively with H_2O until pH 7-7.4 was achieved and lyophilised for approx. 36 hr. For the microwave method, crude CT (250 mg) was weighed into individual microwave vessels (EasyPrep™, CEM, UK) followed by the addition of NaOH (9 mL, 30% w/v). Vessels

were then placed under magnetic stirring for 30 min at 900 rpm to ensure homogenous distribution throughout the solvent. Samples were then subjected to microwave irradiation (MARS5, CEM, UK) for 15 mins, at 900 W followed by a 30 min cool down period. The resultant Cs was then centrifuged (5500 rpm, 20 min, 22 °C) and the pellet washed extensively until neutral pH was reached (7-7.4). The product was then freeze dried for approximately 36 hr and the dried weight recorded.

7.2.3 CT-Determination of the degree of acetylation via ^{13}C-NMR spectroscopy

Solid state ^{13}C-NMR is often used for quantifying and determining the degree of purity of carbohydrates, in particular CT and Cs (Heux *et al.*, 2000) and, as such, was applied to determine the purity and DA% of the CT samples extracted from *A. bisporus*. In the CT molecular structure, the amine group of the glucosamine residue is acetylated and consequently shows two additional resonances in the ^{13}C-NMR spectrum, one related to the carbonyl group at 175 ppm and the other one with the methyl group at 25 ppm. These two signals are very distinctive as they occur at both sides of the signals due to the backbone structure, making them easy to identify. Spectra were recorded using a procedure published Heux *et al.*, 2000 and the DA% calculated using equation 7.1:

$$\boldsymbol{DA}\ (\%) = \frac{\boldsymbol{AUC_{25}}}{\boldsymbol{AUC_{175}}} \times \mathbf{100}$$

(Equation 7.1)

where AUC_{25} relates to the methyl carbons on the glucosamine residue at 25 ppm and AUC_{175} the carbonyl carbons at 175 ppm (Heux, *et al* 2000).

7.2.4 Chitosan-Determination of the DDA% ^{1}H-NMR spectroscopy

DDA% of Cs samples were determined using a procedure published by (de Oliveira *et al.*, 2014) with the following modifications: Cs (100 mg) was suspended in HCl (10 mL, 0.07 M) at room temperature (RT) and left to stir at 800 rpm overnight. Sodium nitrate (15 uL, 1 M) was then added to the solution and then left to stir for four hours at RT. NaOH (1 M) was then added drop wise until pH 10 was reached and the Cs subsequently precipitated out. The Cs pellet was then recovered by centrifugation at 10,000 rpm for 15 min, washing extensively with dH_2O, lyophilising and ion exchanging with D_2O three times. The Cs sample (approximately 10 mg) was then transferred to a 2 mL Eppendorf and D_2O (1.96 mL) was added along with DCl (40 uL, 20% w/v). The solution was then left to agitate for 30 min to ensure full dissolution and was then transferred to a Colorspec™ NMR (Aldrich) tube for ^{1}H NMR analysis. Spectra were recorded on a Bruker Avance 400 spectrometer at 80°C after 128 scans with a delay time of 4 seconds. An elevated temperature was used, with the aim of shifting the HOD signal to a higher field, allowing for the quantification of the glucosamine residue H-1 signals. The DDA% was than calculated using Equation 7.2 (Lavertu *et al*. 2003):

$$\boldsymbol{DDA}\ (\%) = \frac{(\mathbf{1} - (\frac{\mathbf{1}}{\mathbf{3}}\boldsymbol{HAc})}{(\frac{\mathbf{1}}{\mathbf{6}}\boldsymbol{H26})} \times \mathbf{100}$$

(Equation 7.2)

where HAc corresponds to the methyl protons of the acetyl group and H26 represents the signal from protons H2, H3, H4, H5, H6, H6 of both monomers, through use of the integral peak intensity values (Lavertu *et al*. 2003).

7.2.5 Fourier transform infrared spectroscopy (FTIR)

The FTIR spectrum of the extracted Cs was acquired via a Spotlight 400 series spectrometer (Perkin Elmer, USA), using the attenuated total reflectance spectroscopy method (ATR-FTIR), in the range of 650-4000 cm^{-1}. Prior to analysis, Cs samples were lyophilised -40 °C for 36 hrs. The dried Cs solids were then placed on the ATR crystal prism (ZnSe), and 32 scans were acquired at 4 cm^{-1} resolution with background subtraction.

7.2.6 Chitosan molecular weight determination: gel permeation chromatography (GPC)

For all samples, Cs solutions (4.0 mg/mL) were prepared by direct dissolution in mobile phase (acetate buffer: 0.15 M acetic acid:0.1 M sodium acetate:0.2 mM sodium azide) by agitating at 300 rpm, at room temperature for two days, and were then filtered with a syringe filter (0.45 μm, Millipore). Analyses were performed at room temperature using 2 X PL Aquagel-OH MIXED-H 8um 300 x 7.5mm columns (Agilent, UK), at a flow rate of 1 mL/min and a sample injection volume of 20 μL. GPC data was acquired using a Varian 350 refractive index detector coupled to a Varian 210 solvent delivery module. A calibration curve was made by using GPC dextran standards of known MW (25-670 kDa) at 2.0 mg/mL concentration.

7.2.7 Synthesis of trimethyl chitosan

During TMC synthesis, the number of positive charges on the polymer chain is increased (Synman, D. *et al*., 2002) through the addition of methyl groups to the primary amines present on Cs. The use of Iodomethane (MeI) and N-methyl-2-

pyrrolidinone (NMP) allows quaternisation through the nucleophilic substitution of the amine group with MeI and Sodium iodide (NaI). The N-quaternisation process depends on the concentration of NaOH used, the reaction time and the reaction steps. The initial TMC iodide salt is then dissolved in NaCl for exchange of iodide ions with chloride (Sieval, *et al*, 1998) (Figure 7.2). Once produced, TMC can be assessed for its ability to open cellular tight junctions (as determined in a transepithelial electrical resistance (TEER) assay) and thus infer its potential usefulness as a PE.

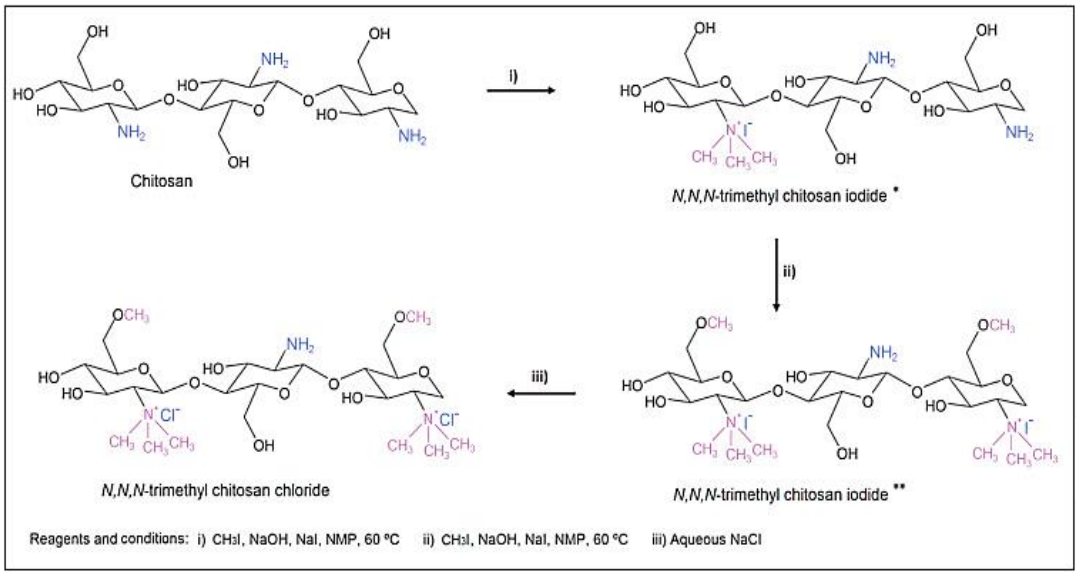

Figure 7.2 The synthesis of N-trimethyl chitosan (TMC).

TMC chloride was synthesised by methylation of fungal (fTMC) or commercial Cs (cTMC) with methyl iodide (MeI) in the presence of NaOH, as per Sieval *et al.*, (1998), with slight modifications. In detail, a mixture of Cs (1 g), sodium iodide (2.4 g) and NaOH (5.5 mL, 15 % w/v) in N-methylpyrrolidinone (NMP) (40 mL) was maintained in an oil bath under magnetic stirring at 60 °C for 30 min in the presence of a Liebig condenser. Then, MeI (5.75 mL) was added to the mixture and the reaction was continued for another 75 min. The product was then precipitated by the addition of ethanol and isolated by centrifugation at 4000 rpm, 4 ºC, for 5 min. The pellet was washed with diethyl ether, dried under vacuum and then resuspended in NMP (40

mL), at 60 ºC and stirred continuously until the product dissolved. Once dissolved, NaI (2.4 g), NaOH (5.5 mL, 15 % w/v) and MeI (3.5 mL) were added to the flask and the reaction was left to proceed for 30 min. MeI (2 mL) and NaOH (0.3 g) pellets were then added to the flask and the reaction was left to proceed for a further 60 min. The product was then precipitated by the addition of ethanol and isolated by centrifugation at (4000 rpm, 4 ºC, 5 min). Resultant pellets were then resuspended in an aqueous NaCl solution (10 % w/v), to exchange iodide for chloride ions and the product was reprecipitated with ethanol, isolated by centrifugation at (4000 rpm, 4 ºC, 5 min). The final product was dissolved in H_2O and centrifuged (5500 rpm, 4 ºC for 10 min) to remove insoluble material (such as demethylated Cs residues N-$(CH_3)_2$). The resultant supernatant was then dialysed against deionised water (changing buffer twice-daily) for 3 days and freeze dried for 36 hr to obtain white purified TMC powder.

7.2.7.1 Water solubility of fTMC and cTMC

Aqueous solubility of the different polymers (fTMC and cTMC) was determined in HPLC grade water (pH 7) solvent at room temperature. Samples were dissolved at concentrations ranging from 1-10 w/v %, and the transmittance of the solutions at 500 nm was measured on an UV/VIS spectrophotometer (TECAN GENios, Grodig, Austria). The polymers were considered insoluble when the transmittance was less than 90% compared to the transmittance of the solvent (Verheul *et al.*, 2008).

7.2.8 Determination of the degree of quaternisation and O-methylation by ^{1}H-NMR

To determine the degree of quaternisation (% DQ) and O-methylation (OMe) the ^{1}H NMR spectrum of TMC was measured in D_2O, using a 400 MHz spectrometer

(Bruker-Biospin, Rheinstetten, Germany) at 80 °C. The % DQ and OMe was calculated by the following equations (Zarifpour 2013):

$$\boldsymbol{DQ = \frac{[(CH_3)_3]}{[H]} \times \frac{1}{9} \times 100\%}$$

(Equation 7.3)

$$\boldsymbol{OMe = \frac{[(CH_3)]}{[H]} \times \frac{1}{3} \times 100\%}$$

(Equation 7.4)

where DQ is the degree of quaternisation, in mole percentage of free amine, $[(CH_3)_3]$ is the integral of chemical shift of the hydrogens of trimethyl amino groups at 3.3 ppm, $[(CH_3)]$ the methylated hydroxyl groups at either 3.4 (OMe-6) or 3.5 (OMe-3) ppm and [H] is the integral of H-1 peaks between 4.7 and 5.7 ppm, related to hydrogen atoms bound to carbon 1 of the Cs molecule, which is taken as the reference signal.

7.2.9 Transepithelial electrical resistance (TEER) measurements

Caco-2, human colon adenocarcinoma cell lines, are regarded as representative of the small intestine (Brayden, Cryan, *et al.*, 2015; Gleeson *et al.*, 2015). When they are grown on semipermeable filters, they spontaneously differentiate in culture to form confluent, polarised, columnar cell monolayers (Woitiski *et al.*, 2011). Therefore, they have widely been selected as an *in vitro* model for evaluation of intestinal drug absorption (Maher, Mrsny and Brayden, 2016). Caco-2 cells were seeded at a density of $6x10^5$ cells per well on 12-transwell plates with a microporous membrane. The cells were cultured in Dulbecco's Modified Eagle's Medium (DMEM) supplemented with L-glutamine (1%), Penicillin and streptomycin (PEST) (1%), non-essential amino acids (1%) and foetal bovine serum (10%), for 21 days until a confluent cell layer was formed. The medium was replaced by Hank's Balanced Salt Solution (HBSS) at the

basolateral side and left to equilibrate for 1 hr before the start of the experiments. Then, 0.5 ml solution of TMC (0.1 w/v), derived from commercial Cs (cTMC) or fungal Cs (fTMC), was applied at the apical side of the cell monolayers. Sodium caprate (0.1 % w/v) was used as positive control and Hanks balanced salt solution (HBSS) as reference. The resistance of the membrane, measured without cells, was used as blank. The TEER of the Caco-2 cells was measured with an Epithelial Voltammeter (EVOM - World Precision Instruments Inc, USA), using the chopstick method (Verheul *et al.*, 2008), at certain time points (0, 10, 30, 60 90 min and 120 min) after addition of the stimuli. After 90 minutes, the cells were washed with HBSS and incubation of the cells was continued in DMEM for 24 hrs at 37 °C, CO_2 5% to determine the recovery of the TEER.

7.3 Results and Discussion

7.3.1 Percentage yield of chitin and chitosan

The CT in cultivated *A. bisporus*, is a stable characteristic of the species and there are no significant differences between the CT content of pileus (cap) and stipes (stalk) of fruiting bodies (Vetter, 2007). In this work, CT was found to account for 6.6 ± 2.2 % of the DMP (Table 7.1), consistent with the observations of Vetter, (2007), who found that 6.68 and 7.25 % of *A. bisporus* pileus and stipes, respectively, existed as CT.

After extraction of CT from the DMP used in this study, two derivatisation methods were employed to produce Cs, which were conventional, and microwave assisted (Section 7.2.2). As can be seen in Table 7.1, a significantly higher yield of Cs was obtained for microwave derived Cs (55%) vs conventional (33%). Moreover, the microwave method entails more than half the reaction time of conventional (45 min vs 3.5 hr). The lower yield recovery from the conventional method may be attributable to the highly basic solvent (KOH 45 w/v %) and the long reflux time (3.5 hr), causing depolymerisation of the CT backbone (through hydrolysation of the amide bond of N-acetylglucosamine) allowing for its subsequent loss during the washing process (Anwar, Anggraeni and Amin, 2017).

Table 7.1 Yield and composition of material obtained during extraction of chitinous material from *A. bisporus* samples. [a]CT yield expressed as percent of DMP, [b]Cs yield expressed as percent of CT, [c]Cs conventionally derived, [d]Cs microwave derived.

Sample	Yield[a] (%)	Yield[b] (%)
DMP	100	-
AIM	25 ± 4.7	-
CT	6.6 ± 2.2	100
[c]Cs	-	33.3 ± 6.8
[d]Cs	-	55.4 ± 5.6

In contrast to the applied, relatively simple and fast method for producing pure fCs with microwave irradiation described in this work, the more common extraction of Cs from crustaceans requires higher concentrations of sodium hydroxide at high temperature and, in general, the whole procedure is costlier and time consuming (Tajdini *et al.*, 2010). Therefore, the fungi could be considered as a good alternative source of Cs.

7.3.2 ^{13}C-NMR -Chitin DA% determination

Figure 7.3 shows the ^{13}C-NMR spectrum of the fungal CT, which exhibits eight main peaks: sharp peaks at 173 and 22 ppm were assigned to the carbonyl and methyl carbons, respectively; the peaks at 103, 82, 74, 72, 59 and 54 ppm were ascribable to the resonances of C1, C4, C5, C3, C6, and C2 on the N-acetyl-D-glucosamine unit of CT, respectively, also illustrated in Figure 7.3. The DA% of the extracted CT was then calculated using the relative integrals of methyl or carbonyl groups related to the carbon integrals of the polysaccharidic backbone (Equation 7.1,) and compared with the commercial CT purchased from Sigma Aldrich (Table 7.2).

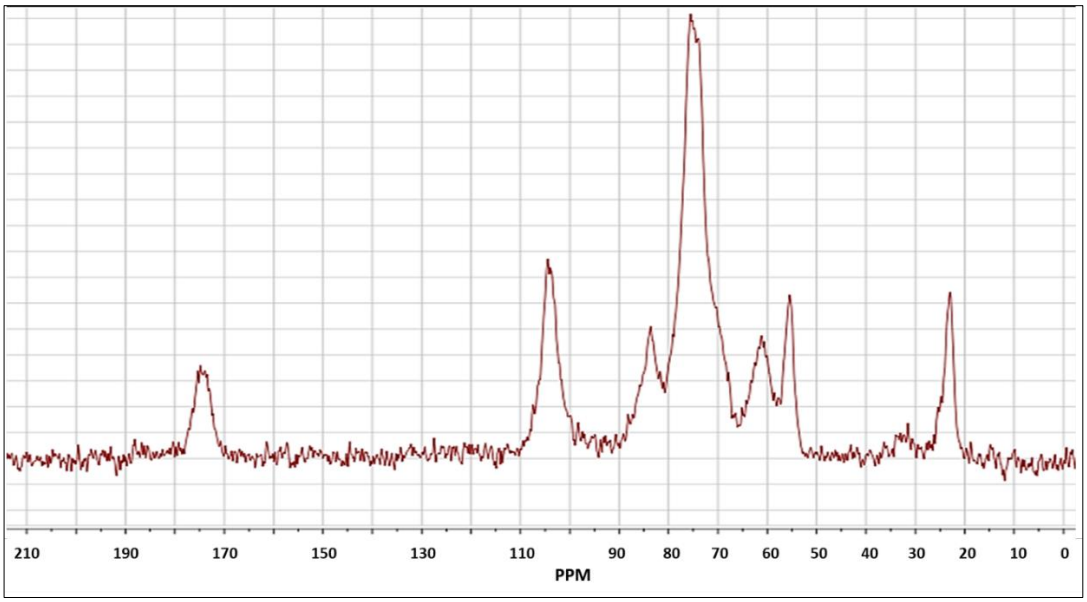

Figure 7.3 Solid state ^{13}C-NMR Spectra of CT extracted from *A. bisporus*.

Well resolved, high purity spectra were observed for both commercial and extracted CT, both having a DA of around 100%. No significant difference in DA was observed between the commercial and extracted CT in this work (Table 7.2), and the high degree to which it is acetylated indicates that the CT produced is a suitable candidate for further derivatisation.

Table 7.2 DA% of extracted CT and SACT, calculated as per Equation 7.1.

Sample	**DA (%)**
SACT (commercial)	96 ± 4.5
CT (extracted)	101 ± 5

Extracted CT was also assessed to establish the crystalline form (α, β or γ) that was present in the *A. bisporus* sample. The α form has chains arranged alternately antiparallel; the β form has all chains parallel, while γ-CT is considered a form of α CT with alternating parallel and antiparallel chains (Figure 7.4 (Kumirska *et al.*, 2011)). It has been shown that β-CT is much more amenable to deacetylation than the α form (Abdou, Nagy and Elsabee, 2008), which is useful when trying to increase the DDA% in order to attain requisite Cs properties for a given application. Notably, the

signals assigned to C3 and C5 of the CT powder existed as a single peak, inferring that the CT extracted from *A. bisporus* was in the β crystal form (Duan *et al.*, 2013). β-chitin has the unique feature of incorporating small molecules, including water, into its crystal lattice to form crystalline complexes (Li, Revol and Marchessault, 1999) and thus is more easily hydrated and soluble in water (Wan and Tai, 2013) The weaker hydrogen-bonding from the parallel-chain structure of β-chitin may account for its higher chemical reactivity (Kurita *et al*., 2005).

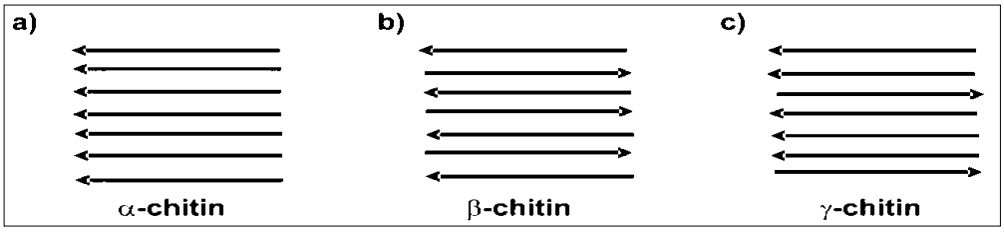

Figure 7.4 Schematic representation of the three polymorphic forms of CT (a) α-CT. (b) β-CT. (c) γ-CT (adapted from Kumirska, Mirko X. Weinhold, *et al*. 2011).

7.3.3 ^{1}H-NMR -Chitosan DDA% determination

Figures 7.5 and 7.6, show the ^{1}H-NMR spectrum of *A. bisporus* Cs, conventionally and microwave derived, respectively. The peak present between 2.0-2.5 ppm represents the methyl protons of the N-acetyl-glucosamine unit (Ac) and the peak between 3.2-3.6 ppm denotes the H-2D proton of the glucosamine (H2, D) residues (Hirai, Odani and Nakajima, 1991). Similar chemical shifts are observed for the non-anomeric protons (H2-H6, A and H3-H6, D) connected to the polymer backbone, due to their similar electron densities, resulting in their signals partially overlapping, causing a broad envelope of signals within the middle of the spectrum, in the range of approximately 3.78-4.32 ppm (Kasaai, 2010). Lastly, the anomeric protons can be seen at higher chemical shifts (approx. 5.33 and 5.01 for H1,D and H1,A respectively)

(Lavertu *et al.*, 2003), attributable to their deshielding glycosidic and ring oxygen neighbours. Additionally, these proton bands possess the least resolution in the ^{1}H-NMR spectra, followed by H3, H4, H5, and H6, while, in contrast, the methyl protons retain the highest resolution of all peaks (Kasaai, 2010).

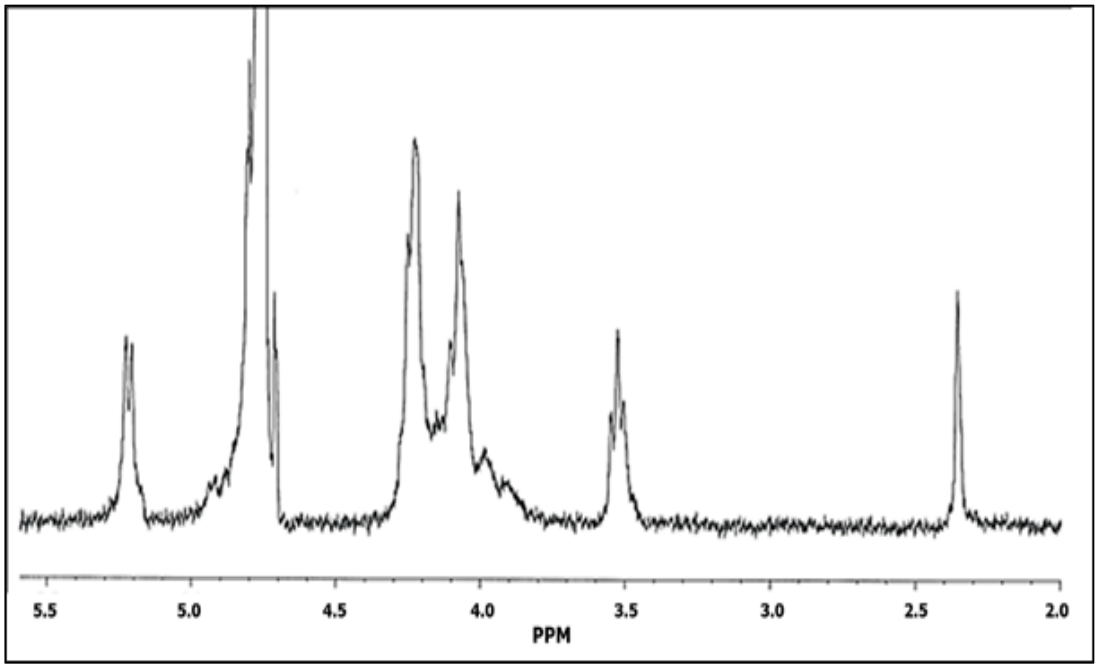

Figure 7.5 ^{1}H-NMR spectra of *A. bisporus* Cs (conventional extraction) at 80°C in DCl 2 wt % in D_2O.

Table 7.3 details the ^{1}H-NMR calculated DDA% of the commercial chitosans (SACs and CL113), which were found to be 85±4% and 81±4.5% respectively. The Cs conventionally derived from the *A. bisporus* was found to have a similar DDA% of 75±6%, in comparison to the microwave extracted (86 ± 6) and, in addition, showed less peak resolution than the microwave Cs samples. This may be attributed to the fact that CT typically exists with associated minerals and proteins that may contain C=O and NH functional groups, similar to those found in Cs (Brugnerotto *et al.*, 2001).

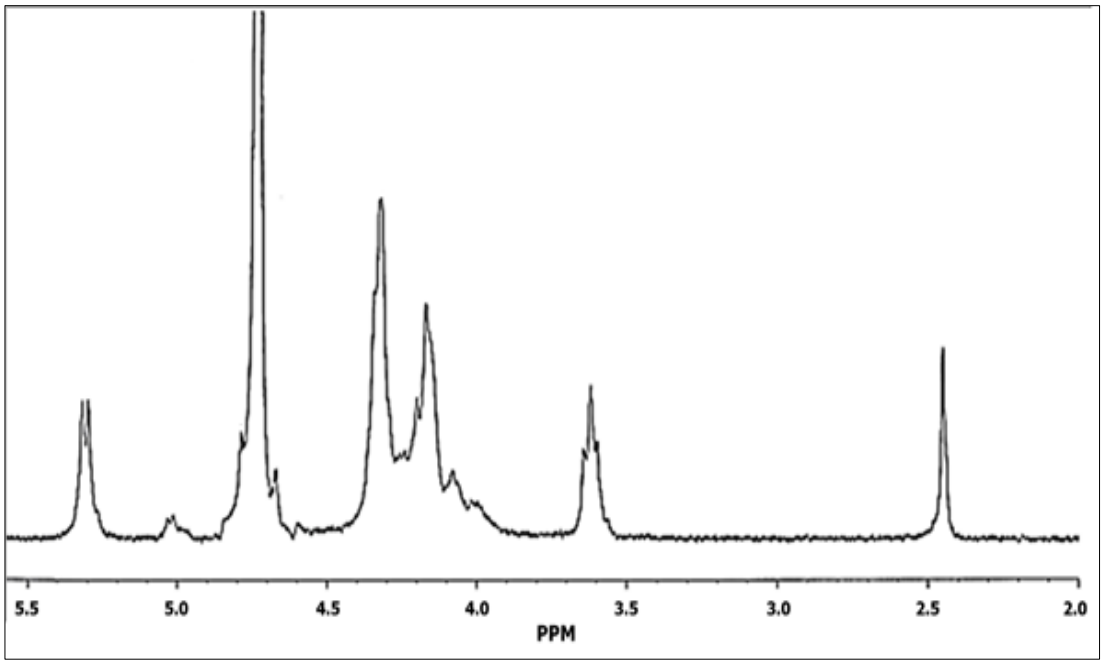

Figure 7.6 ^{1}H-NMR spectra of *A. bisporus* Cs (microwave extracted) at 80°C in DCl 2 wt % in D_2O.

Contamination of Cs with impurities such as these may have contributed to the creation of interference peaks (in addition to change in position and intensity of the signal bands (Brugnerotto *et al.*, 2001; Kasaai, 2010) and the conventional method may not possess the full capacity to remove these impurities. This is evident in the ^{1}H-NMR spectrum of the conventionally derived Cs (Figure 7.5), in which the signal of the H1-A proton appears to have been overlapped by the solvent peak at approximately 4.82 ppm and all other proton signals have been shifted slightly upfield compared to those of the microwave Cs samples (Figure 7.6). Furthermore, the fast and direct heating of reactants using microwave irradiation has been reported to not only give higher yields, but to improve the purity of the desired products (Singh, Kumar and Sanghi, 2012), as reflected in the ^{1}H-NMR observations for microwave derived Cs (Figure 7.6), whereby the H1-A proton is well resolved at 5.1 ppm. Due to the reduction of chemicals usage, reaction time and significantly higher DDA%,

purity and yields (Section 7.3.1) of Cs obtained via microwave derivatisation, it was selected for use in the experiments from this point on.

Table 7.3 DDA% of SACs, CL113 and Cs extracted by conventional or microwave method, calculated as per Equation 7.2.

Sample	DDA (%)	Derivatisation method
SACs	81 ± 4.5	-
CL113 (NovaMatrix)	85 ± 4	-
Cs (*A. bisporus)*	75 ± 6%	Conventional
Cs (*A. bisporus*	86 ± 6	Microwave

7.3.4 FTIR analysis of extracted chitin and chitosan

The structure of the extracted Cs was confirmed by FTIR analysis (Figure 7.7). Table 7.4 provides a comprehensive list of all FTIR spectral bands observed in both commercial and extracted Cs and CT samples; it is worth noting the key peaks associated with the analysis of both compounds, for example the characteristic peak at ≈1550 cm^{-1} that is present in Cs (due to the presence of the primary amine on the D-glucosamine unit) but not in CT.

CT was examined via FTIR (denoted A and B in Figure 7.7) in order to establish the crystalline form (α, β or γ) that was present in the *A. bisporus* sample. Typically, α-CT shows two characteristic bands between ~1660-1620 cm^{-1} (amide I splitting), whereas β-CT displays one band in the amide I region only (Jang *et al.*, 2004). As can be seen, neither commercial or extracted CT displayed peak splitting in the amide I region and, as such, were determined to be in the β crystal form (Raafat and Sahl, 2009), further corroborating the ^{13}C-NMR observations (Section 7.3.4).

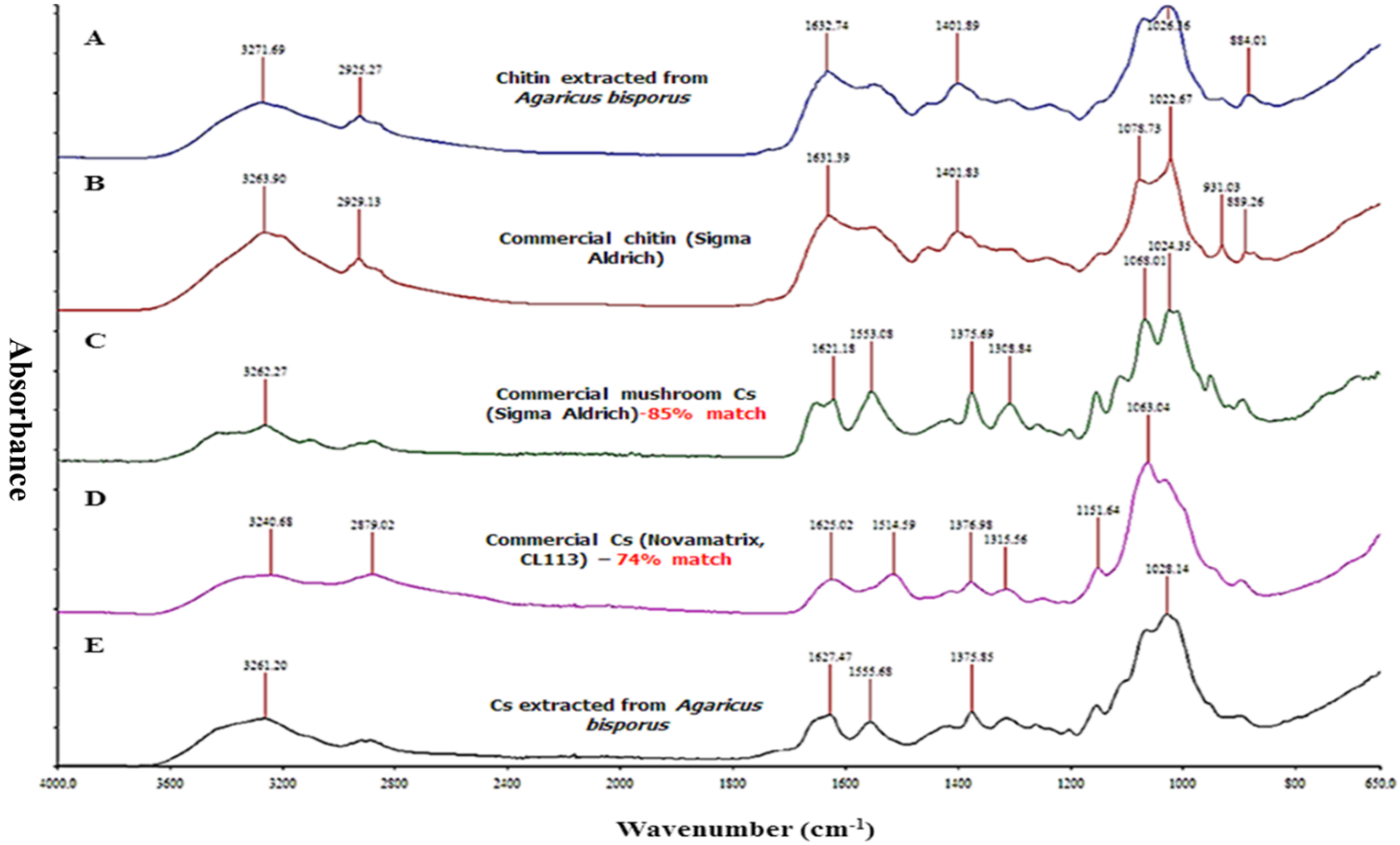

Figure 7.7 IR spectra (off set for clarity) of CT and Cs obtained from, A; CT extracted from *A. bisporus*, B; Commercial CT (Sigma Aldrich), C; Commercial SACs (Cs, Sigma Aldrich), D; Commercial Cs (NovaMatrix, CL113), E; Cs extracted from *A. bisporus*.

Table 7.4 FTIR bands observed in A; CT extracted from *A. bisporus*, B; Commercial CT (Sigma Aldrich), C; Commercial SACs (Cs, Sigma Aldrich), D; Commercial Cs (NovaMatrix, CL113), E; Cs extracted from *A. bisporus*.

Wavenumber (cm^{-1}) frequency					
Figure 7.7	**A**	**B**	**C**	**D**	**E**
Sample	*A. bisporus* CT	SA CT	SACs	CL113	*A. bisporus* Cs
Bond Assignment	**cm^{-1}**	**cm^{-1}**	**cm^{-1}**	**cm^{-1}**	**cm^{-1}**
NH Stretch, amine OH in pyranose ring	3271	3263	3262	3240	3261
CH_2 in CH_2OH group	2925	2929	*	2879	*
C=O in $NHCOCH_3$ group (amide I band)	1632	1631	1621	1625	1627
NH_2 in $NHCOCH_3$ group (amide II)	*	*	1553	1514	1555
CH_2 ending and CH_3 deformation	1401	1401	*	*	*
CH_3 in $NHCOCH_3$ group	*	*	1375	1376	1375
CH in pyranose ring	*	*	1308	1315	*
C-O-C (glycosidic linkage)	*	*	*	1151	*
C-O-C (glycosidic linkage)	*	1078	1068	1063	*
C-O in secondary OH group	1026	1022	1024	*	1028
C-O in primary OH group	*	931	*	*	*
Pyranose ring skeletal vibrations	884	889	*	*	*

*not observed

Regarding Cs analysis, the spectra of all samples analysed (denoted C, D and E in Figure 7.7), both commercial and extracted, showed a broad absorption band in the range 3240 cm^{-1}- 3271 cm^{-1} which is attributed to stretching vibrations caused by the primary amine and pyranose ring hydroxyl groups (Kaya *et al.*, 2014; Rumengan *et al.*, 2014). Key characteristic bands such as amide I band at 1620 cm^{-1} (carbonyl (C=O)) and amide II at 1550 cm^{-1} (amine (NH_2 tensions) were also observed, which is in agreement with literature findings (Abdou, Nagy and Elsabee, 2008; Kaya *et al.*, 2014). The peaks around 2879, 1375 and 1068 cm^{-1} in the FTIR spectrum are due to the stretching vibrations of aliphatic C– H, Amide III and C–O–C bonds, respectively, and are the main characteristics of the Cs polysaccharide (Kaya *et al.*, 2014; Rumengan *et al.*, 2014). Furthermore, FTIR spectral similarities between, SACs, CL113 and chitosan produced from the *A. bisporus* samples in this work displayed a correlation percentage of 85.31% and 74.93% respectively (Figure 7.7).

7.3.5 Molecular weight determination

MW is another important physical property of Cs and is typically determined via viscosity measurements or gel permeation chromatography (GPC) (Baxter *et al*. 2005; Zielinska *et al*. 2014). The size range of fungal derived Cs has been reported as 17-450 kDa by various authors (Miyoshi *et al*. 1992; Niederhofer & Müller 2004; Badawy & Rabea 2009). In terms of determining what size of Cs to use for a given application, low MW Cs is considered to be 10-90 kDa, medium MW in the range of 90-310 kDa and high MW 310-375 kDa (Zappino *et al*. 2015; Lal *et al*. 2012). In this work, GPC was employed to determine the MW of CL113, SACs, fCs and fTMC, and all tested compounds fell within the medium MW range (Table 7.5).

Table 7.5 MW (kDa) of CL113, SACs, fCs and fTMC as determined by GPC, means that do not share a letter are statistically different ($p < 0.05$).

Sample	CL113	SACs	fCs	fTMC
MW (kDa)	110.1 ± 5.9^{a}	$165.5 \pm 39.9^{a,b}$	156.3 ± 23.6^{b}	198.8 ± 16.6^{c}

It was observed that the MW of the produced fCs was significantly higher than that of CL113 (156 vs 110 kDa). Additionally, there was a larger spread of variation in the extracted fCs vs the CL113 (±24 vs ±6) respectively. This is expected, as CL113 is certified to possess a MW of 110-150 kDa and as such is most likely fractionated before sale in order to meet this requirement. Additionally, it has previously been shown that Cs produced via microwave heating tends to have a higher molecular weight than conventionally derived Cs (Sagheer *et al.*, 2009) and this may also be an attributing factor to the higher MW. A strategy to match the fCs further with CL113 in terms of MW would be to depolymerise the chain with $NaNO_2$ (Mao *et al.*, 2004) and subsequently fractionate it with semi-preparative GPC (Nguyen, Winnik and Buschmann, 2009). However, as medium molecular weight Cs, intended for use as a drug delivery vehicle, is considered ideal (Bowman and Leong, 2006), the fCs can be considered acceptable for use in future NP formulations. Interestingly, the commercial SACs was found to possess the highest MW in addition to the largest spread of variation (165±39 kDa) and although this product has not been sold as an ultrapure, highly characterised, Cs, it is worth noting for other researchers, considering its employment in various applications. Lastly, the MW of the fCs was found to increase after synthesis to TMC, which was expected due to the addition of methyl groups to the free amine residues of the Cs backbone (Verheul *et al.*, 2008).

7.3.6 TMC solubility

Table 7.6 shows the water solubility of the synthesised TMCs (derived from CL113 or fungal Cs extracted from *A. bisporus*), both with and without centrifugal purification (Section 7.2.7). As can be seen, a significant improvement in both cTMC and fTMC aqueous solubility (1 vs 10 %, at pH 7) was observed by employing the centrifugal clean up step (Section 7.2.7). This is an expected result, as any residual, insoluble, O-methylated (OCH_3) and dimethylated $(CH_3)_2$ amines would be removed from the final product, thus increasing solubility (Verheul *et al.*, 2008).

Table 7.6 Results of Solubility of Synthesised TMC.

	Non-Purified		**Purified**	
Conc. (%w/v)	**fTMC**	**cTMC**	**fTMC**	**cTMC**
1%	+	+	+	+
2%	-	+	+	+
4%	-	-	+	+
6%	-	-	+	+
8%	-	-	+	+
10%	-	-	+	+

Interestingly, without the clean-up step, cTMC showed solubility up to 2 % w/v, whereas fTMC to only 1 w/v %, most likely attributable to the higher MW of the fCs, which plays an important role in the solubility of the final product, whereby typically, the lower the MW, the higher the solubility (Sajomsang *et al.*, 2010).

7.3.7 ^{1}H-NMR - TMC DQ % determination

Several studies have been performed to determine the optimal DQ% for solubilising TMC in neutral aqueous media and for the trans epithelial delivery of low molecular weight drug molecules and/or proteins (Mourya and Inamdar, 2009; Vongchan *et al.*, 2011; de Britto *et al.*, 2012). For TMC to be soluble in neutral aqueous solvents, it is requisite that

the DQ% be ≥ 28 % and, for trans epithelial delivery of both low molecular weight compounds and proteins, a DQ% of about 40-50% is generally accepted to be optimum (Benediktsdóttir, Baldursson and Másson, 2014). In this work, the calculated DQ% (Equation 7.3) of fTMC and cTMC was found to be 45 ± 6 and 40 ± 4 respectively (Table 7.7) and repeated experiments showed good reproducibility, inferring the suitability of the synthesised polymers to serve as absorption enhancers.

Table 7.7 Degree of quaternisation (DQ %) calculated as per Equation 7.3 and 7.4.

Sample	DQ (%)	OMe-6	OMe-3
fTMC	45 ± 5.5	25 ± 6.5	18 ± 4.0
cTMC	40 ± 3.5	21 ± 2.5	15 ± 2.0

In this work, chitosan was methylated with methyl iodide to yield TMC (Figure 7.2) and the ^{1}H NMR spectrum of the fTMC polymer is presented in Figure 7.8. The amino groups in the C-2 position of Cs were methylated to form quaternary amino groups with fixed positive charges on the repeating units of the TMC polymer chain. According to the results of previous studies (Domard *et al.*, 1987; Sieval *et al.*, 1998), the peak at 3.8 ppm, that was not detected in the ^{1}H NMR spectrum of Cs (Figure 7.5 and 7.6), is attributable to the nine hydrogen atoms of the methyl groups pertaining to trimethylated amino groups, and the peaks between 4.9 and 5.9 ppm are assigned to the ^{1}H protons, which were taken as the reference signal.

An overview of the ^{1}H-NMR results of the O-methylated TMCs is presented in Table 7.7. Although O-methylation is a well-known side-reaction in TMC synthesis, that reduces the aqueous solubility of the product, there are relatively few studies that report the extent of this side reaction (Verheul *et al.*, 2008). The spectrum of fTMC synthesised showed O-methylation of the hydroxyl groups at the C-3 and C-6 of the glucosamine units (peaks observed at 4.0 and 3.9 ppm, respectively) showing that OMe-6 and OMe-3 were 25 and

18%, respectively (Equation 7.4). As the C-6 hydroxyl groups are less sterically hindered than the hydroxyl groups on the C-3, a higher degree of methylation is observed (Verheul *et al.*, 2008).

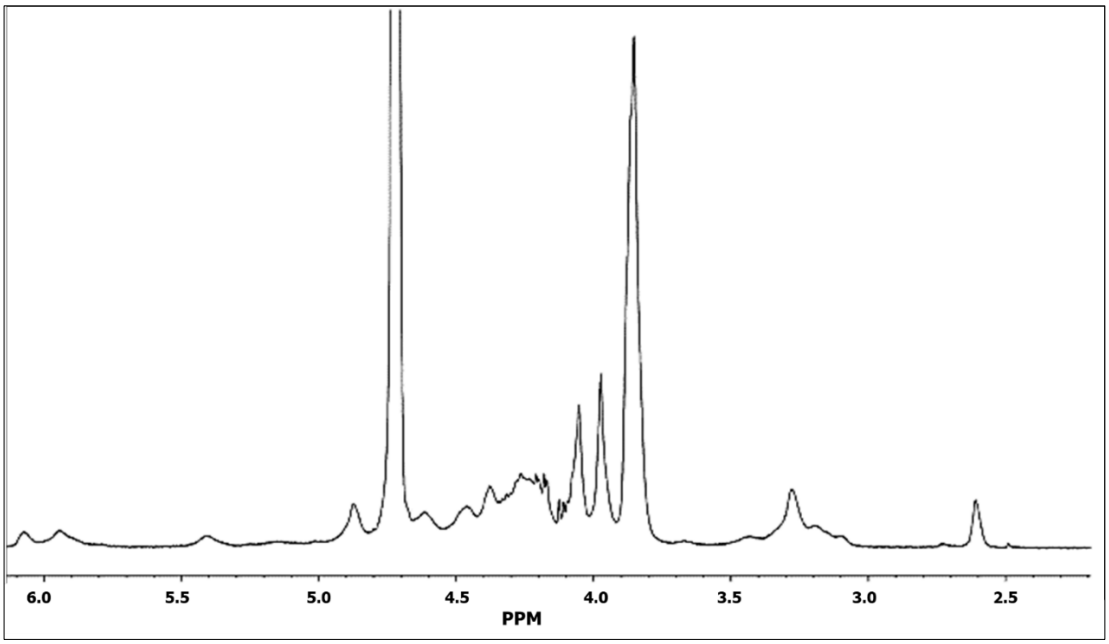

Figure 7.8 ^{1}H-NMR-spectra of fTMC with a DQ of approximately 45 % at 80°C in D_2O.

7.3.8 TEER -TMC as a permeation enhancer

TEER measurements for intestinal membrane models such as Caco-2 human colon adenocarcinoma cell monolayers can be used to predict their paracellular permeability. When the tight junctions (TJs) are open, the TEER of Caco-2 cell monolayers is significantly reduced due to the passing of ions via their paracellular route (Hidalgo, Raub and Borchardt, 1989). TEER has been applied to study the permeation enhancer (PE) effects of compounds such as polyacrylic acid, polycarbophil and TMC, over recent years (Aungst, 2000; Liu *et al.*, 2008; Maher, Mrsny and Brayden, 2016), the latter having been shown to exhibit a reversible time and dose dependant decrease, thus indicating its ability to open the TJs (Ranaldi *et al.*, 2002).

The initial studies in this work looked to compare the TEER measurements across Caco-2 cells incubated with fTMC and cTMC to the well-established PE, sodium caprate (C10) (Brayden, Gleeson and Walsh, 2014) at 0.1 % w/v, vs HBSS as reference (Figure 7.9).

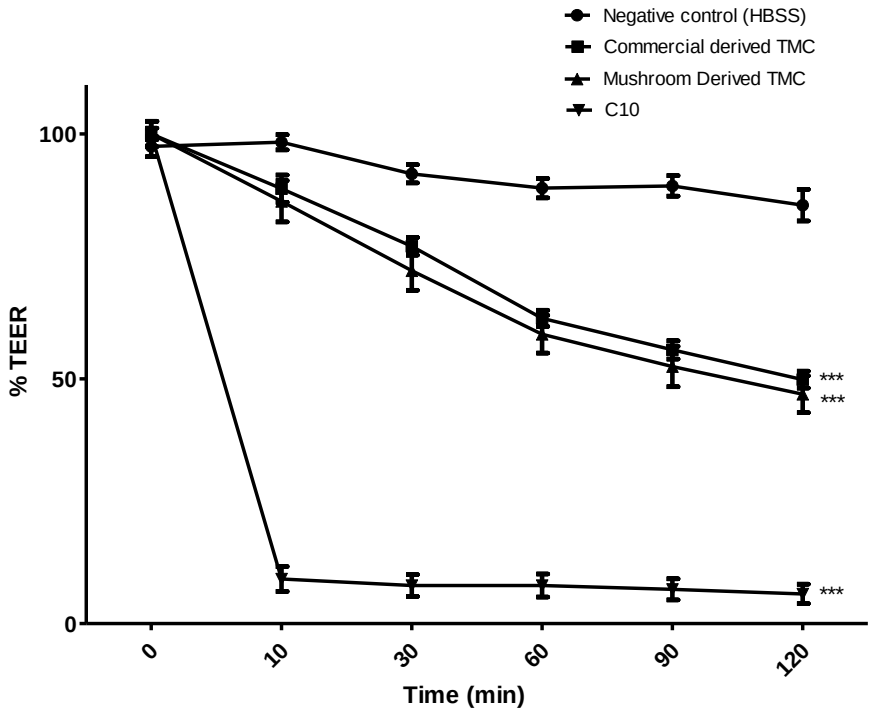

Figure 7.9 TEER assessment of commercial (cTMC) and fungal (fTMC) derived TMC (0.1% w/v) using C10 (0.1% w/v, 10mM) as a positive control. Error bars represent the standard deviation of six measurements.

It was observed that a significant reduction to TEER occurred for both TMCs vs HBSS alone, and no significant difference between cTMC and fTMC was apparent (50±4 % vs 47±6 %, respectively) at the test concentrations employed (0.1% w/v). It is has previously been shown that a decrease of TEER, to a value not exceeding 50% of the initial reference value (HBSS), is insufficient to permit paracellular transport of the marker substances (Borchard *et al.*, 1996). C10 at 0.1 % w/v (10 mM) comfortably achieved a reduction of TEER to 94±4% (Figure 7.9). However, as concentrations of C10 exceeding 10 mM have been shown to elicit substantial cytotoxicity (Gleeson *et al.*, 2015), it was decided to increase the TMC concentration for further investigation, whilst maintaining C10 (10

mM) as positive control. Additionally, as the ultimate goal of this work was to produce and assess fungal derived fTMC as a PE, it was decided that fTMC be solely evaluated for further investigation.

Figure 7.10 presents the TEER assessment of fTMC ranging from 0.2-0.6 % w/v. As can be seen, after 120 min incubation, the initial TEER value in Caco-2 cell monolayers incubated with fTMC, across all test concentrations, decreased by ≥ 75 %. This is consistent with reports from Kotzé *et al.*, (1998), whereby increased TMC concentrations (0.25-1.5 % w/v) lead to further decreases in TEER values, on Caco-2 monolayers. It has recently been reported that exposure of C10 at 10 and 12 mM to Caco-2 monolayers irreversibly reduced TEER ≈90% after 15 min (Brayden, Maher, *et al.*, 2015). The observations in this work are in line with those reported, as the greatest reduction in TEER was again observed for C10 (94 %). However, this decrease in TEER value may be attributable to a decrease in cell viability after long periods of incubation (Marušić *et al.*, 2013). To assess whether this was the case, all test compounds were removed from the monolayers after the 120 min exposure and replaced with DMEM to determine the recovery of the TEER after 24 hr. A recovery of TEER after the experiments would imply that the cells were undamaged and functionally intact and, as the results in Figure 7.10 shows, the TEER of the fTMC monolayer partially recovered after removal of the solutions (≥60 % of initial reference value), whereas that exposed to C10 did not (≈8 %).

It has also been proposed that, due to the high viscosity and adhesive nature of TMC, the reversibility of TEER decrease is gradual, owing to the fact that complete removal of the polymer prior to recovery is unlikely without incurring some damage to the cells (Borchard *et al.*, 1996; Verheul *et al.*, 2008).

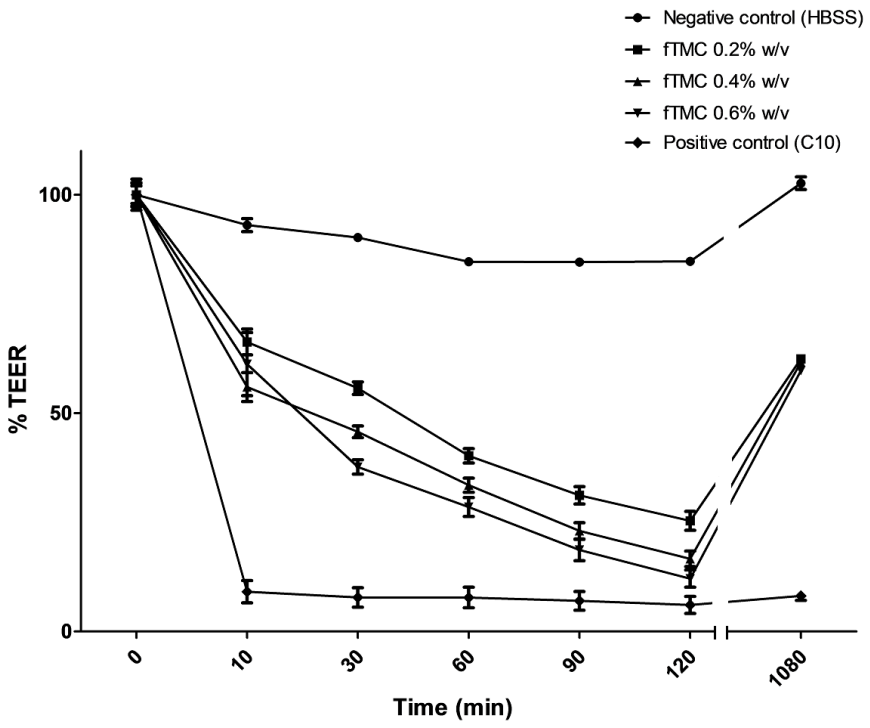

Figure 7.10 TEER assessment of fTMC concentrations (0.2-0.6 w/v %) on Caco-2 cell monolayers. C10 (0.1 % w/v) was used as a positive control. Error bars represent the standard deviation of six measurements.

It has been established that Cs unmodified or TMC with DQ% less than 18 % is unable to significantly reduce TEER. However, at DQ% of 40-60 %, a decrease in TEER of Caco-2 cells and increased mannitol permeation at pH 7.4 can be achieved (Amidi *et al.*, 2010). This study concluded that the prepared fTMC was capable of transiently and reversibly opening the tight junctions between Caco-2 cells and thus merits further investigation as a PE.

7.4 Conclusion

In this work, CT has been extracted from *A. bisporus* with equivalent purity and DA% to a commercial standard, as determined by ^{13}C NMR. The extracted CT was then derivatised to Cs, the optimum method for production being identified as microwave extraction. The Cs produced using this method showed equivalent purity and DDA% to that of commercial fungal Cs purchased from Sigma Aldrich and that of ultrapure CL113 from NovaMatrix, as identified by ^{1}H-NMR and FTIR spectroscopy. As Cs, a positively charged polyelectrolyte, has shown promising potential as a drug delivery vehicle, this may be an application for future use of the product. Lastly, fungal and commercial Cs were then chemically modified to TMC and assessed for permeation enhancing effects using TEER, showing its potential application as a PE. Based on the present knowledge identified in this work, *A. bisporus* can be considered as a good source of CT that can be easily isolated without aggressive treatments, subsequently deacetylated for the production of Cs and chemically modified to TMC, showing these by-products have potential use for many different practical applications.

7.5 References

Abdou, E. S., Nagy, K. S. a and Elsabee, M. Z. (2008) 'Extraction and characterization of chitin and chitosan from local sources', *Bioresource Technology*, 99(5), pp. 1359–1367.

de Alvarenga, E. S., Pereira de Oliveira, C. and Roberto Bellato, C. (2010) 'An approach to understanding the deacetylation degree of chitosan', *Carbohydrate Polymers*, 80(4), pp. 1155–1160.

Amidi, M. *et al.* (2010) 'Chitosan-based delivery systems for protein therapeutics and antigens', *Advanced Drug Delivery Reviews*, 62(1), pp. 59–82.

Anwar, M., Anggraeni, A. S. and Amin, M. H. Al (2017) 'Comparison of green method for chitin deacetylation', *AIP Conference Proceedings*, 1823.

Aranaz, I. *et al.* (2018) 'Cosmetics and Cosmeceutical Applications of Chitin, Chitosan and Their Derivatives', *Polymers*, 10(2), p. 213.

Aungst, B. J. (2000) 'Intestinal permeation enhancers', *Journal of Pharmaceutical Sciences*, 89(4), pp. 429–442.

Barikani, M. *et al.* (2014) 'Preparation and application of chitin and its derivatives: a review', *Iranian Polymer Journal*, 23(4), pp. 307–326.

Baxter, S., Zivanovic, S. and Weiss, J. (2005) 'Molecular weight and degree of acetylation of high-intensity ultrasonicated chitosan', *Food Hydrocolloids*, 19(5), pp. 821–830.

BCC research (2016) *Chitin and Chitosan Derivatives: Technologies, Applications and Global Markets*. Available at: https://www.bccresearch.com/market-research/plastics/chitin-chitosan-derivatives-markets-report-pls085a.html. (Accessed 15 Jan 2018)

Benediktsdóttir, B. E., Baldursson, Ó. and Másson, M. (2014) 'Challenges in evaluation of chitosan and trimethylated chitosan (TMC) as mucosal permeation enhancers: From synthesis to in vitro application', *Journal of Controlled Release*, 173, pp. 18–31.

Bernkop-Schnürch, A. and Dünnhaupt, S. (2012) 'Chitosan-based drug delivery systems', *European Journal of Pharmaceutics and Biopharmaceutics*, 81(3), pp. 463–469.

Boateng, J., Okeke, O. and Khan, S. (2015) 'Polysaccharide based formulations for mucosal drug delivery: A review', *Current Pharmaceutical Design*, 21(33), pp. 4798–4821.

Borchard, G. *et al.* (1996) 'The potential of mucoadhesive polymers in enhancing intestinal peptide drug absorption. III: Effects of chitosan-glutamate and carbomer on epithelial tight

junctions in vitro', *Journal of Controlled Release*, 39(2–3), pp. 131–138.

Bowman, K. and Leong, K. W. (2006) 'Chitosan nanoparticles for oral drug and gene delivery', *International Journal of Nanomedicine*, 1(2), p. 117.

Brayden, D. J., Cryan, S.-A., *et al.* (2015) 'High-content analysis for drug delivery and nanoparticle applications', *Drug Discovery Today*, 20(8), pp. 942–957.

Brayden, D. J., Maher, S., *et al.* (2015) 'Sodium caprate-induced increases in intestinal permeability and epithelial damage are prevented by misoprostol', *European Journal of Pharmaceutics and Biopharmaceutics*, 94, pp. 194–206.

Brayden, D. J., Gleeson, J. and Walsh, E. G. (2014) 'A head-to-head multi-parametric high content analysis of a series of medium chain fatty acid intestinal permeation enhancers in Caco-2 cells', *European Journal of Pharmaceutics and Biopharmaceutics*, 88(3), pp. 830–839.

de Britto, D. *et al.* (2012) 'N,N,N-trimethyl chitosan nanoparticles as a vitamin carrier system', *Food Hydrocolloids*, 27(2), pp. 487–493.

Brugnerotto, J. *et al.* (2001) 'An infrared investigation in relation with chitin and chitosan characterization', *Polymers*, 42(8), pp. 3569–3580.

Domard, A. *et al.* (1987) '13C and 1H n.m.r. spectroscopy of chitosan and N-trimethyl chloride derivatives', *International Journal of Biological Macromolecules*, 9(4), pp. 233–237.

Duan, B. *et al.* (2013) 'High strength films with gas-barrier fabricated from chitin solution dissolved at low temperature', *Journal of Materials Chemistry A*, 1(5), pp. 1867–1874.

Duarte, M. L. *et al.* (2002) 'An optimised method to determine the degree of acetylation of chitin and chitosan by FTIR spectroscopy', *International Journal of Biological Macromolecules*, 31(1), pp. 1–8.

Felt, O., Buri, P. and Gurny, R. (1998) 'Chitosan: a unique polysaccharide for drug delivery', *Drug Development and Industrial Pharmacy*, 24(11), pp. 979–993.

Feofilova, E. P. (2010) 'The fungal cell wall: modern concepts of its composition and biological function', *Microbiology*, 79(6), pp. 711–720.

Fernández-Gutiérrez, M. *et al.* (2015) 'Bioactive Chitosan Nanoparticles Loaded with Retinyl Palmitate: A Simple Route Using Ionotropic Gelation', *Macromolecular Chemistry and Physics*, 216(12), pp. 1321–1332.

Ghormade, V., Pathan, E. K. and Deshpande, M. V (2017) 'Can fungi compete with marine sources for chitosan production?', *International Journal of Biological Macromolecules*, 104, pp. 1415–1421.

Gleeson, J. P. *et al.* (2015) 'Stability, toxicity and intestinal permeation enhancement of food-derived antihypertensive tripeptides, Ile-Pro-Pro and Leu-Lys-Pro', *Peptides*, 71, pp. 1–7.

Gleeson, J. P., Ryan, S. M. and Brayden, D. J. (2016) 'Oral delivery strategies for nutraceuticals: Delivery vehicles and absorption enhancers', *Trends in Food Science & Technology*, 53, pp. 90–101.

Hamed, I., Özogul, F. and Regenstein, J. M. (2016) 'Industrial applications of crustacean by-products (chitin, chitosan, and chitooligosaccharides): A review', *Trends in Food Science & Technology*, 48, pp. 40–50.

Heux, L. *et al.* (2000) 'Solid state NMR for determination of degree of acetylation of chitin and chitosan.' *Biomacromolecules*, 1(4), pp.746-751.

Hidalgo, I. J., Raub, T. J. and Borchardt, R. T. (1989) 'Characterization of the human colon carcinoma cell line (Caco-2) as a model system for intestinal epithelial permeability', *Gastroenterology*, 96(3), pp. 736–749.

Hirai, A., Odani, H. and Nakajima, A. (1991) 'Determination of degree of deacetylation of chitosan by 1H NMR spectroscopy', *Polymer Bulletin*, 26(1), pp. 87–94.

Huang, Y., Cai, Y. and Lapitsky, Y. (2015) 'Factors affecting the stability of chitosan/tripolyphosphate micro- and nanogels: resolving the opposing findings', *Journal of Materials Chemistry B*, 3(29), pp. 5957–5970.

Jang, M. *et al.* (2004) 'Physicochemical characterization of α-chitin, β-chitin, and γ-chitin separated from natural resources', *Journal of Polymer Science Part A: Polymer Chemistry*, 42(14), pp. 3423–3432.

Kardas, I. *et al.* (2012) 'Chitin and chitosan as functional biopolymers for industrial applications', in *The European Polysaccharide Network of Excellence (EPNOE)*, pp. 329–373.

Kasaai, M. R. (2010) 'Determination of the degree of N-acetylation for chitin and chitosan by various NMR spectroscopy techniques: A review', *Carbohydrate Polymers*, 79(4), pp. 801–810.

Katas, H., Raja. and Lam, K. L. (2013) 'Development of chitosan nanoparticles as a stable drug delivery system for protein/siRNA', *International Journal of Biomaterials*. pp.1-9

Kaur, S. *et al.* (2014) 'Waste biomass: a prospective renewable resource for development of bio-based economy/processes', in *Biotransformation of Waste Biomass into High Value Biochemicals*, pp. 3–28.

Kaya, M. *et al.* (2014) 'Extraction and characterization of α-chitin and chitosan from six different aquatic invertebrates', *Food Biophysics*, 9(2), pp. 145–157.

Kim, S.-K. and Rajapakse, N. (2005) 'Enzymatic production and biological activities of chitosan oligosaccharides (COS): A review', *Carbohydrate Polymers*, 62(4), pp. 357–368.

Kotzé, A. F. *et al.* (1998) 'Comparison of the effect of different chitosan salts and N-trimethyl chitosan chloride on the permeability of intestinal epithelial cells (Caco-2)', *Journal of Controlled Release*, 51(1), pp. 35–46.

Kulshreshtha, S., Mathur, N. and Bhatnagar, P. (2014) 'Mushroom as a product and their role in mycoremediation', *AMB Express*, 4, p. 29.

Kumirska, J. *et al.* (2011) 'Biomedical Activity of Chitin/Chitosan Based Materials—Influence of Physicochemical Properties Apart from Molecular Weight and Degree of N-Acetylation', *Polymers*, 3(4), pp. 1875–1901.

Lavertu, M. *et al.* (2003) 'A validated 1H NMR method for the determination of the degree of deacetylation of chitosan', *Journal of Pharmaceutical and Biomedical Analysis*, 32(6), pp. 1149–1158.

Li, J., Revol, J.-F. and Marchessault, R. H. (1999) 'Alkali Induced Polymorphic Changes of Chitin', in *Biopolymers*, pp. 7–88.

Liu, Z. *et al.* (2008) 'Polysaccharides-based nanoparticles as drug delivery systems.', *Advanced Drug Delivery Reviews*, 60(15), pp. 1650–62.

Maher, S., Mrsny, R. J. and Brayden, D. J. (2016) 'Intestinal Permeation Enhancers for Oral Peptide Delivery', *Advanced Drug Delivery Reviews*, 106, pp.277-319.

Mao, S. *et al.* (2004) 'The depolymerization of chitosan: Effects on physicochemical and biological properties', *International Journal of Pharmaceutics*, 281(1–2), pp. 45–54.

Mariod, A. A. (2016) 'Extraction, Purification, and Modification of Natural Polymers', in *Natural Polymers*, pp. 63–91.

Marušić, M. *et al.* (2013) 'The Caco-2 cell culture model enables sensitive detection of enhanced protein permeability in the presence of N-decyl-β-d-maltopyranoside', *New Biotechnology*, 30(5), pp. 507–515.

Miyoshi, H. *et al.* (1992) 'Characterization of some fungal chitosans', *Bioscience, Biotechnology, and Biochemistry*, 56(12), pp. 1901–1905.

Mourya, V. K. and Inamdar, N. N. (2009) 'Trimethyl chitosan and its applications in drug delivery', *Journal of Materials Science: Materials in Medicine*, 20(5), p. 1057.

Muzzarelli, R. a a *et al.* (2012) 'Current views on fungal chitin/chitosan, human chitinases, food preservation, glucans, pectins and inulin: A tribute to Henri Braconnot, precursor of the carbohydrate polymers science, on the chitin bicentennial', *Carbohydrate Polymers*, 87(2), pp. 995–1012.

Nguyen, S., Winnik, F. M. and Buschmann, M. D. (2009) 'Improved reproducibility in the determination of the molecular weight of chitosan by analytical size exclusion chromatography', *Carbohydrate Polymers*, 75(3), pp. 528–533.

de Oliveira, A. M. *et al.* (2014) 'Physicochemical characterization of thermally treated chitosans and chitosans obtained by alkaline deacetylation', *International Journal of Polymer Science*, pp. 1–20.

Philibert, T., Lee, B. H. and Fabien, N. (2017) 'Current status and new perspectives on chitin and chitosan as functional biopolymers', *Applied Biochemistry and Biotechnology*, 181(4), pp. 1314–1337.

Pillai, C. K. S., Paul, W. and Sharma, C. P. (2009) 'Chitin and chitosan polymers: Chemistry, solubility and fiber formation', *Progress in Polymer Science*, 34(7), pp. 641–678.

Prabaharan, M. (2008) 'Chitosan derivatives as promising materials for controlled drug delivery', *Journal of Biomaterials Applications*, 23(1), pp. 5–36.

Raafat, D. and Sahl, H. (2009) 'Chitosan and its antimicrobial potential–a critical literature survey', *Microbial Biotechnology*, 2(2), pp. 186–201.

Ranaldi, G. *et al.* (2002) 'The effect of chitosan and other polycations on tight junction permeability in the human intestinal Caco-2 cell line', *The Journal of Nutritional Biochemistry*, 13(3), pp. 157–167.

Rathke, T. D. and Hudson, S. M. (1994) 'Review of chitin and chitosan as fiber and film formers', *Journal of Macromolecular Science, Part C: Polymer Reviews*, 34(3), pp. 375–437.

Rumengan, I. *et al.* (2014) 'Structural Characteristics of Chitin y Chitosan Isolated from the Biomass of Cultivated Rotifer, Brachionus rotundiformis', *International Journal of Fisheries Aquatic Sciences*, 3(1), pp. 12–18.

Ryan, S. M. *et al.* (2013) 'An intra-articular salmon calcitonin-based nanocomplex reduces experimental inflammatory arthritis', *Journal of Controlled Release*, 167(2), pp. 120–129.

Sagheer, F. A. Al *et al.* (2009) 'Extraction and characterization of chitin and chitosan from marine sources in Arabian Gulf', *Carbohydrate Polymers*, 77(2), pp. 410–419.

Sajomsang, W. *et al.* (2010) 'Quaternization of N-(3-pyridylmethyl) chitosan derivatives: Effects of the degree of quaternization, molecular weight and ratio of N-methylpyridinium and N,N,N-trimethyl ammonium moieties on bactericidal activity', *Carbohydrate Polymers*, 82(4), pp. 1143–1152.

Sieval, A. B. *et al.* (1998) 'Preparation and NMR characterization of highly substitutedN-trimethyl chitosan chloride', *Carbohydrate Polymers*, 36(2–3), pp. 157–165.

Singh, V., Kumar, P. and Sanghi, R. (2012) 'Use of microwave irradiation in the grafting modification of the polysaccharides - A review', *Progress in Polymer Science*, 37(2), pp. 340–364.

Smets, G. and Rüdelsheim, P. (2018) 'Biotechnologically produced chitosan for nanoscale products. A legal analysis', *New Biotechnology*, 42, pp. 42–47.

Sonia, T. A. and Sharma, C. P. (2011) 'Chitosan and its derivatives for drug delivery perspective', in *Chitosan for biomaterials*, pp. 23–53.

Tajdini, F. *et al.* (2010) 'Production, physiochemical and antimicrobial properties of fungal chitosan from Rhizomucor miehei and Mucor racemosus', *International Journal of Biological Macromolecules*, 47(2), pp. 180–183.

Tetens, I. (2010) 'Scientific Opinion on the safety of'Chitin-glucan'as a Novel Food ingredient: EFSA-Q-2009-00762'. European Food Safety Authority.

Tolaimate, A. *et al.* (2000) 'On the influence of deacetylation process on the physicochemical characteristics of chitosan from squid chitin', *Polymers*, 41(7), pp. 2463–2469.

Upadhyay, R. K. (2014) 'Transendothelial Transport and Its Role in Therapeutics', *International Scholarly Research Notices*, 2014.

Verheul, R. J. *et al.* (2008) 'Synthesis, characterization and in vitro biological properties of O-methyl free N,N,N-trimethylated chitosan', *Biomaterials*, 29(27), pp. 3642–3649.

Vetter, J. (2007) 'Chitin content of cultivated mushrooms Agaricus bisporus, Pleurotus ostreatus and Lentinula edodes', *Food Chemistry*, 102(1), pp. 6–9.

Vongchan, P. *et al.* (2011) 'N, N, N-Trimethyl chitosan nanoparticles for the delivery of monoclonal antibodies against hepatocellular carcinoma cells', *Carbohydrate Polymers*, 85(1), pp. 215–220.

Wan, A. C. A. and Tai, B. C. U. (2013) 'Chitin — A promising biomaterial for tissue engineering and stem cell technologies', *Biotechnology Advances*, 31(8), pp. 1776–1785.

Wasikiewicz, J. M. and Yeates, S. G. (2013) '"Green" molecular weight degradation of chitosan using microwave irradiation', *Polymer Degradation and Stability*, 98(4), pp. 863–867.

Weinhold, M. X. *et al.* (2009) 'Strategy to improve the characterization of chitosan for sustainable biomedical applications: SAR guided multi-dimensional analysis', *Green Chemistry*, 11(4), pp. 498–509.

Woitiski, C. B. *et al.* (2011) 'Facilitated nanoscale delivery of insulin across intestinal membrane models', *International Journal of Pharmaceutics*, 412(1–2), pp. 123–131.

Xing, L. *et al.* (2018) 'Chemical Modification of Chitosan for Efficient Vaccine Delivery', *Molecules*, 23(2), p. 229.

Xu, T. *et al.* (2010) 'Synthesis, characteristic and antibacterial activity of N,N,N-trimethyl chitosan and its carboxymethyl derivatives', *Carbohydrate Polymers*, 81(4), pp. 931–936.

Xu, Y. and Du, Y. (2003) 'Effect of molecular structure of chitosan on protein delivery properties of chitosan nanoparticles', *International Journal of Pharmaceutics*, 250(1), pp. 215–226.

Yang, R. *et al.* (2016) 'A review on chitosan-based flocculants and their applications in water treatment', *Water Research*, 95, pp. 59–89.

Zappino, M. *et al.* (2015) 'Bromelain immobilization on microbial and animal source chitosan films, plasticized with glycerol, for application in wine-like medium: microstructural, mechanical and catalytic characterisations', *Food Hydrocolloids*, 45, pp. 41–47.

Zielinska, K., Shostenko, a. G. and Truszkowski, S. (2014) 'Analysis of chitosan by gel permeation chromatography', *High Energy Chemistry*, 48(2), pp. 72–75.

8 FUNGAL CHITOSAN NANOPARTICLES COATED WITH ZEIN FOR IMPROVED ORAL DELIVERY OF SELENOCYSTINE

The work presented in this chapter contains the following elements of research:

An unpublished study of the validation of an extraction and characterisation of selenoamino acids from Irish mushrooms with the objective of demonstrating the availability of the species for supplement production in the Irish context (Sections 8.2.2-8.2.3 and 8.3.1-8.3.2).

A study of the formulation of $SeCys_2$ into nanoparticles produced from *A. bisporus* origin chitosan, using results from previous chapters to demonstrate the feasibility of a supplement formulation containing using mushrooms origin ingredients. This work will be submitted as:

Vozza, G., Khalid, M.D, Forde S, Byrne, H. J., Ryan, S and Frias, J. (2018). Fungal chitosan nanoparticles coated with zein for improved delivery of selenocystine. To the Journal of Innovative Food Science and Emerging Technologies (IFSET), May 2018.

Vozza, G., was the primary author, Khalid, M.D., helped develop the formulation process, Forde, S, conducted experiments in Section 8.3.6 and Byrne, H. J., Frias, J. and Ryan S contributed to layout, design and proofing.

Abstract

Selenoamino acids (SeAAs), have been shown to possess antioxidant and anticancer properties. SeAAs, especially selenocystine ($SeCys_2$) and selenomethionine (SeMet) have been shown to accumulate in mushroom bodies supplemented with Se during cultivation. In this work, a Reverse phase, high performance liquid chromatography, Photodiode Array Detector (RP-HPLC-PDA) method was validated to analyse the SeAAs content of Se supplemented *A. bisporus.* The predominant species found was $SeCys_2$, at 616 ± 23 µg/g dried mushroom powder (DMP), while 18 ± 9 µg/g DMP of SeMet was identified, inferring that Se supplemented mushrooms may be a viable source for organic Se (291±7 µg/g of Total Se). $SeCys_2$, however, can be toxic above the recommended nutritional intake level, and thus improved, targeted delivery methods are desirable. $SeCys_2$ was encapsulated into nanoparticles (NPs) composed of fungal derived chitosan (fCs), via ionotropic gelation with tripolyphosphate (TPP), then coated by zein (a maize derived prolamine rich protein). Optimum NP physicochemical properties for oral delivery were obtained at a 6:1 ratio of Cs:TPP, with a 1:0.75 mass ratio of Cs:zein coating (diameter ~300 nm, polydispersity index ~0.3, zeta potential >38mV). Scanning electron microscopy (SEM) analysis showed spheroidal, well distributed particles. An encapsulation efficiency of 84.4 % was achieved. Cytotoxicity studies of $SeCys_2$ loaded NPs elicited no decrease in cellular viability in Caco-2 (intestinal) cells after 4hrs exposure, although a significant reduction was observed, when compared to pure $SeCys_2$, for all test concentrations in HepG2 liver cells, after 72 hr exposure. Accelerated thermal stability testing of the NPs indicated good stability under normal storage conditions. Lastly, the sustained release profile of the formulation showed that 32 ± 4.5 % of $SeCys_2$ was released from the fCs NPs after 2 hr in simulated gastric fluid, followed by 30 ± 2 % release in simulated intestinal fluid for 4 hr.

Keywords

Agaricus bisporus, Fungal chitosan, selenium, zein, selenocystine, nanoparticles, oral delivery.

Abbreviations

fCs, fungal chitosan; **CL113**, PROTASAN™ UP; **DLS**, dynamic light scattering; **EE%**, Encapsulation efficiency; **GRAS**, Generally recognised as safe; **LDV**, laser doppler velocimetry; **MSC**, methylselenocysteine; **NP**, nanoparticle; **PDI**, Polydispersity; **$SeCys_2$**, selenocystine; **SeMet**, Selenomethionine; **TPP**, Tripolyphosphate; **ZP**, Zeta potential. **CT**, Chitin; **DDA%**, Degree of Deacetylation.

8.1 Introduction

Selenium is an essential micronutrient in human and animal nutrition (Rayman, 2000) that exists in a wide array of different forms, both organic and inorganic. Selenite and selenate salts are the most common inorganic forms, whereas selenoamino acids (SeAAs), such as selenocystine ($SeCys_2$), selenomethionine (SeMet), and methylselenocysteine (MSC) are the most commonly found forms in foods from the *Agaricus*, *Brassica* and *Allium* families (Montes-Bayón, M. J D Molet, *et al.*, 2006; Maseko *et al.*, 2013; Reilly *et al.*, 2014). Health benefits of Se originating from MSC and $SeCys_2$ have been linked to the body's endogenous antioxidant defence system, protecting cellular components such as cell membranes, lipids, lipoproteins and DNA from oxidative damage by free radicals, reactive oxygen and reactive nitrogen species (Ponnampalam *et al.*, 2009). As oxidative damage is linked to the development of cardiovascular and neurodegenerative diseases as well as cancers, several experimental *in vivo* studies of the effects of administration of Se compounds have been undertaken

(Valko *et al.*, 2007; Lobo *et al.*, 2010; de Souza *et al.*, 2014). $SeCys_2$ has been shown to reduce tobacco-derived nitrosamine-induced lung tumour growth and enhance hepatic chemoprotective enzyme activities in mice (Fan *et al.*, 2013), SeMet may have some potential in degenerative disease by decreasing oxidative stress of small molecule antioxidants used as a buffer for free radicals in brain tissue (Song *et al.*, 2014; Reddy *et al.*, 2017), whereas MSC has been shown to offer selective protection against organ specific toxicity induced by clinically active antitumor agents, cisplatin, oxaliplatin, and irinotecan in rat models (Cao *et al.*, 2014). A number of benefits regarding oncology treatments due the modulation of the therapeutic efficacy and selectivity of anticancer drugs has been reported for these SeAAs also (Evans, Khairuddin and Jameson, 2017).

Although essential, Se possesses a low therapeutic index, meaning that there is a fine line between beneficial and toxic doses. Generally, organic Se shows a greater degree of bioavailability than the inorganic forms, as well as a higher threshold for toxicity (Amoako, Uden and Tyson, 2009). Despite the associated health benefits, Se intake in Ireland is remarkably low, whereby, nearly 50% of females and 20% of males aged between 18 – 64 years fail to meet the average recommended requirement (ARR) of 40 µg/day (Murphy and Cashman, 2002). This low Se intake in the Irish population has been attributed to the drop in imports of high-protein wheat for bread-making flour from North America and Canada (Barclay and Macpherson, 1992), which are Se-rich in comparison to Irish flour varieties (Murphy and Cashman, 2001).

Selenium-fortified *A. bisporus* have demonstrated the ability to assimilate inorganic Se (such as sodium selenite) from the growth substrate and convert it to organic forms, such as SeMet, MSC and $SeCys_2$ (Maseko *et al.*, 2013) For this, mushrooms have been proposed as a potential source of Se for Se deficient populations (Falandysz, 2008;

Maseko *et al.*, 2013). While *A. bisporus* generally contain an average of only >1 µg Se/g dry weight (Savic *et al*., 2012), when cultivated in substrates containing Se in either inorganic or organic forms, they exhibit much higher concentrations, ranging from 354 ± 0.19 µg/g to 707 ± 37.3 µg/g of Se (Gergely *et al.*, 2006; Savic *et al*., 2012).

The predominant form of Se identified in *A. bisporus* is $SeCys_2$ (Maseko *et al.*, 2013), which has been shown to exert similar toxicity as that of inorganic forms such as selenite (Takahashi, Suzuki and Ogra, 2017). Additionally, Se from *A. bisporus* has been reported to have poor bioavailability (Thiry *et al.*, 2012), which is further retarded upon cooking (Khanam and Platel, 2016). As such, the efficacy of $SeCys_2$ can be limited by its potential to reach the target site of the jejunum for therapeutic action, thus reducing its bioavailability. To identify Se species present in *A. bisporus*, it is first necessary to isolate fractions of Se from the fruiting bodies of the mushrooms and identify the species present. However, to date, no robust method for complete extraction and analysis of Se from food sources has been developed (Thiry *et al.*, 2012). Careful optimisation of extraction procedures is an essential requirement for Se speciation analysis of solid samples, in order to achieve high extraction efficiencies that also mitigate interconversion of the original species present (Dumont, Vanhaecke and Cornelis, 2006). It is generally recognised that a single step extraction is insufficient for Se liberation due to the varied matrix associations of Se in real samples (Pyrzyńska, 1996). For example, hot water extraction has been employed as a Se leaching solution for three edible wild mushroom species (*Macrolepiota procera*, *Lepista luscina* and *Boletus luridus*), although only 47% of the total Se content present in the sample (present in water soluble proteins) could be recovered (Huerta, Sánchez and Sanz-Medel, 2005). As many Se species are protein bound, several authors have utilised strong acids in extraction procedures, in order to increase liberation of Se from various matrices (Casiot *et al.*, 1999; Wrobel *et al.*, 2003).

Additionally, proteolytic enzymes have been employed for extracting SeAAs incorporated into proteins due to their ability to cleave peptide bonds (Montes-Bayón, Maria José Díaz Molet, *et al.*, 2006). Also, inorganic forms of Se have been found to become entrapped physically or chemically into cell walls and as such, acids and non-proteolytic enzymes such as driselase have been used in Se extraction (Infante, Hearn and Catterick, 2005).

A dedicated analytical approach must be adopted in all areas of interest in the field of Se speciation, especially in the case of the separation technique preceding element or molecule specific detection. A massive challenge to the analyst is the myriad of Se species with different physicochemical properties present in biological systems. Se species must be unambiguously separated, identified and correctly quantified after they are extracted from a given matrix. However, interconversion amongst Se species upon extraction from a food matrix is a common obstacle that needs to be overcome in speciation analysis (Uden *et al*., 2004).

In this work, Se species were extracted from Se supplemented *A. bisporus* samples, using protease enzymes or HCL (0.1 M), under microwave or sonic energy respectively. Se species were then separated by Reverse phase, high performance liquid chromatography (RP-HPLC) coupled to a Photodiode Array Detector (PDA) and subjected to a validation protocol, based on approved guidelines (EMEA, 1995), to assess its suitability for routine work.

All considered, an opportunity presents for developing a drug delivery system that optimises $SeCys_2$ bioavailability, whilst reducing its toxic side effects. One approach is the use of colloidal drug carriers that can provide site specific or targeted bioactive (BA) delivery combined with optimal BA release profiles. Nanoparticle (NP) delivery systems

have shown a higher mobility and cellular uptake compared to systems of larger size which may offer an advantage to the delivery of BA compounds. Mohanraj & Cheng (2007) compared the uptake of 1 and 10 µm particles to that of 100 nm particles in *in vitro* models, observing that an increase of 2.5-6 fold higher uptake respectively for the smaller sized particles. Etheridge *et al*. (2013) observed that the effect of particle size on cellular intake can also be influenced by the constituent material and the particle geometry, a consequence of reduced intestinal clearance mechanisms and an increase in the mass to surface ratio interaction with the biological support.

In recent years, a wide array of constituents, such as natural and synthetic polymers, lipids, and proteins, have been employed to prepare BA containing nanocarriers (Puri *et al.*, 2009; Elzoghby, Samy and Elgindy, 2012; Pridgen, Alexis and Farokhzad, 2015). Among the materials proposed for mucosal delivery, polysaccharides have received increasing attention because of their physical and biological properties (Rampino *et al.*, 2013). The natural polymer chitosan (Cs) is a positively charged mucopolysaccharide, closely related to cellulose and derived from chitin (CT), the second most abundant polymer in nature (Kean and Thanou, 2010). Cs has been used for the development and formulation of nanoparticles by ionotropic gelation due to its physicochemical and biological properties (H. Zhang *et al.*, 2015; Mohammed *et al.*, 2017). This bioactivity includes improved adherence to mucosal surfaces, increased drug residence time (Ryan *et al.*, 2012), and protection of the bioactive drug from intestinal proteases (Ryan *et al.*, 2013; Amaro *et al.*, 2015). Cs can be dissolved in acidic media, due to protonation of the amine residues present in the polymer backbone. Ionotropic gelation allows for the formation of NPs from Cs via crosslinking with oppositely-charged electrolytes (such as tripolyphosphate (TPP)) under mild conditions in which amino acids and peptides will

remain reasonably stable (Janes, Calvo and Alonso, 2001; Wang *et al.*, 2011; Chen *et al.*, 2013).

Typically, Cs is manufactured commercially on a large scale by alkaline N-deacetylation of crustacean origin CT (Philibert, Lee and Fabien, 2017). However, the preparation of Cs with controlled properties, by means of microorganisms such as fungi is of increasing interest as it offers several advantages over its crustacean counterparts. For example, fungal Cs (fCs) has significantly lower heavy metal association than that of crustaceans, allowing for milder production methods in its isolation, and year-round growth that is not seasonally dependant (Muzzarelli *et al.*, 2012). In this context, production and purification of Cs from the cell walls of waste fungal mycelium may offer the advantage of being more sustainable with potential for a more consistent product.

To date, the vast majority of Cs research in a drug delivery context has used crustacean derived Cs (Ryan *et al.*, 2013; Umerska, Corrigan and Tajber, 2014; Diop *et al.*, 2015; Danish *et al.*, 2017a), For example, PROTASAN™ CL113, an ultrapure commercial Cs, derived from crustacean shells and sold by NovaMatrix, FMC Corporations, has been previously promoted for its ability to encapsulate and deliver food derived BAs such as Retinyl Palmitate (a vitamin A isomer) and possesses the following physicochemical properties: MW of 110-150 kDa, DDA% ≥80 % and minimal metal contamination (Fernández-Gutiérrez *et al.*, 2015). However, one drawback of NPs formulated with Cs is that the ability of the BA to be encapsulated within the NP matrix is often limited by the availability of its the ionisable groups (Lin, Liu and Ping, 2007). Additionally, they can often display fast release rates in the stomach environment, due to the enhanced solubility of Cs at acidic pH (Mohammed *et al.*, 2017). To overcome these limitations, coating of Cs NPs with anionic polyelectrolytes has been investigated (Banerjee *et al.*,

2016). Zein a GRAS approved prolamine-rich protein derived from maize, has been used in the formulation and coating of peptide oral delivery systems (Y. Zhang *et al.*, 2015), to increase encapsulation efficiency (Luo and Wang, 2014) and improve the control of gastric release of labile bioactives (Luo *et al.*, 2010; Paliwal and Palakurthi, 2014). By exploiting the physical interactions between protein and polysaccharide (in this instance zein and Cs), it is possible to improve and broaden the range of the physical and chemical stability properties of the NP delivery systems (Benshitrit *et al.*, 2012).

In the previous work of Vozza *et al.*, (2018a, Chapter 5) a Design of Experiments (DoE) approach was used to establish optimum formulation conditions that would produce SeAA (SeMet) loaded NPs, via ionotropic gelation. DoE identified the conditions of mass ratio 6:1 (Cs:TPP), with TPP dissolved in NaOH (0.1 M) and Cs dissolved in acetate buffer (pH 3) prior to crosslinking, produced NPs with physicochemical properties (Size ~ 300 nm, PDI <0.5 and ZP >30 mV) suitable for oral delivery (des Rieux *et al.*, 2006). Additionally, by coating the produced NPs with zein, the encapsulation efficiency (EE%) was significantly improved from < 65% to >80%.

In a further study, Vozza *et al.*, (2018b, Chapter 6), employed the optimised formulation conditions to encapsulate $SeCys_2$ and MSC, based on the rationale that $SeCys_2$ (with a pKa of 4.7 (Lacourciere and Stadtman, 1999)), and MSC (with a pKa of 4.9 (Mishra, Priyadarsini and Mohan, 2007)), contain comparably ionisable groups to SeMet. The findings showed that, by employing the previously established DoE parameters, similar formulations (e.g. physicochemical properties and EE%) to those achieved for the SeMet loaded NPs could be produced.

As the Cs employed for the NP formulations in Vozza *et al.*, (2018a, 2018b, Chapters 4-6), was CL113, a further study by Vozza *et al.*, (2018c, Chapter 7) looked at the extraction of CT from the edible basidiomycete mushroom *A. bisporus* and its derivatisation to fCs, with equivalent properties (DDA%, MW and purity) to that of CL113.

The aim of this study was to qualitatively and quantitatively identify SeAAs present in *A. bisporus* as a potential source for organic Se and to build directly on the previous work on encapsulation in Cs NPs. This was achieved by applying the optimum DoE formulation conditions, detailed in Vozza *et al.*, (2018a, 2018b, Chapters 4-6), to fCs, produced as per Vozza *et al.*, (2018c, Chapter 7) with synthetic $SeCys_2$ (to avoid natural variance from *A. bisporus* $SeCys_2$). Once the encapsulating fCs NPs were prepared, they were extensively assessed for their physicochemical properties, morphology, thermal stability, cytotoxicity and *in vitro* controlled release, utilising the methods developed in the previous studies (Vozza *et al*., 2018a, Chapter 5).

8.2 Materials and Methods

8.2.1 Materials

Fungal Cs (fCs), with MW of 156±24 kDa and degree of deacetylation (DDA%) of 86 % was derived as per Vozza *et al.*, (2018c, Chapter 7), Seleno-DL-cystine (>98 % purity), D (+) - Trehalose dihydrate, Sodium Tripolyphosphate (TPP), and zein, of ≥99 % purity, were obtained from Sigma Aldrich, Ireland. Acetic acid, ACS reagent, ≥99.7%, sodium hydroxide solution 50 wt % in H_2O, hydrochloric acid (HCL) 37 wt % in H_2O were purchased from Fisher Scientific, Ireland. All other reagents, chemicals and solvents were of analytical grade from Sigma Aldrich, Ireland. Deionised water (dH_2O) ≥18 MΩcm was obtained using Millipore Simplicity® Water Purification System and used for all manipulations unless otherwise specified.

8.2.2 RP-HPLC-PDA Method Validation

RP-HPLC-PDA was employed to quantify the SeAAs present in the mushroom samples, as previously described (Ward, Connolly and Murphy, 2012) with the following modifications. Samples were analysed with a Waters 2998 HPLC coupled to a Photodiode Array Detector, (Waters, USA), using a Pursuit 5 C18, 250 x 4.6 mm column, (Agilent Technologies, UK). Isocratic elution was carried out at a flow rate of 0.8 mL/min, column temperature 45.0 ± 5.0 °C with a mobile phase of water/methanol/trifluoroacetic acid (97.9:2.0:0.1). Samples were monitored according to their UV absorbance at 218 nm.

The chromatographic method was validated for linearity, precision, accuracy, limit of detection (LOD) and limit of quantification (LOQ). To establish linearity, primary standard stock solutions for SeMet, MSC and $SeCys_2$ were prepared separately in aqueous tris hydrochloride (10 mM) at 1 mg/mL concentration. Solutions were further diluted with the mobile phase to obtain eight working standard solutions of 4-500 μg/ml and ran on RP-HPLC-PDA, under the conditions denoted in Section 8.2.2. Assay precision was estimated by analysing each standard compound in six replicates and expressed as percentage of relative standard deviation (%RSD). All the samples were prepared freshly at the same nominal concentration, injected on three separated days (inter-day precision) and calculated based on retention time (RT) and peak area of each standard compound. The accuracy of the method was validated based on determination of percentage recovery of standard compounds after spiking the sample with known concentrations of standard compounds. The limit of detection (LOD) and limit of quantification (LOQ) were established by analysing the standard deviation (STD) of the calibration curve and its slope (S) using the multipliers suggested by the International Conference on Harmonisation guidelines (ICH, 2005), of 3.3 for LOD or 10 for LOQ and calculated using Equations 8.1 and 8.2. All values were calculated as means ± standard deviation of three replicates and repeated twice, (n = 6).

$$\boldsymbol{LOD = \frac{3.3 \times STD}{S}}$$

(Equation 8.1)

$$\boldsymbol{LOD = \frac{10 \times STD}{S}}$$

(Equation 8.2)

8.2.3 Sample extraction

A. bisporus samples supplemented with sodium selenite (60 mg/L) on day 4 of production, were provided by Monaghan Mushrooms (MM), Tyholland Farm, Monaghan, Ireland. Mushroom bodies were freeze-dried, ground to a powder (DMP), sieved through a 500 uM sieve and stored in a desiccator at room temperature for further analyses. To identify SeAA species present, mushroom samples were subjected to acid or enzymatic digestions. For acid extractions, HCL (1 mL,1 M) was added to DMP (40 mg), sonicated (55 ºC, 1 hr) in a Bransen 2200 water bath sonicator (Bransen Ultrasonics, UK) and centrifuged (14,000 rpm, 15 min, 4 ºC) to obtain clear supernatant. The samples were then diluted 1:2 with mobile phase, filtered (0.25 μm) and ran on RP-HPLC-PDA as per Section 8.2.2, both with and without SeAA spike additions. In terms of enzymatic extractions, Protease XIV (0.5 mL, 60 mg/mL) was added to DMP (40 mg) and vortex mixed (1 min), then ultrasonicated for 30 s at 45 % amplitude and the probe tip washed with 0.25 mL of protease solution to ensure maximum recovery of the analytes. Samples were then placed into individual microwave vessels (EasyPrep™, CEM, UK) and subjected to microwave irradiation (MARS5, CEM, UK), for 15 mins at 80 W, followed by a 30 min cool down period. The resultant extracts were then centrifuged (14,000 rpm, 15 min, 4 °C) to obtain the clear supernatant and the pellet washed with H_2O (1 mL). The final volume was then made up to 5 mL using mobile phase, before removing an aliquot (2 mL) for filtration (0.25 μm), dilution (1:2) and spike addition, prior to RP-HPLC-PDA analysis.

Measurements of Se totals were conducted by an accredited third-party laboratory (Eurofins, Ireland), using ICP-MS and used for comparison against the developed RP-HPLC-PDA method.

8.2.4 Preparation of Se loaded fCs nanoparticles, coated with zein - Particle size, PDI and ZP

fCs (Vozza *et al*, 2018c, Chapter 7), $SeCys_2$ loaded NPs were formed via the ionotropic gelation method (Vozza *et al*, 2018b, Chapter 6) with small modifications from the original method from Calvo *et al.*, (1997). In Brief, aqueous TPP solution (3 mg/mL) was prepared in NaOH (0.01 M), with a $SeCys_2$ concentration of 400 ug/mL. and added in equal volumetric proportions to stirring fCs solution (3 mg/mL, 700 rpm) prepared in acetate buffer (pH 3). The NPs formed were left to stabilise for 30 min, after which absolute EtOH (8 mL) was added whilst the stirring speed (700 rpm) of the solution was maintained. Filtered zein (2 mL, 5.625 mg/mL), dissolved in aqueous EtOH (80% v/v), was then added dropwise to the solution to yield zein:Cs NPs of mass ratio 0.75:1 and left to stabilise for 30 min. NPs were isolated by centrifugation (3000 rpm, 30 min) using a 20 kDa MWCO (Vivaspin 20, Sartorius) centrifugal filter. Filtered EtOH (80% v/v) (equivalent in volume to the recovered supernatant) was added to the purified NPs and subsequently sonicated at 35% amplitude for 30 s with 5 s pulse intervals. The NP formulations were then concentrated under vacuum (175 mbar) at 40 °C until EtOH was completely removed. To ensure stability of the optimised formulation after lyophilisation, 10 mL of the cryoprotectant trehalose 5 % w/v in H_2O were added to each formulation and they were lyophilised for 36 hr (Danish *et al*, 2017b)

8.2.5 Physicochemical characterisation of $SeCys_2$ loaded NPs

8.2.5.1 Particle size, PDI and Zeta potential

Dynamic light scattering (DLS) was used to determine the mean particle size and polydispersity index (PDI) of the NP formulation. Laser doppler velocimetry (LDV) was used to measure the zeta potential (ZP). Both DLS and LDV analysis were performed with a Zetasizer Nano series Nano-ZS ZEN3600 fitted with a 633 nm laser (Malvern Instruments Ltd., UK), using a folded capillary cuvette (Folded capillary cell-DTS1060, Malvern, UK), at 25 °C. The values presented herein were acquired from three separate experiments, each of which included three replicates. N=3 (Chapter 3, Section 3.2.1).

8.2.5.2 Scanning electron microscopy (SEM)

SEM analysis was used to visualise the morphology of the NPs formed at an accelerating voltage of 20 kV, using a secondary electron detector (Hitachi, SU6600 FESEM, USA). NP solutions were spin coated onto Si wafers, dried at room temperature and then sputter coated with 4 nm Au/Pd prior to imaging (Mukhopadhyay *et al.*, 2013), (Chapter 3, Section 3.2.2).

8.2.5.3 Encapsulation efficiency of SeCys in Cs:TPP nanoparticles

The EE% of $SeCys_2$ in the fCs NPs was determined by the separation and quantification of $SeCys_2$ left in the supernatant after ultracentrifugation isolation of the formed NPs, using the RP-HPLC-PDA method denoted in Section 8.2.2.

The encapsulation efficiency was calculated using Equation 8.3 (Xu and Du, 2003), (Chapter 3, Section 3.2.3):

$$\boldsymbol{EE\%} = \frac{\boldsymbol{Total\ amount\ of\ Se\ Met - Free\ amount\ of\ SeMet}}{\boldsymbol{Total\ amount\ of\ SeMet}}\ \boldsymbol{X\ 100}$$

(Equation 8.3)

8.2.6 Cytotoxicity

The potential cytotoxicity of pure $SeCys_2$, unloaded and $SeCys_2$ loaded fCs NPs, was studied in Caco-2 human epithelial cells, and HepG2 human liver hepatocellular cells. Both cell lines are routinely employed to assess the potential toxicity of orally delivered compounds (Gleeson *et al*., 2015; Brayden *et al*., 2015). Caco-2 and HepG2 cells were seeded at a density of 2 x 10^4 cells/well and cultured on 96 well plates in Dulbecco's Modified Eagle Medium (DMEM) and Eagle's Minimum Essential Medium (EMEM) respectively, supplemented with 10 % foetal bovine serum, 1 % L-glutamine, 1 % penicillin-streptomycin and 1 % non-essential amino acids at 37 °C in a humidified incubator with 5 % CO_2 and 95 % O_2. Time points were selected with the intention to mimic *in vivo* conditions for each cell type. As the maximum time NPs will be exposed to the intestine, a 4 hr exposure time was used in Caco-2 cell lines (Neves *et al*., 2016), while to mimic the liver exposure, a 72-h exposure time was used for HepG2 cell lines (Brayden *et al*., 2014). Triton X-100™ (0.05%) was used as a positive control. The concentrations of the test compounds applied were 0.25, 2.5, 5, 10, 25, 50 and 100 uM. After exposure, treatments were removed and replaced with MTS(3-(4,5-dimethylthiazol-2-yl)-5-(3-carboxymethoxyphenyl)-2-(4-sulfophenyl)-2H-tetrazolium). Optical density (OD) was measured at 490 nm using a microplate reader (TECAN GENios, Grodig, Austria). Each value presented was normalised against untreated control and calculated from three separate experiments, each of which included six replicates.

8.2.7 Accelerated stability analysis

NPs were suspended at a concentration of 0.1 mg/mL, in aqueous KCl solution (10 mM) and stored at accelerated conditions: 60 °C for 720 min, 70 °C for 300 min and 80 °C for 120 min (Danish *et al.*, 2017a). The particle size, PDI and zeta potential were measured using the Nanosizer ZS (Malvern Instruments Ltd, UK) over time intervals to determine the degree of degradation. The generated data was then analysed via R software (R Core Team, 2016). The temperature dependence of the kinetic parameters of SeMet-loaded NPs stability was measured by calculating the observed rate constants. This was plotted in an Arrhenius representation and apparent activation energy, E_a and reaction rate constant, k_{ref} were calculated according to Equation 8.4:

$$\boldsymbol{P = Po + e^{ln(k) - \frac{Ea}{R}(\frac{1}{T} - \frac{1}{T_{ref}})} t}$$

(Equation 8.4)

where P is the property (particle size, PDI or ZP) at time t, Po is the initial property conditions, k is the apparent zero order reaction constant, E_a is the energy of activation, R is the universal gas constant, T is the temperature of the experiment in Kelvin (K) and T_{ref} is the reference temperature (343 K).

8.2.8 *In vitro* controlled release studies

$SeCys_2$ release from the NPs was carried out using a dialysis bag diffusion technique (Hosseinzadeh *et al.*, 2012) over 6 hr (Calderon L. *et al.*, 2013; Yoon *et al.*, 2014). Freeze dried $SeCys_2$ loaded fCs NPs, coated with zein, were suspended in 5 mL H_2O and sonicated at 35 % amplitude for 30 s with 5 s intervals and placed into a Float-A-Lyzer®G2 dialysis membrane with a pore size of 25 kDa (Spectrum Laboratories, USA). The sample was placed into 40 mL of simulated gastric fluid (SGF) or simulated intestinal

fluid (SIF) specified according to the British Pharmacopoeia (Pharmacopoeia, 2016). SGF was composed of 0.1 M HCL and SIF was composed of 1 volume of 0.2 M trisodium phosphate dodecahydrate and 3 volumes of 0.1 M HCL (adjusted to pH 6.8), without enzymes (British Pharmacopoeia Commission, 2016). Samples were placed in a thermostatic shaker at 37 ºC and agitated at 100 rpm. At predetermined time points, 1 mL of release fluid was analysed and replaced with simulated fluid to maintain sink conditions.

$SeCys_2$ release was measured by RP-HPLC-PDA (Section 8.2.5). Equation 8.5 was used to determine the % drug release:

$$\boldsymbol{Drug_{rel}}\ \% = \frac{\boldsymbol{D(t)}}{\boldsymbol{D(l)}} * \mathbf{100}$$

(Equation 8.5)

where $Drug_{rel}$ is the percentage of $SeCys_2$ released, D(*l*) represents the concentration of $SeCys_2$ loaded and D(t) represents the amount of $SeCys_2$ released at time t, respectively.

8.3 Results and Discussion

8.3.1 RP-HPLC-PDA Method Validation

Most often, for Se speciation analysis in food samples, Liquid chromatography-tandem mass spectrometry (LC-MS/MS) is the method commonly employed, owing to its excellent sensitivity and short run time (Schaumlöffel and Tholey, 2011). However, the apparatus is expensive and many analytical laboratories cannot support such equipment because of the high maintenance costs (Capelo *et al.*, 2006).

In this work, RP-HPLC-PDA was employed for the determination of SeAAs ($SeCys_2$, SeMet and MSC) in *A. bisporus*, supplemented with sodium selenite. The proposed method was validated with respect to linearity, LOD, LOQ, recoveries and precision according to the International Conference on Harmonization (ICH) guidelines for method validation (ICH, 2005). The linearity of calibration curves was calculated using linear regression analysis of area versus concentration, for eight concentration levels of each standard compound, injected in triplicate. Table 8.1 shows the regression equation and correlation coefficient relationship between concentrations and peak area. Over the range tested (5-400 ug/mL), all the analytes exhibited a good linearity with correlation coefficients ranging from 0.9995 to 0.9998. The LOD and LOQ were estimated from the calibration curve and values subsequently ranged from 0.33 to 2.64 µg/L and 1–8 µg/mL, respectively (Table 8.1). The precision of the method was assessed by the percent relative standard deviation (%RSD) using retention times and peak areas of standard compounds. The results suggest a satisfactory intermediate precision value (%RSD) which ranged

from 0.5 to 4.43 and 2.87–3.78 with respect to retention time and peak-area, respectively (Table 8.1).

Table 8.1 Precision of the method, linearity data for calibration curves and retention time (RT) of reference SeAAs studied. LOD and LOQ calculated according to Equations 8.1 & 8.2. RSD (%): percentage relative standard deviation of mean recovery. N=6.

SeAA	**Linearity range (ug/mL)**	**Retention time (min)**	**Slope (m)**	**Intercept (c)**	**Correlation coefficient (R^2)**
$SeCys_2$	4-500	4.33	5.30±0.80	12.95±7.42	0.9998
MSC	4-500	7.24	8.80±0.40	16.81±12.86	0.9997
SeMet	4-500	15.60	9.54±0.10	11.80±27.59	0.9995
SeAA	**Recovery (%)**	**LOD (ug/mL)**	**LOQ (ug/mL)**	**RSD (%) RT**	**RSD (%) Peak area**
$SeCys_2$	96	2.6	8.0	0.52	3.78
MSC	94	1.3	4.0	2.45	2.87
SeMet	88	0.3	1.0	4.43	3.40

For evaluation of the accuracy of the method, recovery assays were performed, whereby mushroom extracts were spiked with a known amount of standard compound and the percentage recoveries were determined to range from 88-96 % (Table 8.1). These findings suggest that the proposed RP-HPLC-PDA method is sufficiently accurate and sensitive for the determination of the SeAAs selected for assessment in *in vitro* studies, without the use of expensive instrumentation setups such as LC-MS/MS.

8.3.2 Qualitative and Quantitative analysis of SeAAs in *A. bisporus*

The first part of this experiment focused on comparing the acidic and protease extractions for the three SeAAs ($SeCys_2$, SeMet and MSC) selected for study in the dried mushroom powder (DMP) samples. As can be seen in Figure 8.1, significantly more $SeCys_2$ and SeMet (66-fold and 5-fold higher, respectively) was liberated from the DMP through use of a proteolytic digestion when compared to that of acidic digestion. The enzymatic hydrolysis was most likely better equipped to liberate SeMet and $SeCys_2$ associated with

high molecular weight compounds (such as proteins) from the mushroom matrix, due to them being protein bound (Kápolna *et al.*, 2007). Although MSC has been identified by others in Se supplemented *A. bisporus* samples (Gergely *et al.*, 2006; Maseko *et al.*, 2013), spike additions failed to identify MSC in the DMP investigated in this study. MSC is a non-protein bound, water soluble SeAA and as such it was expected to be present in the acid extractions (Gergely *et al.*, 2006). However, as concentrations of MSC present in Se supplemented mushrooms are reported to be ≈ 0.8 ug/mL (Maseko *et al.*, 2013) and the validated RP-HPLC-PDA method having an LOD of 1.3 ug/mL (for MSC), it is likely that it is present in the DMP but not detectable by the RP-HPLC-PDA method employed.

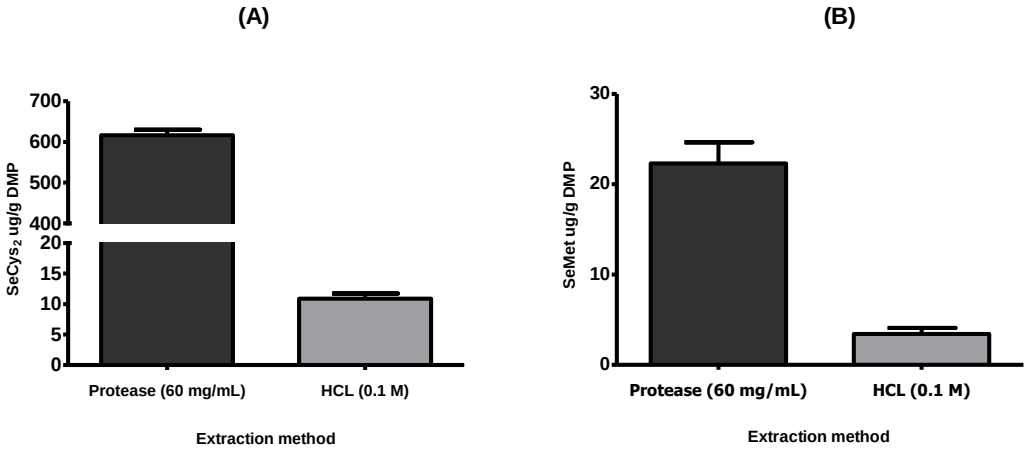

Figure 8.1 Comparison of acid and protease extractions for the liberation of $SeCys_2$ (A) and SeMet (B) from DMP. N=3.

Table 8.2, shows the quantitative data for SeMet and $SeCys_2$ identified in the DMP after protease digestion, the latter being shown to be the predominant species, present at 616 ± 23 µg/g DMP, while a modest amount of 18 ± 9 µg/g DMP SeMet was identified. Se equivalent values were then calculated for the identified SeAAs (40 and 45 % of SeMet and $SeCys_2$ exist as Se, respectively), tallied together, and compared to total Se values as identified by the third party accredited lab Eurofins, Ireland (Table 8.2).

Table 8.2 Concentration of Se species in DMP after protease extraction, determined by RP-HPLC-PDA. N=6.

SeAA	Se AA µg/g DMP	Se equivalent µg/g DMP
$SeCys_2$	616.69 ± 23.64	283.68 ± 10.87
SeMet	18.97 ± 9.64	7.59 ± 3.85
MSC	n.d	n.d
Sum of Species[a]	635.66 ± 16.64	291.27 ± 7.36
Total Se[b]	-	356.25 ± 61.87

n.d (not determined), [a] Sum of $SeCys_2$ and SeMet as determined by RP-HPLC-PDA, [b] Total Se, as measured by ICP-MS, Eurofins, Ireland.

The total Se identified using the RP-HPLC-PDA method developed was 291 ± 7 µg/g vs 356 ± 61 µg/g from Eurofins (Figure 8.2), showing that approx. 80 % of the total Se content was identified using the current method. Several other SeAA species, such as selenite, selenite, selenoethionine, have been reported to be present in Se supplemented *A. bisporus* (Stefánka *et al*., 2001; Haberhauer-Troyer *et al*., 2003), which were not targeted for identification in this study and could account for the discrepancy in Se totals.

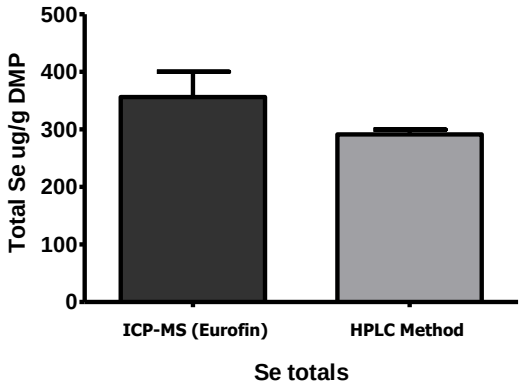

Figure 8.2 Se totals, Eurofins vs developed RP-HPLC-PDA method. N=3.

Although Se totals for *A. bisporus* have been reported previously, there appears to be several conflicting findings. For example, Maseko (2013), found total Se to be 137 ug/g of dried stalks and mushroom caps. However, in that study, the Se provided to the mushroom bodies during cultivation was as sodium selenite at a maximum of 40 mg/L,

which is less than the 60 mg/L used in the *A. bisporus* provided by Monaghan mushrooms. On the other hand, Gergely *et al.*, (2006) reported the ability of *A. bisporus* to accumulate 770.7 ± 37.3 µg/g after supplementation of mushroom compost with only 10 mg/kg of selenised yeast, and Werner and Beelman, (2002), demonstrated the ability of *A. bisporus* to accumulate Se up to 1300 µg/g DMP, after supplementing cultivation media with up to 300 mg/L. Perhaps the reason for the reported discrepancies in these studies is related to the variances in the cultivation or extraction methods. Moreover, it is worth noting that these studies did not test/validate the robustness of the employed analytical methods for Se determination or use certified reference material as a reference check point. The current study, however, did assess the suitability of the analytical method for employment in Se determination, in addition to employing an independent ISO accredited third party laboratory to assess the provided samples for Se content and thus comparison with the proposed RP-HPLC-PDA method. Overall, given the high concentrations of Se present in the fungal samples (291 µg/g DMP, equivalent to 23 ug/g fresh weight), Se supplemented mushrooms may be a feasible source for Se in the diet. To meet the Se recommended daily allowance (RDA) (40 ug/day), ingestion of just 2 g fresh mushroom bodies would be required. However, it is worth noting that Se from *A. bisporus* has been reported to have poor bioavailability (Thiry *et al.*, 2012), which is further retarded upon cooking (Khanam and Platel, 2016). As such, the efficacy of the predominant Se species present in the supplemented mushroom bodies ($SeCys_2$) may be limited by its potential to reach the target site of the jejunum for therapeutic action, thus encapsulating $SeCys_2$ into a NP delivery system may offer an advantage.

8.3.3 Characterisation of fCs NPs loaded with $SeCys_2$ - Particle size, PDI and surface charge

Table 8.3 displays the physicochemical properties of the $SeCys_2$ loaded NPs produced with the fCs developed in Vozza *et al.*, (2018c, Chapter 7) For ease of comparison, the properties of NPs produced with CL113 (Vozza *et al.*, 2018b, Chapter 6) are displayed in this table also. No significant difference between size and PDI of the fCs and CL113 NPs was observed, although for ZP and EE%, NPs formulated with fCs were significantly higher vs the CL113 NPs (ZP 38 vs 31 mV, EE% 84 vs 80 %) (Table 8.3).

Table 8.3 Physiochemical results for $SeCys_2$ loaded NPs, coated with zein. Size, PDI, ZP and EE% are presented for each NP formulated with either fCs or CL113. N=3.

fCs $SeCys_2$ NPs	**Size (nm)**	**PDI**	**ZP**	**EE%**
Average	299.5 ± 47.1	0.324 ± 0.176	38.7 ± 2.1	84.4 ± 1.2
CL113 $SeCys_2$ NPs	**Size (nm)**	**PDI**	**ZP**	**EE%**
Average	262.1 ± 11.1	0.243 ± 0.061	31.5 ± 1.0	78.9 ± 1.5

Previous observations have shown the importance of the final Cs:TPP mass ratio, the formulation media pH and zein coating mass ratio in determining the physicochemical properties of ionotropic formed Cs NPs (Vozza *et al.*, 2018a, Vozza *et al.*, 2018b, Chapters 4-6). Other variables which have been shown to affect Cs NP properties (e.g. size, PDI, ZP and morphology) include the ionic strength of the formulation medium, concentration of both polyelectrolytes prior to crosslinking and the degree of deacetylation (DDA%)/MW of the employed Cs (Qinna *et al.*, 2015). It is worth noting that the latter two factors confer different properties to Cs, which can affect properties associated with the NPs it produces:

- Cs ability to complex with opposing charged polyelectrolytes is dependent on the DDA% (Anitha *et al.*, 2014)

- NP dimensions and ZP; larger size and higher ZP reported with higher MW and DDA% Cs (Alameh *et al.*, 2017)
- NP toxicity; lower MW and DDA%, reported to have less toxicity than that of high MW Cs (Kean and Thanou, 2010)
- NP EE%; higher in NPs produced with high MW and DDA% Cs (Jelvehgari *et al.*, 2010)
- Release kinetics; Slower for high MW Cs NPs (Gan and Wang, 2007)

The DDA% and MW of the Cs used to produce NPs play a significant role in their final properties. Vozza *et al.*, (2018b Chapter 7), ^{1}H-NMR calculated the DDA% of CL113 and fCs, to be 85 ± 4% and 86 ±6 % respectively. As such, the variance between the ZP and EE% values for the produced NPs is unlikely to be related to the DDA% of the Cs used for their production. In this regard, for CL113 vs fCs NPs, the apparent difference in ZP and EE%, may be a result of a difference in their MW (156±24 vs 110±6 kDa).Gan and Wang, (2007), reported that the EE% of BSA in Cs NPs was increased from 61.1 to 69.9 and 78.2 % as a result of an increase in Cs molecular weight from low to medium and high, indicating that the longer Cs chains could offer more reactive sites for the formation of hydrogen bonds with the BSA protein molecules. Additionally, at low pH, Cs is fully extended in solution and the higher the MW weight of Cs, the greater the electrostatic repulsion between the primary amines on the backbone (thus reduced steric hinderance), which would allow for increased interactions between opposing polyelectrolytes and thus increased EE% (Almalik *et al.*, 2013). With this in mind, it is reasonable to suggest that the higher MW of the fCs used to produce the NPs in this work allowed for higher EE% and ZP compared to their CL113 counterparts, which is consistent with the findings of other authors (Ing *et al.*, 2012).

8.3.4 NP morphology - Scanning electron microscopy

Figure 8.3 shows the SEM images of $SeCys_2$ loaded NPs formulated with fCs (A) or CL113 (B). Spheroidal, well distributed particles with slightly irregular surface morphology were observed for $SeCys_2$ loaded CL113 NPs (8.3 B). This may be attributable to the electrostatic interaction of the negatively charged carboxyl groups of zein facilitating a thin layer membrane around the positively charged amines residues of Cs (Luo *et al.*, 2011) with variation in surface density of zein protein on the Cs NP surface and porosity of Cs core (Pan *et al.*, 2015). Additionally, low MW Cs NPs have been reported to facilitate surface binding of negatively charged polyelectrolytes such as hyaluronic acid, due to their less porous more compact dimensions (Almalik *et al.*, 2013). fCs NPs showed smooth, dense, spheroidal morphologies with higher polydispersity than that of the CL113 NPs, which agrees with the DLS observations for PDI (Table 8.3). This may be related to the distribution of the polymer chains of fCs in comparison to CL113, which is certified to possess a MW of 110-150 kDa, and as such is likely fractionally separated to this range prior to sale. The larger the spread of the Cs chain lengths, the larger the variance in NP PDI to be expected. Additionally, hyaluronic acid has appeared to diffuse more deeply into the bulk of high MW Cs NPs, reducing the observable surface coating appearance via SEM and atomic force microscopy (Almalik *et al.*, 2013), which agrees with the observed properties of the higher MW fCs NPs. In terms of the particle size, comparing SEM and DLS measurements, larger sizes were observed by SEM imaging (approx. 90-150 nm larger), which may be due to the rapid evaporation of residual ethanol (present in the final suspension media) during the spin casting process and subsequent flattening of the particles on the grid (da Rosa *et al.*, 2015).

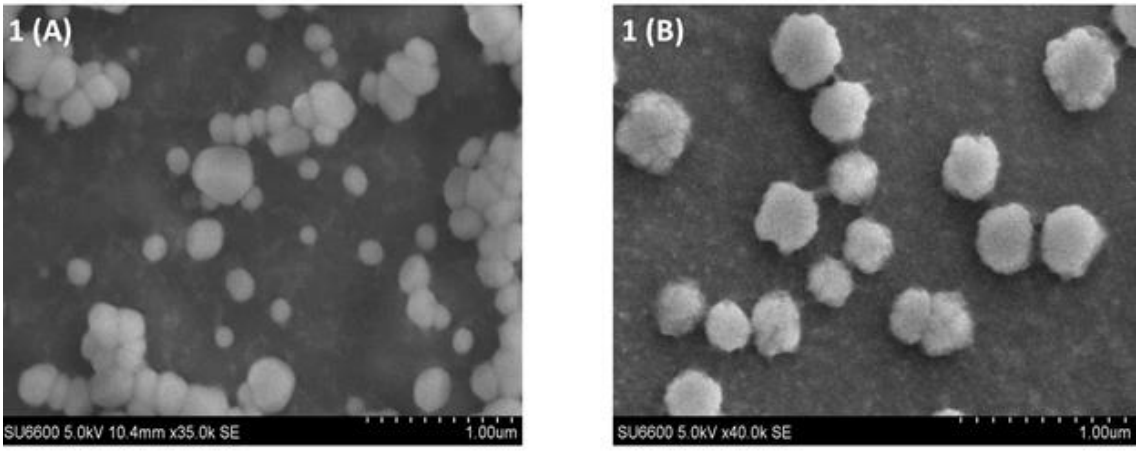

Figure 8.3 SEM image of (A) $SeCys_2$ fCs NPs and (B) $SeCys_2$ CL113 NPs coated with zein.

8.3.5 Accelerated stability analysis of fungal derived fCs NPs loaded with $SeCys_2$

Figure 8.4 shows the kinetic behaviour of the $SeCys_2$ loaded fCs NP properties: size (A), PDI (B) and ZP (C), at temperatures ranging from 60-80 °C. The stability of the NPs decreased with increasing temperature. Little change was detected for all properties at 60 °C, over the course of 720 min, whereas a more pronounced influence on size and PDI and a decrease in ZP was observed at 70 °C after 300 min. At 80 °C, destabilisation of the NP complexes was evident according to all properties, whereby size increased from approximately 300 nm to > 700 nm, PDI from approximately 0.2 to >0.9 and ZP reduced from approximately 36 mV to < 18 mV, indicating that aggregation of the NPs had occurred (Wu, Zhang and Watanabe, 2011).

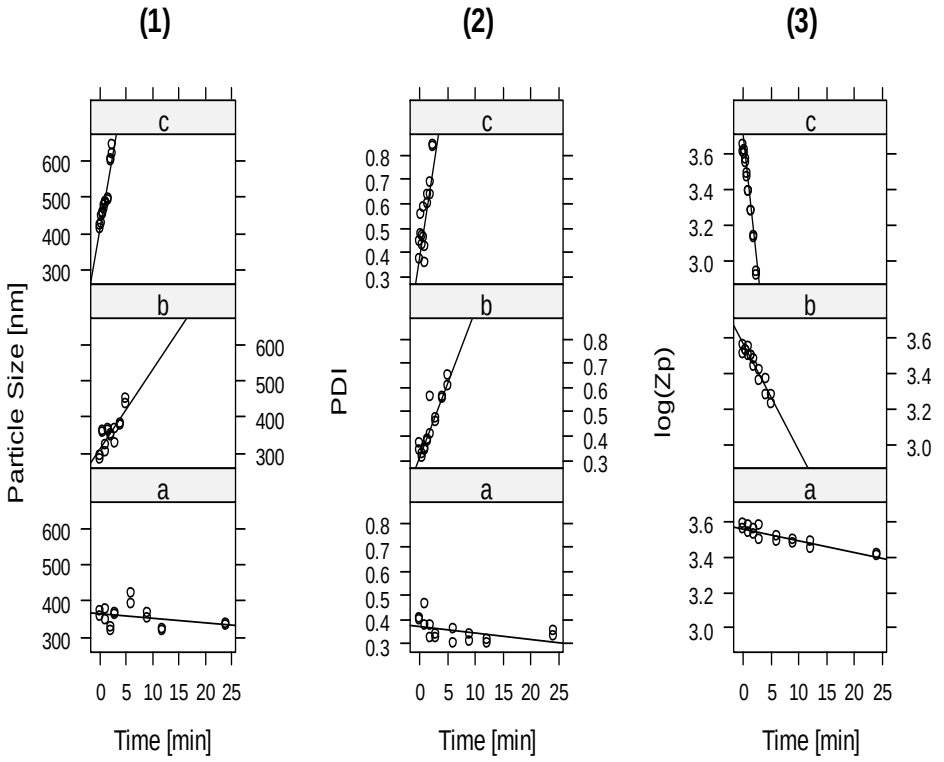

Figure 8.4 (1) Particle size, (2) PDI and (3) ZP analysis of fCs $SeCys_2$ loaded NPs exposed to (a) 60 °C, (b) 70 °C and (c) 80 °C, over time periods of 120, 300 and 720 min, respectively. N=3.

The one-step nonlinear regression analysis of the kinetic experiments shows that the particle size and PDI of $SeCys_2$ loaded fCs NPs fit to a zero-order kinetic behaviour, with an Arrhenius dependence of ln (kref@70 °C) = 6.43 ± 4.12 min^{-1} and Ea = 291.35 ± 62.35 kJ/mol for size, and a ln (kref@70 °C) = 0.026 ± 0.007 min^{-1}, and an Ea = 192.39 ± 24.05 kJ/mol for PDI respectively (Figure 8.4). Regarding ZP, an apparent first order mechanism fits the data better than an apparent zero order model, with an Arrhenius dependence of ln (kref@70 °C) = 0.051 ± 0.004 min^{-1} and Ea = 148.10 ± 6.581 kJ/mol. Lastly, a linear correlation is evident between 1/T and ln k, indicating that the formulations will be stable under normal storage conditions (Figure 8.5).

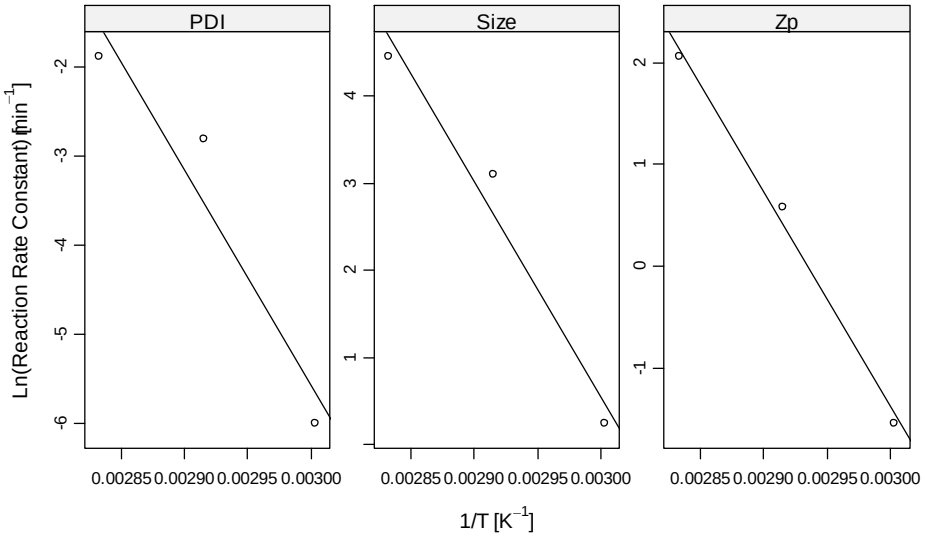

Figure 8.5 Arrhenius plots for the PDI, Size and ZP accelerated studies of $SeCys_2$ loaded NPs. N=3.

No significant difference in kinetic behaviour was observed between the $SeCys_2$ loaded CL113 and fCs NPs properties (size (A), PDI (B) and ZP (C)) at temperatures ranging from 60-80 °C. As shown previously by Vozza *et al.*, (2018a, 2018b, Chapters 5 & 6), the SeAAs (SeMet, MSC or $SeCys_2$) used to load the NPs did not have an effect on the formulation stability, which lends weight to the argument that the contributing factors to the formulation stability lies with the Cs:zein complex rather than the loaded SeAA. The complexation of protein (in this instance zein) with polysaccharide (Cs) systems involves non-covalent interactions that can change the interfacial behaviour and stability of food colloids (Ghosh *et al.*, 2012). When Cs is blended with a polymer, the miscibility between their molecules is a very significant factor, especially for the mechanical properties of the blend (Sakurai, Maegawa and Takahashi, 2000). For example, previous differential scanning calorimetry studies have shown that pure zein has a transition temperature around 150 °C, which was attributed to thermal denaturation of this protein (Neo *et al.*, 2013). By harnessing the thermal stability of Cs (transition temperature of 203°C) and combining it with the aromatic side groups and double bonds of zein, it is possible to

greatly increase the stability of labile nutraceuticals against thermal degradation and oligomerization (Torres-Giner, Ocio and Lagaron, 2009; Luo *et al.*, 2013).

Zein coated tablets exhibit stronger resistance to abrasion, high humidity and high temperatures than a variety of commercial sugar-coated tablets (Y. Zhang *et al.*, 2015). Moreover, it has been reported that the bi-layer approach for encapsulation of BAs leads to a better control of the NP interface structure, charge, thickness and permeability, and substantially enhanced stability (Hu and McClements, 2014). Notably, the net attractive and net repulsive strength character of protein–polysaccharide non-covalent physical interactions can vary substantially, depending primarily on environmental conditions such as pH, ionic strength, and temperature (Semenova *et al.*, 2014). In this work, the conditions (presence of salt) used to prepare the NPs, in addition to the strong bonding between the zein and Cs complex, may have been a contributing factor to the enhanced stability of the formulation and is consistent with our previous observations (Danish, *et al.*, 2017a; Vozza *et al.*, 2018a, 2018b).

8.3.6 Cytotoxicity assessment of fungal derived Cs NPs loaded with $SeCys_2$

In the work of Vozza *et al.*, (2018b, Chapter 6), the tested concentrations of native $SeCys_2$ and loaded CLL3 NPs (25, 50 & 100 uM) where more reflective of supra-nutritional Se levels, reported to be involved in the prevention of several types of cancer, including lung, colorectal, and prostate cancers (Rikiishi, 2007; Suzuki *et al.*, 2010; Bao *et al.*, 2015). To gain more insight into the potential cytotoxicity of $SeCys_2$ as a basal nutritional supplement (in native form and encapsulated within fCs NPs), additional test concentrations for nutritionally low (0.25, 2.5 uM) and adequate (5, 10 uM), Se status, were investigated (Hawkes *et al.*, 2008). The supra-nutritional concentrations (25, 50 and

100 uM), were also assessed, to maintain consistency in comparing the $SeCys_2$ loaded CL113 NPs to the fCs NPs, in Caco-2 human epithelial cells, and HepG2 human liver hepatocellular cells, using the MTS assay. As the NPs will be exposed to the intestinal epithelium following oral delivery (leading to its facilitated transport and uptake), time points were selected with the intention to mimic *in vivo* conditions for each cell type, to assess the potential cytotoxicity of the formulated NPs (Gleeson *et al*., 2015; Brayden *et al*., 2015). Caco-2 cells were exposed for 4h (Figure 8.6, A, B)) and HepG2 cells for 72h (Figure 8.7, A).

In Caco-2 exposures, no cytotoxicity was observed for $SeCys_2$ native, unloaded or $SeCys_2$ loaded NPs, in comparison to the negative control, across all tested concentrations (Figure 8.6 A, B). This is consistent with previous observations (Vozza *et al.*, 2018b, Chapter6) and in agreement with the works of others (Marschall *et al.*, 2016; Takahashi, Suzuki and Ogra, 2017).

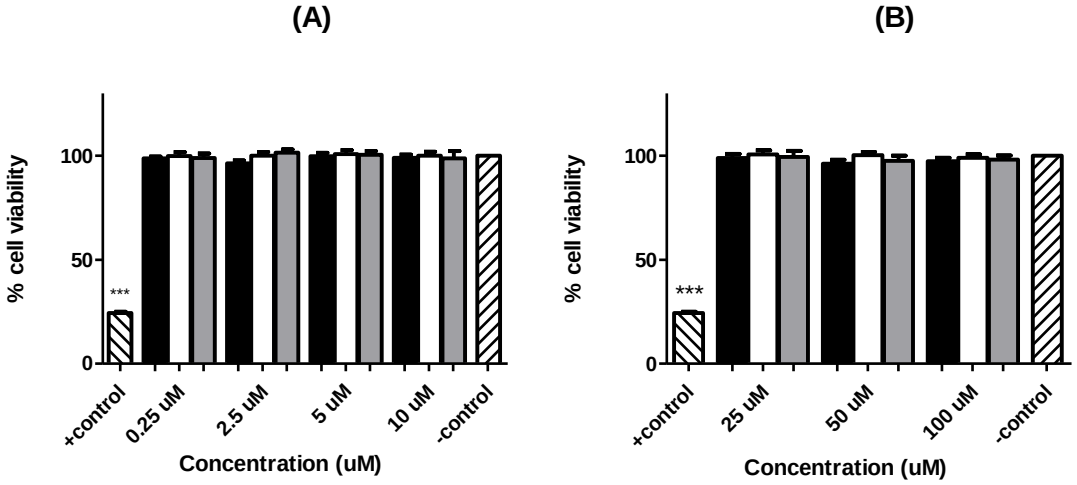

Figure 8.6 Cytotoxicity assessment of ■ $SeCys_2$, □ unloaded fCs NPs and ▭ $SeCys_2$ loaded fCs NPs, exposed for 4h in Caco2 cell lines at (a) low (0.25, 2.5 uM) and adequate nutritional level (5-10 uM) and (b) supra-nutritional level (25-100 uM) concentrations. Percentage (%) of MTS converted was compared to untreated control. 1-Way ANOVA with Dunnett's post-test *** $p < 0.001$. Each value presented was normalised against untreated control and calculated from three separate experiments, each of which included six replicates. N=3.

Regarding native $SeCys_2$ exposure to HepG2 cell lines, no significant toxicity was observed for test concentrations ranging from 0.25-5 uM (≤94 % viability). However, a dose dependant reduction in cell viability was observed for concentrations exceeding 5 uM, which levelled off at 50 uM test concentrations (≤40 % viability). As can be seen in Figure 8.7 A, the encapsulation of $SeCys_2$ within the fCs NP matrix conferred protection to the HepG2 cells after 72 hr exposure, from 0.25-25 uM test concentrations. However, this shielding effect was lost at concentrations >50 uM, showing equivalent toxicity to that of the native $SeCys_2$ (≤40 % viability). Nevertheless, the IC_{50} of native $SeCys_2$ was found to be 12.8 ± 3.6 uM vs 32.5 ± 1.4 uM for $SeCys_2$ loaded fCs NPs, showing that the cytotoxic effects of pure $SeCys_2$ can be reduced with the applied formulation (Figure 8.7 B, C)

Similar results for the toxicity of native $SeCys_2$ were observed by Takahashi, Suzuki and Ogra, (2017), who reported no significant change in the viability of Caco-2 cell lines after 6 hr, although significant toxicity to HepG2 cells was observed at 100 uM, comparable to that of the inorganic form selenite, after prolonged exposure (48 hr). As the toxicity of $SeCys_2$ has been shown to be comparable to that of selenite, it has been proposed by others that the cellular overload of metabolites (such as selenide moieties ($-Se^-$) and (HSe^-) produced during selenoprotein formation or excretion (Rayman, Infante and Sargent, 2008; Marschall *et al.*, 2016) is responsible for this affect. This is conceivable, as the reduction of $SeCys_2$ to SeCys in the cell would result in the generation of a highly reactive and sensitive to oxidation selenyl group (-SeH), whose relatively low pKa of 5.2 would promote the formation of ($-Se^-$) at physiological pH (Iwaoka, 2014).

Lastly, the unloaded NPs showed a significant proliferative effect in HepG2 cells over the range of 0.25-50 uM test concentrations, although at 100 uM, this effect was lost. Previous studies have shown the combination of zeins demonstrated cytocompatibility with NIH 3T3 and human liver cells (HL-7702) in terms of cell adhesion and proliferation (Dong, Sun and Wang, 2004), and an increase in fibroblast production caused by the presence of Cs (Rajam *et al.*, 2011). Thus, it is reasonable to suggest that the observed protective effects of the encapsulated native $SeCys_2$ is attributable to the fCs:zein NP matrix.

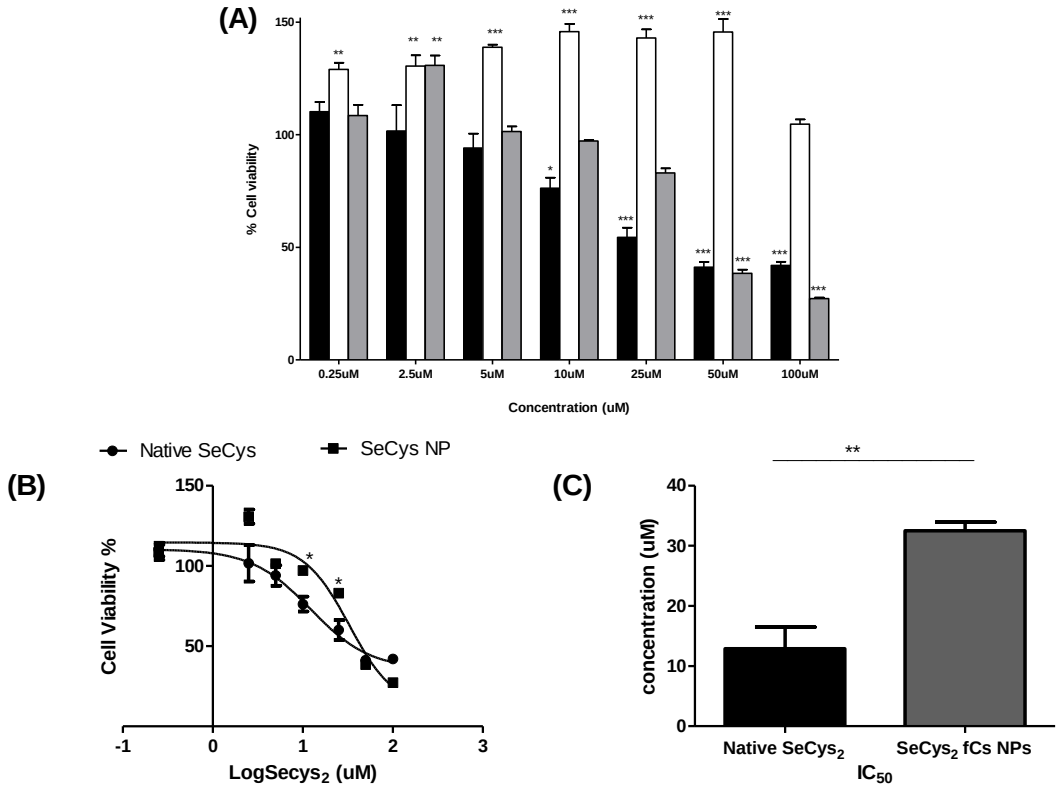

Figure 8.7: (A) Cytotoxicity assessment of ■ $SeCys_2$, □ unloaded fCs NPs and ▭ $SeCys_2$ loaded fCs NPs, exposed at test concentrations of 0.25-100 uM, for 72 hr in HepG2 cell lines. MTS converted was compared to untreated control. (B) Dose-response curve was constructed by plotting cell viability versus log concentration of (-●-) $SeCys_2$ and (-■-) $SeCys_2$ loaded fCs NPs, and (C) corresponding IC_{50} values of ■ $SeCys_2$ and ▭ $SeCys_2$ loaded fCs NPs**.** * p< 0.05, ** p< 0.01, *** P< 0.001, 1-Way ANOVA with Dunnett's post-test (A), 2-Way ANOVA with Bonferroni post-test (B), and Students t-test (C). N=3.

8.3.7 *In vitro* release studies

Figure 8.8 shows the cumulative release profile of the $SeCys_2$ loaded fCs NPs, coated with zein, after subjection to 2 hrs in an SGF environment (pH 1.2) representative of the stomach, followed by a compartmental change to SIF (pH 6.8), representative of the intestine, for 4 hrs. For ease of comparison, the release of $SeCys_2$ from NPs produced with CL113 (Vozza *et al.*, 2018b, Chapter 6) is displayed in this figure also. As can be

seen, 32 ± 4.5 % of $SeCys_2$ was released from the fCs NPs after 2 hr in SGF, followed by 30 ± 2 % release in SIF for 4 hr. In comparison, the release of $SeCys_2$ from NPs formulated with CL113 was significantly faster in SGF (45 ± 4 %) after 2 hr, with a marginally slower release (24 ± 4 %), compared to fCs NPs, after subjection to a SIF environment (4 hr).

Three basic mechanisms that are typically employed to describe the release of drugs from polymeric particles are, swelling/erosion, diffusion, and degradation (Liechty *et al.*, 2010). The prominence of each can depend on the conditions of the environment. Therefore, the release kinetics of $SeCys_2$ loaded fCs NPs were monitored sequentially in SGF and SIF controlled release experiments. As two different simulated fluids were used for this study, representing the pH environment in the stomach (SGF) and the jejunum target site in the intestine (SIF), their release profile was modelled using a swelling, Peppas equation (8.6) and (8.7) (Siepmann and Peppas, 2011, Danish *et al*., 2017a).

For the SGF:

$$\frac{\boldsymbol{M_t}}{\boldsymbol{M_\infty}} = \boldsymbol{ks_1} * \sqrt{\boldsymbol{time}} + \boldsymbol{ks_2} * \boldsymbol{time}$$

(Equation 8.6)

where M_t is the diffused mass at a given time, M_∞ is the asymptotic diffused mass at infinite time, and ks_1 and ks_2 are the diffusive and relaxation rate constants respectively.

For the SIF:

$$\frac{\boldsymbol{M_t}}{\boldsymbol{M_\infty}} - \frac{\boldsymbol{M_{120}}}{\boldsymbol{M_\infty}} = \boldsymbol{ki_1} * \left(\sqrt{\boldsymbol{time - 120}}\right) + \boldsymbol{ki_2} * (\boldsymbol{time - 120})$$

(Equation 8.7)

where M_{120} is the predicted diffused mass at the time of changing from SGF to SIF (120 min), ki_1 and ki_2 are diffusive and relaxation rate constants.

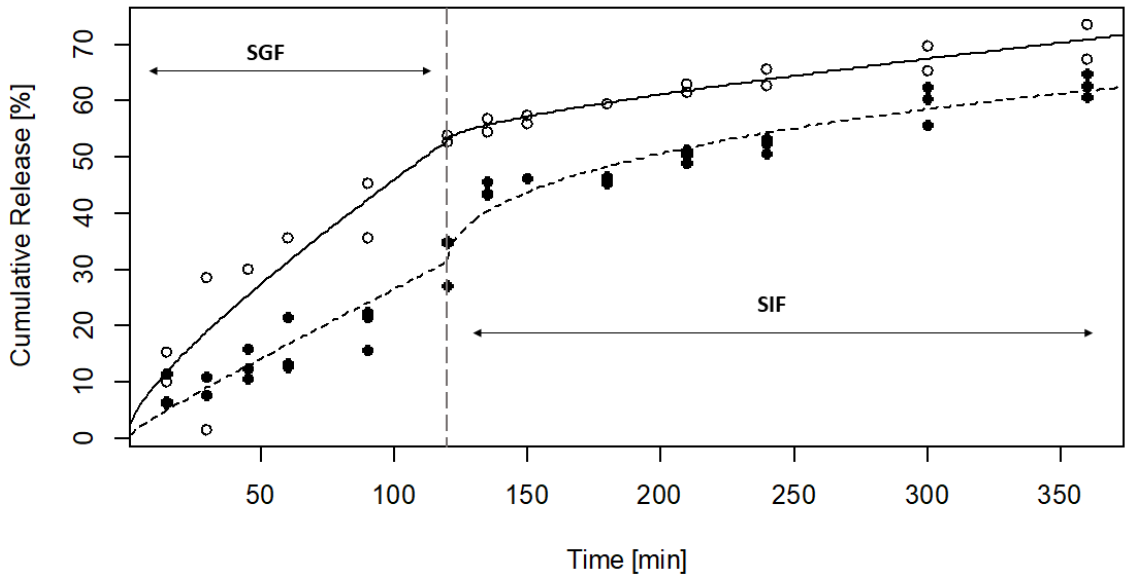

Figure 8.8 Release kinetics of $SeCys_2$ loaded CL113 (–○–) and fCs (--●--) NPs, coated with zein, after 2 hr in SGF (pH 1.2) and 4 hrs in SIF (pH 6.8). Lines indicate the model predictions of Equations 8.6 and 8.7. N=3.

The release of $SeCys_2$ from the CL113 and fCs nanoparticles was best fitted with a combination of diffusion and relaxation mechanisms. The fits of the model are illustrated by solid lines in Figure 8.8. Table 8.4 presents the fitted values for the rate constants in SGF (ks) and SIF (ki) for both $SeCys_2$ loaded (CL113and fCs) NPs, divided into diffusion and relaxation mechanisms ($_1$ and $_2$) (Equations 8.6 & 8.7).

For $SeCys_2$ loaded fCs NPs, subjected to the simulated stomach environment (SGF, pH 1.2), no statistically significant ks_1 parameter was found, indicating that the primary mechanism for release in the stomach was via relaxation, i.e. slower release, approaching zero-order kinetics. Conversely, after 2 hr subjected to the SGF environment, a compartmental change was employed to mimic the movement of the $SeCys_2$ fCs NPs to the intestinal environment (SIF, pH 6.8), whereupon a diffusion (ki_1) mechanism was observed ($p<0.05$) indicating that the primary mechanism for release in the stomach was via diffusion, i.e. slower release, approaching zero-order kinetics.

In contrast, a combination of ki_1 and ki_2 mechanisms in the stomach (SGF) was observed for the release of the $SeCys_2$ loaded CL113 NPs and no statistically significant ki_2 parameter was found for the intestinal compartment, indicating that, in the small intestine (jejunum), at pH 6.8, relaxation is the primary mechanism of release for $SeCys_2$.

Table 8.4 Swellable model parameters for kinetic release studies of $SeCys_2$ loaded fCs or CL113 NPs, coated with zein. ks represents the stomach compartment and ki the intestinal compartment, divided into diffusion and relaxation mechanisms ($_1$ and $_2$). All parameters listed where statistically significant, ($^*p < 0.05$).

CL113 $SeCys_2$ loaded NPs	
Coefficients	**Estimate ($min^{-1/2}$)**
ks_1	2.29±0.68
ks_2	0.22±0.07
ki_1	1.15±0.20
fCs $SeCys_2$ loaded NPs	
ks_2	0.24±0.05
ki_1	1.98±0.16

As the only variable between these two formulations relates to the Cs used to produce the NPs, which matched regarding DDA%, it is conceivable that the reduced release rate observed for the fCs NPs may be related to the MW of the precursor fCs being higher than that of CL113 (156±24 vs 110±6 kDa). On exposure to the dissolution fluids (SGF and SIF), the Cs complex will become hydrated forming a viscous gel layer that slows down further seeping-in of dissolution fluids towards the core of the NP (Miladi *et al.*, 2015). The subsequent Cs swelling under these conditions allows for the drug release to follow a diffusion oriented mechanism, which is then typically trailed by the mechanical erosion of the swollen Cs hydrogel (Mohammed *et al.*, 2017). In tandem, subsequent hydration and swelling of the system is heavily dependent upon whether the Cs erodes further. With this in mind, it was observed that the release of $SeCys_2$ from both Cs:zein NPs was pH dependent, indicative of Cs solubility in acidic media (Yuan *et al.*, 2013), although the slower release observed for the fCs NPs was most likely attributed to its

higher MW. For example, Gan and Wang, (2007), showed that the release kinetics of BSA from Cs NPs decreased significantly upon increasing molecular weights. The reduction observed in that study was postulated to arise from the protein requiring increased swelling and degradation of the NPs which was hindered by a greater crosslink density of TPP with high MW, causing increased chain packing and rigidity, as well as increased inter-chain bonding. Additionally, the higher the MW, the larger proportion of ($-NH_2$) residues, allowing for the encapsulated drug to be associated multiple sites on the Cs polymer, thus reducing the overall release from the system (Dash *et al.*, 2011). Overall, despite the high-water solubility of $SeCys_2$ there was good control of drug release in the simulated physiological environment of stomach and small intestine for both fCs and CL113 NPs, with fCs displaying the most optimum release profile, most likely a consequence of higher MW.

8.4 Conclusion

A RP-HPLC-PDA method was validated to analyse Se supplemented *A. bisporus*. The predominant species was $SeCys_2$ at 616 ± 23 µg/g DMP, with modest amounts of SeMet identified also, inferring that Se supplemented mushrooms may be a feasible source for organic Se. fCs was then used to formulate $SeCys_2$ loaded NPs, with optimum properties for oral delivery formed by coating the produced NPs at a 1:0.75 mass ratio of Cs:zein, resulting in sizes of 299.5 ± 47.1 nm, PDI 0.324 ± 0.176, ZP 38.7 ± 2.1, and EE% of 84.4 ± 1.2. SEM analysis showed smooth spheroidal, well distributed particles were produced. MTS cytotoxicity studies on $SeCys_2$ loaded NPs showed no decrease in cellular viability in Caco-2 (intestinal) cells after 4 hr exposures across all test concentrations. However, a significant reduction was observed when compared to pure $SeCys_2$, across all test concentrations in HepG2 liver cells after 72 hr exposure. Accelerated thermal stability of the produced NPs indicated good stability under normal storage conditions. After 6 hr exposure to simulated gastrointestinal tract environments, the sustained release profile of the formulation showed that 62.0 ± 2.5 % $SeCys_2$ was released. By encapsulating $SeCys_2$ into a NP delivery system, improved oral administration of this molecule may be achieved, which could be of beneficial use for the supplementation of food products with these essential nutrients. All assessments on the fCs NPs properties were compared against $SeCys_2$ CL113 NPs developed in previous work by Vozza *et al.*, (2018b, Chapter 6), showing that equivalent NPs formulations could be produced. This study provides robust methods to formulate and assess $SeCys_2$ fCs NPs, in addition to the speciation analysis of SeAAs in supplemented *A. bisporus*, inferring that the encapsulation of $SeCys_2$ into a NP delivery system can be achieved using food-derived components whilst also providing a viable approach to oral administration of this molecule.

8.5 References

Alameh, M. *et al.* (2017) 'siRNA Delivery with Chitosan: Influence of Chitosan Molecular Weight, Degree of Deacetylation, and Amine to Phosphate Ratio on in Vitro Silencing Efficiency, Hemocompatibility, Biodistribution, and in Vivo Efficacy', *Biomacromolecules*, 19(1), pp. 112–131.

Almalik, A. *et al.* (2013) 'Hyaluronic acid-coated chitosan nanoparticles: Molecular weight-dependent effects on morphology and hyaluronic acid presentation', *Journal of Controlled Release*, 172(3), pp. 1142–1150.

Amaro, M. I. *et al.* (2015) 'Formulation, stability and pharmacokinetics of sugar-based salmon calcitonin-loaded nanoporous/nanoparticulate microparticles (NPMPs) for inhalation', *International Journal of Pharmaceutics*, 483(1–2), pp. 6–18.

Amoako, P. O., Uden, P. C. and Tyson, J. F. (2009) 'Speciation of selenium dietary supplements; formation of S-(methylseleno)cysteine and other selenium compounds', *Analytica Chimica Acta*, 652(1–2), pp. 315–323.

Anitha, A. *et al.* (2014) 'Chitin and chitosan in selected biomedical applications', *Progress in Polymer Science*, 39(9), pp. 1644–1667.

Banerjee, A. *et al.* (2016) 'Role of nanoparticle size, shape and surface chemistry in oral drug delivery', *Journal of Controlled Release*, 238, pp. 176–185.

Bao, P. *et al.* (2015) 'Selenite-induced toxicity in cancer cells is mediated by metabolic generation of endogenous selenium nanoparticles', *Journal of Proteome Research*, 14(2), pp. 1127–1136.

Benshitrit, R. C. *et al.* (2012) 'Development of oral food-grade delivery systems: Current knowledge and future challenges', *Food & Function*, 3(1), p. 10.

Brayden, D. J., Cryan, S.-A., *et al.* (2015) 'High-content analysis for drug delivery and nanoparticle applications', *Drug Discovery Today*, 20(8), pp. 942–957.

Brayden, D. J., Maher, S., *et al.* (2015) 'Sodium caprate-induced increases in intestinal permeability and epithelial damage are prevented by misoprostol', *European Journal of Pharmaceutics and Biopharmaceutics*, 94, pp. 194–206.

Brayden, D. J., Gleeson, J. and Walsh, E. G. (2014) 'A head-to-head multi-parametric high content analysis of a series of medium chain fatty acid intestinal permeation enhancers in Caco-2 cells', *European Journal of Pharmaceutics and Biopharmaceutics*, 88(3), pp. 830–839.

British Pharmacopoeia Commission (2016) *British Pharmacopoeia: Appendix XII B. Dissolution*. London: TSO.

Calderon L. *et al.* (2013) 'Nano and microparticulate chitosan-based systems for antiviral topical delivery', *European Journal of Pharmaceutical Sciences*, 48, pp. 216–222.

Calvo, P. *et al.* (1997) 'Novel hydrophilic chitosan-polyethylene oxide nanoparticles as protein carriers', *Journal of Applied Polymer Science*, 63(1), pp. 125–132.

Cao, S. *et al.* (2014) 'Se-methylselenocysteine offers selective protection against toxicity and potentiates the antitumour activity of anticancer drugs in preclinical animal models', *British Journal of Cancer*, 110(7), p. 1733.

Capelo, J. L. *et al.* (2006) 'Trends in selenium determination/speciation by hyphenated techniques based on AAS or AFS', *Talanta*, 68(5), pp. 1442–1447.

Casiot, C. *et al.* (1999) 'Sample preparation and HPLC separation approaches to speciation analysis of selenium in yeast by ICP-MS', *Journal of Analytical Atomic Spectrometry*, 14(4), pp. 645–650.

Chen, M. C. *et al.* (2013) 'Recent advances in chitosan-based nanoparticles for oral delivery of macromolecules', *Advanced Drug Delivery Reviews*, pp. 865–879.

Danish, M. K. *et al.* (2017a) 'Comparative study of the structural and physicochemical properties of two food derived antihypertensive tri-peptides, Isoleucine-Proline-Proline and Leucine-Lysine-Proline encapsulated into a chitosan based nanoparticle system', *Innovative Food Science & Emerging Technologies*, 44, pp. 139–148.

Danish, M. K. *et al.* (2017b) 'Formulation, Characterization and Stability Assessment of a Food-Derived Tripeptide, Leucine-Lysine-Proline Loaded Chitosan Nanoparticles', *Journal of Food Science*, 82(9), pp. 2094–2104.

Dash, M. *et al.* (2011) 'Chitosan - A versatile semi-synthetic polymer in biomedical applications', *Progress in Polymer Science*, 36(8), pp. 981–1014.

Diop, M. *et al.* (2015) 'Design, characterisation, and bioefficiency of insulin-chitosan nanoparticles after stabilisation by freeze-drying or cross-linking', *International Journal of Pharmaceutics*, 491(1–2), pp. 402–408.

Dong, J., Sun, Q. and Wang, J.-Y. (2004) ‘Basic study of corn protein, zein, as a biomaterial in tissue engineering, surface morphology and biocompatibility’, *Biomaterials*, 25(19), pp. 4691–4697.

Dumont, E., Vanhaecke, F. and Cornelis, R. (2006) ‘Selenium speciation from food source to metabolites: a critical review’, *Analytical and Bioanalytical Chemistry*, 385(7), pp. 1304–1323.

Elzoghby, A. O., Samy, W. M. and Elgindy, N. a. (2012) ‘Protein-based nanocarriers as promising drug and gene delivery systems’, *Journal of Controlled Release*, 161(1), pp. 38–49.

EMEA (1995) ‘Validation of analytical prrocedures: definitions and methodology’, *ICH Harmonised Tripartite Guideline*, 20(121), p. 278.

Etheridge, M. L. *et al.* (2013) ‘The big picture on nanomedicine: the state of investigational and approved nanomedicine products.’, *Nanomedicine : Nanotechnology, Biology, and Medicine*, 9(1), pp. 1–14.

Evans, S. O., Khairuddin, P. F. and Jameson, M. B. (2017) ‘Optimising Selenium for Modulation of Cancer Treatments’, *Anticancer Research*, 37(12), pp. 6497–6509.

Falandysz, J. (2008) ‘Selenium in edible mushrooms’, *Journal of Environmental Science and Health Part C*, 26(3), pp. 256–299.

Fan, C. *et al.* (2013) ‘Selenocystine potentiates cancer cell apoptosis induced by 5-fluorouracil by triggering reactive oxygen species-mediated DNA damage and inactivation of the ERK pathway’, *Free Radical Biology and Medicine*, 65, pp. 305–316.

Gan, Q. and Wang, T. (2007) ‘Chitosan nanoparticle as protein delivery carrier-Systematic examination of fabrication conditions for efficient loading and release’, *Colloids and Surfaces B: Biointerfaces*, 59(1), pp. 24–34.

Gergely, V. *et al.* (2006) ‘Selenium speciation in Agaricus bisporus and Lentinula edodes mushroom proteins using multi-dimensional chromatography coupled to inductively coupled plasma mass spectrometry’, *Journal of Chromatography A*, 1101(1–2), pp. 94–102.

Ghosh, A. K. *et al.* (2012) ‘Polysaccharide-protein interactions and their relevance in food colloids’, *The complex world of polysaccharides*. InTech.

Haberhauer-Troyer, C. *et al.* (2003) ‘Comparison of different chloroformates for the derivatisation of seleno amino acids for gas chromatographic analysis’, *Journal of Chromatography A*, 1015(1–2), pp. 1–10.

Hawkes, W. C. *et al.* (2008) 'Response of selenium status indicators to supplementation of healthy North American men with high-selenium yeast', *Biological Trace Element Research*, 122(2), p. 107.

Hosseinzadeh, H. *et al.* (2012) 'Chitosan-Pluronic nanoparticles as oral delivery of anticancer gemcitabine: Preparation and in vitro study', *International Journal of Nanomedicine*, 7, pp. 1851–1863.

Hu, K. and McClements, D. J. (2014) 'Fabrication of surfactant-stabilized zein nanoparticles: A pH modulated antisolvent precipitation method', *Food Research International*, 64, pp. 329–335.

Huerta, V. D., Sánchez, M. L. F. and Sanz-Medel, A. (2005) 'Qualitative and quantitative speciation analysis of water soluble selenium in three edible wild mushrooms species by liquid chromatography using post-column isotope dilution ICP–MS', *Analytica Chimica Acta*, 538(1), pp. 99–105.

ICH (2005) 'ICH Topic Q2 (R1) Validation of Analytical Procedures : Text and Methodology', *International Conference on Harmonization*, 1994 (November 1996), p. 17.

Infante, H. G., Hearn, R. and Catterick, T. (2005) 'Current mass spectrometry strategies for selenium speciation in dietary sources of high-selenium', *Analytical and Bioanalytical Chemistry*, 382(4), pp. 957–967.

Ing, L. Y. *et al.* (2012) 'Antifungal activity of chitosan nanoparticles and correlation with their physical properties', *International Journal of Biomaterials*, 2012.

Iwaoka, M. (2014) 'Antioxidant organoselenium molecules', *Organoselenium Chemistry: Between Synthesis and Biochemistry*. Bentham Books, pp. 361–378.

Janes, K. A., Calvo, P. and Alonso, M. J. (2001) 'Polysaccharide colloidal particles as delivery systems for macromolecules', *Advanced Drug Delivery Reviews*, 47(1), pp. 83–97.

Jelvehgari, M. *et al.* (2010) 'Development of pH-sensitive insulin nanoparticles using Eudragit L100-55 and chitosan with different molecular weights', *AAPS Pharmscitech*, 11(3), pp. 1237–1242.

Kápolna, E. *et al.* (2007) 'Selenium speciation studies in Se-enriched chives (Allium schoenoprasum) by HPLC-ICP–MS', *Food Chemistry*, 101(4), pp. 1398–1406.

Kean, T. and Thanou, M. (2010) 'Biodegradation, biodistribution and toxicity of chitosan', *Advanced Drug Delivery Reviews*, pp. 3–11.

Khanam, A. and Platel, K. (2016) ‘Bioaccessibility of selenium, selenomethionine and selenocysteine from foods and influence of heat processing on the same’, *Food Chemistry*, 194, pp. 1293–1299.

Lacourciere, G. M. and Stadtman, T. C. (1999) ‘Catalytic properties of selenophosphate synthetases: comparison of the selenocysteine-containing enzyme from Haemophilus influenzae with the corresponding cysteine-containing enzyme from Escherichia coli’, *Proceedings of the National Academy of Sciences*, 96(1), pp. 44–48.

Liechty, W. B. *et al.* (2010) ‘Polymers for Drug Delivery Systems’, *Annual Review of Chemical and Biomolecular Engineering*, 1, pp. 149–173.

Lin, A. H., Liu, Y. M. and Ping, Q. N. (2007) ‘Free amino groups on the surface of chitosan nanoparticles and its characteristics’, *Acta Pharmaceutica Sinica*, 42(3), pp. 323–328.

Lobo, V. *et al.* (2010) ‘Free radicals, antioxidants and functional foods: Impact on human health’, *Pharmacognosy Reviews*, 4(8), p. 118.

Luo, Y. *et al.* (2010) ‘Preparation, characterization and evaluation of selenite-loaded chitosan/TPP nanoparticles with or without zein coating’, *Carbohydrate Polymers*, 82(3), pp. 942–951.

Luo, Y. *et al.* (2011) ‘Preparation and characterization of zein/chitosan complex for encapsulation of ??-tocopherol, and its in vitro controlled release study’, *Colloids and Surfaces B: Biointerfaces*, 85(2), pp. 145–152.

Luo, Y. *et al.* (2013) ‘Encapsulation of indole-3-carbinol and 3,3′-diindolylmethane in zein/carboxymethyl chitosan nanoparticles with controlled release property and improved stability’, *Food Chemistry*, 139(1–4), pp. 224–230.

Luo, Y. and Wang, Q. (2014) ‘Zein-based micro- and nano-particles for drug and nutrient delivery: A review’, *Journal of Applied Polymer Science*, 131(16), pp. 1–12.

Marschall, T. A. *et al.* (2016) ‘Differing cytotoxicity and bioavailability of selenite, methylselenocysteine, selenomethionine, selenosugar 1 and trimethylselenonium ion and their underlying metabolic transformations in human cells’, *Molecular Nutrition & Food Research*, 60(12), pp. 2622–2632.

Maseko, T. *et al.* (2013) ‘Chemical characterisation and speciation of organic selenium in cultivated selenium-enriched Agaricus bisporus.’, *Food Chemistry*, 141(4), pp. 3681–3687.

Miladi, K. *et al.* (2015) ‘Enhancement of alendronate encapsulation in chitosan nanoparticles’, *Journal of Drug Delivery Science and Technology*, 30, pp. 391–396.

Mishra, B., Priyadarsini, K. I. and Mohan, H. (2007) 'Effect of pH on one-electron oxidation of selenium aminoacids', *BARC Newsletter*, 285, p. 220.

Mohammed, M. A. *et al.* (2017) 'An overview of chitosan nanoparticles and its application in non-parenteral drug delivery', *Pharmaceutics*, 9(4).

Montes-Bayón, M., Molet, M. J. D., *et al.* (2006) 'Evaluation of different sample extraction strategies for selenium determination in selenium-enriched plants (Allium sativum and Brassica juncea) and Se speciation by HPLC-ICP-MS', *Talanta*, 68(4), pp. 1287–1293.

Montes-Bayón, M., Molet, M. J. D., *et al.* (2006) 'Evaluation of different sample extraction strategies for selenium determination in selenium-enriched plants (Alliumsativum and Brassicajuncea) and Se speciation by HPLC-ICP-MS', *Talanta*, 68(4), pp. 1287–1293.

Mukhopadhyay, P. *et al.* (2013) 'Oral insulin delivery by self-assembled chitosan nanoparticles: in vitro and in vivo studies in diabetic animal model.', *Materials Science & Engineering. C, Materials for Biological Applications*, 33(1), pp. 376–82.

Muzzarelli, R. a a *et al.* (2012) 'Current views on fungal chitin/chitosan, human chitinases, food preservation, glucans, pectins and inulin: A tribute to Henri Braconnot, precursor of the carbohydrate polymers science, on the chitin bicentennial', *Carbohydrate Polymers*, 87(2), pp. 995–1012.

Neo, Y. P. *et al.* (2013) 'Encapsulation of food grade antioxidant in natural biopolymer by electrospinning technique: A physicochemical study based on zein–gallic acid system', *Food Chemistry*, 136(2), pp. 1013–1021.

Neves, A. R. *et al.* (2016) 'Nanoscale delivery of resveratrol towards enhancement of supplements and nutraceuticals', *Nutrients*, 8(3), p. 131.

Paliwal, R. and Palakurthi, S. (2014) 'Zein in controlled drug delivery and tissue engineering.', *Journal of Controlled Release*, 189, pp. 108–22.

Pan, Y. *et al.* (2015) 'Effect of barrier properties of zein colloidal particles and oil-in-water emulsions on oxidative stability of encapsulated bioactive compounds', *Food Hydrocolloids*, 43, pp. 82–90.

Pharmacopoeia, B. (2016) 'British Pharmacopoeia Commission: London'. UK.

Philibert, T., Lee, B. H. and Fabien, N. (2017) ‘Current status and new perspectives on chitin and chitosan as functional biopolymers’, *Applied Biochemistry and Biotechnology*, 181(4), pp. 1314–1337.

Ponnampalam, E. *et al.* (2009) ‘Nutritional strategies to increase the selenium and iron content in pork and promote human health’, *Co-operative Research Centre for an Internationally Competitive Pork Industry, Pork CRC, Australian Government*.

Pridgen, E. M., Alexis, F. and Farokhzad, O. C. (2015) ‘Polymeric nanoparticle drug delivery technologies for oral delivery applications’, *Expert Opinion on Drug Delivery*, 12(9), pp. 1459–1473.

Puri, A. *et al.* (2009) ‘Lipid-based nanoparticles as pharmaceutical drug carriers: from concepts to clinic.’, *Critical Reviews in Therapeutic Drug Carrier Systems*, 26(6), pp. 523–580.

Pyrzyńska, K. (1996) ‘Speciation analysis of some organic selenium compounds. A review’, *Analyst*, 121(8), p. 77R–83R.

Qinna, N. A. *et al.* (2015) ‘Influence of molecular weight and degree of deacetylation of low molecular weight chitosan on the bioactivity of oral insulin preparations’, *Marine Drugs*, 13(4), pp. 1710–1725.

Rajam, M. *et al.* (2011) ‘Chitosan nanoparticles as a dual growth factor delivery system for tissue engineering applications’, *International Journal of Pharmaceutics*, 410(1–2), pp. 145–152.

Rampino, A. *et al.* (2013) ‘Chitosan nanoparticles: Preparation, size evolution and stability’, *International Journal of Pharmaceutics*, 455(1), pp. 219–228.

Rayman, M. P., Infante, H. G. and Sargent, M. (2008) ‘Food-chain selenium and human health: spotlight on speciation.’, *The British Journal of Nutrition*, 100(2), pp. 238–253.

Reddy, V. S. *et al.* (2017) ‘A systematic review and meta-analysis of the circulatory, erythrocellular and CSF selenium levels in Alzheimer’s disease: A metal meta-analysis (AMMA study-I)’, *Journal of Trace Elements in Medicine and Biology*, 42, pp. 68–75.

Reilly, K. *et al.* (2014) ‘A note on the effectiveness of selenium supplementation of Irish-grown Allium crops’, *Irish Journal of Agricultural and Food Research*, pp. 91–99.

des Rieux, A. *et al.* (2006) ‘Nanoparticles as potential oral delivery systems of proteins and vaccines: a mechanistic approach’, *Journal of Controlled Release*, 116(1), pp. 1–27.

Rikiishi, H. (2007) ‘Apoptotic cellular events for selenium compounds involved in cancer prevention’, *Journal of Bioenergetics and Biomembranes*, 39(1), pp. 91–98.

da Rosa, C. G. *et al.* (2015) ‘Characterization and evaluation of physicochemical and antimicrobial properties of zein nanoparticles loaded with phenolics monoterpenes’, *Colloids and Surfaces A: Physicochemical and Engineering Aspects*, 481, pp. 337–344.

Ryan, K. B. *et al.* (2012) ‘ Nanostructures overcoming the intestinal barrier: drug delivery strategies’, *Nanostructured Biomaterials for Overcoming Biological Barriers*, (22), p. 63.

Ryan, S. M. *et al.* (2013) ‘An intra-articular salmon calcitonin-based nanocomplex reduces experimental inflammatory arthritis’, *Journal of Controlled Release*, 167(2), pp. 120–129.

Sakurai, K., Maegawa, T. and Takahashi, T. (2000) ‘Glass transition temperature of chitosan and miscibility of chitosan/poly(N-vinyl pyrrolidone) blends’, *Polymers*, 41(19), pp. 7051–7056.

Savic, M. *et al.* (2012) ‘The fungistatic activity of organic selenium and its application to the production of cultivated mushrooms Agaricus bisporus and Pleurotus spp.’, *Archives of Biological Sciences*, 64(4), pp. 1455–1463.

Schaumlöffel, D. and Tholey, A. (2011) ‘Recent directions of electrospray mass spectrometry for elemental speciation analysis’, *Analytical and Bioanalytical Chemistry*, 400(6), pp. 1645–1652.

Semenova, M. G. *et al.* (2014) ‘Protein–Polysaccharide Interactions and Digestion of the Complex Particles’, in *Food Structures, Digestion and Health*, pp. 169–192.

Siepmann, J. and Peppas, N. A. (2011) ‘Higuchi equation: Derivation, applications, use and misuse’, *International Journal of Pharmaceutics*, pp. 6–12.

Song, G. *et al*. (2014) “Selenomethionine ameliorates cognitive decline, reduces tau hyperphosphorylation, and reverses synaptic deficit in the triple transgenic mouse model of alzheimer”s disease’, *Journal of Alzheimer’s Disease*, 41(1), pp. 85–99.

de Souza, V. R. *et al.* (2014) ‘Determination of the bioactive compounds, antioxidant activity and chemical composition of Brazilian blackberry, red raspberry, strawberry, blueberry and sweet cherry fruits.’, *Food Chemistry*, 156, pp. 362–8.

Stefánka, Z. *et al.* (2001) ‘Comparison of sample preparation methods based on proteolytic enzymatic processes for Se-speciation of edible mushroom (Agaricus bisporus) samples’, *Talanta*, 55(3), pp. 437–447.

Suzuki, M. *et al.* (2010) 'Differential apoptotic response of human cancer cells to organoselenium compounds', *Cancer Chemotherapy and Pharmacology*, 66(3), pp. 475–484.

Takahashi, K., Suzuki, N. and Ogra, Y. (2017) 'Bioavailability comparison of nine bioselenocompounds in vitro and in vivo', *International Journal of Molecular Sciences*, 18(3), pp. 1–11.

Thiry, C. *et al.* (2012) 'Current knowledge in species-related bioavailability of selenium in food', *Food Chemistry*, 130(4), pp. 767–784.

Torres-Giner, S., Ocio, M. J. and Lagaron, J. M. (2009) 'Novel antimicrobial ultrathin structures of zein/chitosan blends obtained by electrospinning', *Carbohydrate Polymers*, 77(2), pp. 261–266.

Uden, P. C. *et al.* (2004) 'Selective detection and identification of Se containing compounds—review and recent developments', *Journal of Chromatography A*, 1050(1), pp. 85–93.

Umerska, A., Corrigan, O. I. and Tajber, L. (2014) 'Intermolecular interactions between salmon calcitonin, hyaluronate, and chitosan and their impact on the process of formation and properties of peptide-loaded nanoparticles', *International Journal of Pharmaceutics*, 477(1), pp. 102–112.

Valko, M. *et al.* (2007) 'Free radicals and antioxidants in normal physiological functions and human disease', *The International Journal of Biochemistry & Cell Biology*, 39(1), pp. 44–84.

Vozza, G. *et al.* (2018a) 'Application of box-behnken experimental design for the formulation and optimisation of selenomethionine-loaded chitosan nanoparticles coated with zein for oral delivery', *International Journal of Pharmaceutics*, (submitted for publication).

Vozza, G. *et al.* (2018b) 'Formulation, characterisation, and in vitro evaluation of methylselenocysteine and selenocystine loaded chitosan nanoparticles-coated with zein', *Food Hydrocolloids*, (submitted for publication).

Vozza, G. *et al.* (2018c) 'Potential of mushroom by-products for nutrient delivery applications: production and characterisation of chitin from *Agaricus bisporus* and its derivatisation to chitosan and trimethyl chitosan', *Carbohydrate Polymers*, (submitted for publication).

Wang, J. J. *et al.* (2011) 'Recent advances of chitosan nanoparticles as drug carriers.', *International Journal of Nanomedicine*, pp. 765–774.

Ward, P., Connolly, C. and Murphy, R. (2012) 'Accelerated Determination of Selenomethionine in Selenized Yeast: Validation of Analytical Method', *Biological Trace Element Research*, 151(3), pp. 446–450.

Werner, A. R. and Beelman, R. B. (2002) 'Growing high-selenium edible and medicinal button mushrooms (Agaricus bisporus) as ingredients for functional foods or dietary supplements', *International Journal of Medicinal Mushrooms*, 4(2).

Wrobel, K. K. *et al.* (2003) 'Hydrolysis of proteins with methanesulfonic acid for improved HPLC-ICP-MS determination of seleno-methionine in yeast and nuts', *Analytical and Bioanalytical Chemistry*, 375(1), pp. 133–138.

Wu, L., Zhang, J. and Watanabe, W. (2011) 'Physical and chemical stability of drug nanoparticles', *Advanced Drug Delivery Reviews*, 63(6), pp. 456–469.

Xu, Y. and Du, Y. (2003) 'Effect of molecular structure of chitosan on protein delivery properties of chitosan nanoparticles', *International Journal of Pharmaceutics*, 250(1), pp. 215–226.

Yoon, H. Y. *et al.* (2014) 'Glycol chitosan nanoparticles as specialized cancer therapeutic vehicles: Sequential delivery of doxorubicin and Bcl-2 siRNA', *Scientific Reports*, 4, p. 6878.

Yuan, Z. *et al.* (2013) 'Chitosan-graft-β-cyclodextrin nanoparticles as a carrier for controlled drug release', *International Journal of Pharmaceutics*, 446(1–2), pp. 191–198.

Zhang, H. *et al.* (2015) 'Preparation and physicochemical properties of chitosan broadleaf holly leaf nanoparticles', *International Journal of Pharmaceutics*, 479(1), pp. 212–218.

Zhang, Y. *et al.* (2015) 'Zein-based films and their usage for controlled delivery: Origin, classes and current landscape', *Journal of Controlled Release*, 206(2699), pp. 206–219.

9 CONCLUSIONS AND FUTURE PERSPECTIVES

9.1 Overview

Nanotechnology has been touted as the next revolution in many industries, including the pharmaceutical and food industry (Srinivas *et al.*, 2010; Safari and Zarnegar, 2014; Divya, 2015). It is not surprising that the nutraceutical industry has expanded within the past two decades (DeFelice 1995; Verbeke 2005; Lagos *et al*. 2015) given that consumers now acknowledge the ability of certain foods to reduce disease risk or improve health (Hasler, 2000). Aqueous solubility and permeability of BA compounds have been highlighted among the major challenges in early and late product research and development (R&D), affecting up to 40 % of drugs on the pharmaceutical market (Censi and Di Martino, 2015). Attrition of many molecules in the pharmaceutical R&D program can be ascribed to lack of efficacy and the onset of secondary effects (Basavaraj and Betageri, 2014). The oral route, being the most popular, can be particularly challenging due to the harsh environment of the associated biological fluids found in the GIT, leading to limited absorption and limited bioavailability, (Sosnik, das Neves and Sarmento, 2014). That considered, an opportunity presents itself for development of a drug delivery carrier system that can optimise stability and bioavailability, whilst reducing its toxic side effects. One approach is the use of colloidal drug carriers that can provide site specific or targeted BA delivery, combined with optimal BA release profiles (Joye, Davidov-Pardo and McClements, 2014).

This project was carried out at the food and pharma interface, to produce oral formulations of nutraceutical SeAAs, which have been reported to possess narrow therapeutic indices and to be poorly absorbed in the small intestinal epithelium (Amoako, Uden and Tyson, 2009). Pharmaceutical drug delivery formulation techniques, such as ionotropic gelation, were employed to produce NP delivery systems that could potentially

improve the permeation, bioavailability and toxicity of the SeAAs. In tandem, process techniques common to the food industry, such as DoE (statistical experimental designs), were used to develop optimum NP formulations for oral delivery. The precise conditions identified through efficient estimation of process parameters enabled the production of NPs with target physicochemical properties (size, PDI and ZP), as identified by DLS. *In vitro* evaluation of the produced NPs was then conducted to assess the likelihood of oral compatibility in terms of stability, cytotoxicity and release profiles. Lastly, mushroom by-products were isolated and purified for the formulation of these NP systems.

9.2 Research Findings

In Chapter 4, a CCD and mathematical modelling approach was employed to assess the method of ionic gelation between the biopolymer chitosan (Cs) and tripolyphosphate (TPP), for production of NPs with physicochemical properties suitable for oral delivery. The mass ratio of Cs:TPP is one of the most influential variables that determines the size, PDI, ZP and morphology of ionotropically formed Cs NPs. The results of the CCD design identified that, at approximate concentrations of Cs (1.68 - 1.8 mg/mL) and intermediate concentrations of TPP (0.20 - 0.37 mg/mL), a feasible region was identified in which NP target properties could be achieved. The physicochemical properties of the NPs produced from the validation of the CCD study were assessed by DLS, showing that, under optimum conditions of Cs:TPP (6:1), NPs with sizes of 161 ± 43 nm, PDI of 0.39 ± 0.02 and ZP of 42 ± 3 could be produced. The information acquired from the CCD enabled further development and understanding of the model variables for NP production.

In Chapter 5, the main variables which affect EE%, particle size, PDI and ZP were optimised by use of a BBD. The SeAA, SeMet, was used as a prototype encapsulant, and

increasing the EE% of SeMet in the formulation was one of the driving targets for study. It was in this work that the importance of ionisable groups present on the BA to be encapsulated was highlighted, and a fundamental understanding of the formulation variables was gained. Through modulation of the formulation media pH, it was possible to induce higher protonation of Cs and ionisation of SeMet and thus electrostatic interactions between the two. This modification resulted in an increase of the EE% of the NPs from 39 ± 3 % to 66 ± 1 %, whilst their physicochemical properties remained within the target range for oral delivery. To further increase the EE%, the NPs were coated with the prolamine rich protein zein, which resulted in a final EE% of >80%, with NP diameters of 377±47nm, whilst the PDI and ZP values were maintained. Once satisfactory NPs for oral delivery were attained, it was necessary to then assess their suitability as a delivery system *in vitro*. Techniques were developed to evaluate their stability, cytotoxicity and release profiles and overall, the NPs performed well, showing high colloidal stability and thermal resistance over prolonged periods of time and no decrease in cellular viability in either Caco-2 or HepG2 cells after 4 and 72 hr exposures, respectively. Lastly, after 6 hr exposure to simulated intestinal buffers, the cumulative release profile of SeMet from the NPs showed that ≤ 60% of the drug had been released, indicating that degradation of the NP was slow and thus the mechanism may be diffusion/relaxation oriented. Overall, the findings inferred that it was possible to use DoE for the encapsulation of SeMet into a NP delivery system comprising food-derived components and that the oral administration of this molecule was plausible.

The strength of the DoE methodology was then tested in Chapter 6, in which the optimised formulation conditions, as previously identified, were employed to encapsulate the SeAAs $SeCys_2$ and MSC. The rationale for this approach was based on the fact that $SeCys_2$ and MSC contain comparable ionisable groups to SeMet and, as such, similar

formulations (e.g. physicochemical properties and EE%) as those achieved for the SeMet loaded NPs could be achieved. It was here that the reliability and usefulness of DoE was evidenced, as the responses that were estimated using the derived quadratic polynomial equations in Chapter 5, produced $SeCys_2$ and MSC loaded NPs, with equivalent physicochemical properties to those of SeMet. Differences between the encapsulated SeAAs were then identified by the *in vitro* techniques developed previously, whereby SeMet and MSC were shown to elicit little to no toxicity at test concentrations of 25-100uM in Caco-2 and HepG2 cell lines after 4 and 72 hr exposures. Although native $SeCys_2$ mirrored SeMet and MSC in terms of no apparent toxicity to Caco-2 cell lines, it elicited significant toxicity in HepG2 cells, across all tested concentrations. The feasibility of the formulation was then evidenced, as the encapsulation of $SeCys_2$ within the Cs:zein NP matrix conferred protection to the HepG2 cells after 72 hr exposure, indicating that, at the test concentrations used in the study (25-100 uM), the cytotoxic effects of pure $SeCys_2$ could be reduced. Interestingly, variances in the release profiles of the SeAAs were identified in this work, appearing to be intrinsically linked with their pKa values. A slower release in the stomach was observed for SeAAs with increasing pKa ($SeCys_2$, $_{pKa=4.66}$ < MSC, $_{pKa=4.93}$ < SeMet, $_{pka=5.53}$) and it was postulated that this systematic variance was attributable to their chargeable properties and interactions with the protonated 1º amines of Cs. In terms of stability, all formulations displayed high colloidal stability and thermal resistance over prolonged periods of time, independent of the encapsulated SeAA, with evidence that the Cs:zein matrix was responsible for this stability.

In Chapters 4-6, all the NPs developed were produced using PROTASAN™ UP (CL113), a well-known commercially pure Cs derived from crustaceans. Chapter 7 then looked at extracting chitin (the precursor to Cs) from the edible basidiomycete mushroom *A.*

bisporus and its subsequent derivatisation to Cs using microwave radiation. The target of that study was to reduce the time taken for the production of Cs compared to traditional methods and to produce a product with equivalent properties (such as DDA% and MW) to CL113, that could be potentially used in future NP formulations. The study indicated that fungal Cs (fCs) could be produced with equivalent DDA% to that of CL113 (86±6 vs 85±4 %). Notably, the produced fCs possessed a higher MW (180±19 vs 110±4 kDa), although it still fell within the medium molecular range suitable for oral delivery (110-225 kDa) (Bowman and Leong, 2006)). Once Cs with satisfactory properties was produced from the *A. bisporus* samples, a further modification was investigated, whereby the free amine groups present on the polymer backbone, were subjected to exhaustive methylation to give rise to trimethyl-chitosan (TMC). TMC was then assessed *in vitro* and showed potential application as a permeation enhancer. Based on the findings of Chapter 7, *A. bisporus* can be considered as a good source of chitin that can be easily isolated without aggressive treatments, subsequently deacetylated for the production of Cs and chemically modified to TMC, showing these by-products have potential use for many different practical applications.

Lastly, in Chapter 8, fCs was used to formulate NPs loaded with synthetic $SeCys_2$ by employing the optimised formulation conditions previously identified (Chapter 5). Once again, the robustness of the DoE formulation model was evidenced, as although fCs was used in place of CL113, NPs with equivalent physicochemical properties (sizes of 299.5 ± 47.1 nm, PDI 0.324 ± 0.176, ZP 38.7 ± 2.1, and EE% of 84.4 ± 1.2) were produced. The effect of Cs MW on NP production was also highlighted in this study, whereby the higher MW fCs NPs showed increased EE% / ZP values and a slower controlled release profile, most likely attributable to the larger proportion of ˚1 amines present on the polymer backbone available to interact with the ionised groups of $SeCys_2$. No apparent

toxicity to Caco-2 cell lines was observed after 4 hr exposure, although, for HepG2 cells, the IC_{50} of native $SeCys_2$ was found to be 12.8 ± 3.6 uM vs 32.5 ± 1.4 uM for $SeCys_2$ loaded fCs NPs, showing that the cytotoxic effects of pure $SeCys_2$ can be reduced with the applied formulation. Finally, a preliminary study to assess the feasibility of Irish mushrooms providing Se species for supplementation purposes was conducted. In that study, a RP-HPLC-PDA method was validated to analyse Se supplemented *A. bisporus* and the predominant species identified was $SeCys_2$ at 616 ± 23 µg/g DMP. Modest amounts of the SeAA, SeMet were also identified, at 18 ± 9 µg/g DMP. These findings infer that, Se supplemented mushrooms may be a feasible source for organic Se supplementation purposes and warrant further investigation.

9.3 Considerations and Future Perspectives

The work in this thesis raises several important points for consideration. Firstly, the physicochemical properties of the carrier system are critical considerations and ultimately, the desired targets (e.g. size, PDI, ZP) will rely heavily on the desired delivery route. Time spent on achieving these target properties can be substantially reduced, by employing a DoE approach, to develop optimum processes, via efficient screening of process parameters. In this work, a robust formulation model was produced using SeMet as a prototype encapsulant, which allowed for the subsequent encapsulation of structurally similar SeAAs, in a fraction of the time it would take compared to a OFAT approach, proving the benefits of a systematic approach to NP carrier design. While for the food industry, DoE has become standard practice for R&D of improved manufacturing processes (Carneiro and Azevedo, 2017), in comparison, the pharmaceutical industry has been late in adopting these paradigms (Politis *et al.*, 2017). The FDA, have recognised that "quality cannot be tested into products, i.e. quality should

be built in by design" (Ich.org, 2009) and the benefits of a DoE approach have started to become apparent to the industry (Politis *et al.*, 2017). The work in this thesis shows that an experimental planning approach together with a knowledge of the physical chemistry phenomena involved can enable the achievement of formulation target properties with application to similar targets/cargo successfully.

Further exploration of the application of other DoE strategies might increase research efficiencies, for example with the extension from laboratory experiments in this thesis to industrially oriented experiment DoE such as Taguchi methodology. The Taguchi method utilises orthogonal array (OA), signal-to-noise ratios (S/N), main effects, and analysis of variance (ANOVA) (Fei, Mehat and Kamaruddin, 2013). OA provides a set of well-balanced (minimum experimental runs) experiments and S/N, which are logarithmic functions of desired output, which serve as objective functions for optimisation (Datta, Bandyopadhyay and Pal, 2008). The approach provides an easy to interpret set of results that help experimenters determine the appropriate set of factor levels to create a robust system that performs on target. Static mixers are composed of several tortuous motionless elements, that allow for rapid combination of flow streams through mixers with low energy requirement, low cost, compact space requirement and continuous operation (Dong *et al.*, 2013). As such, coupling of a static mixer system with a Taguchi DoE method may offer a future approach for industrial scale up of the NPs developed in this work.

Regarding the use of these SeAA loaded NPs for supplementation purposes, this current work optimised physicochemical properties (size, PDI, ZP and morphology) suitable for oral delivery, in addition to ensuring high enough encapsulation of the cargo for commercial applications. These formulations were then screened *in vitro* to assess their

stability, release profiles and potential cytotoxicity for suitability for oral delivery. The findings of this work indicate that the formulation will be orally compatible and suitable for supplementation purposes.

The role of selenocompounds as potent cancer chemopreventive agents has been evidenced in several epidemiological studies, preclinical investigations and clinical intervention trials. However, these reports have often conflicted (Novotny *et al.*, 2010; Mandair *et al.*, 2014) and accumulated evidence suggests that the important determinants of the chemopreventive activities of Se compounds are both dose and chemical species dependant (El-Bayoumy, Sinha and Richie Jr, 2015). Additionally, the metabolic products from the various Se forms present in food and Se supplements, aimed at increasing selenium body status, are typically based on the indirect analysis of selenoproteins such as glutathione peroxidase (GPX) and selenoprotein P, as they are the major forms of Se present in the body (Kieliszek and Błażejak, 2013). The question, however, regarding what happens to selenium, from when it is ingested until it is excreted from the body, largely remains open (Kokarnig *et al.*, 2015). The antioxidant properties of the GPX selenoproteins, have been presumed to be the main factor in preventing carcinogenesis, largely based on animal and cellular studies (Chen, Prabhu and Mastro, 2013). However, this is likely to be an oversimplification, and emerging evidence suggests that certain forms of Se might exclusively elevate the level of Se-binding protein (SBP) (suggested to play a role in tumour suppression) rather than GPX (Mandair *et al.*, 2014). Amoako *et al.*, addressed the issue of stability of un-encapsulated Se species in selenium supplements (comprising multiple complex species in yeast-based and non-yeast-based supplements), exposing their predisposition to interconvert at the expense of long-term stability (Amoako, Uden and Tyson, 2009). No other work has focused on the encapsulation of organic Se species prior to their assessment as either supplementary,

chemo-preventative or therapeutic agents. The evidence provided in this thesis presents a formulation cargo system that can be used in future research in Se supplementation/therapy which may prevent biases in this research area and possibly lead to industrial applications.

Lastly, the $SeCys_2$ fCs NPs formulation developed in this work, may warrant a future investigation as a potential chemotherapeutic, based on literature evidence and the ability of the formulation to provide stability against Se degradation. Over the last decade, chemotherapy and targeted therapy combinations have helped to significantly improve patient outcomes (Kemp *et al.*, 2016). Although chemotherapeutic agents can be highly effective, small biological differences in the host and cancer cells makes treatment more challenging (Hoelder, Clarke and Workman, 2012). Often, antineoplastic agents are toxic chemicals and biologics designed to destroy cancer cells. However, while exerting their desired pharmacological effects, they can often precipitate severe toxic effects. Nausea, hair loss, compromised immune system, cardiotoxicity, are some of the adverse physical effects of these agents (Keefe and Bateman, 2012). As such, strategies are evolving to reduce or eliminate these unfavourable side effects by targeted delivery of the chemotherapeutic agent to the specific areas of cancer (Byers *et al.*, 2016). Molecular targeting for cancer chemoprevention has recently been focused on intracellular-signalling cascades (Wada, 2012). The anticancer activity of Se has been postulated to include inhibition of cell proliferation, modulation of redox state, detoxification of carcinogen, stimulation of the immune system, inhibition of angiogenesis and induction of cell apoptosis (Sanmartín *et al.*, 2011; Narayan *et al.*, 2015; Wrobel, Power and Toborek, 2016). In an *in vitro* study, $SeCys_2$ was identified as a novel agent with a broad-spectrum of antitumour activity, whereby a panel of eight human cancer cell lines was shown to be susceptible to $SeCys_2$, with IC_{50} values ranging from 3.6 to 37.0 μM (Chen

and Wong, 2009). More specifically, $SeCys_2$ has been reported to induce normalisation of the tumour vasculature, and a 4-fold increase in intra-tumoral doxorubicin levels, upon oral administration in mouse models, indicating its selective uptake by tumour tissues *in vivo* (Fernandes and Gandin, 2015). Studies by Estevez *et al.*, assessed the effects of Cs stabilised, elemental Se (Se_0) NPs on cell proliferation, apoptosis and cell cycle pattern in HepG2 cells and compared their peformance to other Se species. They found that the Se_0 NPs, stabilised with Cs, modestly inhibit a key enzyme known as CDK1, which is responsible for cell division and postulated that Se could be used as a chemotherapeutic by causing cell cycle arrest in cancer cells through CDK1 inhibition. Interestingly, they observed that native $SeCys_2$ induced a more potent inhibitory effect on CDK1, but argued that strong inhibition of this enzyme would likely be toxic to both cancerous and healthy cells (Estevez *et al.*, 2014). It is worth noting that, in that study, the authors neglected to stabilise the $SeCys_2$ with Cs for use as a control, so a true conclusion cannot be drawn on whether the Se_0 NPs were solely responsible for the observed effects and not the synergy between the Cs and Se_0 complex.

A challenge in the use of Se as a cancer therapeutic is to deliver redox active selenium, preferentially directly to the tumour and/or metastatic cells (Misra *et al.*, 2015). Interestingly, a significant number of Cs-based NPs have been reported to be selectively accumulated into tumour sites, primarily owing to the enhanced permeability and retention (EPR) effect (Prabaharan, 2008; Na *et al.*, 2011; Maeda, Nakamura and Fang, 2013). The EPR affect relates to the defective tumour vasculature and disorganised endothelium with poor lymphatic drainage at the tumour sites, allowing for the selective accumulation of macromolecular drugs in tumour tissues (Wolinsky and Grinstaff, 2008). As Cs is biodegradable and easily metabolised from the body, it has become quite clinically attractive for use in drug delivery applications (Kumari, Yadav and Yadav,

2010). Moreover, the biocompatibility of Cs is dependent on its purity, MW, and DDA% and, as this work evidenced, can be modulated accordingly, given the right production conditions. Considering the apparent selective cancer targeting properties of both $SeCys_2$ and Cs and the reported antitumour activity of $SeCys_2$, in addition to the observed ability of Cs to confer protection to non-cancerous cells, it seems reasonable to suggest that the $SeCys_2$ loaded fCs NPs, as described in this work, may warrant investigation as anticancer formulations.

Crustacean derived Cs is dependent on the source itself, whereby, to yield a product with reproducible properties, the same species must be harvested, at the same time (seasonally), in the same geographical location and at the same life stage cycle and different batch materials require different processing conditions (Weinhold *et al.*, 2009). fCs offers several advantages over its crustacean counterparts, owing to the highly controlled environments in which it is cultivated, year-round growth that is not seasonally dependant and significantly lower heavy metal association than that of crustaceans (Muzzarelli *et al.*, 2012). The present work shows the reproducibility of laboratory based fCs production as well as the ability to match industry standards. However, to make fCs sustainable and competitive in the market, especially for pharmaceutical applications, the assessment of reproducibility of fCs product batches is imperative. Currently, there are two companies that are actively selling enzymatically derived fCs for weight-loss products (Kiytozyme, Belgium) and for R&D applications (Mycodev, Canada) at a cost range of €177-213 per gram (www.sigmaaldrich.com). There are many potential reasons for this apparent high cost, which may relate to the enzymes being employed, the initial investment cost of the scale-up instrumentation and their subsequent energy consumption. Although it is difficult to provide an exact comparison of cost of the fCs produced in this small-scale work, with that of commercially available products, a crude

estimate can be made. For instance, the initial investment of a MARS 6, 40 vessel turntable microwave, as used in this project, is €15,000 and it can process 10 g of chitin at a time, using > 400 mL of NaOH (30 % w/v, ≈ €15) with a 15 min reaction time in a 600W microwave at a cost €23.79 per Kwh (www.energyusecalculator.com, accessed in May 2018). The weight yield of fCs using this method is 5.5g, with a DDA% of 86 ± 6 % and MW of 180±19 kDa. Excluding the initial €15,000 investment of the microwave, the apparent cost of fCs using the method developed in this research is ≈ €6.2/g, showing considerable potential for a mark-up that would quickly recover the initial investment cost and offer a significantly more competitive price compared to the current market providers.

Consumers may see purchasing non-animal products as an ethical obligation, whilst others trade it off against price and other product attributes (Vanhonacker *et al.*, 2007; Vanhonacker and Verbeke, 2014). Varying preferences and perceptions may also stem from norms and values within specific subcultures, such as those linked to religious (e.g. pigs in Muslim and cows in Hinduism countries) and cultural differences at the national level (Van Riemsdijk *et al.*, 2017). Regardless, with the rise in consumer demand for non-animal constituents in food (Bord Bia Insight Centre, 2016), cosmetic (Hennigs, Karampournioti and Wiedmann, 2016) and pharmaceutical (Murtaugh *et al.*, 2017) products, industrial companies are very interested in fungal-based alternatives, (Martin Zaki, Lambson Ltd, private communication) for use in product formulations. As such, fCs, produced as per this current work, may be well placed to address this demand and would warrant further investigation.

Additionally, in this thesis, the Cs derivative TMC, which is a permeation enhancer presently used in both academic and pharmaceutical research and development (Kulkarni

et al., 2017), was produced from fungal chitosan. A recommendation for future work regarding further optimisation of TMC production from fCs would be the employment of parallel synthesis for potential optimisation of the DDQ % and further reduction in the extent of O-methylation. For example, variation of the alkylhalides (e.g. chloromethane, bromomethane), bases (e.g. KOH, K_2CO_3), and/or aprotic solvents (e.g. DMF, DMSO) employed may identify improved synthetic routes. It would also be interesting to employ a CCD to investigate the use of microwave irradiation for the synthesis of TMC, which would allow for both optimisation and comparison to the conventional method employed in this research, as it may result in a significantly reduced production time, similar to that attained for the fCs.

9.4 References

Amoako, P. O., Uden, P. C. and Tyson, J. F. (2009) 'Speciation of selenium dietary supplements; formation of S-(methylseleno)cysteine and other selenium compounds', *Analytica Chimica Acta*, 652(1–2), pp. 315–323.

Basavaraj, S. and Betageri, G. V. (2014) 'Can formulation and drug delivery reduce attrition during drug discovery and development—review of feasibility, benefits and challenges', *Acta Pharmaceutica Sinica B*, 4(1), pp. 3–17.

Bord Bia Insight Centre (2016) 'Exploring global meat trends', (October). Available at: http://www.bordbia.ie/industry/manufacturers/insight/publications/bbreports/RecentMarketingReports/Global Meat Trends October 2016.pdf. (Accessed 10 Jan 2018).

Bowman, K. and Leong, K. W. (2006) 'Chitosan nanoparticles for oral drug and gene delivery', *International Journal of Nanomedicine*, 1(2), p. 117.

Byers, T. et al. (2016) 'The American Cancer Society challenge goal to reduce US cancer mortality by 50% between 1990 and 2015: results and reflections', *Cancer Journal for Clinicians*, 66(5), pp. 359–369.

Carneiro, F. and Azevedo, A. (2017) 'A six sigma approach applied to the analysis of variability of an industrial process in the field of the food industry', *Industrial Engineering and Engineering Management (IEEM)*, pp. 1672–1679.

Censi, R. and Di Martino, P. (2015) 'Polymorph impact on the bioavailability and stability of poorly soluble drugs', *Molecules*, 20(10), pp. 18759–18776.

Chen, Y.-C., Prabhu, K. S. and Mastro, A. M. (2013) 'Is Selenium a Potential Treatment for Cancer Metastasis?', *Nutrients*, 5(4), pp. 1149–1168.

Datta, S., Bandyopadhyay, A. and Pal, P. K. (2008) 'Grey-based Taguchi method for optimization of bead geometry in submerged arc bead-on-plate welding', *The International Journal of Advanced Manufacturing Technology*, 39(11–12), pp. 1136–1143.

DeFelice, S. L. (1995) 'The nutraceutical revolution: its impact on food industry R&D', *Trends in Food Science & Technology*, 6(2), pp. 59–61.

Divya, S. D. P. * and D. (2015) 'Nanotechnology and Nutraceuticals', *International Journal of Nanomaterials, Nanotechnology and Nanomedicine*, 1(2), p. 4.

Dong, Y. et al. (2013) ‘Scalable ionic gelation synthesis of chitosan nanoparticles for drug delivery in static mixers’, *Carbohydrate Polymers*, 94(2), pp. 940–945.

El-Bayoumy, K., Sinha, R. and Richie Jr, J. P. (2015) ‘7 Forms of Selenium in Cancer Prevention’, Diversity of Selenium Functions in Health and Disease. *CRC Press*, 38, p. 137.

Estevez, H. et al. (2014) ‘Effects of chitosan-stabilized selenium nanoparticles on cell proliferation, apoptosis and cell cycle pattern in HepG2 cells: Comparison with other selenospecies’, *Colloids and Surfaces B: Biointerfaces*, 122, pp. 184–193.

Fei, N. C., Mehat, N. M. and Kamaruddin, S. (2013) ‘Practical Applications of Taguchi Method for Optimization of Processing Parameters for Plastic Injection Moulding: A Retrospective Review’, *ISRN Industrial Engineering*, pp. 1–11.

Fernandes, A. P. and Gandin, V. (2015) ‘Selenium compounds as therapeutic agents in cancer’, *Biochimica et Biophysica Acta (BBA)*, 1850(8), pp. 1642–1660.

Hasler, C. M. (2000) ‘The changing face of functional foods’, *Journal of the American College of Nutrition*, 19(sup5), p. 499S–506S.

Hennigs, N., Karampournioti, E. and Wiedmann, K.-P. (2016) ‘Do as You Would Be Done by: The Importance of Animal Welfare in the Global Beauty Care Industry’, *Green Fashion*, pp. 109–125.

Hoelder, S., Clarke, P. A. and Workman, P. (2012) ‘Discovery of small molecule cancer drugs: Successes, challenges and opportunities’, *Molecular Oncology*, 6(2), pp. 155–176.

ICH.org (2009) ‘Pharmaceutical Development Q8’, ICH Harmonised Tripartite Guideline, 8, pp. 1–28.

Joye, I. J., Davidov-Pardo, G. and McClements, D. J. (2014) ‘Nanotechnology for increased micronutrient bioavailability’, *Trends in Food Science & Technology*, 40(2), pp. 168–182.

Keefe, D. M. K. and Bateman, E. H. (2012) ‘Tumour control versus adverse events with targeted anticancer therapies’, *Nature Reviews Clinical oncology*, 9(2), p. 98.

Kemp, J. A. et al. (2016) ‘“Combo” nanomedicine: co-delivery of multi-modal therapeutics for efficient, targeted, and safe cancer therapy’, *Advanced Drug Delivery Reviews*, 98, pp. 3–18.

Kieliszek, M. and Błażejak, S. (2013) ‘Selenium: Significance, and outlook for supplementation’, *Nutrition*, 29(5), pp. 713–718.

Kokarnig, S. et al. (2015) ‘Concurrent quantitative HPLC-mass spectrometry profiling of small selenium species in human serum and urine after ingestion of selenium supplements’, *Journal of Trace Elements in Medicine and Biology*, pp. 83–90.

Kulkarni, A. D. et al. (2017) ‘N, N, N-Trimethyl chitosan: An advanced polymer with myriad of opportunities in nanomedicine’, *Carbohydrate Polymers*, 157, pp. 875–902.

Kumari, A., Yadav, S. K. and Yadav, S. C. (2010) ‘Biodegradable polymeric nanoparticle based drug delivery systems.’, *Colloids and Surfaces. B, Biointerfaces*, 75(1), pp. 1–18.

Lagos, J. B. et al. (2015) ‘Recent patents on the application of bioactive compounds in food: A short review’, *Current Opinion in Food Science*, 5, pp 1-7.

Maeda, H., Nakamura, H. and Fang, J. (2013) ‘The EPR effect for macromolecular drug delivery to solid tumors: Improvement of tumor uptake, lowering of systemic toxicity, and distinct tumor imaging in vivo’, *Advanced Drug Delivery Reviews*, 65(1), pp. 71–79.

Mandair, D. S. et al. (2014) ‘The impact of diet and nutrition in the prevention and progression of hepatocellular carcinoma.’, *Expert review of Gastroenterology & Hepatology*, 8(4), pp. 369–82.

Misra, S. et al. (2015) ‘Redox-active selenium compounds—From toxicity and cell death to cancer treatment’, *Nutrients*, 7(5), pp. 3536–3556.

Murtaugh, M. P. et al. (2017) ‘The science behind One Health: at the interface of humans, animals, and the environment’, *Animals of the New York Academy of Sciences*, 1395(1), pp. 12–32.

Na, J. H. et al. (2011) ‘Real-time and non-invasive optical imaging of tumor-targeting glycol chitosan nanoparticles in various tumor models’, *Biomaterials*, 32(22), pp. 5252–5261.

Narayan, V. et al. (2015) ‘Epigenetic regulation of inflammatory gene expression in macrophages by selenium’, *The Journal of Nutritional Biochemistry*, 26(2), pp. 138–145.

Novotny, L. et al. (2010) ‘Selenium as a chemoprotective anti-cancer agent: reality or wishful thinking’, *Neoplasma*, 57(5), pp. 383–391.

Politis, S. N. et al. (2017) ‘Design of experiments (DoE) in pharmaceutical development’, *Drug Development and Industrial Pharmacy*, 43(6), pp. 889–901.

Prabaharan, M. (2008) ‘Chitosan derivatives as promising materials for controlled drug delivery’, *Journal of Biomaterials Applications*, 23(1), pp. 5–36.

Van Riemsdijk, L. et al. (2017) ‘Marketing animal-friendly products: Addressing the consumer social dilemma with reinforcement positioning strategies’, *Animals*, 7(12).

Safari, J. and Zarnegar, Z. (2014) ‘Advanced drug delivery systems: Nanotechnology of health design A review’, *Journal of Saudi Chemical Society*, 18(2), pp. 85–99.

Sanmartín, C. et al. (2011) ‘Selenium and clinical trials: new therapeutic evidence for multiple diseases’, *Current Medicinal Chemistry*, 18(30), pp. 4635–4650.

Sosnik, A., das Neves, J. and Sarmento, B. (2014) ‘Mucoadhesive polymers in the design of nano-drug delivery systems for administration by non-parenteral routes: A review’, *Progress in Polymer Science*, 39(12), pp. 2030–2075.

Srinivas, P. R. et al. (2010) ‘Nanotechnology research: applications in nutritional sciences.’, *The Journal of Nutrition*, 140(1), pp. 119–24.

Vanhonacker, F. et al. (2007) ‘Segmentation based on consumers’ perceived importance and attitude toward farm animal welfare.’, *International Journal of Sociology of Agriculture and Food*, 15(3), pp. 91–107.

Vanhonacker, F. and Verbeke, W. (2014) ‘Public and consumer policies for higher welfare food products: Challenges and opportunities’, *Journal of Agricultural and Environmental Ethics*, 27(1), pp. 153–171.

Verbeke, W. (2005) ‘Consumer acceptance of functional foods: socio-demographic, cognitive and attitudinal determinants’, *Food Quality and Preference*, 16(1), pp. 45–57.

Wada, S. (2012) ‘Colorectal cancer and the preventive effects of food components’, Cancer Prevention-From Mechanisms to Translational Benefits. InTech.

Weinhold, M. X. et al. (2009) ‘Strategy to improve the characterization of chitosan for sustainable biomedical applications: SAR guided multi-dimensional analysis’, *Green Chemistry*, 11(4), pp. 498–509.

Wolinsky, J. B. and Grinstaff, M. W. (2008) ‘Therapeutic and diagnostic applications of dendrimers for cancer treatment’, *Advanced Drug Delivery Reviews*, 60(9), pp. 1037–1055.

Wrobel, J. K., Power, R. and Toborek, M. (2016) ‘Biological activity of selenium: revisited’, *IUBMB life*, 68(2), pp. 97–105.

Dissemination

Publications

Vozza, G., Khalid, M., Byrne, H. J., Ryan, S., & Frias, J. (2016). Nutrition - Nutrient delivery. In: Nanotechnology in the Food Industry, Volume 5. (U. K. Oxford, Ed.) (1st ed.).

Vozza, G., Danish, M. K., Byrne, H. J., Frias, J. M., & Ryan, S. M. (2018). Application of Box-Behnken experimental design for the formulation and optimisation of selenomethionine-loaded chitosan nanoparticles coated with zein for oral delivery. International Journal of Pharmaceutics, (submitted for publication, April 2018).

Vozza, G., Danish, M. K., Byrne, H. J., Frias, J. M., & Ryan, S. M. (2018). Formulation, characterisation, and *in vitro* evaluation of methylselenocysteine and selenocystine loaded chitosan nanoparticles-coated with zein. Food Hydrocolloids, (submitted for publication, May 2018).

Vozza, G., Danish, M. K., Byrne, H. J., Frias, J. M., & Ryan, S. M. (2018). Potential of mushroom by-products for nutrient delivery applications: production and characterisation of chitin from *Agaricus bisporus* and its derivatisation to chitosan and trimethyl chitosan. Carbohydrate Polymers, (submitted for publication, May 2018).

Danish, M. K., **Vozza, G**., Byrne, H. J., Frias, J. M., & Ryan, S. M. (2017). Formulation, Characterization and Stability Assessment of a Food-Derived Tripeptide, Leucine-Lysine-Proline Loaded Chitosan Nanoparticles. Journal of Food Science, 82(9). https://doi.org/10.1111/1750-3841.13824

Danish, M. K., **Vozza, G**., Byrne, H. J., Frias, J. M., Ryan, S. M., Khalid, M., Ryan, S. M. (2017). Comparative study of the structural and physicochemical properties of two food derived antihypertensive tri-peptides, Isoleucine-Proline-Proline and Leucine-Lysine-Proline encapsulated into a chitosan based nanoparticle system. Innovative Food Science & Emerging Technologies, 44, 139–148. https://doi.org/10.1016/j.ifset.2017.07.002

Conference Presentations

Innovations in Encapsulation, Royal Society of Chemistry (RSC) conference, Dec 2017, London, UK. Giuliana Vozza, Minna Khalid, Hugh J. Byrne, Sinead Ryan and Jesus Frias. **Oral presentation** – "*Methylselenocysteine loaded chitosan:zein nanoparticles: Formulation, characterisation, and in vitro evaluations*"

American Association of Pharmaceutical Scientists (AAPS) conference, Nov 2017, San Diego, California. **Poster presentation** – "*Formulation, characterisation and in vitro assessment of Selenocystine loaded chitosan nanoparticles for oral delivery*"

The European Federation of Food Science & Technology (EFFoST) conference, Nov 2017, Sitges, Spain. Giuliana Vozza, Hugh J. Byrne, Sinéad Ryan and Jesús Frías **Poster presentation** – "*Isolation and characterisation of chitin and chitosan from the cultivated mushroom Agaricus bisporus*"

The International Union of Food Science and Technology (IUFoST) conference, Aug 2016. Dublin, Ireland. Giuliana Vozza, Minna Khalid, Hugh J. Byrne, Sinéad Ryan and Jesús Frías **Poster presentation** – "*Protein-polysaccharide delivery systems: A systematic approach for the formulation and optimisation of selenomethionine-loaded chitosan: zein nanoparticles*"

United Kingdom and Ireland Controlled Release Society (UKICRS) symposium, April 2016. Giuliana Vozza, Minna Khalid, Hugh J. Byrne, Sinéad Ryan and Jesús Frías **Poster presentation** - "*Preparation, optimization and characterization of selenium-loaded chitosan nanoparticles for oral delivery*"

The European Federation of Food Science & Technology (EFFoST) conference, Nov 2015, Athens, Greece. Giuliana Vozza, Minna Khalid, Hugh J. Byrne, Sinéad Ryan and Jesús Frías **Oral presentation** - "*Encapsulation efficiency and physicochemical properties of a selenomethionine-loaded chitosan nanoparticles formulation for oral delivery*"

Delivery of Functionality in Complex Food Systems (DOF), July 2015, Paris, France. Giuliana Vozza, Minna Khalid, Hugh J. Byrne, Sinéad Ryan and Jesús Frías **Poster presentation** - "*Preparation and characterisation of selenomethionine-loaded chitosan nanoparticles for oral delivery*"

43rd Institute of Food Science and Technology of Ireland (IFSTI), Nov 2014. Dublin, Ireland. Giuliana Vozza, Minna Khalid, Hugh J. Byrne, Sinéad Ryan and Jesús Frías **Poster presentation** - "*Preparation and characterization of selenomethionine loaded chitosan/TPP nanoparticles for oral delivery*".

Modules

- PGD (Postgraduate Demonstrator) Training (Sept 2014)
- Applied Modelling in Environment, Food and Health (Sept 2015)
- Thesis writing group workshop (July 2015)
- PhD (and beyond) master class (Feb 2016)
- Science Writing and Presenting Skills (April 2016)
- Statistics for the Agri-Food Researcher (Aug 2017)
- Agri-Food Career Management (Dec 2017)
- Leadership Skills for the Agri-Food sector (Jan 2018)